Characterisation in mice of a conserved sequence, Mcr2, associated with the Wilms' tumour 1 (Wt1) locus

Meza Menchaca, Thuluz

Award date:
2010

Awarding institution:
University of Bath

Characterisation in mice of a conserved sequence, Mcr2, associated with the Wilms' tumour 1 (Wt1) locus

Submitted by

Thuluz Meza Menchaca

for the degree of Doctor in Philosophy

of the

University of Bath

Department of Biology and Biochemistry

September 2010

Signature of the Author.....  .....

I

Abstract

The Wilms' tumour suppressor gene WT1, encodes a structurally diverse and multifunctional protein with tightly controlled expression throughout the development of several organ systems. Although initially defined as a tumor suppressor, WT1 has been found to be overexpressed in some cancers. How WT1 contributes to the shift from normal to aberrant development, or from normal function to oncogenic function, is poorly understood. Recent studies have shown an abundance of bidirectional transcription across metazoan genomes suggesting that non-coding antisense transcripts may have important roles in cell function. WT1-AS transcripts are capable of positively modulating WT1 protein levels in vitro, but relatively little is known about the functions of these antisense transcripts in vivo. The aim of this thesis was to characterize the role of a highly conserved region, Mcr2, located upstream of human and mouse WT1. Our data suggests that Mcr2 is not translated into protein and is transcribed in an antisense orientation. Mcr2 was found partially conserved in fish and well conserved in terrestrial vertebrates. By analysing novel mouse strains with genetically modified Mcr2 we have identified that Mcr2 may have a role in both fertility and embryonic survival, as well as regulating liquid homeostasis in the adult mouse.

Acknowledgements

First and foremost I offer all my gratitude to my supervisor, Dr. Andrew Ward, who has supported me throughout my thesis. It is also a great pleasure to thank Dr. Kim Moorwood who has co-supervised during my studies. I would also like to thank Joanne Stewart-Cox and all the rest of wonderful people in our laboratory.

In particular I wish to express my gratitude to Dr. Karim Malik, Dr. Anne Hancock and Dr. Robert Kelsh, for invaluable contributions during the course of this project. For their expert technical help, I would like to thank Dr. Wolf Woltersdorf, Lesley Moore, Iryna Withington, Rosalind West and David Jeffery.

Finally I want to thank the National Council of Science and Technology (Mexican funding) that has been supporting me during my PhD studies.

…for my mother Dr. María del Socorro Menchaca Dávila.

Table of contents

List of Figures

List of Tables

List of Abbreviations

aa: amino acid

Ago: Argonaute

AML: acute myeloid leukemia

AMPS: ammonium persulfate

ANOVA: analysis of variance

ARR: antisense regulatory region

AUG: adenine uracile guanine

AWT1: alternative WT1 transcript

BMC: bone mineral content

BMD: bone mineral density

bp: base pairs

BSA: bovine serum albumin

BWS: Beckwith-Weidemann syndrome

c M: centimorgan

C: cytosine

Ca^{2+}: calcium ion

cDNA: complementary deoxyribonucleic acid

cm: centimeter

CpG: cytosine guanine dinucleotide

Cre: Cre recombinase

CTCF: CCCTC binding factor

DDS: Denys Drash syndrome

DDT: dithiothreitol

DEPC: diethyl pyrocarbonate

DMSO: dimethyl sulfoxide

DNA: deoxyribonucleic acid

DNase: deoxyribonuclease

dNTPs: 2'-deoxynucleotide-5'-triphosphates

DPX: distryrene plasticiser in xylene

DTA: diphtheria toxigene

DTT: dithiothreitol

E: gestational day

EDTA: ethylenediaminetetraacetic acid

EGR1: early growth reponse-1

EMSA: electro mobility shift assays

ENCODE: encyclopedia of DNA elements

EOC: endometrial ovarian cancer

eRNA: enhancer non-coding RNA

ES: embryonic stem

EST: expressed sequenced tag

FANTOM: functional annotation of mouse

FS: Fraiser syndrome

G: guanine

GDNF: glial cell line derived neurotrophic factor

H&E: haematoxylin and eosin

H: homologue

he: heterozygote

ho: homozygote

IPTG: isopropyl-B-D-thiogalactoside

IU: international unit

K: potassium

kb: kilobase pairs

kDa: kilo Daltons

KI: knock-in

KO: knock-out

KTS: lysine, threonine, serine

l: liter

lncRNA: long non-coding ribonucleic acid

LOH: loss of heterozygosity

LOI: loss of imprinting

M: moles

MAR: matrix attachment region

MCR: Mouse Conserved Region

mg: milligram

min: minute

ml: milliliter

mm: millimeter

mM: millimolar

mOsm:milliosmol

n: population size

Na: sodium

NAT: natural antisense transcript

NCBI: National Centre for Biotechnology Information

ncRNA: non-coding RNA

ng: nanogram

ºC: degrees Celsius

P: probability value

PAGE: polyacrylamide gel electrophoresis

PAS: periodic acid-Schiff

PBS: phosphate buffered saline

PCR: polymerase chain reaction

PD: postnatal date

PFA: paraformaldehyde

PIP: percentage identity plot

PVDF: polyvinylidene fluoride

qPCR: quantitative real time polymerase chain reaction

R T: room temperature

RNA: ribonucleic acid

RNAi: RNA interference

RNase: ribonuclease

RNP: ribonucleoprotein

RO: reverse osmosis

RPA: ribonuclease protection assay

RT: reverse transcriptase

SDS: sodium dodecyl sulphate

SHM: somatic hypermutation

siRNA: small interfering RNA

smRNA: small modulatory RNA

snoRNA small nucleolar RNA

SNP: single nucleotide polymorphism

snRNA: small nuclear RNA

snRNP: small nuclear ribonucleoprotein

sRNA: small RNA

SSC: saline sodium citrate

T: thymine

TAE: Tris base, acetic acid and ethylenediaminetetraacetic acid.

TE: Tris base and ethylenediaminetetraacetic acid

Tm: melting temperature

Tris: Tris (hydroxymethyl) amino methane

TSG: tumour suppressor gene

TTS: transcriptional terminator sequence

Tukey's test: Tukey's multiple comparison analyses

U: units of enzyme

UTR: untranslated region

UV: ultra violet

V: volts

WAGR: Wilms' tumour, aniridia, genitourinary abnormalities and mental retardation.

wt: wild type

WT: Wilms' tumour

$WT1^{-/-}$: WT1 homozygous

$WT1^{-/+}$: WT1 heterozygous

$WT1^{+/+}$: Wilms' tumour gene 1 wild type

X^2: Chi-squared

YAC: yeast artificial chromosome

Chapter 1: Introduction

1.1 The Wilms' tumour 1 gene *WT1*

The *WT1* gene encodes for multifunctional zinc finger proteins and is well known for its complexity. This gene is mostly conserved across vertebrates and is important in organ development as well as tumourigenesis. Mouse models have proved *WT1* to be essential for normal kidney function and also for the development of other organs. In human, the lack or malfunction of this gene is associated with Wilms' tumour (WT), as well as other solid tumours and hematological diseases. It is currently a target for cancer immunotherapy.

1.1.1 Identification

Characterization of the short arm of chromosome 11, while studying constitutional heterozygous deletions in WAGR syndrome (Wilms' tumour, aniridia, genitourinary malformations, mental retardation) (Francke *et al*., 1979; Riccardi 1980; Shannon 1982), enabled the identification of 11p lost of heterozygosity (LOH) in sporadic WT (Fearon *et al*., 1984; Koufos *et al*., 1984; Orkin *et al*., 1984; Reeve *et al*., 1984). This led to identification of *WT1* that was mapped to chromosome 11p 13 and cloned by three different groups (Call *et al*., 1990; Gessler *et al*., 1990; Rose *et al*., 1990). Further pedigree analysis of families with hereditary predisposition to WT found the linkage to 11p genetic markers absent, uncovering the presence of more than one WT predisposition locus (Huff *et al*., 1988; Grundy *et al*., 1988; Lewis *et al*., 1988). However, preliminary studies confirmed *WT1* to be tissue specific (Call *et al*., 1990) and highly expressed on the developing kidney (Haber, 1990; Pritchard-Jones, 1990).

Identification of the *WT1* homologue in the mouse (*Wt1*) followed a similar route. A deletion encompassing the small eye (*Sey*) locus in the mouse model called Sey^{Dey} which resembled the phenotype cause by the human l1pl3 WAGR deletions (see Section 1.1.9.1.5) (Gessler *et al*., 1990) contributed to the isolation and characterization of *Wt1* in chromosome 2 (Buckler *et al*., 1991).

1.1.2 *WT1* gene structure

Both human and mouse *WT1* genes span about 50 kb of the genome, comprising 10 exons (Figure 1.1). The last four exons encode a Krüppel' type zinc finger domain employed by a broad array of transcription factors that play important roles in gene regulation. *WT1* produces four major distinct isoforms due to two alternative splicing events.

1.1.2.1 *WT1* isoforms

WT1 gives a clear example of how, due to transcriptional and post-transcriptional alternative mechanisms, a plethora of protein isoforms that can each display distinct biological properties. Differential pre-mRNA splicing of *WT1* produces a diverse range of mRNA species (Call *et al.*, 1990; Dallosso *et al.*, 2003; Gessler *et al*., 1990; Gessler *et al*., 1992; Haber *et al*., 1991). In human and in mouse the gene encodes in theory at least 32 different 36-62 kDa protein isoforms by a combination of alternative mRNA splicing (Haber *et al*., 1991) plus RNA editing (Sharma *et al*., 1994) and non-AUG translational initiations (Bruening and Pelletier, 1996; Figure 1.1 A).

Of the known alternative splicing events two are the most well studied. One leads to inclusion or exclusion of exon 5 (+/- exon 5) (Figure 1.1 C) which encodes 17 amino acids (aa) and this splice-isoform event is conserved exclusively in mammalian species (Miles *et al*., 2003), whose exact function *in vivo* remains unclear given that mice lacking this exon do not appear to have altered development or fertility (see Section 1.1.9.1.4) (Natoli *et al*., 2002). Later studies did suggest it to be involved in cell survival in cell culture systems (Renshaw *et al*., 2004). Also it has been found that the +/- exon 5 ratio is altered in WTs (Baudry *et al*., 2002) and in acute myeloid leukemia (AML) (Gu *et al*., 2010; Siehl *et al*., 2004).

A different splicing event takes place in exon 9 (Figure 1.1 E). This isoform arises from the use of an alternate 5' splice junction at exon 9 and results in the insertion or omission of three aa (Lysine-Threonine-Serine, KTS) between zinc fingers 3 and 4 (+KTS/-KTS), which modulates DNA binding specificity (Rauscher *et al*., 1990) and

subnuclear localization (Larsson *et al*., 1995). Transfection of constructs expressing differential levels of either WT1 + KTS or WT1 –KTS into two different P53 negative cells lines shows in both cell types that WT1 –KTS induced apoptosis, whereas WT1 +KTS isoforms did not (Menke *et al*., 1997). This became relevant because WT1 +/- KTS ratio is altered in Fraiser syndrome (FS), where a germline mutation in the splice consensus sequence (resulting in reduced WT1 +KTS isoform) produces characteristic severe kidney and gonad developmental abnormalities *in vivo* (see Section 1.1.9.1.3) (Hammes *et al*., 2001). In normal tissues isoforms including the WT1 +KTS aa account for about 80% of the cellular mRNA, while those encoding +/- exon 5 account for at approximately 60% (Haber *et al*., 1991). The WT1 +exon 5 splicing is exclusive from mammals, whereas the WT1 +KTS isoform is conserved even in lower vertebrates (Kent *et al*., 1995; Miles *et al*., 1998; 2003; Semba *et al*., 1996). The WT1 –KTS isoforms appear to function as transcription factors (Madden *et al*., 1990), whereas the WT1 +KTS isoform associate with splicing complexes in the nucleus and might be involved in RNA metabolism (Menke *et al*., 1998). In mammals the different WT1 isoforms were initially shown to be present in fixed ratios of 8.3:3.8:2.5:1 (WT1 +exon 5/+KTS : -exon 5/+KTS : +exon 5/-KTS : -exon 5/-KTS) (Haber *et al*., 1991). Nevertheless, the ribonuclease protection assay (RPA) gave multiple bands from a very long RPA probe, making it difficult to discern which band identifies a particular isoform. Subsequent studies have re-examined the isoform ratios in different species combining reverse transcription-PCR (RT-PCR) and RPA assays (Kent *et al*., 1995). Even though these two techniques gave consistent results they did not confirm the expression ratios proposed by Haber *et al*., 1991. Also later studies showed that there is no differences of isoform ratios between species and that it remains static during nephrogenesis (Hammes *et al*., 2001), giving a ratio of 1.1-1.5 for WT1 +/-KTS using the mouse model.Other evidence shows that ratios can change according to cell/tissue context (Baudry *et al*., 2002). It has been proposed that altered WT1 isoform ratios may be involved on the etiology of sporadic WT and leukemia (Baudry *et al*., 2002; Klamt, *et al*., 1998; Shen *et al*., 2007).

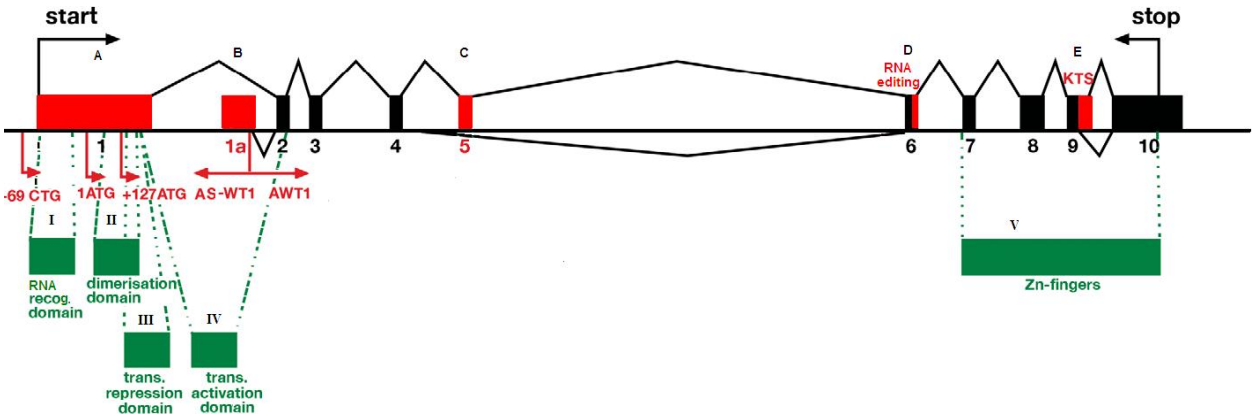

Figure 1.1 Schematic representation of *WT1* gene. Alternative start codons in exon 1, fixed exons in black, alternative exons marked in red (A-E). Red arrows show start of transcription. Green boxes (I-V) represent protein functional domains described in the text. Figure adapted from Hohestein & Hastie, 2006.

The latest splice-isoform identified was named Alternative WT1 (AWT1) (Figure 1.1 B), and was detected in hematopoietic and renal cells. It lacks exon 1 and it arises through transcription from an alternative promoter located in intron 1. This protein has a shorter N-terminal and smaller size, of 33 kDa, and exhibits normal 17aa and WT1 KTS splices as in the canonical *WT1* transcripts (other isoform transcripts) (Dalloso *et al*., 2004). Although the functional consequences have not been elucidated, it is known that *AWT1* is imprinted in the maternal allele with expression driven from the paternal allele. However, in WTs *AWT1* is expressed on both alleles, an example of loss of imprinting (LOI). In addition to this alternative splicing, for the variety in *WT1* mRNA/protein species has been reported as a result of post-transcriptional RNA editing in exon 6 (leucine to proline at codon 280, Figure 1.1 D) (Sharma *et al*., 1994). Also the use of an upstream non-AUG (CUG) alternative initiation codon has been reported to happen from upstream CUG in-frame with the main AUG start site and (Bruening and Pelletier., 1996), producing higher molecular weight proteins (approximately 68 kDa). The use of alternative start codons and RNA editing appears to occur exclusively in mammalian organisms (Scharnhorst *et al*., 1999).

1.1.3 Functional WT1 protein domains

There are three characteristic main domains of WT1 proteins: self recognition, activation and repression. Self-association domains have been described within the first 182 aa residue (Figure 1.1 II) (Englert *et al*., 1995a; Reddy *et al*., 1995b; Holmes *et al*., 1997) although this domain is still not well understood. The amino (N) terminus is rich in prolines and glutamines, and resembles the transactivation or repression domains of other transcription factors. WT1 protein can act as an activator or repressor of genes. Using hybrid protein domain-mapping experiments GAL4-fusion proteins were use to identify the transcriptional repressor domain within the N-terminus of WT1 (Madden *et al*., 1993b) localized to residues 71–180 (Figure 1.1 III). Later on, the suppression domain was further localized by cotransfection of WT1 deletion mutants with a reporter construct to aa 92-101 (Carpenter *et al*., 2004).

A transcriptional activation domain (residues 180-294) was characterized by transient cotransfection assays in a murine fibroblasts cell line (NIH3T3) of WT1 binding sites either side of a minimal promoter of the *Platelet-derived growth factor A-chain* (PDGF A-*chain*) gene (a gene transcriptionally suppressed by WT1) (Wang *et al*., 1993) (Figure 1.1 IV). WT1 can activate or down-regulate transcription depending on cofactors present in specific cell types. Using deletion analysis revealed regions required for transcriptional repression (Wang *et al*., 1995a), although is quite interesting that the isoform *AWT1* lacks the repression domain as well as the putative RNA recognition motif, self association, transcriptional repression and activation domains (Figure 1.1, I, II, III and IV), but the biological relevance of skipping these domains has not been elucidated (Dalloso *et al*., 2004). However, in isoforms with the repression domain, there occurs oligomerization which may block a repression domain and /or reveal an activation domain (Wang *et al*., 1995a). The suppression domain is also known to recruit a transcriptional cosuppressor, BASP1 (Carpenter *et al*., 2004). WT1 encodes a typical Krüppel-type zinc-finger protein (Figure 1.1 V) with affinity for GC-rich sequences that are closely related to the EGR-1 sequence. EGR-1 and WT1 share 67% of homology in the amino acid sequence of the zinc

finger domains. The N-terminal region of the WT1 zinc finger domains have been shown to have properties of nuclear localization signals (Englert *et al*., 1995a, Bruening *et al*., 1996). A potential RNA recognition motif was identified in the N-terminus of WT1 by computer modeling by Kennedy *et al*., (1996), although its role still not proved experimentally.

1.1.4 Transcriptional regulatory properties

1.1.4.1 WT1 DNA Binding

Interactions between proteins and DNA play an important and fundamental role in the regulation of gene expression. However, the mechanisms by which WT1 proteins select target genes to modify their expression still not fully understood. Work by several groups indicate that the choice of cell system, expression vector or reporter construct can all have an impact on the transcriptional regulators (reviewed by Menke *et al*., 1998; Little *et al*., 1999). This can be especially contradictory for those genes that are very context-dependent due to the fact that reporter constructs have shown to influence the activity of WT1 proteins (Reddy *et al*., 1995a). So, it has been observed through transfection experiments that WT1 can either enhance or repress the expression of specific targets or gene constructs depending on where the WT1 binding site is in relation to the transcriptional start site, as well as which cell type is employed and how the experiments were performed (Laity *et al*., 2000; Lee and Pelletier, 2001; Reddy *et al*., 1995a; Wang *et al*., 1995b).

Studies identified specific sequences that might be hot spots of interaction between WT1 and DNA. By its four zinc fingers, WT1 can bind to a variety of GC-rich sequences, for example, the early growth reponse-1 (*EGR1*) DNA sequence binding sites (5'-GNGNGGGNG-3') (Rauscher *et al*., 1993), and the WT1 high affinity 10 bp site (5'-GCGTGGGAGT-3') or (TCC) motif (Wang *et al.*, 1993). These sites are linked with WT1-dependent genes that can be up or down regulated as it has been found *in vitro* (Hamilton *et al*., 1995; Nakagama *et al.*, 1995). Earlier studies proposed that binding sequences are likely to be isoform specific. The WT1 +KTS isoform binds the consensus sequence 5'-GCGGGGGCG-3', where the WT1-KTS

does not (Rauscher *et al*., 1993). More recent studies have demonstrated stronger binding (including both WT1+/-KTS) to a series of longer sites defined as 5′-GCG-(T/G)GG-GG-(G/G)(A/G)(T/G)-3′ (Borel, *et al*., 1996; Hamilton *et al*., 1995), where this 12-base pair site defines more accurately the topological binding of the four zinc fingers, with each zinc finger binding to a 3-base pair triplet (Pavletich *et al*., 1991).

In a recent report Hartwig *et al*., (2010), analyzed *WT1* targets in nephron progenitor cells in embryonic explants. A pool of 1663 candidate genes were obtained by looking for a *EGR1* DNA consensus site under bioinformatic analyses. Co-immunopresipited-PCR was used to indicate biological significance together with a novel *in vivo* model, using modified *WT1* morpholino loss-of-function in embryonic kidney explants. By this triangulation of techniques the result was a corroboration of genes previously identified as *WT1* targets in the developing nephron such as: *Bmp7*, *Pax-2* and *Sall1*. Additionally, other 8 novel candidates were found *Cxxc5, Lsp1* , *Pbx2, Plxdc2 ,Rps6ka3, Fgfr3, Scx , Sox11*.

1.1.4.2 *WT1* in RNA binding

In eukaryotic cells, numerous RNA binding proteins and small RNAs play key roles in the post-transcriptional regulation of gene expression, including pre-mRNA splicing and polyadenylation. RNA binding proteins can also form stable ribonucleoprotein (RNP) complexes that transport and localize RNAs. Mutations in RNA binding proteins are known to account for some genetic disorders and, potentially, malignancy (reviewed in Burd and Dreyfuss, 1994). Suggesting the possible participation of *WT1* in RNA processing, Larsson *et al*., (1995), showed subnuclear co-localization of WT1 and small nuclear RNP (snRNP) proteins in “speckles” and coiled bodies inthat was splice-isoform dependent. The highest affinity binding was seen for the WT1 +KTS isoforms. Furthermore, computer modeling has identified a putative RNA recognition motif at aa 11-72 (Kennedy *et al*., 1996). In subsequent studies WT1 +KTS protein was shown to be directly associated with the ubiquitous splicing factor, U2AF65 which is part of the splicing machinery (Davies *et al*., 1998). Apparently this interaction does not require the first 180 aa implying that RNA binding is not essential for interaction with U2AF65 so

another part of the protein might be required for this interaction. Subsequent analysis has shown that WT1 co-purifies by chromatography with nuclear proteins present in large (>2mDa) RNP complexes (Ladomery *et al*., 1999).

Both WT1 +/- KTS protein were shown to be able to bind the *IGF2* (insulin-like growth factor type-2) exon 2 mRNA transcript as an RNA-protein interaction (Caricasole *et al*., 1996), mediated by the zinc finger motifs that bind to a target site overlapping (but not identical to) that for DNA binding. Moreover, via RNA-RNA interaction *WTl* may be autoregulatory (Moorwood *et al*., 1999), the *WT1* locus is complex and is characterized by antisense transcription of RNA initially called *WIT-1* (Huang *et al*., 1990), which is expressed in the same temporal and spatial manner as WT1 protein (Yeger *et al*., 1992; Moorwood *et al*., 1998). Later on the same region renamed as *WT1* antisense (*WT1-AS*) was shown to be transcribed from a promoter located in *WT1* intron 1 (Figure 1.1 B). *WT1* is thought to bind a complementary antisense in human RNA and as this is an important topic for this thesis it will be discussed later on in more detail.

1.1.4.3 WT1 protein-protein interactions

Analysis of native WT1 protein from human kidney and WTs shows WT1 present in homodimers (approximately 120 kDa), and association in complexes of 70kDa-80kDa, suggesting complex formation with other proteins beside WT1 (Iben and Roger-Pokora, 1999). WT1 can dimerise via interactions at its N-terminal domain, shown by yeast two-hybrid *in vitro* assays, GST pull-down assays and co-immunoprecipitation (Englert *et al*., 1995b; Holmes *et al*., 1997; Reddy *et al*., 1995b). Interactions are also mediated via domains within the zinc fingers (Bruening *et al*., 1996). P53 was identified by coimmunoprecipitation as a protein that interacts with WT1 in baby rat kidney cells expressing WT1 and from WT specimens (Maheswaran, 1993). The tumour suppressor p53 can associate with the first two zinc-fingers of WT1. When WT1 is coexpressed with wild type p53 in (p53 null), the interaction of exogenous p53 and WT1 prevents apoptosis of cells after UV irradiation (normally mediated by p53) representing an anti-apoptotic function of

WT1 (Maherswaran *et al*., 1995). Data in the literature also suggests that these two proteins can reciprocally modify each other's biological activities, in WT1 this occurs through the zinc fingers domain. More recent studies in mice suggest that WT1 and p53 can cooperate in tumourigenesis (Menke *et al*., 2002). WT1 also forms a complex with the transcription factor PAX-2, which was proposed to form a regulatory feedback to the expression of both the PAX-2 and the *WT1* genes during kidney development.

It has been found that the Brain Acid Soluble Protein 1 (BASP1) is a WT1 transcriptional cosuppressor (Carpenter *et al*., 2004). More recent studies using cell model mimicking the differentiating podocyte was used to show how the interaction between WT1-BASP1 is required for differentiation by Green *et al*., (2009). Both proteins colocalized to regulate the expression of *Bak*, *c-myc* and *podocalyxin* gene promoters, demonstrating that BASP1 can localize to gene promoters that are regulated by WT1.

WT1-interacting protein (WTIP) was isolated by a yeast two-hybrid screen experiment. In a podocyte cell line, WTIP is expressed at the cell surface, as part of the filtration barrier of the glomeruli where WTIP is inhibiting transcriptional activation of WT1. (Srichai *et al*., 2004). Other studies have identified interactions of WT1 with the prostate apoptosis response factor (Par4) (Johnstone *et al*., 1996), the p53 homologues p63 and p73 (Scharnhorst *et al*., 2000), ubiquitin-conjugation enzyme 9 (Nachtigal *et al*., 1998), and FHL2 (Du *et al*., 2002), with components of the splicing machinery (Larsson et l., 1995), Ciao_1 (Johnstone *et al*., 1999) and the transcriptional co-activator CBP (Wang et l., 2001). So, in addition to all this WT1 also has other roles in gene regulation dependent on interactions with several different proteins (reviewed by Riviera & Haber 2005; Lee and Haber2001; Wagner *et al*., 2003; Roberts, 2005).

1.1.5 WT1 targets of transcriptional regulation

WT1 isoform (e.g. AWT1), specific WT1 DNA binding site and the cell type in which the experiment was performed has resulted in the identification of many targets, that exhibit either up or downregulation of their expression (Table 1.1). It has been recently demonstrated that exogenous expression of WT1 in the human breast cancer cell lines, MDA-MB and MCF-7 and in human leukemic cell lines, can activate the *c-Myc* promoter and stimulate cellular proliferation (Han *et al*., 2004). In contrast, studies reported in HeLa cells, with the CAT reporter assays showed repression of the *c-Myc* promoter by WT1 indicating an antiapoptotic function. A role for WT1 in differentiation is proved by its action on the *amphiregulin* gene, which encodes a member of the epidermal growth factor family that stimulates epithelial branching in organ cultures of embryonic mouse kidney (Lee *et al*., 1999). *WT1* and *amphiregulin* mRNAs are co-expressed in the podocyte layer of developing glomeruli in the differentiating kidney (Lee *et al*., 1999). WT1 protein containing or excluding the WT1 +KTS amino acids inhibit expression of *cyclin E*, a critical step in promoting initiation of S phase of the cell cycle. WT1 -KTS shows the strongest effect, suppressing cyclin E promoter activity by 4-5 fold (Loeb *et al*., 2002). This target gene was identified by the use of inducible WT1 expression in tissue culture, and was confirmed by co-transfection and electro mobility shift assays (EMSA). Interestingly, the inhibition appears to be cell-line specific. WT1 can downregulate growth factor receptors such as EGFR modifying it expression of the Early Growth Response (*EGR*) family, primarily due to similarities in the consensus sequences of *WT1* and *EGR1*. This introduces the possibility that WT1 activity and/or binding to this target sites (consensus sites are present in the *cyclin E* promoter) can be also modified by cellular context. However, the consequences of binding are most often mutually opposing; EGR1 activates the transcription of genes that WT1 repress (Madden *et al*., 1991).

Table 1.1 Selected WT1 target genes.

Target Gene	Activation/Repression	Reference
Cyclin E	Repression	Loeb *et al*., 2002
EGR-1	Repression	Madden *et al* 1991
PDGF-A	Activation	Reddy *et al*., 1995b
EGFR	Repression	Englert *et al*., 1995a
IGF1R	Repression	Werner *et al*., 1994
Bcl-2	Activation/Repression	Mayo *et al*., 1999
TGF-β1	Repression	Dey *et al*., 1994
IGF-2	Activation	Ward *et al*., 1995
Amphiregulin	Activation	Lee *et al*., 1999
P21	Activation	Englert *et al*., 1997
c-Myb	Repression	McCann *et al*., 1995
Pax-2	Repression	Ryan *et al*., 1995
Erythropoietin	Activation	Dame *et al*., 2006
Snai1	Activation	Martinez- Estrada *et al.*, 2010
Cdh1	Repression	Martinez- Estrada *et al.*, 2010
EpoR	Activation	Kirschner *et al*., 2008
Dax-1	Repression	Chang *et al*., 2009
Scel	Activation	Ratelade *et al*., 2010
Sulf1	Activation	Ratelade *et al*., 2010
α4-integrin	Activation	Kirschner *et al*., 2006
c-myc	Activation	Madden *et al*., 1991
Raldh2	Activation/Repression	Norden *et al*., 2010
VEGF	Activation	Graham *et al*., 2006
GAL-4	Repression	Madden *et al*., 1993a
Bak	Activation	Morison *et al*., *2005*
JunB	Activation	Chen *et al*., 2010

1.1.6 The functional roles of *WT1*

1.1.6.1 *WT1* as a tumour suppressor gene

The failure of cellular mechanisms that normally control growth can result in the abnormal cell proliferation characteristic of cancer. WT1 is a zinc-finger transcription factor which regulates the expression of multiple growth factors such as colony stimulating factor (Harrington *et al*., 1993), insulin-like growth factor I (Sarfstein *et al*., 2006). Loss of WT1 inactivation leads to upregulation of these growth factors and the formation of WTs, leading to its original classification as a tumour suppressor (Little & Wells *et al*., 1997). WT1 appears to show lower levels of expression during

differentiation of the leukemic cell line K562 (Phelan *et al*., 1994). Also by antisense experiments the inactivation of *WT1* in K562 cells leads to reduced proliferation followed by apoptosis (Algar *et al*., 1996).

In addition to this, the ability of *WT1* to induce growth suppression *in vivo* in mice might support its role as a tumour suppressor. *In vitro* experiments indicated that ectopic expression of WT1 +KTS isoforms in murine M1 leukemic cells produced spontaneously monocytic differentiation. The WT1/+KTS expressing cells were inoculated into C.B-17 *scid/scid* mice. Tumours arising in these mice exhibited a loss of ectopic WT1 protein expression and M1 cells stably expressing WT1/+KTS isoforms exhibited a reduction in tumour formation (Fraizer *et al*., 2004; Smith *et al*., 2000).

1.1.6.2 *WT1* as an oncogene

Oncogenesis is an abnormal process of cell proliferation. Divergently from its initial characterization as a tumour suppressor gene, mounting evidence suggests that *WT1* can also act as an oncogene. It has been observed that disruption of *WT1* function has been implicated in the formation of many different tumour types. However it has been found that in ovarian cancer is currently reported that nuclear undisrupted WT1 protein is observed in most serous carcinomas and also 30% of endometrioid carcinomas (Mandore *et al*., 2010). Aberrant expression might be the mechanism by which suggested tumour suppressor gene (TSG) function of *WT1* is disrupted. In contrast, it has been found without mutations and overexpressed revealing putative role as an oncogene. Consistently with what happen with leukemia, in which mutations of the *WT1* gene are rare, an absence of *WT1* mutations in 98 different cancer samples of non hematopoietic origin were found (Oji *et al*., 2002, 2004). Since it is up-regulated in a variety of human cancers such as astrocytic tumours (Oji, 2004), breast cancer (Loeb, 2001), leukemia (Miwa, 2003) and many sporadic WTs (Ghanem, 2000; Grubb, 1994), which accounts for ~85% of all WTs, *WT1* cannot be classified as a TSG. Interestingly, using immunohistochemistry analysis of WT1 protein was frequently aberrantly present in the cytosol instead of the nucleus.

How *WT1* promotes oncogenic effects remains to be established, but genes that are key to the control of apoptosis have been highlighted as targets of WT1, including c-myc, Bcl2, Bcl2A1, Bak, and JunB (Han *et al*., 2004; Mayo *et al*., 1999; Morrison *et al*., 2005; Simpson *et al*., 2006; Kim *et al*., 2007; Green *et al*., 2009; Renshaw *et al*., 2004; Udtha *et al*., 2003). For example, exogenous expression of *WT1* in the human breast cancer cell lines, MDAMB-468 and MCF-7 and in human leukemic K562 cells can activate the *c-Myc* promoter and stimulate cellular proliferation.

The isoform +exon 5 WT1/+KTS has been associated with a strong anti-apoptotic response (Ito, 2006), given that an exon 5 *WT1*-specific siRNA induced apoptosis in three *WT1*-expressing leukemia cell lines, but not in *WT1*-non-expressing lymphoma cell line (Ito *et al*., 2006). Interestingly as it has been stated earlier, mice lacking this exon do not have a discernable abnormal phenotype which might suggest that exon 5 plays a role directly in disease processes rather than in development. In tumours its expression is highly abundant which suggesting a potential therapeutically target (Renshaw *et al*., 2004). *WT1* has been proposed as a prognosis marker in AML (Sakamoto 2009), breast cancer (Gupta *et al*., 2009) and endometrian ovarian cancer (EOC), is a putative gynecological biomarker that is differentially expressed among gynecological epithelia (Shimizu *et al*., 2000). Nuclear WT1 protein is present in tubal and ovarian epithelium (Shimizu *et al*., 2000). In contrast, *WT1* is not expressed in endometrial epithelium in the nucleus (Shimizu *et al*., 2000), therefore, *WT1* is been a potential biomarker candidate. In ovarian cancers, it is currently reported that nuclear WT1 protein is observed in the majority of serous carcinomas and also 30% of endometrioid carcinomas (Acs *et al*., 2004; Cathro *et al*., 2005; Waldstrom *et al*., 2005). However, it is unclear whether this is a reflection of the actual incidence of WT1 protein expression in these two histotypes, or whether *WT1*'s efficiency as a biomarker uncertain by the misclassification of progression of such serous carcinomas.

1.1.7 *WT1* in disease

1.1.7.1 Wilms' Tumour

WT also known as nephroblastoma is the commonest solid tumour in childhood (Bennington and Beckwith, 1975) affecting 1 in 10,000 children and accounting for approximately 6% of all paediatric cancers (Matsunaga *et al*., 1981). Wilms' tumours arise from aberrant differentiation of metanephric mesenchyme before age of 5. Current radio therapy treatment success is achieved in about 85% of cases were previously were uniformly lethal.

Most WTs are unilateral and most likely arise from sporadic in about 10-15% of WTs with inactivating mutations (Coppes *et al*., 1993a; Varnasi *et al*., 1994). Most of these mutations include nonsense and missense changes. Sporadic mutations may correspond to an early event in the etiology of WT, and such have been found in nephrogenic rests (Park *et al*., 1993). Nephrogenic rests appear to be precursor lesions that originate from the blastema in the developing kidney and may progress to WT (Beckwith *et al*., 1990). A multi step model of WT genesis has been proposed by Charles and *et al*., (1998). WT is believed to begin from a single cell progenitor already transformed within a pluripotent cell population which undergoes aberrant differentiation. About 10% of sporadic WTs express elevated levels of an in frame deletion of exon 2, they may alter the transactivational function of the encoded protein (Haber *et al*., 1993b). In most of the cases of sporadic WTs the *WT1* gene is not mutated but *WT1* is still expressed at high levels. Such tumours may have alterations in downstream targets of *WT1* or result from genetic or epigenetic alterations in other cellular pathways upstream to produce over expression. In a minority of WTs, *WT1* is truncated in the DNA-binding domain. In 70% of cases the wild-type allele was lost, proving that this *WT1* can act as a recessive tumour suppressor gene. Although most cases are spontaneous, small number are associated with hereditary predisposition such as familial WT, BWS, Denys-Drash syndrome (DDS), WAGR and also Fraiser Syndrome (FS) (see Table 1.2) which will be briefly

described next (Beckwith *et al*., 1969; Francke *et al*., 1979; Pelletier *et al*., 1991b; Weidemann *et al*., 1964).

1.1.7.2 Human syndromes associated with Wilms Tumour

A group of syndromes which involve *WT1* are found to present a set of related features, including urogenital abnormalities and WT predisposition (Table 1.2), some of them will be described next.

1.1.7.2.1 WAGR syndrome

WAGR syndrome comprises sporadic aniridia (lack of an iris), genitourinary malformation, mental retardation and a high risk of developing WT (Francke *et al*., 1979). Karyotype analysis detects deletions encompassing band 11p 13 in pediatric patients. This chromosomal deletion includes *WT1* and also a gene involved in aniridia *PAX-6*. *WT1* acts recessively and therefore requires a second mutation described as the Knudson double hit hypothesis model (Knudson, 1971). The increased incidence of WT in WAGR is due to any somatic *WT1* mutation in kidney being a 2nd hit, therefore WT in WAGR is an example of the role of *WT1* as a TSG. In contrast loss of only one allele *PAX-6* is necessary to result in aniridia.

1.1.7.2.2 Denys-Drash syndrome

DDS is an infrequent syndrome in children, which is characterized by nephropathy, genital abnormalities and a predisposition to WT (Denys 1967; Drash, 1970) also characterized by a focal or diffuse mesanglial sclerosis. Nephropathy generally occurs during the first couple of years and progresses to renal failure due to nephrotic syndrome by the 4th year, which results in increasing proteinurea. Cases have been reported where children do not exhibit the full spectrum of pathological feature. These patients can have a normal karyotype and generally have normal developments of genitals. In contrast patients may have external abnormalities while presenting an XY karyotype where phenotype includes ambiguous genitalia and male pseudohermaphroditism (Little *et al*., 1994; Mueller, 1994; Pelletier *et al*., 1991a).

The vast majority (90%) of patients with DDS carry constitutional mutation in the *WT1* gene, most of which are located in exons 8 and 9, (Baird *et al*., 1992). Mutations are dominant, as patients are frequently heterozygous for *WT1* mutation. In contrast to WAGR, most individuals with classic DDS harbours missense mutations. These are located in the zinc finger DNA binding region (Little *et al*., 1995; Roger-Pokora *et al*., 2004) affect the DNA binding capability of WT1. There is a clear contrast between DDS and WAGR, although both display a broad variability in the severity of their genital abnormalities, in DDS the presence of mutated *WT1* leads to a more severe effect on genitourinary development and a less dramatic effect when only one allele is lost. In addition to these differences, WAGR patients do not get renal failure as a consequence of mesangial sclerosis whereas DDS patients do.

1.1.7.2.3 Frasier syndrome

The current diagnosis of Frasier syndrome is usually is based on the association of male pseudohermaphroditism (gonadal dysgenesis), with steroid-resistant nephritic syndrome due to glomerular sclerosis, which progresses to end-stage renal failure during adolescence or adulthood. Frasier *et al*., (1964) described a syndrome that associates nephrotic syndrome (due to focal and segmental glomerular sclerosis) with pseudo hermaphroditism (as a result of XY gonadal dysgenesis). One of the differences between this and DDS is that renal failure becomes present during adolescence or older and gonadoblastoma and more frequent than WT (Barbaux *et al*., 1997). In FS mutations in intron 9 affect the expression of WT1–KTS from one allele (Bruenin *et al*., 1992) which modifies the normal WT1 + and – KTS ratio.

1.1.7.2.4 Beckwith-Weidemann syndrome

Beckwith-Weidemann syndrome (BWS) occurs with a frequency of 1 in 13,700 births and is characterized by growth abnormalities, particularly unbilical hernia, macroglosia and gigantism with hemihypertrophy and also in association with neonatal hypoglycaemia, typically ear creases and pits. This condition also predisposes to developmental cancer including adenocortcal carninoma, hepatoblatoma, rhabdomyosarcoma and most often, WT (Beckwith, 1983). The

localization of BWS to 11p15 follows linkage analysis and association of BWS with chromosomal abnormalities. Furthermore, evidence for genomic imprinting in this region is given by loss of heterozygosity in WTs always occurring on the maternal allele (Schrieder *et al*., 1987, Williams *et al*., 1989). However, there are several imprinted genes such as *H19*, *L1T1* and *p57*, which may also play a crucial role on this syndrome (Brown *et* al., 1996; Ward, 1997).

Table 1.2 Comparative of WT related syndromes.

Syndrome	Abnormalities	Germ line associated
Beckwith-Weidemann	WT, Organomegaly, hypoglycemia, umbilical hernia, predisposition to adrenal cortex carcinoma, hepatoblastoma,	Genetic lesion unclear, ncRNAs *H19* and *KvLQT1* with loss of imprinting may be involved
Denys Drash	WT, genitourinary defects, diffuse mesangial sclerosis	Heterozygous missense mutations in *Wt1*
Fraiser	Low risk of WTs, genitourinary defects, focal segmental glomerular sclerosis, ambiguous genitalia,	Heterozygous point mutation at the donor splice of intron 9 KTS in WT1: >50% WT1 +KTS
WAGR	WT, aniridia, genitourinary defects, mental retardation	Heterozygous deletion chromosome 11p13

Adapted from Bong-Lee *et al*., (2001).

1.1.8 *WT1* in development

The *WT1* gene is important not only in cell proliferation or cancer but also in cell differentiation, in developmental morphogenesis and in subsequent physiological organ maintenance (Hastie, 1994). Indeed it expression pattern suggested for the normal development and homeostasis of several organs and tissues through the modulation of proliferation and differentiation in a cell-specific manner (reviewed by Dizcensa 2005; Scholz and Kirschner 2005). WT1 protein products act as transcriptional and post-transcriptional regulators and in consequence it shows fundamental roles in nephrogenesis, haematopoiesis, cardiogenesis and sex determination (Scharnhorst *et al*., 2001; Roberts 2005).

In varied cell organogenic contexts *WT1* expression pattern indicates that the function of the gene can have either negative or positive effect on proliferation and/or differentiation. *Wt1* KO mouse proved to be essential for the normal development of kidney. Also in the urogenital system as gonads (Kreidberg *et al*., 1993), but also other mesothelium-derived organs such as epicardium, spleen (Herzer *et al*., 1999), adrenal glands (Moore *et al*., 1999), as well as in olfactory system (Wagner *et al*., 2005) and neuronal tissues specifically retinal ganglia (Wagner *et al*., 2002). However, *WT1* function in the kidney has received the most attention because of its functional role in development.

1.1.8.1 Kidney Morphogenesis and function

In Mammals and birds kidney development is characterized by induction of a mesenchymal to epithelial transition where three different systems are formed at different developmental stages. The earliest is the pronephros, with excretory function in larval stages in amphibians and fish and with unknown function in higher vertebrates. The next is the mesonephros (the excretory gland of the mammalian embryo), and the last metanephros (which becomes the permanent kidney). These correspond to three main different developmental stages, the first two stages: onset of nephrogenesis and the progression of nephrogenesis are both transitory, and the third establishment and the maintenance of normal podocyte function, which persists as a

functional kidney (Saxen and Sariola, 1987) (Figure 1.2). The kidney is formed through the reciprocal interaction of the *WT1* expressing metanephric mesenchyme and a caudal outgrowth from the Wollfian duct (called the ureteric bud) during epithelization (Figure 1.2).

At mouse E11, human E34–E35 is possible to find *WT1* expression but at very low level in uninduced metanephric mesenchyme. However at E35-36 in humans; E10.5-11.5 in mice, the ureteric bud arises and invades the intermediate mesoderm. In the beginning the Wolffian duct and the metanephric mesenchyme (which are derived from intermediate mesoderm) are involved in a restricted regulated manner at E11.5 in the mouse (E36-37 in humans). Then the mesenchymal cells condense and form the blastema around the uteric bud to from caps that undergo mesenchymal-epitelial transition (Figure 1.2, 2). The blastema then develops into the renal vesicle (Figure 1.2, 3) and matures further via comma and S-shaped bodies into epithelial cells that form the proximal tubules, distal tubules and the glomerulous of the nephron. *WT1* expression is low in the developing blastema and increases in the structures known as the comma- and S-shaped bodies (Figure 1.2, 4-5).

In mammals, the pronephric tubules and the anterior portion of the pronephric duct degenerate, but the more caudal portions of the pronephric duct persist and serve as the central component of the excretory system. Following differentiation, *WT1* expression is generally downregulated, and restricted to the podocytes which form the filtration barrier within the mature glomerulous where *WT1* expression will persist during adulthood. Three genes known to be directly controlled by *WT1* in the podocyte include *podocalyxin* (Palmer *et al*., 2001), *nephrin* (Wagner, 2004), and *Pax-2* (Ryan *et al*., 1995).

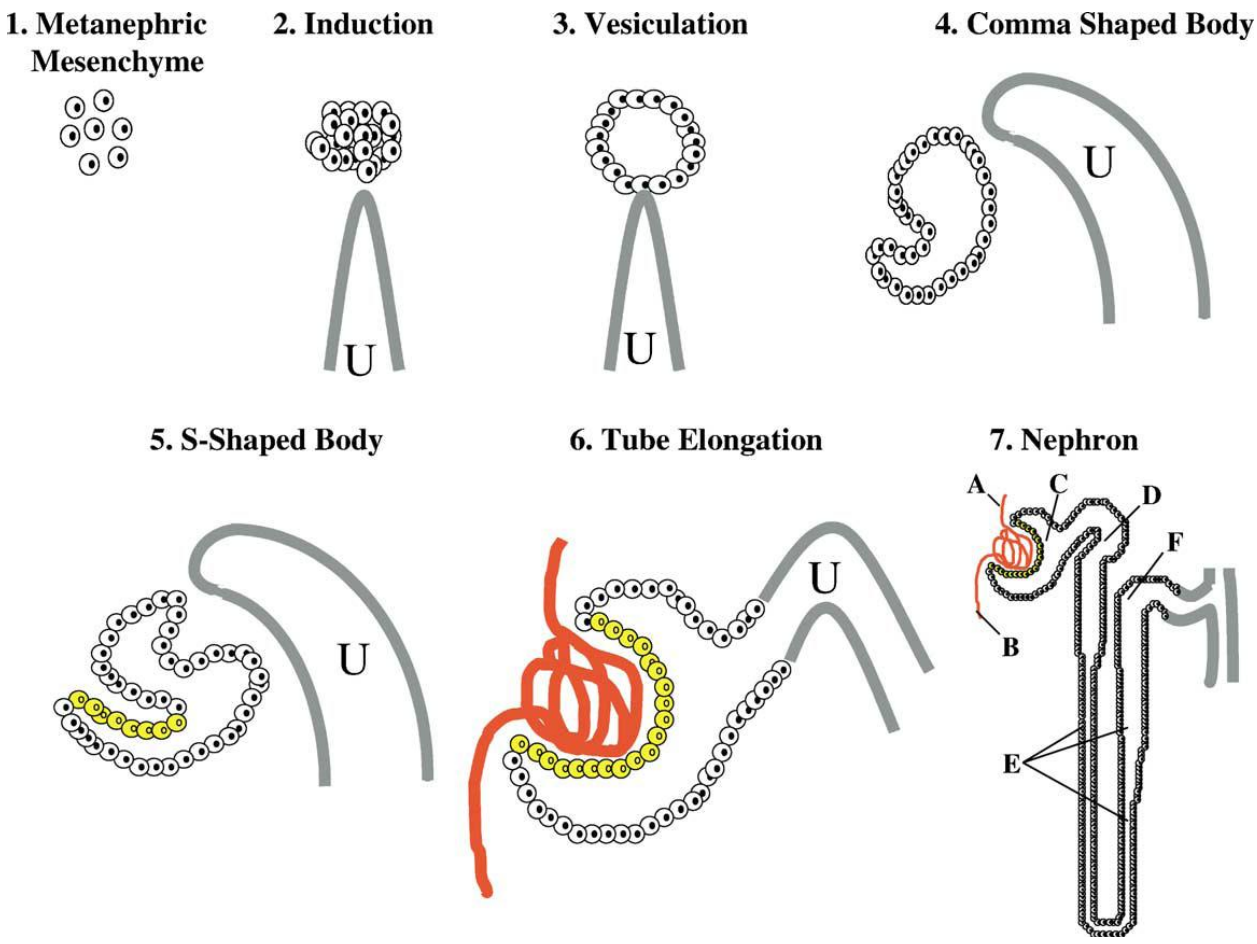

Figure 1.2 Diagram representing neprhogenesis. Nephrogenic development (1-6) and develped nephron structure (7). A, vas afferens; B, vas efferens; C, Bowman's capsule or glomerulous; D, proximal tubule; E, Loop of Henle; F distal tubule; U ureteric bud. Yellow cells are developing podocytes. This figure was reproduced with permission of the author (Menke ad Schedl, 2003).

The glomerulous is responsible for blood filtration in the kidney. It consists of four different cell types: endothelial cells, supporting mesangial cells, and epithelial cells of the Bowman's capsule (Figure. 1.2, 7-C). Coordinated cross-talk between these cells is required for the normal development and maintenance of the filtration barrier. The glomerulous is made by arrays of capillaries in a looped shape sustained by mesangial cells. While blood plasma is filtered through the glomerular capillary, the local intracapillary pressures plasma to pass through the glomeruli filtration barrier, which consists of three components displayed in layers: the glomerular endothelial cells, the basement membrane and the podocyte (Figure 1.3). The glomerular endothelial cells are flattened cells that regulate homeostasis and vasomotor tone

(Ballermann *et al*., 2005), and also divides the blood and tissue compartments. At this point filtration is not considerably highly permeable to water and small solutes. The endothelium completely covers the basement membrane. This second layer is a dense cluster of extracellular matrix components which provide local high blood pressure for the capillary wall. The recent finding of proteins critical for permeability highlight the podocytes as the ideally specialized to perform the main filtration barrier (Zenker *et al*., 2004) and interestingly is where *WT1* is highly expressed during life time in mouse and human as well as other vertebrates.

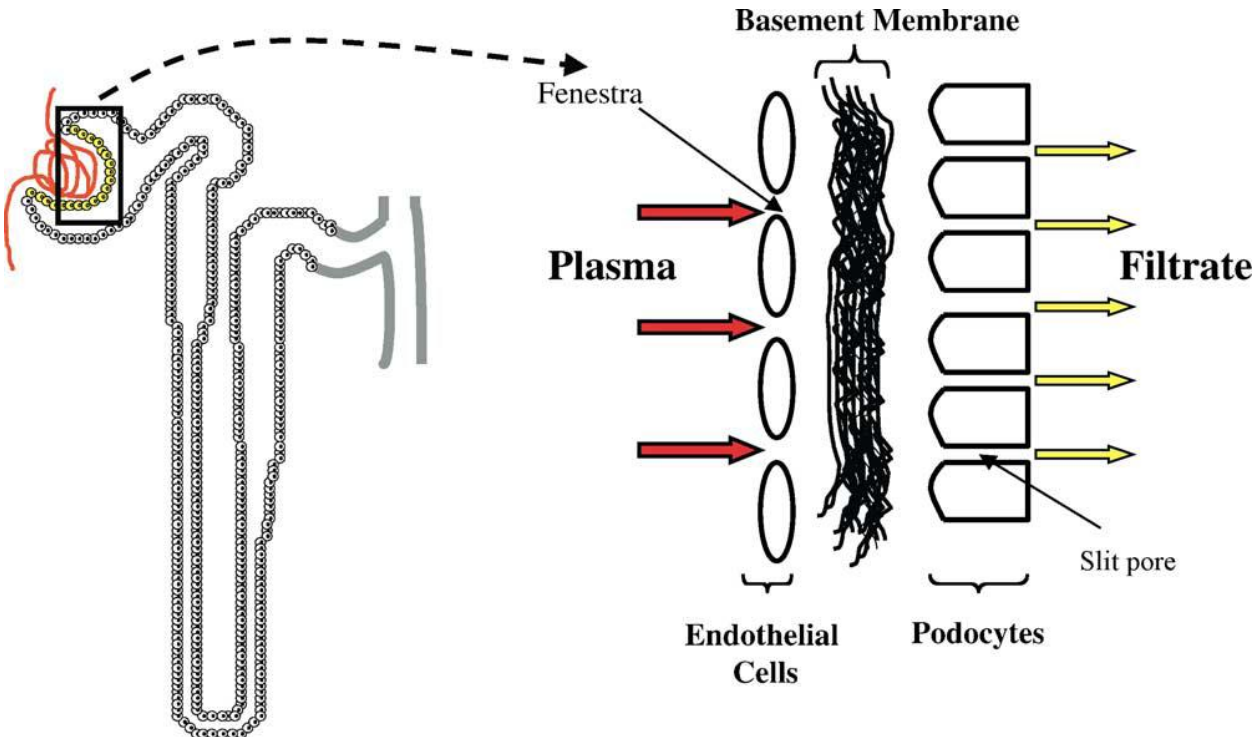

Figure 1.3 Schematic structure of the glomerular filtration barrier. On the left side Bowman's capsule shown in square. On the right plasma fluid through endothelial cells (red arrows) followed by basement membrane and ends up in the podocyte barrier (yellow arrows). This figure was reproduced with permission of the author. Original source: Menke and Schedl (2002).

1.1.8.2 *WT1* in gonad development and sex determination

Typical defects of aberrant reproductive system development and impaired masculinisation are well defined for WAGR, Denys Drash syndrome (DDS), and FS as urogenital abnormalities associated with mutations in *WT1* (reviewed by Scharnhorst *et al*., 2001). Also it has been shown using $Wt1^{-/-}$ mice, that a thickening of the epithelium rises toward the gonad primordium at embryonic stage day 11 but that gonad development fails to progress further, and is followed by apoptosis. Further WT1/–KTS was shown to be required for the survival and proliferation of biopotential gonadal cells. In knock-out mice with lacking only the WT1/–KTS isoform gonads begin to regress by embryonic day 12.5 (Hammes *et al*., 2001; Kreidberg *et al*., 1993).

A second role for *WT1* during gonad formation occurs at the level of sex determination. In mammals during the early development the gonadal system has potential to develop either into testes or ovaries independently of external ambient factors. The fact that *WT1* is already expressed within the undifferentiated gonad and lacking of WT1/ +KTS isoforms in gonads specifically exhibit male-to female sex reversal indicate a role for *WT1* in sex determination (Hammes *et al*., 2001). Other factors are involved, including as the product of the steroidogenetic factor 1 (*Sf1*) gene, and the Lim homoebox protein LHX-9. Expression of *Sry* is important for the activation of the male differentiation pathway. *In vitro* experiments suggested that *WT1* is responsible for transcriptional activation of *Sry* (Berta *et al*., 1990). As expected, only the "DNA binding" variant WT1/–KTS can transactivate this gene, since the WT1/+KTS isoforms showed no effect in cotransfection assays (Hossain and Saunders, 2001). Expression of *Sf1* and expression of *WT1* in the gonad begin at roughly the same time and might be dependent. Indeed, Wilhelm and Englert (2002) demonstrated that *WT1*, and more specifically both isoforms (Hammes, 2002) can activate the *Sf1* promoter *in vitro* and *in vivo*. The programmed cell death phenotype in *Wt1*-knockout mice can be explained by a lack of *Sf1* expression.

WT1 expression in Sertoli cells in testes and in granulose cells in ovaries, uterus, oviduct and endometrium in adulthood could indicate a third role of *WT1* in the

maintenance of cellular functions in these reproductive cell types (Hsu *et al*., 1995; Pelletier *et al*., 1991a; Pritchard-Jones *et al*., 1990). Using a tissue specific RNA interference technique in Sertoli cells it shows that *Wt1* expression in the germ cells have an anti-apoptotic role proving *WT1* to be essential for survival and maturation of sperm (Rao *et al*., 2006).

1.1.8.3 Hematopoiesis

WT1 expression has been detected in foetal spleen, liver and thymus in which the development of blood cells takes place during gestation (Junqueira and Carneiro, 1995). In addition, *WT1* is transcribed in bone marrow, lymph nodes and peripheral blood throughout life suggesting that *WT1* is involved in erythroid myeloid and lymphoid cell formation and also its maintenance (Fraizer *et al*., 1995; Menke *et al*., 1998). *Wt1* expression is mainly found in earlier stages but not in mature blood cells suggesting its involvement in hematopoiesis. A *Wt1* knockout mouse model was employed to elucidate the role of *Wt1* in haematopoiesis, finding that cells lacking *WT1* were deficient in hematopoietic stem cell function making only minimal contribution to the hematopoietic system.

Alberta *et al.,* (2003) observed a reduction 75% in erythroid blast-forming unit, erythroid colony-forming unit and colony-forming unit-granulocyte macrophage-erythroid-megakaryocyte. It was found that embryonic stem cells lacking *Wt1* failed to contribute effectively to the developing haematopoietic system in chimeric embryos in a competitive situation, providing evidence a role for *Wt1* in differentiating haematopoietic cells (Alberta *et al*., 2003). Furthermore, induced expression of *Wt1* by retroviral infection activated myelomonocytic differentiation of CD34 human hematopoietic progenitors and dominance of a subset of immature CD38/CD34 cells (Ellisen *et al*., 2001). In mouse, expression of *Wt1* also resulted in an enhanced differentiation, 32D cl3 cells, were differentiated in response to granulocyte colony stimulating factor (G-CSF) (Loeb *et al*., 2003).

The proposed role of *Wt1* in murine hematopoiesis was challenged by King-Underwood *et al*., (2005), who stated that *Wt1* is not required for hematopoiesis given that (in experiments similar to results those shown by Alberta *et al*., 2003) *Wt1*-null murine fetal liver cells are capable of reconstituting hematopoiesis following transplantation into irradiated recipients. Also they could not establish any difference in *in vitro* colony-forming ability of wild-type and *Wt1*-null cells. In a transgenic mouse system, *WT1* was detectable in adult bone marrow, but undetectable in subsets of different hematopoietic cells, finding no differences between the clonogenic potential of hematopoietic progenitor cells from the aorta-gonad-mesonephros between wild-type and *Wt1*-null. King-Underwood *et al*., (2005), conclude that *Wt1* is not essential for hematopoiesis in the mouse.

Even though the primary role of *Wt1* in the murine remains to be resolved, worthwhile evidence of the function of *Wt1* during hematopoiesis can be elucidate from its downstream target genes from hematopoietic precursor cells.

1.1.9 The mouse as a model in comparative physiology

Due to data obtained by exhaustive research in human and mouse genomes it is possible to elucidate their similitude. The mouse genome mouse is 2.5 Gb long only ~14% smaller than the human genome (Waterston *et al*., 2002). Among the 30,000 protein-coding genes 80% of mouse genes, can be identified that have human orthologue, and less than 1% appear to be truly unique (Mouse sequencing consortium, 2002). Shared regions of synteny (e.g. *WT1* gene in human chromosome 11, and in mouse chromosome 2) have been conserved regardless of over 75 million years of evolutionary divergence (Nei *et al*., 2001). According to the mouse sequencing consortium (FANTOM3), 1,022 human genes are involved in disease and 807 of these are also present in the mouse. There is still much to be done to clarify the physiological role of each of these. Functional genomics is still an emerging field that, due to the vast amount of candidates still to be functionally defined *in vivo*. In the mouse, only about one third of the genes have been studied at some level. The number of homologous genes suggests a transdisciplinary effort including different areas in biology and medicine.

1.1.9.1 Mouse models with *WT1*-targeted mutation

Biomolecular and biochemical studies of the *WT1* gene have contributed enormously to the understanding of transcriptional or post-transcritional roles. All this work gave very relevant information of how WT1 isoforms interact how they may function within the cell. Nevertheless, understanding the role of *WT1* in organogenesis must take in account of interactions between a multiplicity of cell types and tissues. *WT1* related mouse models allow us to study in detail the role this gene plays in normal and abnormal development that would be impossible to gauge from cell culture system alone. Gene modification in the mouse can result in measurable changes in morphogenetic and physiological properties that can be attributed to *WT1*. In this way mouse models with modified *WT1* expression have confirmed unequivocally that *WT1* plays a central role in kidney development and maintenance.

However, it should be considered that in the mouse model, kidneys are significantly smaller and their life-span shorter than the cell population in human kidneys. Also, human kidney development occurs over a period of 31 weeks compared with mice 21 days in mice, during which there might be significantly fewer post zygotic mutations resulting in less probability of oncogenesis occurring. Besides, while in human more than one tumour-related genes reside on the same chromosome (11p13 and 11p15), in mice these two loci are on different chromosomes (2 and 7). Consequently, in humans heterozygosity can be achieved for both of these loci with a single hit, whereas in the mouse analogous events must involve independent chromosomes. Moreover, differences in urogenital systems between mammals and the rest in the animal kingdom (e.g. fish) suggests it must be difficult to make final conclusions using model organisms if the final interest is to better understand *WT1* molecular biology in development and disease in humans.

1.1.9.1.1 The *Wt1* null mouse

One of the key findings to confirm *WT1* as a central gene in kidney development was phenotype of *Wt1*$^{-/-}$ knock-out mice in which lethality happened by E12 (Herzer *et al*., 1999; Kreidberg *et al*., 1993). In the Kreidberg knockout mouse model a replacement-type targeting vector with a deletion of *Wt1* exon 1 and 0.5 kb of upstream sequence was used to knockout Wt1. The most prominent finding was the lack of kidneys and gonads in the mutant embryos. Further defects were observed in diaphragm, peritoneum, epicardium, and tissues derived from mesothelium as well as in heart, adrenal glands (Moore *et al*., 1999; Kreidberg *et al*, 1993), and spleen (Herzer *et al*., 1999), olfactory system (Wagner *et al*., 2005) and neuronal tissues, specifically retinal ganglia (Wagner *et al*., 2002).

In mutant mice, the kidney development was arrested after establishment of the metanephric blastema from intermediate mesoderm. Blastemal cells were present initially but then soon after underwent apoptosis with embryos becoming oedematous after E12 and then reabsorbed between E13 and E15. Metaneprhic mesenchyme that undergoes apoptosis never manages to reach the ureteric bud and is unable to be formed, which might suggest upregulation of apoptosis-inducing genes (Kreidberg *et al*., 1993). On further analyses it was found that *WT1*$^{-/-}$ mesenchyme had a different histological appearance and also showed the presence of Pax-2 mRNA but not protein, suggesting that Pax-2 may be regulated by *WT1* at a post-transcriptional stage. Other mouse models with increased mesenchymal apoptosis include *Bmp7*$^{-/-}$ (Luo *et al*., 1995) and *Sall1*$^{-/-}$(Nishinakamura *et al*., 2001) knockouts. However, only the *WT1*$^{-/-}$ model also presented gonadogenesis, a reduced and shapeless thorax with discontinuities in the diaphragm, and small heart and lungs.

In contrast, the heterozygous *WT1*$^{+/-}$ mice survived into adulthood and initially no abnormal phenotype was detected. Later studies back crossing the Kreidberg mouse model into mixed genetic background revealed that after 400 days post-gestation 40% of the mice had died and this was associated with a predisposition to glomerulosclerosis (Menke *et al*., 2003).

In homozygote *Wt1* mouse during gonadal development displayed phenotypes similar to those found in DDS (Pelletier *et al*., 1991a). When the mutant mesenchyme was examined for the expression of genetic markers for early mesenchyme differentiation, *Pax-2*, *Six2*, and glial cell line derived neurotrophic factor (GDNF) mRNAs were detected at a level comparable to those in wild-type mice. Unlike individuals with the WAGR syndrome, which retain only one functional copy of the *WT1* gene, mice heterozygous for a functional *Wt1* allele revealed no predisposition for WT tumourgenesis. This is also true of *Sey*^{Dey} mice (to be discussed in Section 1.1.9.1.5), which are heterozygous for a large deletion in the *Wt1*-aniridia region (Glaser *et al*., 1990) and might reflect a distinct initial genetic predisposition in mice and humans or distinctive mechanisms for preventing carcinogenesis.

1.1.9.1.2 Denys-Drash mouse models *Wt1*^{tmT396} and *Wt1*^{R394W}

To make a the DDS mouse model, the DDS mutation named *Wt1*^{tmT396} truncates zinc finger 3 at the codon 396 which was been introduced into embryonic stem (ES) cells, (Patek *et al*., 1999). Targeted ES cells produce wild-type and mutant transcripts of the *Wt1* gene in equal amounts, but analysis of the protein products revealed that the mutant protein was only 5% of the total Wt1 protein produced. As a consequence of this truncation mesangial sclerosis in adult heterozygote mice was observed as well as male genital defects resembling what it occur in human DDS. Also there was one case of WT implying a potential link between *WT1* malfunction and WTs. However, in this mouse model the mutant allele did not affect the glomerular lineage in early nephrogenesis (Patek *et al*., 1999). This shows two things: First, by some mechanism expression from the mutant allele is compensated. Second, a very small proportion of mutated Wt1 protein can produce a dramatic disruption in the genitourinary system. However, a very few mutant animals were analysed in this initial report (Patek et al., 1997).

On a subsequent attempt by Patek *et al*., (2008) to generate heterozygotes *Wt1*$^{tmT396/+}$ which where back crossed with the MF1-N2 strain mice with no abnormal phenotype were obtained, male and female heterozygotes were fertile. Sporadic proteinuria and glomerulosclerosis was observed but predisposition to WT or male pseudohermaphroditism did not occur. So the authors conclude that effects initially observed on kidney disease and fertility were genetic background-dependent, or possibly the inheritance might be subject of imprinting (parent-of-origin effect), or stochastic effects might prevent to set up disease. Initial observation was probably due to *WT1*-independant alterations in the knockout ES cells used to generate these mice.

A more recent mouse knockout was made with the most frequent mutation observed in DDS patients that substitutes a tryptophan for an arginine aa 394 affecting the DNA-binding domain in *WT1* (Gao *et al*., 2004). The heterozygous mice did not show gonadal dysgenesis or male pseudohermaphrotitism, nevertheless mice had proteinurea as a consequence of diffuse mesangial sclerosis. WT1 protein levels were decreased by 20% from wild type controls. Electron microscopy showed an abnormally thickening of the glomeruli, however, no difference in the number of cells were observed, corroborating that mesangial proliferation is not how *WT1* mutation leads to glomerulosclerosis. Although mechanisms of how this mutation start the process of disease is still unknown, this study suggest it could involve some deregulations of *WT1* downstream target genes.

1.1.9.1.3 Fraiser Syndrome mouse model

As mentioned in Section 1.1.2.1, FS is characterized by splicing defects resulting in an inability to express from one allele the WT1/+KTS isoform, suggesting that there is an important equilibrium maintained between the different isoforms in normal renal and testicular development. Based on previous *in vitro* evidence distinct functions for

WT1 +/– KTS isoforms were suggested. Genetically modified mice were generated which express either the WT1/+KTS wt1 isoform or only the WT1/-KTS Wt1 isoform (FS) (Hammes *et al*., 2001). Homozygote Fraiser mice die at birth due to kidney defects specifically affecting the glomerular podocyte layer and also have defects in male sex determination. WT1/+KTS mice are more severely affected and have hypodysplastic kidneys and streak gonads. Clearly, both isoforms are necessary for correct development, although the appearance of normal adrenal glands and spleen in both models indicates that there is some functional redundancy between the two isoforms, perhaps because WT1/+KTS isoforms are more critical for kidney and testis development than spleen. Nevertheless, the authors could consider re-examine if there is any differential expression earlier in development at the Wolffian duct which gives rise to both kidneys and gonads.

1.1.9.1.4 *Wt1* targeted mice with disruption and CUG-initiated translation

To elucidate the role of the mammal specific exon 5 *in vivo* the mammal specific features of embryonic implantation and lactation, were analyzed in mice in lacking Wt1 +exon 5. Mice were generated by gene targeting in a two-step approach to delete exon 5 without disrupting Wt1 isoforms (Natoli *et al.*, 2002a). These mice apparently were able to develop, grow and breed normally, without a discernable abnormal phenotype, indicating that exon 5 is not required in lactation, or embryonic implantation. WT1/+exon5 isoforms have also been studied in DDS WT1/+exon5 transgene experiments (Natoli *et al*., 2002b). These results showed that WT1 isoforms lacking exon 5 have a greater role in directing podocyte differentiation. Normal urogenital development occurs in the absence of the mammalian specific exon 5 and the CUG-initiated translation isoforms, but this redundancy in mice may not be reflected in humans due to evolution of mammalian-specific features.

1.1.9.1.5 The Dickie small-eye (*Sey*) mouse

The Harwell Dickie's small eye (*Sey*) deletion in mouse is another type of Wt1 knockout model highly comparable to cytogenetic deletions identified at human 11p 13 in children with WAGR syndrome and Peter's anomaly which is characterized by defects in the cornea (Glaser *et al*., 1990). The *Sey* mouse model has a semi-dominant mutation that is phenotypically consistent with aniridia, but none of the other abnormalities typically found in human WAGR. The Dickie small-eye (Sey^{Dey}) allele in mice is an interstitial deletion on chromosome 2 encompassing the *Wt1, Rcn* and *Pax-6* genes (Glaser *et al*., 1990). The *Rcn* gene encodes retiuculocalbin, which is a Ca^{2+} -binding protein expressed in the lumen of the endoplasmic reticulum. In both heterozygote and homozygous renal neoplasms were absent and kidneys, gonads and mesothelium appeared to be morphologically normal.

1.1.9.1.6 *WT1*:Trp53 compound mice

The interaction of different genes through development can be studied by crossing of mutant mice to create double knockout compound mutant mice. P53 and WT1 have a reciprocal effect on their own functions (Maheswaran *et al*., 1998,), both can induce apoptosis (Menke *et al*., 1997). Therefore, to corroborate if WT1 interacts *in vivo* with p53, mice harboring $Wt1^{+/-}$ and $p53^{+/-}$ mutation interbred. The only new phenotype, other than inherited glomeruloesclerosis that what was previously reported for $wt1^{+/-}$ mice, was earlier onset of lymphoma, the most prevalent tumour associated with $Trp53^{+/-}$ mice.

1.1.9.1.7 *Wt1*:*Pax-2* compound mice

Both *WT1* and *Pax-2* are expressed during kidney organogenesis suggesting the possibility of a regulatory interaction between them. Mouse embryos containing targeted heterozygous disruptions and/or sporadic mutations for *Pax-2* (Favor *et al*., 1996) as well as transgenic mice with overexpression showed structural defects and impaired kidney function (Dressler *et al*., 1993). Both mouse models exhibit structural defects producing an abnormal renal function in adulthood.

Characterization of *Wt1*$^{+/-}$:*Pax2*$^{1Neu/-}$ offspring revealed that kidneys were 50% smaller than in wild-type controls and 20% smaller than the *Pax2*$^{1Neu/+}$ kidneys (Discenza *et al*., 2003). Kidneys in compound mutant animal had an abnormal the renal medulla, and reduced development of the calyces and renal pelvis. In heterozygote renal cortex development was comparable with that of *Pax2*$^{1Neu/-}$ cortex. The authors conclude that *wt1* is a modifier of *Pax-2*. On subsequent review Discenza and Pelletier (2004) conclude haploinsufficiency, as a result diminution of total protein to enable heterodimeration on these two proteins.

1.2 Non-protein-coding RNA

In multicellular organisms diverse phenotypic variation makes it possible to differentiate and classify phyla through an evolutionary line. Nevertheless, only ~1.2% of the human genome is translated to protein (Venter *et al*., 2001) a feature that is similar across the vertebrates and indeed all metazoa, making this genomic feature uninformative for discriminating between major groups of organisms despite remarkable differences in developmental complexity (Figure 1.4 B). On the other hand, sequencing projects have found that the number of protein-coding genes and the extent of their sequences remain relatively static. In concordance with this, annotations show that the nematode worm *Caenorhabditis elegans*, containing only ~1,000 cells, has ~20,000 protein-coding genes (Stein *et al*., 2003), roughly the same number as human (Goodstadt and Ponting, 2006) which has ~100 trillion cells in precisely formed tissues, including ~100 billion neurons with an estimated 1014 synaptic connections in the neocortex (Andersen *et al*., 2003). In contrast the number of intronic, and intergenic sequences does appear to correlate with developmental complexity, increasing remarkably along the phylogenetic scale. This suggests that these sequences may contain elaborate regulatory information (Figure 1.4 A), although the biological relevance of the non-coding sequence is stills a matter of debate (Dennis 2002; Brosius, 2005; Struhl, 2007; Pauler *et al*., 2007).

Recently it has become clear that the majority of the eukaryotic genome is transcribed in a developmentally regulated manner to produce a large class of RNAs with little or

no protein-coding potential RNAs (ncRNAs); (Carninci *et al*., 2005; Cheng *et al*., 2005; Kaprankov *et al*., 2007b; Mattick and Makunin, 2006), that are often rapidly degraded (Yazgan and Krebs, 2007). Dissecting the mouse genome the RIKEN Mouse Gene Encyclopedia project used cell lines and tissues to create a full-length cDNA library of 5'-capped and 3'-poly(A) tailed RNAs with many putative RNAs without open read frames were identified (Hayashizaki *et al*., 2003). In 2005 the FANTOM3 genome sequencing consortium annotated 103,000 cDNA sequences that were classified as non-coding RNA. Sequencing of a large set of these cDNA by the FANTOM3 consortium, found that 47% had absent open reading frame (ORFs) so were classified as putative ncRNAs (Carninci *et al*., 2005; Katayama *et al*., 2005).

To evaluate whether ncRNAs have a functional role a study was undertaken by Ravasi *et al*., (2006). Using a combination of RT-PCR, microarrays and Northern hybridization it was shown that ncRNAs are expressed in a tissue-specific manner suggesting they have biological function. The FANTOM3 Consortium, 2005 found that the extent of ncRNA length does not change across metazoan species, in spite of large differences in developmental complexity (Taft *et al*., 2007). Often, many transcripts are expressed from a single locus. Analysis of expressed sequence tags (EST) has indicated that an average of 5.6 different transcripts are produced from each locus, with protein coding RNAs often capable of producing two or more variants, as we could see in Section 1.1.2.1 for *WT1* locus. According to the ENCODE consortium 90% of the mammalian genome is estimated to be actively transcribed (Birney *et al*., 2007). Due to the frequent occurrence of this ncRNAs in species with higher developmental complexity therefore is proposed to be strictly regulated during developmentally manner (Mattick, 1994, 2001).

Recent growing evidence suggests that ncRNA transcripts are functional, particularly in the regulation of epigenetic processes, leading to the hypothesis that there exists a hitherto hidden layer of genomic programming in humans and other multicellular organisms (Dallosso *et al* 2007).

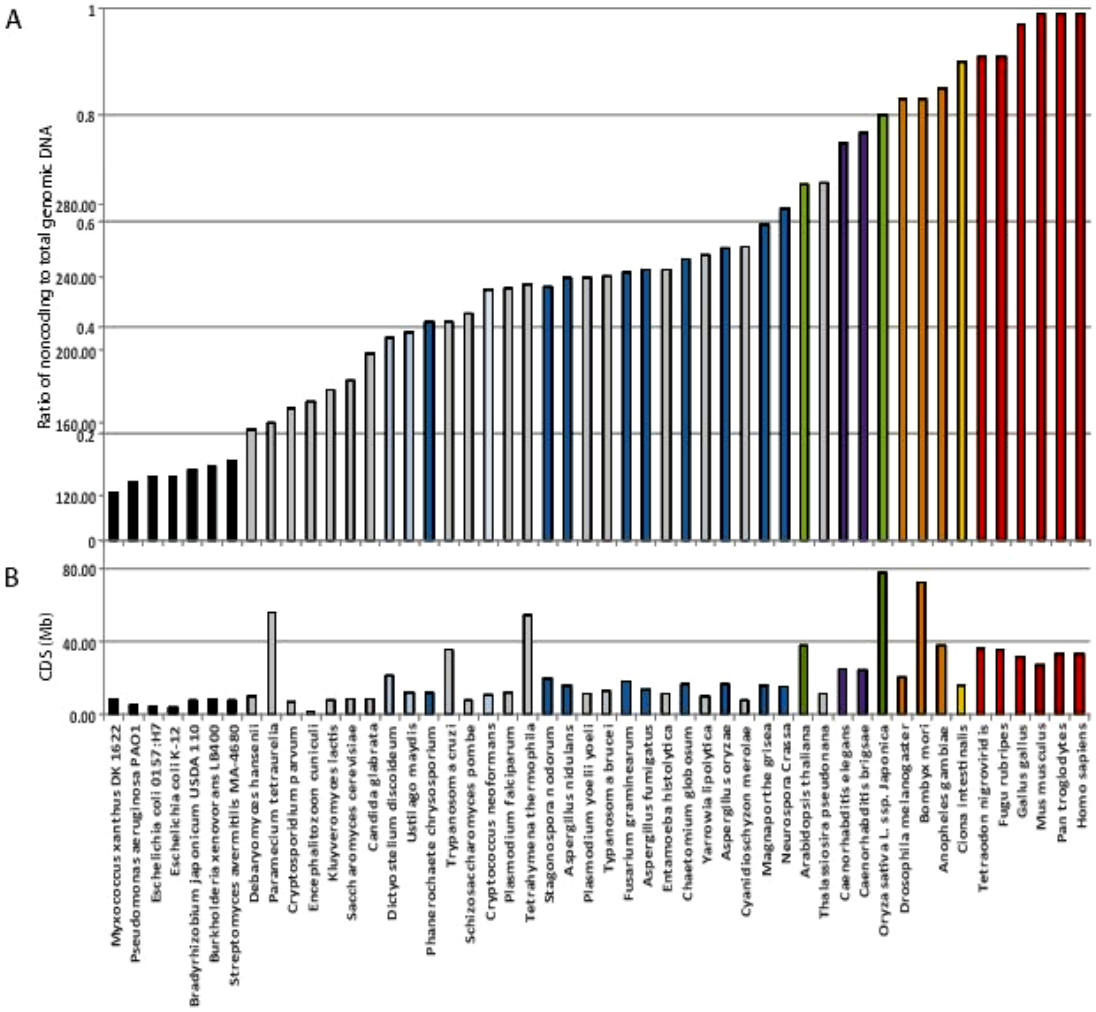

Figure 1.4 The fraction of non-protein-coding DNA and megabases of protein coding sequence (CDS) per haploid genome in different species. (A) The ratio of the total bases of non-protein-coding to the total bases of genomic DNA per sequenced genome across phyla (i.e. the fraction of non-protein-coding DNA). The four largest prokaryote genomes and two well-known bacterial species are depicted in black. Single-celled organisms are shown in gray, organisms known to be both single and multicellular depending on lifecycle are light blue, basal multicellular organisms are blue, plants are green, nematodes are purple, arthropods are orange, ascidians are yellow, and vertebrates are red. Species names are listed below B. (B) The amount (in megabases) of CDS per genome for species ranked by fraction of non-protein-coding DNA. Original source Mattick *et al.*, (2007). This figure was reproduced with permission of the author.

1.2.1 Categories of ncRNA

ncRNAs can be generally classified according to their sizes which may indicate specific length-dependent functions. The following section will briefly described the three best known types of ncRNAs, long, small and micro, although other types have been recently discovered (see Table 1.3).

1.2.1.1 Long non-coding RNAs >~200 nt

Tiling arrays tested on the human genome, revealed that the majority of transcription occurs as long ncRNAs (lncRNAs) (Kapranov *et al*., 2007b). Although a small number of lncRNAs have been functionally characterized (Prasanth & Spector 2007) they seem to exhibit a broad range of functions (Prasanth & Spector 2007,) each with restricted expression in specific cell types and localization to specific cellular compartments (Clemson *et al*., 1998; Ginger *et al*., 2006; Prasanth *et al*., 2005; Willingham *et al*., 2005). Their functions are extremely diverse comprising events such as: DNA demethylation, X-inactivation, modulation of transcription and genomic imprinting (Avner *et al*., 2001), but also in subcellular dynamics, including chromatin modification, transcriptional activation, transcriptional interference, nuclear transportation, and generation of the other classes of ncRNAs (Costa, 2005; Chen *et al*., 2010; Storz, 2002).

LncRNAs are thought to be involved in the regulation of protein-coding genes in normal development and also oncogenesis. Some lncRNAs may be precursors of smaller RNAs, but many are detected as relatively stable polyadenylated and non-polyadenylated transcripts (Bartel *et al*., 2004; Cheng 2005; Kim, 2005; Kiyosawa *et al*., 2007; Mallory & Vaucheret, 2006).

The first mammalian ncRNA that proved to have a gene silencing function was the *Xist* ncRNA, which inactivates one of the two X chromosomes in female mammals (Marahrens *et al*., 1997). The Telomerase RNA is also lncRNA and an integral part of

the telomerase enzyme serving as a template for the synthesis of chromosome ends (Chen *et al*., 2000). Even larger transcripts that can be 200->10,000 nucleotides in length belong to a group known as medium or large RNAs (reviewed in Storz *et al*., 2002). Extremely long ncRNAs >10,000 nt detected in insects and mammalian cells have been associated with gene silencing and in modifying chromatin structure along large chromosomal regions, e.g. human *Xist* RNA required for X chromosome inactivation and mouse antisense *Igf2r* (insulin-like growth factor type-2 receptor) (*Air*) RNA required for autosomal gene imprinting antisense *Igf2r*, of the 108kb *Igf2r* gene (reviewed in O'Neil *et al*., 2005).

1.2.1.2 Small non-protein-coding RNAs ~21-22nt

Transcripts ~21-22 nucleotides in length are a group which comprise small RNAs (sRNAs). These are potent regulators of postranscriptional and transcriptional gene expression (Voinnet *et al*., 2009). The effects of sRNAs gene expression and control are generally inhibitory as long as the regulatory mechanisms underlie RNA silencing. Control of gene expression of sRNAs was discovered in 1993 while analyzing the nematode *Caenorhabditis elegans* larvae sRNAs were found complemented the sense strand of a larger mRNA and bound to its 3' untranslated region, thus inhibiting translation (Bartel, 2004; Lee *et al*., 1993). Since then a number of different sRNAs have been found with a variety of mechanisms of transcriptional regulation. They also can be divided in two main groups the small interfering RNAs (siRNAs) and the micro RNAs (miRNAs).

The siRNAs are double-stranded RNA molecules (~21 bp), generated by the cleavage of dsRNA by an enzyme called Dicer, a member of the RNase III family. SiRNA is thought to be exogenous in origin derived directly from virus, transgenes trigger or transposons, which is excised from fully complementary double stranded, that is not encoded in the genome. (Tomari and Zamore 2005). siRNAs regulate the degradation by cleavage of mRNA complementary sequences, resulting in the down regulation of protein synthesis (Fuchs and Boutros, 2007; Kittler *et al*., 2003; Mocellin *et al*., 2006; Sledz *et al*., 2005). They have roles in virtually all developmental processes,

including stem cell and germline maintenance, development and differentiation, transcriptional and post-transcriptional gene silencing and subcellular localization. The 186nt human U2 small nuclear RNA involved in RNA splicing (Will *et al*., 2001). siRNAs can also silence gene expression by obstructing the promoter by directing gene methylation or chromatin condensation, roles that have been associated with involved in transposon control and viral defence. SiRNA sequences can be phylogenetically conserved.

The other class of sRNAs are the microRNAs (miRNAs) (~21 bp), these are a diverse class of sRNAs molecules (Table 1.3) and typically endogenous gene products, miRNAs appear to originate from stem-loop precursors with incomplete double-stranded hairpins. Like siRNAs, Dicer enzymes excise miRNAs from their precursors, and Argonaute (Ago) proteins appears to perform the signature of silencing effectors' function being part of the catalytic components of the RNA-induced silencing complex (Meister and Tuschl, 2004) (Table 1.3).

miRNAs are involved in a wide variety of biological processes, such as development, metabolism and cell cycle (Boehm *et al*., 2005; Carleton *et al*., 2007; Harfe *et al*., 2005), as well as human diseases, such as diabetes, cancer and neuro- and immune-degenerative processes (Jin *et al*., 2004; Poy *et al*., 2004; Volina *et al*., 2006). miRNAs are a highly conserved between species with diverse functions in the regulation of gene expression in multicellular eukaryotes and some unicellular eukaryotes (Kato and Slack, 2008). It has been estimated that miRNAs regulate ~30% of human genes (Bartel, 2004), and that half of the known miRNAs are inside or next to polymorphism hot-spots sites in minimal regions of loss of heterozygosity and regions of amplification, near common breakpoints associated with cancer (Garzon *et al*., 2009; Lu *et al*., 2005; Volinia *et al*., 2006). In particular miR-15a and miR-16-1 have been stipulated to affect level of *WT1* in leukemia cell lines (Calin *et al*., 2008).

Table 1.3 Classes of non-coding RNA in mammals

NcRNA class	
Long non-coding RNAs (lncRNAs)	The broadest class, encompass all non-protein-coding RNA spencies >~200 nt, including, mRNA-like ncRNAs. Their functions include epigenetic regulation, acting as a sequence-specific tethers for protein complexes and specifying subcellular compartments or localizations
Small interfering RNAs (siRNAs)	Small RNAs ~21-22 nt long, produced by Dicer cleavage of complementary dsRNA duplexes siRNAs form complexes with Ago protein and are involved in gene regulation, transposon control and viral defense.
MicroRNAs (miRNAs)	Small RNAs ~22 nt long, produced by Dicer cleavage of imperfect RNA hairpins encoded in long primary transcripts or short introns. They associate with Ago proteins and are predominately involved in post-transcriptionaly regulations.
Promoter-associated RNAs (PARs)	A general term encompassing a suite of long and short RNAs, including promoter-associated RNAs (PASRs) and transcription initiation RNAs (tiRNAs) that overlap promoters and TSSs. These transcripts may regulate gene expression.
Small nucleolar RNAs (snoRNAs)	Traditionally viewed as guides of rRNA methylation and pseudouirydylation. However, there is emerging evidence that they also have gene-regulatory roles.
<u>Recently described classes</u>	X-inactivation RNAs (xiRNAs)
X-inactivation RNAs (xiRNAs)	Dicer-dependent small RNAs processed from duplexes of two lncRNAs, Xist and Tsix, which are responsible for X-chromosome inactivation in placental mammals.
Sno-derived RNAs (sdRNAs)	Small RNAs, some of which dicer dependent, wich are processed from small nucleolar RNAs (snoRNAs). Some sdRNAs have been shown to function as miRNA-like regulators of translation.

microRNA-offset RNAs (moRNAs)	Small RNAs ~20nt, derived from de regions adjacent to pre-miRNAs. Their function is unknown.
tRNA-derived RNAs	tRNAs can be processed into small RNA species by conserved RNase (angionin). They are able to induce translational repression.
MSY2-associated RNAs (MSY-RNAs)	MSY2-RNAs are associated with the germ cell-specific DNA/RNA binding protein MSY2. Like piRNAs, they are largely restricted to the germline and are ~26-30 nt long. Their function is unknown.
Telomere small RNAs (tel-sRNAs)	Dicer-independent 24 nt RNAs principally derived from G rich strand of telomeric repeats. May have a role in telomere maintenance

This table was reproduced with permission of the author (Mattick, 2005)

1.2.1.2.1 The influence of *H19* on *Igf2*

The *IGF2* and *H19* genes are reciprocally imprinted transcripts, both located at 11p15.5 in human and distal chromosome 7 in mouse. *H19* codes for a 2.3 kb spliced and polyadenylated RNA product. *H19* is a member of the class of genes transcribed by the RNA polymerase II that was the first example identified of a non-coding RNA (Brannan *et al*., 1990). Coexpression of *H19* and it *IGF2* occurs in parallel in most of the same tissues during embryogenic development. *IGF2* encodes a potent mitogen, transcribed from four promoters P1-4, of which promoters P2-4 are imprinted and transcription occurs only from the paternal allele (Ogawa *et al*., 1993; Rainier *et al*., 1993) whereas *H19* is expressed from the maternal allele. The modulation of imprinting of *H19/IGF* requires binding of the vertebrate insulator protein, CCCTC binding factor (CTCF) a multivalent zinc finger protein whose DNA binding is prevented by DNA methylation, CTCF binds to the maternally differentially

hypomethylated domain (DMD) and is involved in blocking access of enhancer sequences to *IGF2* promoters. On the paternal allele, methylation of the DMD blocks CTCF binding and repressing H19 transcription while allowing enhancers to interact with *IGF2* promoters (Figure 1.6). Loss of imprinting of *IGF2* and *H19* is common in WTs, and *IGF2*, as an autocrine growth factor is an appealing target in playing a causal role in tumorigenesis (Arima *et al*., 1997; McCann *et al*., 1996).

Recent studies of BWS have found in inherited mutations in WT (Riccio *et al*., 2009). This might be correlated with the LOI mechanism allowing the paternal allele of *IGF2* to be expressed and H19 to be silenced. Nevertheless, the abrogation of H19 might also be a factor in tumour progression, as this conserved molecule (Juan *et al*., 2000) has been correlated with TS activity (Brannan *et al*., 1990; Hao *et al*., 1993). Additionally, evaluation of IGF2 peptide levels in WTs with relaxation of imprinting, indicate little change in protein levels (Baccarini *et al*., 1993; Haselbacher *et al*., 1987), though this does not exclude a role for elevated *IGF2* at early stages of tumourigenesis. Interestingly, mice inheriting a truncated maternal *H19* allele and a deleted paternal *IGF2* allele had no discernable phenotype whereas mice inheriting only a deleted maternal *H19* showed body overgrowth.

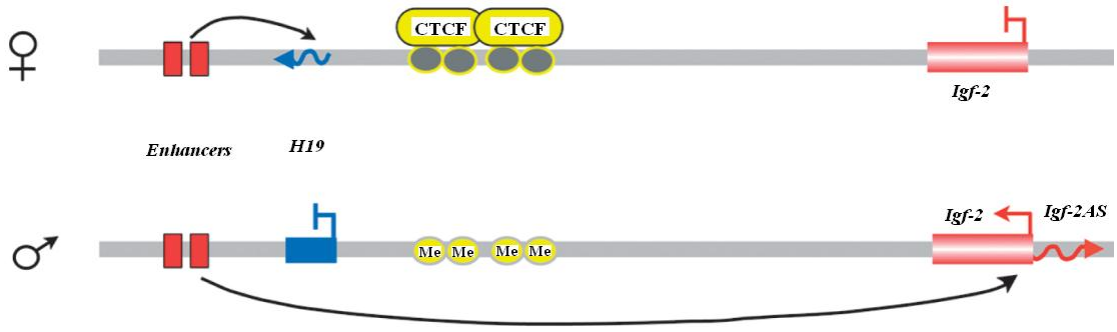

Figure 1.5 Long noncoding RNA-mediated transcription regulation by enhancer competition. The *H19* lncRNA is transcribed only maternally from the imprinted *H19/Igf2* locus, which is controlled by chromatin insulators that lie upstream of the H19 gene. On the maternal chromosome, the insulator sequence is unmethylated and binds CCCTC-binding factor (CTCF), and thus prevents the enhancers from interacting with the *Igf2* promoter, but instead activates *H19* gene transcription. On the paternal chromosome, insulators are methylated and do not bind CTCF, thus allowing the enhancers to activate *Igf2* transcription.

On the other hand mice inheriting only a deleted paternal *IGF2* gene displayed somatic undergrowth when compared to control mice. This indicates that the loss of *H19* is not lethal, *H19* expression governs *IGF2* repression, and the overexpression of *IGF2* is responsible for the overgrowth phenotype observed in the maternal inheritance of a deleted *H19* (Leighton *et al*., 1995).

1.2.2 Antisense RNA transcripts

By definition antisense transcripts are RNA molecules that are transcribed from opposite strand of conventional (sense) genes. Such antisense transcripts may overlap or not with mature sense (Figure 1.6) (Williams and Fried, 1986). Many ncRNAs are divergently expressed that overlap protein-coding genes and are a widespread phenomenon in mammalian genomes (Table 1.4). In the last several years, attention has been addressed to the fact that a considerable fraction of the transcriptome comprises endogenous transcripts with inverse orientation serving as a template of RNA polymerase II (Goodrich *et al*., 2006).

Antisense RNA molecules are transcribed from the opposite strand and in the reverse direction compared with a sense transcript which commonly is a protein coding RNA is translated. They are classified into two groups: One is the natural antisense transcript (NAT) which has partial or complete complementary transcript sequences shared with a sense counterpart. The second type is non-overlapping with the sense transcript but may be complementary to DNA (Figure 1.6). Antisense transcripts can be spliced, polyadenylated and imprinted, although it has been reported that they have a tendency to undergo fewer splicing events than is typically displayed by their sense counterparts (He *et al*., 2008).

1.2.2.1 Discovery

The first NATs were discovered in 1981. These were small plasmid-encoded RNA regulators which control the copy number of *Escherichia coli* plasmids CoE1 and R1 (Tomizawa *et al*., 1981; Stougard *et al*., 1981; reviewed in Brantl *et al*., 2002). Antisense RNAs can be coding or non-coding. An example of a protein coding

antisense RNA is mitotic apparatus protein one. It is an antisense transcript of Interleukin 18 binding protein and overlaps the 3' untranslated region (UTR). However, naturally occurring antisense RNAs are usually ncRNAs and represent around 98% of all humans ncRNA transcriptional output.

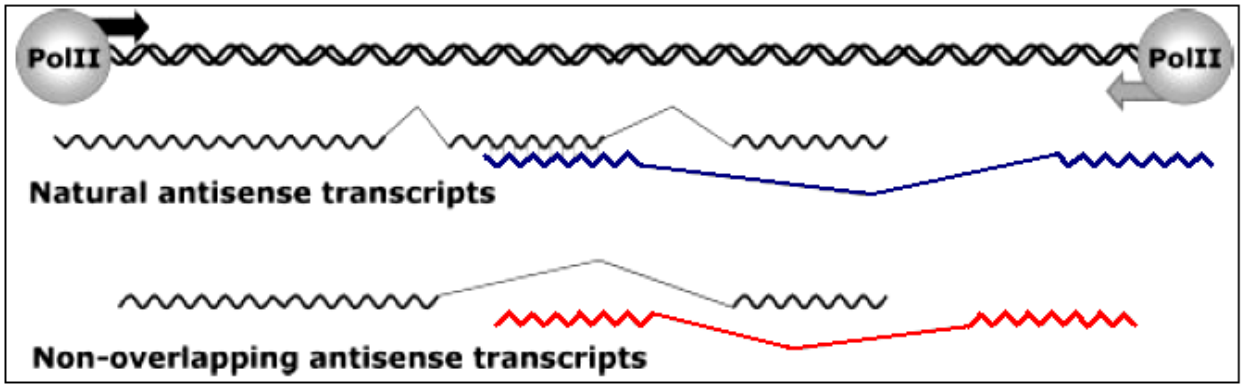

Figure 1.6 Schematic representing antisense transcripts. An example of complementary "natural" antisense in blue, and "non-overlapping" of a given sense transcript in red. At the top double chain showing polymerase enzyme and transcription orientation.

Conventionally, the sense strand is considered to encode the protein since it has the same sequence as the mRNA. However, long open reading frames in the antisense strand can exist which might encode "antisense" proteins (Meckler, 1969; Merino *et al*., 1994). Yomo *et al*., (1992), interpreted the discovery of long antisense open reading frames in certain plasmid genes as indicating that some "unknown force" is protecting the frames from mutations generating stop codons. In later studies, Yomo and Urabe (1994) have generalized these arguments taking into account the observation that the frequencies of individual codons in sense strands are often similar to their frequencies in the antisense strands (when read in the same phase and with the correct polarity; Alff-Steinberger 1984, 1987; Yomo and Ohno 1989).

Others have suggested that the genetic code may initially have evolved to enable the simultaneous emergence of sense and antisense peptides (Alff-Steinberger, 1984; Konecny *et al*., 1993; Zull & Smith, 1990). Codons for hydrophilic and hydrophobic aa on the sense strand may sometimes be complemented, in frame, by codons for

hydrophobic and hydrophilic aa on the antisense strand. Furthermore, antisense proteins may sometimes interact with high specificity with the corresponding sense proteins (Blalock and Bost, 1986; Blalock, 1990; Clarke and Blalock, 1991). The interactions involve multiple contacts along the lengths of the polypeptide chains (Tropsha *et al*., 1992).

The presence and abundance of genes with antisense transcripts have been estimated by distinct methodological approaches, including bioinformatics analysis of expressed sequence tag (EST), Ref Seq and data bases (Zhang *et al*., 2006), single-strand RT-PCR (Yeung and Lau, 2002), hybridization techniques (Rosok and Sioud, 2004), strand specific microarrays (Ge *et al*, 2008), sequencing (Katayama, 2005; Kiyosawa *et al*., 2003), serial analysis of genomic expression (SAGE) libraries (Ge *et al*., 2006), global run-on sequencing (GRAO-seq)(Core *et al*., 2008) and asymmetric strand-specific analysis of gene expression (He *et al*., 2008). These techniques provide ample evidence that the mammalian genomes code for numerous antisense transcripts. At least a 1,000 NATs were have been found conserved between human and mouse (Engstrom *et al*., 2006) However, this information remains limited because not all of the mammalian transcriptome has been sequenced fully and more information is needed to map antisense elements which are transcribed in low copy number. For instance, in the mouse due to large scale sequencing of cDNA clones by the FANTOM3 consortium NATs were shown to be associated with 70% of sense transcribed transcribed genes, with most lacking protein-coding capacity (Katayama, 2005). The abundance of non over lapping antisense RNAs has not yet been estimated. This suggests that there is a higher prevalence of antisense RNAs in mammals and alludes to their importance (Table 1.4). The occurrence of an imprinted ncRNA with some an imprinted gene cluster has been observed (Sleutels & Barlow 2002) however ncRNA, have also been identified in several bi-allelically expressed genes such as *N-myc*, *BFGF*, *Hox11*, *RPS14* and *Kelch-like 1* (Benzow & Koob, 2002; Krystal et al., 1990; Li *et al*., 1996; Potter & Bradford, 1998; 1990; Tashev & Roufa, 1995). Antisense transcripts identified within imprinting regions so far are expressed from the paternal allele only, apart from *Tsix*, the antisense transcript to *Xist* (Sado *et al*., 2001).

1.2.2.2 Functional validation

As it has been stated before mammalian genomes code for numerous antisense transcripts, but their function remain poorly understood. Several authors have identified that endogenous expression levels may have a positive reciprocal correlation between the presence of sense and antisense transcripts, within specific tissues or cell lines (Katayama *et al*., 2005; Li *et al*., 1996; Sado *et al*., 2001,), however this interaction may not occur between tissue or cell-type (Alenina *et al*., 2002, Okada *et al*., 2008). Although very little is known about the biological functions of NATs (reviewed in Lavorgna *et al*., 2004), recent evidence indicates that antisense transcripts are frequently functional and use diverse transcriptional and post-transcriptional gene regulatory mechanisms to carry out a wide variety of biological roles (Table 1.4). The biochemical function of NATs has been assessed in various organisms, and evidence for RNA interference, RNA editing, RNA splicing, transcriptional interference, or direct RNA-protein interaction has been reported. These important findings have been reviewed in detail (Faghihi and Wahlestedt, 2009; Mattick 2005). However, the extent to which these mechanisms contribute to the phylogenetic drive to accumulate antisense transcripts in eukaryotic genomes is a matter of debate.

Antisense RNAs can cause messenger RNA (mRNA) destruction, repression and activation, altered RNA processing (such as editing), effects on transcription, inhibition of mRNA transport and alteration in mRNA stability. Antisense RNA mechanism of action can be via DNA, RNA or protein-interaction. The RNA may affect the DNA level if the sense and antisense promoters compete for shared enhancers or the antisense RNA may occlude the promoters directly. At the RNA level transcription is clearly important in gene control, but translation is also extensively regulated. Translation repression can occur by inhibition of ribosome elongation, but only very tight binding antisense agents can also block this progression (Huttenhofer *et al*., 2005; Morey *et al*., 2004; Storz, 2002).

Translation initiation can be inhibited by mRNA structure or antisense sequences which cover/mask recognition signals. In prokaryotes, trans-encoded antisense sequences typically work by binding to the start codon region of mRNA whereas in eukaryotes most NATs repress translation by binding sequences within the 3'UTR. It may seem surprising that binding to sites in the 3'UTR can repress translation; however this region interacts with the 5'UTR where translation begins. Connective tissue growth factor (CTGF) exhibits repression of translation mediated by the antisense (Kubota *et al*., 1999).

Table 1.4 Compilation of reported antisense transcripts and their possible targets.

Sense–antisense transcripts	**Proposed function or disease relevance**	**Suggested mechanism**	**Species**
BACE1 and *BACE1-AS*	Alzheimer's disease	Stability	H, M
APOE and *APOE-AS1*	Alzheimer's disease	Not known	H, M
PU.1 and *PU.1-AS*	Haematopoiesis	Translational block	H, M
Δ5-desaturase and *reverse Δ5-desaturase*	Fatty acid metabolism	Translational block, transcriptional interference, mRNA stability	H, R
P15 and *P15-AS*	Tumour suppressor	Chromatin modification	H
P21 and *P21-AS*	Tumour Suppressor	Chromatin modification	H
NKx2.2 and *NKx2.2-AS*	Neuronal cell differentiation	Not known	H
Zfh-5 and *zfh-5AS*	Transcription factor	Not known	M
Progesteron receptor and *PR-AS*	PR activation / inhibition	Promoter activation/inhibition through heterochromatin protein 1	H
HAR1F and *HAR1R*	Neuro-development	Not known	H
WT1 and *WT1-AS*	Kidney development	Methylation	H
BDNF and *BDNFOS*	Neurotrophic factor	RNA duplex formation	P
PINK1 and *naPINK1*	Mitochondrial function	Not known	H
FMR1 and *ASFMR1*	Fragile X mental retardation	Epigenetic changes	H, M
EPO-R and *asEPO-*	Lung growth	Stability, translation	H, C

R			
Ghrelin and *ghrelinOS*	Anxiety, depression	Not known	H
Rad 18 and *NAT-Rad18*	Apoptosis	Post-transcriptional control	H, R
HFE and *HFE antisense RNA*	Iron storage disorder	Translation repression	H
Zeb2 and *Zeb2 NAT*	Epithelial–mesenchymal transition	Splicing	H, M
TSP1 and *TSP1-AS*	Platelet aggregation	Not known	H
Urocortin, Ucn and *Ucn-AS*	Neuro-transmission	Post-transcriptional	
Sphk1 and *Khps1*	Calcium mobilization	Demethylation	H, R
Pdcd2 and *Tbp*	Apoptosis	Editing, alternative splicing and polyadenylation	H, M, Ch
Msh4 and *Hspa5*	Meiotic DNA recombination	RNA degradation	M
Pax-6 and *Pax-6OS* *Pax-2* and *Pax-2OS* *Six3* and *Six3OS* *Six6* and *Six6OS* *Otx2* and *Otx2OS* *Crx* and *CrxOS* *Rax* and *RaxOS* *Vax2* and *Vax2OS*	Eye development	Not known	M, H
Hyaluronan synthase 2 and *HASNT*	Hyaluronan biosynthesis	Not known	M, H
Msx1 and *Msx1_AS*	Skeletal terminal differentiation	Splicing, imprinting	R, H
FGF-2 and *FGF-AS (bFGF* and *bFGF-AS)*	Haematological tumours, endometriosis	Polyadenylation, translational block, editing, stability	Mm
p53	Differentiation	Transport	M
N-myc	Oncogenesis	Splicing	M, H
Tsix and *Xist*	X chromosome inactivation	X inactivation	Mm
HIF-1α and *aHIF*	Poor prognosis marker in breast cancer, renal cancer	RNA destabilization, pre-mRNA splicing	H, R
Survivin and *EPR-1*	Colon cancer	Not known	H

α-globulin and *LUC7L*	A-Thalassaemia	Methylation	H
IGF2R and *Air*	Tumour suppressor	Imprinting	H, M
KvLQT1	BWS	Imprinting	H
SNURF-SNRPN and *UBE3A*	Prader-Willi and Angelman syndrome	Imprinting	H
GNAS	Signal transduction	Imprinting	H, M
BCMA and *BCMA-AS RNA*	B-cell maturation	Translation block, editing	H
Bcl-2 and *IgH*	Follicular B-cell lymphoma	RNA stabilization	H
c-erbA and *Rev-ErbAα*	Thyroid hormone receptor	Splicing	H, R
Thymidylate synthase and *rTSα DNA*	Replication And repair	Editing	H
CHRNA3 and *CHRNA5*	Neuronal nicotinic receptor	Stabilization	H, B
Myelin basic protein (MBP and *MBP-AS)*	Myelin formation	Transport	M
eNOS and *NOS3AS (sONE)*	Vascular disease	Inverse S–AS correlation	H, M
Neuronal nitric oxide synthase and *NOS*	Nervous system signalling	Post-transcriptional, translation	S, H, R
Inducible nitric oxide synthase (iNOS and *iNOS AS)*	Inflammatory diseases	Stability	R
NOS2A and *anti-NOS2A*	Neuronal differentiation	Inverse S–AS correlation	P
SMAD5 and *DAMS*	TGF-β/BMP inhibitory signals	Transcriptional interference, translational block	H, R
eIF2α	T cell mitogenesis	RNA degradation	H
ERCC-1, RAF49 (ASE-1)	DNA repair	Stability, localization	H
α1 collagen	Chondrogenesis	Competitive transcriptional interference	Ch
MKRN2 and *RAF1*	Cancer	Polyadenylation	Mm
Hoxa 11	Development	Epigenetic	Mm
Cardiac troponin 1	Myocardial function	Translation	H, R
pMCH and *pMCH*	Food intake	Splicing	H, R

antisense			
CDYL and *CDYL-AS*	Spermatogenesis	Not known	B
FGFR-3 and *psiFGFR-3*	Bone and haematopoietic maturation	RNA degradation, translation inhibition	M
TOP1 and *TOP1-AS*	Cell cycle	Translational regulation	H
EP1 prostanoid receptor and *PKN protein kinase*	Intracellular signalling	Not known	M
EMX2 and *EMX2OS*	Development	Splicing, polyadenylation	H, M
Thymidine kinase and *TK-AS*	Cell cycle	Inverse S–AS correlation	M
DIPLA1 and *DIPAS*	Placenta specific	Not known	H
GnRH and *SH*	Gonadotropin-releasing hormone (GnRH)	Not known	R
HLA-J cluster *HZFw* and *HZFc* *HZFw* and *HCGV* *HTEX6* and *HTEX4*	MHC class I	Alternative splicing, alternative polyadenylation	H, M
MHC IIa, IIx, IIb and *antisense aII, xII, bII*	Skeletal muscle myosin heavy chain regulation	Transcriptional interference and/or promoter methylation	R
Cardiac βMHC and *AS- βMHC*	Cardiac myosin heavy chain α–β gene switching	Transcriptional regulation at promoter	H, R
ABO and *ABOAS*	Blood group, ABO gene expression	Post-transcriptional, methylation	H
Frequency, frq and *antisense-frq*	Circadian clock function	Inverse S–AS correlation	F
ORCTL2 and *ORCTL2S*	Wilm's tumour	Imprinting	H
Tenascin-X and *P450c21B*	Adrenal function	Post-transcriptional	H
NPT and *NPT-AS*	Na/Pi co-transporter, Phosphate homeostasis	Translation interference	M, Z
PKN and *EP1*	Protein kinase	Alternative polyadenylation	M
COX10 and *C17ORF1*	Charcot-Marie-Tooth	Post-transcriptional	H

c-myc and *c-myc-antisense*	Oncogene	Pre-mRNA processing, transcription interference	R, H

Species, P: primate, C: canine, Mm: mammal, B: bovine, F: fungus, Z: zebrafish, H: human, M: mouse, R: rat, Ch: Chicken. Information modified from Faghihi and Wahlestedt, 2009. This table was reproduced with permission of the author.

1.2.2.3 Proposed mechanisms of NATs-mediated regulation of sense mRNA

The first model to explain NAT-mediated regulation of sense RNA expression maintains that RNA duplexes require overlap a region of at least 6- to 8-bp to form stable double stranded RNA through complementary base pairing sequences, to result in inhibition of the of protein synthesis (Lai 2002; Lewis *et al*. 2005). The second model involves methylation of promoters included in regions transcribed by antisense mRNAs repressing the transcription of sense mRNAs (Reik and Walter 2001; Tufarelli *et al*. 2003; Wutz *et al*. 1997). A third method suggests the usage of differential transcriptional regulatory elements. Antisense transcripts participate in processes in development, physiology, and responses to external stimuli. Although numerous NATs have been predicted in various species the mechanisms they use to regulate gene expression remain unclear. To elucidate these mechanisms four routes have been proposed (Lavorgna *et al*. 2004):

A) Mechanisms related to transcription
B) RNA-DNA interactions
C) RNA-RNA interactions in the nucleus
D) RNA-RNA interactions in the cytoplasm

1.2.2.3.1 Mechanisms related to transcription.

This model centers on transcriptional collision. The RNA polymerase encoding sense and antisense transcripts clashes within the overlapping region, stopping their transcription. This model was implied from the analyses of the expression levels of cis-NATs in yeast (Peterson and Myers 1993; Puig *et al*. 1999). In more recent studies, the collision of *Escherichia coli*, and *Saccharomyces cerevisiae* (Prescott and Proudfoot 2002), RNA polymerases were observed by atomic force microscopy

(Crampton *et al*. 2006) showing that RNA polymerases do not displace each other, but instead stall in front of each other. Bioinformatic analysis in human and mouse reveals that the size of shared regions between sense and antisense transcripts is inversely correlated with the level of antisense transcript expression, suggesting a putative clash of RNA polymerases. The point of collision increases the length of spanning region. In this model, the antisense RNA is not required to be transcribed, in order to interfere with transcription of the sense RNA.

1.2.2.3.2 RNA–DNA interactions

The RNA-DNA model proposes that NATs can have a direct or indirect participation in RNA–DNA or RNA–chromatin interactions (Bernstein *et al*., 2005). This comprises genomic imprinting (Kanduri *et al*., 2008), X-chromosome inactivation (Reviewed by Avner and Heard 2001) and random endogenous monoallelic exclusion. In each of these cases NAT's interact with one of the two alleles of a gene, enabling monoallelic expression. NAT participate in other forms of epigenetic regulation, involving DNA methylation (Tufarelli *et al*., 2003). Antisense transcripts may bind to specific region of DNA strand, resulting in either DNA methylation or in histone-modifying enzyme recruitment and subsequent alterations in chromatin structure (Yu *et al.*, 2008). These roles for antisense transcripts in epigenetic silencing are likely to be independent of Dicer therefore small RNA production. However, antisense RNA can be processed by Dicer to small RNA in the cytoplasm. Divergently, antisense transcripts stay binding DNA or act chromatin modifications in which may interfere with adjacent regions.

1.2.2.3.3 Nuclear and cytoplasmic RNA-RNA duplex formation

Another type of proposed mechanism involves the formation of nuclear or cytoplasmic sense–antisense RNA duplexes. Nuclear RNA duplex can produce alternative splicing in mRNA by masking the splice sites and there by changing isoform ratios. In addition to this mechanism, RNA may act as a substrate enzymes altering the localization, transport or stability of the sense mRNA transcript. In the cytoplasm, where RNA hairpins can interact with sense mRNA modifying stability and/or translation efficiency. The RNA duplex can mask miRNA or create a template,

within the hairpin loops, for producing endogenous siRNA. The RNA-RNA hybrid can help mRNA stability by preventing mRNA decay.

Interestingly, through these diverse types of mechanisms antisense transcripts in human cell lines are not always linked to expression of the sense gene. The function of ncRNAs, are not restricted only to antisense transcripts, also it may be dependent largely on their interactions with RNP complexes. For example, knockdown or blockade of endogenous antisense transcripts can have different outcomes, either increasing or decreasing sense transcript expression (Wahlestedt *et al*., 2006). Certainly, there are examples of parallel expression of sense and antisense transcripts (Krystal et al., 1990, Moorwood *et al*., 1998). This indicates the metabolism of sense: antisense hybrid is transcript or context-specific, with diverse downstream effects.

1.2.2.4 Antisense RNAs associated with tumour suppressor genes and oncogenes

Antisense transcripts are present in some tumour suppressor genes and could have a role in carcinogenesis as they have been found over expressed in carcinomas. Recently a NAT of *p53* was characterized and named as *Wrap53* that regulates endogenous *p53* mRNA levels by targeting the 5' untranslated region of *p53* mRNA. siRNA knockdown of *Wrap53* results in downregulation of p53 mRNA and suppression of *p53* induction upon DNA damage. On the contrary, overexpression of *Wrap53* increases *p53* mRNA and protein levels strongly suggesting that *Wrap53* influences *p53* via *Wrap53/p53* RNA interaction (Mahesharan *et al*., 1993).

Many ncRNas show abnormal expression patterns in cancerous tissues, including miRNAs telomerase RNA, lncRNA. Details of the biogenesis and function of siRNA, are still largely unknown especially in mammals. On the other hand, miRNA are mostly known to function in differentiation and development as part of a large scale of regulatory network of many protein coding genes. Many microRNAs have been found in primary human tumours (Calin *et al*., 2002; Calin *et al*., 2004; He *et al*., 2005; Lu *et al*., 2005). Moreover, many human microRNAs are transcribed at genomic regions linked to cancer (Calin *et al*., 2004; McManus, 2003). Of particular

interest is the *mir-17* microRNA cluster, which is in a region on human chromosome 13 that is frequently amplified in B-cell lymphomas (He *et al*., 2005). Overexpression of the *mir-17* cluster was found to co-operate with *Myc* to accelerate tumour development in a mouse B-cell lymphoma model. Further evidence for such a link between *Myc* and the *mir-17* cluster has come from microarray expression studies, which showed that *mir-17* cluster gene expression was induced by the overexpression of Myc (O'Donnell *et al*., 2005). Also for the case of single nucleotide polymorphisms have been found in a transcript called *rs11614913* that overlaps *has-mir-196a2* has been found to be associated with non-small cell lung carcinoma (Hu *et al*., 2008). Likewise, a screen of 17 miRNAs that have been predicted to regulate a number of breast cancer associated genes, were found to be regulated by microRNAs *miR-17* and *miR-30c-1*. (Shen, et la., 2009)

1.2.2.5 Antisense RNAs at imprinted genes

Among the range of non-coding RNAs so far identified, a subgroup can be delimited associated with genes regulated by genomic imprinting. By definition, genomic imprinting is an epigenetic differential expression of autosomal alleles dependant on parent of origin (Reik *et al*., 2001a). Currently about 100 imprinted genes are known in the mouse and human genome (some annotated in Table 1.5).

NcRNA transcripts have been identified at a number of imprinted loci, which often occur as may contain both protein coding and noncoding genes (http://www.har.mrc.ac.uk/research/genomic_impriting). Imprinted expression has been found in diverse mammals, except in the egg-laying mammals, reinforcing the fundament of the proposed relation between genomic imprinting and the maternal allele control during gestation (O'Neill *et al*., 2005; Reick *et al*., 2003; Wilkins and Haig 2003). NcRNAs found at imprinted clusters include two classes of small regulatory RNAs. These are snoRNAs and miRNAs. In some cases lncRNAs are expressed from imprinted loci may be the precursors of these small ncRNAs.

Table 1.5 List of imprinted sense-antisense genes.

Gene	Organism	Chromosomal Location	Sense transcript allele	Antisense transcript allele
WT1	Human	11p13	Variable	Paternal
ZNF215	Human	11p15	Maternal	Unknown
KCNQ1	Human	11p15.5	Maternal	Paternal
ZNF127	Human	15q11-13	Paternal	Unknown
UBE3A	Human	15q11-13	Maternal	Paternal
GNAS1	Human	20q13.11	Variable	Paternal
Nesp	Mouse	Distal 2	Maternal	Paternal
Cop2	Mouse	Proximal 6	Maternal	Paternal
Zfp127	Mouse	Central 7	Paternal	Paternal
Igf2	Mouse	Distal 7	Paternal	Paternal
Kvlqt	Mouse	Distal 7	Maternal	Paternal
Igf2r	Mouse	Proximal 17	Maternal	Paternal
Xist	Mouse	X 42 cM	Paternal	Both
Dlk1-Gtl2	Mouse	Distal 12	Maternal	Paternal
Wrap53	Mouse	17p13	Maternal	Paternal

Adapted from gene catalogue published by University of Otago, New Zealand (htt://www.otago.ac.nz/igc).

In some cases one or more protein-coding genes are expressed from one allele whereas the other allele silences these genes and instead expresses an antisense ncRNA gene instead. Thereby, imprinted ncRNAs display discordant expression in *cis* with imprinted protein-coding mRNA genes, indicating that they may act as epigenetic silencers. Of the three imprinted ncRNAs so far tested, a silencing function has been shown for the *Air* and *Kcnq1ot1* ncRNAs (Mancini-Dinardo *et al*., 2006; Sleutels *et al*., 2002). The *H19* ncRNA, however, does not act as a silencer, despite showing a similar discordant expression pattern (Schmidt *et al*., 1999).

Deletion of the ncRNA promoters in three other imprinted clusters is linked with loss of imprinting of cis-linked imprinted mRNA genes, suggesting that these ncRNAs may have a role on silencing (Chamberlain and Brannan, 2001; Lin *et al*., 2003; Williamson *et al*., 2006). These imprinted overlapping pairs are linked with a wide range of pathologies, exhibiting a typical LOI in many cancers. In most of these examples except from *Igf2* the sense transcript is maternally expressed and the antisense paternally expressed in either mouse or human. *Igf2* and *Igf2as* are both paternally transcribed in the mouse. *Air* and also *Tsix*, have very long continuous and unspliced transcripts, however *Tsix* has also been shown to undergo complex alternative splicing (Table 4).

1.2.2.5.1 The antisense RNA transcript *AIR*

A nuclear ncRNA antisense transcript called *AIR* (*Air* for the mouse), partially overlaps with *Igf2r*. *Air* is a ~108-kb, capped, polyadenylated, and is transcribed exclusively by RNA pol II from the paternal allele (Braidotti *et al*., 2004; Seidl *et al*., 2006; Wutz *et al*., 1997). The *Igf2r*/Air transcription at the *Igf2r/Air* locus (proximal chromosome 17) in the mouse genome is maternally expressed and paternally methylated. However it has been found overexpressed in WT in human (Vu *et al*., 2003). *Air* is an unusual ncRNA because it has a conserved unspliced structure escaping from cotranscriptional splicing and persists as a nuclear transcript (Seidl *et al*., 2006).

In this imprinting cluster a bidirectional silencer stops *AIR* transcription from the paternal allele whereas maternal expression persists from three protein coding genes *Igf2*, *Slc22a2* and *Slc22a3.* This is due to methylation and silencing promoter in cis as is expressed through 79 kb upstream the antisense (Rougeulle and Heard 2002; Sleutels *et al*., 2002; Zwart *et al*., 2001) (Figure 1.7). The silencing of these three genes (*Igf2*, Slc22a2 and Slc22a3) is a consequence of an unmethylated CpG island located in *IGF2R* intron 1 that serves as the *AIR* promoter. *AIR* overlaps with only one of the three imprinted genes in the domain, *IGF2R*, but not the other two *Slc22a2* and *Slc22a3* suggesting that there might be more than one mechanism of silencing. Silencing by *Air* is also restricted to specific tissues at particular stage in development, specifically in the brain and placenta, the fundaments of how still unknown (Sleutels *et al*., 2002; Yamasaki *et al*., 2005). *Air* is expected to act by other mechanism than base paring RNA-RNA duplex mechanisms for imprinting (Sleutels *et al*., 2002; Spencer and Lee 2006). The model of *Air* action involves two different steps. First, during *Air* silencing overlaps *Igf2r* by RNA interference (RNAi). Nevertheless, other work by Barlow and colleagues (Sleutels *et al*., 2003) does establish that when *Igf2r* expresion is silenced in the mouse model imprinting of *Slc22a2*, *Slc22a3*, and also *Air* persists.

In addition to a direct interaction with *Igf2r*, *Air* could recruit chromatin modifier proteins to specific regions of the imprinted locus in a manner similar to the role suggested for *Xist* RNA, in order to repress *Slc22a2*, *Slc22a3* (Sleutels *et al*., 2003). Consistent with this, *Igf2r* exhibits allele-specific histone modifications (Fournier *et al*., 2002). However, RNA FISH analysis using specific probes against *Air* RNA did not show coating by *Air* RNA of the imprinted chromosomal region (Braidotti *et al*., 2004).

In the *Air* knockout the mouse model when the targeted allele was present from the maternal allele the phenotype of the mice was not discernible. When the targeted allele was inherited from the paternal *Igf2r* paternal methylation was lost, and paternal silencing of two other genes within the same imprinted gene cluster divergently expressed in relation to *Air*. Also was found a 15% reduction in weight in

new born animals. This phenotype was reversible in a different experiment where male mice with *Air* truncation were combined with female mice containing a 3cM chromosomal deletion spanning the *Igf2r* locus. In normal conditions maternal inheritance of the *Igf2r* deletion is lethal at embryonic stage between E15.5-17.5. After interbreeding with the Air truncated allele mice these double heterozygous were of normal size, viable and fertile indicating that the lethal *Igf2r* knockout phenotype was rescued by the paternal truncation of *Air* due to *Igf2r* expression from the paternal allele (Sleutels *et al*., 2002).

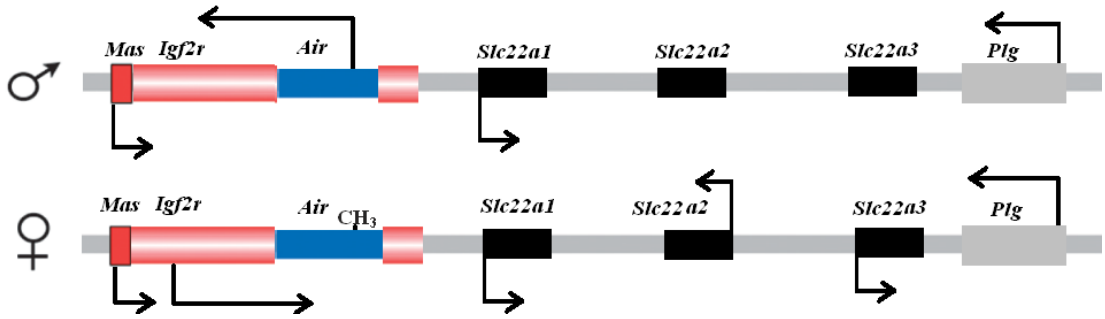

Figure 1.7 *Igf2r/Air* imprinted cluster. Figure showing parent-of-origin imprinting expression of *Air, Igf2r, Slc22a2* and *Slc22a3* and non-imprinted genes *Slc22a1*, *Plg* and *Mas*.

1.3 *WT1* antisense transcription

1.3.1 Identification

As an additional ingredient to the complexity present at the *WT1* locus is the presence of RNAs that do not appear to encode protein products. The *WT1* antisense transcript was first isolated from WT RNA and mapped to the human 11p13 locus showing the same temporal expression pattern as *WT1* although initially thought to be non-overlapping. Those transcripts initially identified were between 2.1-2.7kb in length, polyadenylated, with three introns as indicated by the identification of four cDNAs of dissimilar lengths with common 3' end. They were thought to be transcribed from a bi-directional promoter serving both *WT1* and *WT1-AS* (Bonetta *et al*., 1990; Huang *et al*., 1990). These antisense transcript was initially called *WIT-1* (now known as *WT1-AS*) with a telomeric-to-centromeric direction (antisense to *WT1* transcription),

without discernable overlapping regions with the sense transcript initially named *WIT-2* (now known as *WT1*), that were thought to arise from a single CpG island, a common feature to many promoters regions (Huang *et al*., 1990). Even though transcripts were not cloned and sequenced, it was predicted that these two transcripts may span and work as a bidirectional promoter based on the fact of a pair of TATA boxes plus a CCAAT box. The identification of a divergent transcription at the *WT1* locus in the human was observed in the *WT1* locus (Gessler and Burns, 1993). Studies found more than one splice through exon/intron boundaries in that transcript by RT-PCR product from human foetal kidney. It was also found in WTs cDNA to have a common shared single splice site.

The initially identified WIT-1 antisense transcript does not harbor a long open reading frame and is expressed in the opposite sense with regard to *WT1*. Later experiments discovered multiple-spliced RNA isoforms produced from several transcriptional start sites, some of which produced antisense transcripts overlapping with the 5'end of *WT1*, exon 1 and intron 1 (Figure 1.8). Using RNase protection assays were performed to look for *WT1* exon 1-spanning antisense transcripts in mouse tissues (Campbell *et al*., 1994) and strand-specific Northern blot in human (Eccles *et al*., 1994). The *WT1-AS* promoter has been identified in *WT1* intron 1 (Malik *et al*., 1995) called antisense regulatory region (ARR). Primer extension was used to show the *WT1-AS* transcriptional start site, within the ARR. However further functional analysis indicate the antisense isoform named as AS1 to be a potential regulator of *WT1* (Dallosso *et al*., 2004).

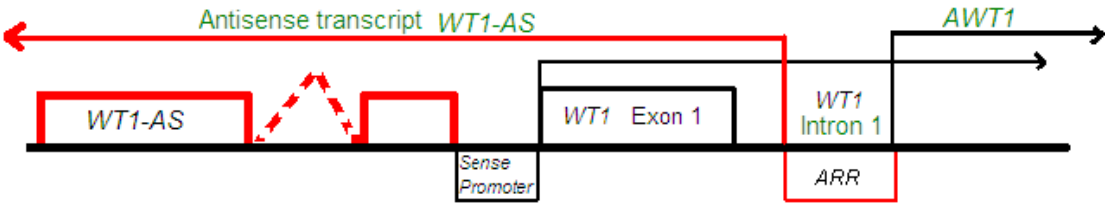

Figure 1.8 Scheme resuming the *WT1* sense/antisense locus in human. The antisense transcription elements in red and sense transcription in black. Arrows show direction of transcription, boxes over the line indicate exons and boxes on below promoters.

1.3.2 Functional characterization

Deregulation of both sense and antisense transcripts was observed in a subset of WTs (Yeger *et al*., 1992). Prompted by this looking the biological relevance of *WT1-AS*, Moorwood (*et al*., 1998) found by co-transfection analysis with antisense *WT1* exon I constructs evident a physiological role for the antisense transcript in regulation of its sense counterpart (Moorwood *et al*., 1998). High level of exon of exogenous WT1-*AS* expression led to down-regulation of the endogenous sense transcript. Lower levels (more physiological) of *WT1-AS* actually enhanced sense *WT1* expression, resulting in increased WT1 protein. Interestingly, parallel expression of *WT1* sense and antisense RNA, and also protein was observed in both WT and normal tissues from human foetal kidneys (Moorwood *et al*., 1998). In contrast to upregulation of *WT1* by *Wt1-AS* found in 293 cells *WT1* antisense reduced WT1 protein levels and inhibited the growth of several *WT1*-expressing cancer cell lines (Eccles *et al*., 1994; Oji *et al*., 2002). Using a *WT1* intron 1 probe identified a 7-10kb transcript in foetal kidney and WT samples.

RNA duplex analysis has revealed that the 5' regions of *WT1* sense transcripts can duplex *in vivo* with overlapping antisense transcripts (Dallosso *et al*., 2004). This is analogous to N-myc sense and antisense transcript expression in neuroblastoma cells, which are found as hybridized duplexes *in vivo* (Krystal *et al*., 1990). Studies from Krystal et al., (1990), found that not every single *N-myc* sense/antisense duplex transcripts match equally, which might suggest being the same behaviour on *WT1* generating more transcripts upstream its major transcriptional starting sites. These may play a significant role modulating the splicing pattern on the antisense transcripts. In addition to this it has to be taking in account that function may not be purely dependent on the sequence properties but also the formation at least on secondary structure or in transcription from restricted chromosome spots with a repercussion in the structure of the chromatin of neighbour regions adjacent or parallel.

A genome-wide screen of hypermethylated loci in breast cancer identified the *WT1* ARR in intron 1 (Huang *et al*., 1997). A subsequent study (Kleymenova *et al*., 1998) examined *Wt1* alterations in rat mesothelioma (a well-established model of the human disease) and identified tumour-specific methylation in *Wt1* intron 1. Plass *et al*., (1999) used methylation sensitive restriction landmark genomic scanning (RLGS-M) to identify WIT-1 as a gene that was specifically hypermethylated in intron 1 and 2 of relapsed, similar to AML and complete remission (CR) samples. Malik *et al*., (2000b) discovered that the *WT1-AS* transcript is imprinted in human adult kidney. In the developing kidney *WT1-AS* transcription is expressed from both alleles (paternal and maternal). Differential methylation of the ARR was found in normal kidneys, accompanied by monoallelic expression of *WT1-AS*. In a subset of WT ARR hypomethylation was concordant with biallelic expression of *WT1-AS* suggesting incidence of the epigenetic state (Malik *et al*., 2000). Recent work (Dallosso *et al*., 2007) has identified imprinting of *WT1-AS* in human postnatal kidney, and ARR hypomethylation together with loss of imprinting of the *WT1-AS* as an early event in WT tumourgenesis. This suggests an epigenetic deregulation involving *WT1-AS* in a range of cancer types. Therefore the characterization of the WTI-AS transcript and elucidation of its function are of increasing significance.

A further *WT1-AS* transcript was identified from a foetal kidney EST library, and its presence was confirmed by real time RT-PCR in adult and foetal kidney, spleen and WT tissue. However it was absent in liver or brain, whereas the antisense transcript isoforms were also expressed in these tissues (Dallosso *et al*., 2007). Such tissue specificity might suggest that certain aberrations of splicing may play a critical role in the etiology of carcinomas. This was supported by the finding that *WT1-AS* transcript isoforms were aberrant in more than 50% of patients with AML and 25% of patients with acute lymphocytic leukemia (Dallosso *et al*., 2007).

In the mouse, *Wt1* exon 1-spanning antisense transcripts have been reported very similar to *Wt1-AS* transcripts (Campbell *et al*., 1994). Other reports have identified divergent transcripts upstream of mouse *Wt1*, but failed to detect Wt1-overlapping RNAs (Gong *et al*., 2001). In the latter case, a mouse metanephric cell line which

expresses w*t1* (M15 cells) and organs from neonatal mouse were analysed by RPA using probes to detect either far upstream, exon 1 or the intron 1/exon 1 boundary within *Wt1*. An antisense transcript was identified with a 5' end upstream of *Wt1* in the M15 cell line, kidney and spleen, but none that overlapped *WT1* exon 1 or intron 1 (Gong *et al*., 2001). More recently three alternatively spliced *Wt1-AS* were isolated from neonatal mouse tissue overlapped with *Wt1* exon 1 and intron 1, and had a large splice of ~25kb, upstream of main *Wt1* transcriptional start site (Dallosso *et al*., 2007).

1.3.3 A transgenic mouse model for *Wt1-AS*

In the last few decades mutant mouse models have proven to be one of the most useful tools for collecting details about *WT1* gene expression and its role during urogenital system development. These models are providing a more comprehensive approach, useful for discovering the role of a particular gene looking at the normal and abnormal function. Furthermore, they have allowed for the discovery of organs other than kidneys whose development is regulated by *WT1* (Discenza and Pelletier 2004).

The analysis of human and mouse sequence data has highlighted two upstream conserved regions, termed MCR1 and MCR2 which lie ~12 and 5kb upstream of *WT1* exon 1 respectively (Figure 1.9). Using a gene-targeting approach, a mouse model was created with the aim of comparing the function of MCR2 as an RNA species and as a DNA element with respect to regulation of *Wt1* expression and overall mouse development. Both (MCR1 and MCR2) elements are located at the 3' termini of alternately spliced, non-coding antisense transcripts from human kidney, and MCR2 shares 94% sequence identity between mouse and human over 289 bp. This high inter-species homology implies a functional role for MCR2. Although it might have been more informative to knockout *Wt1-AS* expression, perhaps by mutating the *WT1-AS* promoter, this may have also directly interfered with *Wt1* expression making it impossible to differentiate the role of *Wt1-AS* on its own. Transient transgenic mice that have been generated with a construct containing the 298 bp conserved MCR2 region linked to a minimal promoter-lacZ cassette show a

subset of *WT1* expression (Colin Miles, personal communication) demonstrating that this conserved region can have enhancer activity.

Two different animal models were created to analyze the role of *WT1-AS*, one with truncated allele and another one with a deleted allele. Different data can be recovered from each model if *WT1-AS* has a separate function, respectively either as a DNA enhancer element or as an RNA element at the transcriptional level.

The targeting construct incorporates Mcr2 and surrounding *Wt1* homologous regions (H), a neomycin resistance gene (GKneo) that allows for positive selection within ES cells, a transcriptional terminator sequence (TTS) orientated to cause a premature termination of *WT1-AS* transcripts and a diphtheria toxin (DTA) that allows negative selection of ES cells those that incorporate the targeting construct at a random location. LoxP sites have been strategically introduced to allow a cre-recombinase mediated 2-step targeting strategy after introduction into ES cells. Deletion between the two LoxP sites flanking the neomycin gene (Δ1) leaves Mcr2 intact, but result in transcripts that are terminated before transcription of Mcr2. Deletion between the two LoxP sites flanking both the neomycin gene and Mcr2 (Δ2) however, will in result the removal of the Mcr2 region as well as premature termination antisense transcripts (Figure 1.10).

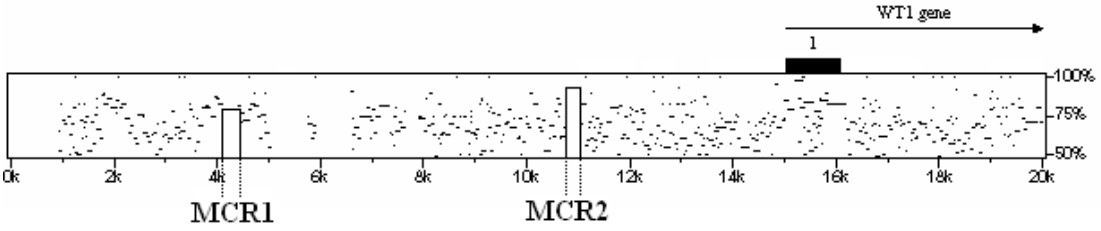

Figure 1.9 Schematic of the WT1 5' upstream region, showing nucleotide identity between human and mouse genes. A percentage of identity plot between human (NT-009237) and mouse (AL512584) upstream *WT1*. The highly conserved regions MCR1 and MCR2 are indicated below. Scale is indicated in kb pairs with conserved features positioned relative to a major *WT1* transcriptional start site (Hoffmann *et al*., 1993). Regions of sequence identity between 50-100% are display by continuous lines of alignment (CLIC Sargent Research Group, University of Bristol, personal communication).

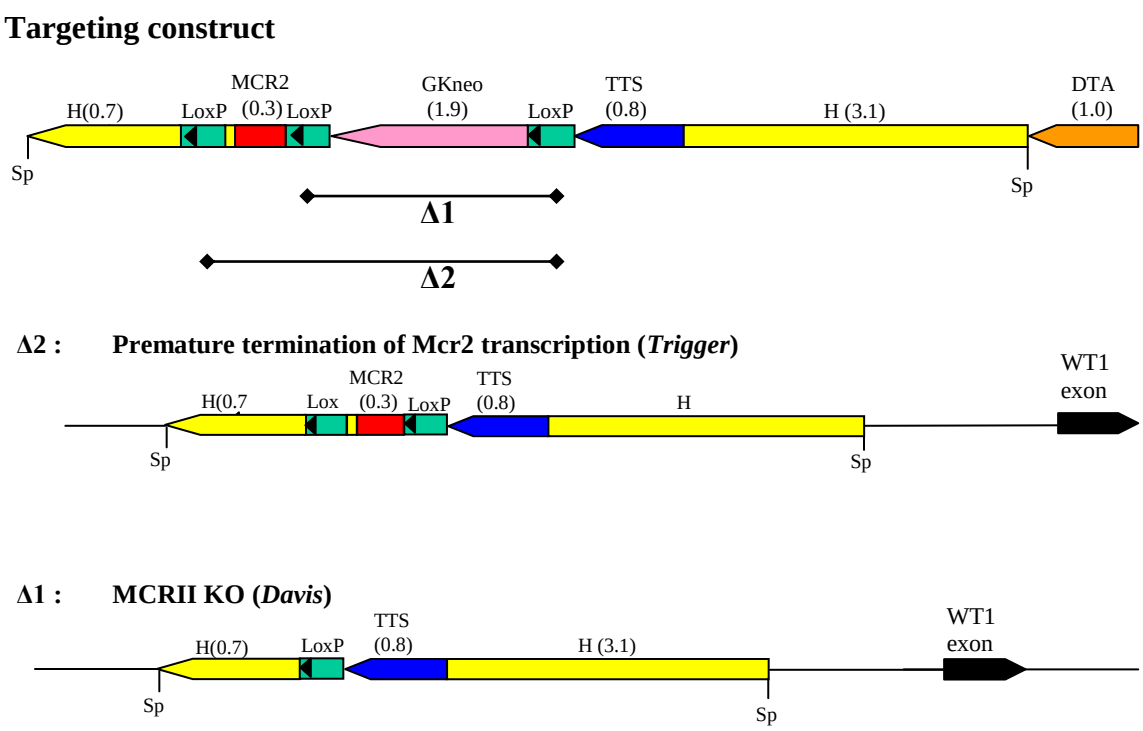

Figure 1.10 Targeting constructs upstream at the 5' region of the *WT1* locus. At the top shows the construct before genomic rearrangements were made from LoxP recombination. In middle Δ2 construct (*Trigger*) shows Mcr2 flanked by LoxP sites and a transcriptional terminator sequence (TTS). These elements are surrounded by homologous regions (H). At the bottom Δ1 (*Davis*) shows the same organization but without Mcr2. Image provided by Dr. Kim Moorwood and Dr. Joanne Stewart-Cox. This figure was reproduced with permission of the author.

Aims

1. To look at conservation of Mcr2 in vertebrates.

2. To establish whether the WT1 antisense gene is indeed truncated in the mutant mouse.

3. To characterize the role of an endogenous antisense transcript in the regulation of expression from the mouse Wt1 locus:

3.1 To determine whether the introduced mutation results in any changes in the expression of sense Wt1 and Awt1 at the level of mRNA or protein.

3.2 To establish if the introduced mutation results in any phenotypic changes.

Chapter 2 Materials and Methods

2.1Bioinformatics analyses

2.1.1 Vertebrate conservation analyses

Multiple alignments of 30 vertebrate species were performed using the NCBI genome Browser and the July 2007 (NCBI37/mm9) mouse genome assembly. This was provided by University of California Santa Cruz (http://genome.ucsc.edu, Rosenbloom *et al*., 2009). The multiple alignments were generated using "multiz" and other tools in the UCSC/Penn State Bioinformatics comparative genomics alignment pipeline. The conservation measurements were created using the "phastCons" package from Adam Siepel at Cornell University.

2.1.2 Open Reading Frame search

The analyses of possible start and stop codons of translational open reading frame (ORF) were performed by the Swiss Institute of Bioinformatics (http://www.isb-sib.ch/).

2.1.3 Protein structure prediction

The Protein Structure Prediction Server (PSIPRED) aggregates several of the structure prediction methods into one location and was used to predict protein structure. This was performed using the informatics browser (http://bioinf.cs.ucl.ac.uk/psipred)

2.1.4 CpG island prediction

A CpG island search was made using the public server provided by the European Bioinformatics Institute (http://www.ebi.ac.uk/).

2.1.5 QTL

The Map of Quantitative Trait Loci (QTL) was obtained from Mouse Genome Informatics (MGI), annotated by NCBI (http://www.ncbi.nlm.nih.gov) and made by

the Mouse Genome Database (MGD): mouse biology and model systems (http://www.informatics.jax.org, Bult *et al*., 1999).

2.2 Mice usage

2.2.1 Animal husbandry

All animals were maintained in accordance with the United Kingdom Home Office Regulations of animal studies. This involves on an artificial light/dark cycle, receiving 13 hours of light and 11 hours of darkness (including 30 min of false dawn and dusk lightning). Ambient temperature was kept at 21± 2ºC and a relative humidity of 55± 10%. Cages were individually ventilated with a housed density of up to 6 animals per cage. Animals were provided with food (CRM formula, Special Diets Services; Witham, Essex, UK) and water *ad libitum*.

2.2.2 Methods of sacrifice

Animals used during the course of this study were culled according to the Home Office Schedule 1 Kill. Embryos were sacrificed by immediate immersion in ice cold PBS upon removal from the uterine horns. Neonatal animals were sacrificed by decapitation due to the requirement for intact organ tissue. Adult animals were sacrificed by cervical dislocation.

2.2.3 Mouse lines with genetically modified Mcr2

The Mcr2 *Davis* and *Trigger* lines used in this study were generated from a gene-tageted embryonic stem cell line. The gene targeting construct shown in Figure 1.10 was integrated into a genomic location upstream Wt1 promoter. Chimeras were generated by Dr Kim Moorwood and Dr Joanne Stewart-Cox. Mosaic LoxP re-arrangements were induced by crossing gene-targeted mice with mencre 40 mice. Both lines were maintained on 129/C56BL/6/CBA mixed background.

2.2.4 Genotyping of mice

Genotyping of mice was done by polymerase chain reaction (PCR) (see Section 2.5.4). Biopsy samples were dependent upon the developmental stage of the whole animal, as follows: embryo, tail clip; neonate, tail clip; adult, ear clip.DNA was

prepared by boiling tissue for 10 min in 600 µl of 0.1 M NaOH. Samples were then neutralized by addition of 50 µl 1 M Tris-HCl pH8.0 and vortexed for 30 sec. 1 µl of each boiled sample was used as template each PCR.

2.3 Histological analyses

2.3.1 Postnatal organ dissections

Neonatal and adult mice were sacrificed as described in section. Whole body weight was recorded. Individual organs were then dissected from the body. Tissues were dabbed dry of fluid and their weights recorded.

2.3.2 Fixation and wax embedding of tissues

Dissected tissues were biopsied and incubated into PBS containing 4% PFA (w/v paraformalidehyde, Sigma-Aldrich) overnight at 4ºC. The following day organs were washed briefly in PBS then transferred to 70% ethanol and stored at 4ºC until processed (no later than 72 hr following fixation). Processing was carried out in a Leica TP machine with 2x 2 hour washes in 70% ethanol, 90% ethanol, 100% ethanol, histoclear clearing solution, followed by 3x 2 hour washes in 40ºC molten wax (Raymond Lamb). Following processing, tissues were embedded in 40ºC molten wax within histology cassettes and allowed to cool until solid on a 4ºC cooled platform embedding station (Leica, EG1160).

2.3.3 Sectioning of wax embedded tissues

Sections of 8 um in thickness were cut using a microtome (Leica, RMA2155) and placed onto Superfrost plus coated slides (Fisher) (antibody staining) or APTS subbed sides (for histological staining), dried at 38ºC overnight then stored a t 4º C.

2.3.4 Subbing slides with APTS

Slides were initially washed in hot soapy water followed by thorough rinsing in hot water and a quick rinse in reverse osmosis (RO) water then in a solution of were then placed in to 2% 3-triethokysilpropilamine (APTS) in acetone for 10 min followed by

rinsing twice in acetone for 10 sec the twice in RO water for 10 sec. Finally slides were baked dry at 37ºC.

2.3.5 Hematoxylin and eosin (H&E) staining of sectioned tissues

Slides with 8 µm wax sections were washed twice in histoclear clearing solution (National Diagnostics) for 2 min to remove wasx. The slides were then hydrated though a descending ethanol series for 2x 1 min each in 100% ethanol followed by 1x 1 min each in 95 ethanol, 90% ethanol, 70% ethanol, 50% ethanol. The slides were placed in milliQ water for 1 min before staining in hematoxylin for 15 min. To eliminate non-specific binding of haematoxylin, slides were placed under gently running tap water for 3 min, followed by 30 sec wash in 1% concentrated ammonia (NH3) in 70% ethanol and a final 30 sec wash in 70% ethanol. Slides were then dehydrated through an ascending ethanol series for 3 sec and 70% ethanol, 5 sec in 95% ethanol, 2x 1min in 100% ethanol, washed twice in histoclear solution for 2 min each and mounted using DPX mount (Sigma) overlaid with coverslip.

2.3.6 Periodic acid-Schiff (PAS) staining

Slides with 8µm wax embedded organ sections were washed twice in histoclear clearing solution (National Diagnostics) for 2 min to remove wax. The slides were then hydrated through descending ethanol series for 2x 1 min in 100% ethanol followed by 1x 1 min each in 95% ethanol, 90% ethanol, 70% ethanol, 50% ethanol. The slides were placed in milliQ water for 1 min then transferred to freshly prepared 1% periodic acid for 6 min. Slides were washed by placing them under gently tap water for 3 min then into miliQ water for 1 min. Staining was carried out at room temperature in Schiff's reagent (Sigma) fro 15 min. Slides were washed by placing them under gently running tap water for 5 min then counter staining in haematoxylin for 1.5 min. Finally slides were dehydrated through an ascending ethanol series as in section 2.3.5, washed in histoclear twice for 2 min each then mounted using DPX mount (sigma) overlaid with a coverslip.

2.4 Other analytical methods

2.4.1 Dual X-ray absoptiometry analysis (DXA)

Body composition was quantified by subjecting whole carcasses of adult mice to DXA analysis using a PIXImus scanner (Lunas Maddison; WI, USA) with small animal software. Physiological parameters recorded included total area, total weight, lean weight, fat weight, bone mineral density (BMD) and bone mineral content (BMC) (Samuels *et al*., 2001).

2.4.2 Urine collection from mice

Urine samples were collected form mice either by scruffing and holding a 1.5 ml microcentrifuge tube under urethra or by individually housing the mice in cages without sawdust and using a Pasteur pipette to collect urine from the bottom cage. The urine samples were immediately frozen until needed.

2.4.3 Urine Osmolarity

Urine osmolarity was measured by Micro-Osmometer 3300 (Advanced instruments, USA). To measure samples a tip was loaded with 20 µl of sample. Before starting test the sampler was within the operating cradle and beneath the cradle top. To start the test the entire operating cradle was pushed down until it reached a positive stop. After one minute the machine displayed a reading.

2.4.4 Urine composition analyses

Electrolytes (Na^+ and K^+) were measured by indirect ion selective electrode (ISE). Creatinine was detected and measured by the Jaffe method. Urea was quantified by using kinetic UV spectrophotometer. Urine composition analyses were performed by Dr. David Jeffrey at the NHS in Bristol.

2.4.5 Statistical analyses

All statistical analyses were performed using GraphPad (v3.0 Graphpad Software, CA, USA). The exact tests employed for each analysis are denoted in the corresponding figure legends in Chapter 5. One way ANOVA non-parametric was performed for comparing three groups. This was followed by Tukey test. For comparing two groups T-student was employed.

2.5 Molecular Biology Techniques

All solutions were made according to Sambrook and Russell (2001) with purified and deionised water, prepared with the MilliQ water filtration system (Millipore Corporation, MA, US) using reagents supplied by Fisher Scientific unless otherwise mentioned.

2.5.1 Agarose gel electrophoresis

Agarose gels were made using between 1 % and 2% weight per volume (depending on the nucleic acid expected) by melting agarose (invitrogen) in 1x TAE (0.04M Tris-acetate, 0.001M EDTA pH 8.0). Before pouring into a gel casting tray, 2.5 ul of ethidium bromide (10mg/ml) per 50 ml agarose was added to allow visualization of nucleic acids. One sixth volume 6X loading dye (Promega) was added to each DNA/RNA sample before loading into the wells of the gel. Samples were electrophoresed at 90-100V for 45min or until the DNA ladder was separated. The DNA or RNA samples were visualized under uv light. When RNA samples were run, the gel tank, gel tray and combs were soaked first with 3% hydrogen peroxide for 30 min, then rinsed with sterile diethyl pyrocarbonate (DEPC)-treated water (1ml DEPC 0.1% (Sigma Aldrich) v/v). Nucleic acids were viewed under uv radiation and photographed using an Alpha imager 3400.

2.5.2 RNA isolation from tissue samples

After schedule I Killing (2.2.2). Organs, whole embryos or tissue biopsies were isolated and snap-frozen in liquid Nitrogen. RNA was purified from frozen samples using TRI reagent (Sigma Aldrich), following the manufacturer's instructions. 50-100 mg tissue was homogenized thoroughly in 1 ml ice-cold TRI reagent using a T8.01

homogenizer (GMBH and Co., Germany). Samples were stored for 5 min at room temperature. After the incubation 0.2 ml chloroform per 1 ml of TRI reagent was added, vortexed and centrifuged at 12,000 x g for 10 minutes in a microcentrifuge at 4ºC. Aqueous phase was placed in a new tube where RNA was precipitated with one volume isopropanol v/v and centrifuged at 12,000 for 8 min 4ºC. Washes were made with 75% ethanol and subsequent centrifugation at 7,500 g for 5 min. The RNA pellet was air-dried for 3-5 min. RNA was resuspended in RNase-free water.

2.5.3 cDNA synthesis

For semi-quantitative reverse transcription PCR (RT-PCR) 1 µg of DNase I-treated RNA using RNA used for cDNA synthesis was first treated using the "DNA-free" kit (Ambion) which contains DNAseI, to remove contaminating genomic DNA (as per manufacturer's protocol). Sample was heated to 65 ºC for 5 minutes in a G-Storm mark 1 thermal cycler in a total volume of 13 µl. with 1 mM dNTP mix (Invitrogen) and 5 uM random primers (Promega). The thermal cycler was paused and samples incubated on ice for 1 min. The SuperScript III reverse transcriptase system (Invitrogen) was used to synthesize cDNA. A control as set up for each sample, in which the reverse transcriptase enzyme was omitted, permitting accurate interpretation of subsequent PCR amplification. For strand specific cDNA synthesis RNA samples, sense or antisense primer and dNTPs were heated at 65 ºC amplification and then placed on ice for one minute. Then all components except SuperScript III reverse transcriptase were mixed and centrifuged. The mix of reaction was then incubate at 25 ºC for 2 minutes. Immeditly after the reverse transcriptase was added and incubated at 25ºC (10 minutes), 65ºC (50 minutes) and 70ºC (15 minutes). cDNA samples were then stored at -20ºC.

2.5.4 Polymerase Chain Reaction

1 µl of template (e.g. 0.1-1 µg purified genomic DNA, 5-50 pg plasmid DNA, cDNA, bacterial colony lysates, or ear clip was used for PCR. Samples were amplified in a total volume of 15 µl containing 1X GoTaq Green master mix (Promega, USA) and 0.6 µM each relevant primer using the following experimental parameters: Initial denaturation, 5 min 94ºC followed by 25-40 cycles of 30 sec at 94ºC, 30 sec at 60ºC,

30º sec at 50-68ºC and completed with a final extension step of 5 min at 72ºC. Conditions for specific primer pairs are described in Table 4.1 Fragments longer than1.5 kb were amplified using a high performance polymerase Kod Hot-start DNA polymerase (Novagen-Germany), according to the manufacturer's instructions. Amplification of all samples was performed on a G-Storm mark 1 thermal cycler (Gene Technologies Ltd., UK). DNA oligonucleotides used as PCR primers were purchased commercially (Invitrogen, UK). PCR products were visualized by agarose gel electrophoresis (see Section 2.5.1).

2.5.5 Real time quantitative PCR

Comparative quantification of RNA levels real-time PCR was performed using SYBR green technology on an Mx3000P detection system (Stratagene). The 20 mL reactions were performed using Platinum SYBR Green qPCR supermix-UDG (Invitrogen). Samples were normalized relative to the housekeeping gene Tbp. This experiment was performed by Dr. Anne L. Hancock, University of Bristol, UK.

2.5.6 Western blotting

Whole neonate kidneys were homogenized in 1 ml Igepal CA-630 lysis buffer (50mM Tris-HCl pH 8.0, 150 mM NaCl, 1% (v/v) Igepal CA-630 (Sigma Aldrich), plus one protease inhibitor cocktail tablet (Roche) per 10 ml buffer). Samples were incubated on ice for 30 min to permit cell lyses and passed through a gauge needle 5 times. Suspensions were centrifuged at 100,000 x g for 30 min (Beckman TL-100 ultracentrifuge) at 4ºC and the pellet discarded.

Total protein concentration was determined using the BCA protein assay kit (Pierce, USA) and samples stored at -20ºC. 20 µg of each sample was mixed with 2x reducing sample buffer (250 mM Tris HCl pH 6.8, 2% (w/v) SDS, 10% (v/v) glycerol (Sigma Aldrich), 10% (v/v) β-mercaptoethanol (Sigma Aldrich), 0.02% (w/v) bromophenol blue (Sigma Aldrich), heated to 95ºC for 5 min then kept on ice. Samples were loaded onto a polyacrylamide gel (resolving gel: 8% polyacrylamide (National Diagnostics, GA, USA), 0.37 M Tris-HCl pH 8.8, 0.1% SDS, 0.05% ammonium persulfate (AMPS) (Sigma Aldrich), 0.05% TEMED (Sigma Aldrich); stacking gel: 5%

polyacrylamide, 0.12 M Tris-HCl pH 6.8, 0.0% AMPS, 0.1% TEMED) alongside pre-stained protein standards (Fermentas, UK), and run at 100 V for 90 min in running buffer (0.1% SDS, 25 mM Tris-HCl, 208 mM glycine (Fluka, Sigma Aldrich). Protein was transferred onto PVDF membrane (Bio-Rad Laboratories) by wet transfer (25 mM Tris, 192 mM glycine, 20% (v/v) methanol (Fisher Scientific) Transfer Buffer. All subsequent incubations were performed on an orbital shaker. The membrane was blocked in TBS-T (recipe) with 5% powdered skimmed milk (Tesco, UK) for 2 hours at room temperature. Primary antibodies were diluted in TBS-T (50mM Tris-HCl pH 7.4, 200 mM NaCl 0.01% Tween-20) and %5 powdered milk (see Table X.X for antibody concentrations used) and applied to the appropriate membranes. Overnight incubation was performed at 4ºC. Membranes were washed three times in PBS-T for 15 min per wash, and incubated in peroxidase-conjugated goat anti-rabbit secondary antibody (Vector Laboratories, CA, USA) diluted 1/10,000 in TBS-T with 5 % powdered milk and applied to the membrane for 1 hour at room temperature (Table 2.2). Three further washes were performed as before and protein detection was achieved using the ECL-Plus system (GE Healthcare), as directed by manufacturer. Autoradiography film (GE Healthcare) was developed using an X-ray processor.

2.5.7 Immunohistochemistry

Tissue sections were prepared from wax blocks as in section 2.3.3. Slides were prepared as in section 2.3.5. Antigen retrieval was done by boiling slides in urea solution (0.8M, pH6.4) for 2 x 10 min in a microwave oven. This was followed by a 10 min PBS wash. All washes were performed at RT on rocking platform. Each section was drawn around section with a wax pen. Incubation with the primary antibody was done by dilution in 0.1% BSA/Blocking serum.Non-specific binding was blocked for 20 min with 1 drop serum per 3.3 ml PBS. This was followed by PBS wash with gentle shaking 2x 5min. Before blocking non-specific binding the slide was drawn around the section with a wax pen. Blocking was subsequently done for 20 min (1 drop blocking serum 3.3ml 1XPBS) overnight at 4°C. After incubation washes were done with PBS/0.25% Triton X-100 wash 1x 5 min then PBS with gentle shaking 1x 5 min. Biotinylated secondary antibody was incubated for 30 min

(3 drops serum in 10ml PBS with 1 drop 2° antibody) at RT. Washes from incubation were performed using PBS/0.5% Triton X-100 1x 30 min then PBS 1x 5 min. In order to quench endogenous peroxidase activity sections were incubated 5 min with 3% Hydrogen Peroxide (H_2O_2 (Sigma Aldrich) (w/w) solution. This was followed by a wash in PBS 1x10 min. Pre-formed AB complexes (vector) were applied to the sections for 30 min at RT then washed in PBS with gentle shaking 1x 10 min. DAB staining was used to detect anybody complexes, this was applied for 5 min (DAB peroxidase substrate kit (Vector). Excess stain was removed by washing in running tap water for 5min. Haematoxylin counterstain was applied as in then slides were dehydrated, cleared and mounted under a coverslip as in section 2.3.5.

Table 2.1 List of primers used for PCR

Primer name	Sequence	Product size	Annealing temperature
A B	$^{5'}$CAAAGTTGAATCTGGGGTCAGG$^{3'}$ $^{5'}$GACGCCACACCACGGGTTCC$^{3'}$	297 bp	58 º
TF S	$^{5'}$CCCAGTTCTGCCTGGTCTTTC$^{3'}$ $^{5'}$CTGGTGCAGATGCAAATTTGC$^{3'}$	WT= 1,002 bp D=1.46 kb	58 º
CNlong B	$^{5'}$AGATGGTGCGCTCTGGACTGG$^{3'}$ $^{5'}$GACGCCACACCACGGGTCC$^{3'}$	243	60º
Actin F R	$^{5'}$ GACCCGATCATGTTTGAGACC$^{3'}$ $^{5'}$GTTGGCATAGAGGTCTTTACGG$^{3'}$	620 bp (DNA) 530 (RNA)	60 º
Lox2x2-5P MWTPro-R	$^{5'}$AGGCAGGAGGATCGGAAGTTC$^{3'}$ $^{5'}$AGCTCAAATAAGAGGGGCCGGCAG$^{3'}$	270 bp	54 º
SF VR	$^{5'}$GCAAAATTTGCATCTCGCACC$^{3'}$ ^{5}GCTCATTTCCAGACTAGCGC$^{3'}$	Strain dependent	58 º

Table 2.2 Primary and secondary antibodies utilized for Western blotting and immunohistochemistry.

Primary Antibody	Secundary	Dilution
α-Tubuline	α-mouse	1:30,000
C-19	α-rabbit	1:100
6HF2	α-mouse	1:100

Chapter 3: Insights into Mcr2 sequence and conservation analysis

3.1 Introduction

In mouse as well in human transcription upstream of *WT1* is abundant and has not fully described in the literature and has unknown function. In order to elucidate their biological function we set out find conserved elements within this region which we predicted might fulfill this putative functional role.

As described in Section 1.3.3 two genomic sequences were previously discovered in human and mouse with a high level of sequence conservation named Mcr1 and Mcr2 both within 20 kb upstream of *WT1* exon 1 (Figure 1.6). Mcr1 was longer in length with a lower overall sequence identity and further upstream from *WT1*. Therefore the present work was focused on Mcr2 (sequence shown in Figure 3.1). Due to the high level sequence identity between human and mouse Mcr2, was of interest to extend the conservation analyses to other vertebrate species. This was also carried on for other relevant sequences such as Mcr1, reported neighbouring transcripts, *Wt1* exonic sequences and known ncRNAs.

In the case of Mcr2 we also looked at ultraconserved sequences which are defined as DNA fragments of at least 100 bp with 100% sequence identity between mouse, human and rat (Bejarano *et al*., 2004). These may have functional roles, particularly as transcriptional enhancers (Pennachio *et al*., 2006). However ultraconserved elements represent a class of genetic elements whose functions and evolutionary origins remain to be determined. In order to predict other possible functional features of Mcr2, its sequence was analyzed for putative open reading frames (ORF). Protein coding sequences are more highly conserved than sequences expressed as ncRNA. Therefore we wished to establish whether Mcr2 might have protein coding capacity. All six possible translational ORF were tested. Start codons were not considered necessary because Mcr2 could represent a single exon belonging to a longer spliced mRNA. Thereby using software analysis we were able to look at protein structure predictions as well as predicting matrix attachment regions (MARs) within Mcr2.

Previous evidence showed that untranslated conserved regions have a role as a transcriptional enhancers (Pennacchio *et al*., 2006). Due to the high identity between Mcr2 in mouse and human it has been previously tested and shown to be an enhancer element in lacZ reporter transgenic mice (unpublished observations, Colin Miles, personal communication). In a recent study an element comprising part of Mcr2 was also identified as a zebrafish transcriptional enhancer. This element was found to bind members of the retinoic acid receptor family factors and to mediate responsiveness to retinoic acid (Bollig et al., 2009). However this sequence has not previously been functionally characterized in any mammalian model. In a different aspect we also ran CpG island predictions for Mcr2 and its local genomic sequence environment and looked in to Quantitative Trade Loci shown to map to Mcr2 on the NCBI database.

ttatcatttctaggttaaaaacataaaaacacaaatactttgaaagaattttctaaggtgagaagattaaagtctctgtcataagt
tctcctcctcctcctcctcctcctcttcttctttttcttcttcttccttttttttttcaccgcccccacccTTGTTTGCAAAGT
TGAATCTGGGGTCAGGAGTTCTAATTGTAACCTCAGACTGGAATTCCAGA
TGGTGCGCTCTGGACTGGAAGCAACTCTCAGTTCATCAATTTCATGGGCTT
CCATATCTGCTCTGGCCACGGCCTGGTCTCCATCCCCACTGTGGCATTAAT
GCAGAACAAATTGAGACATATCCTCTATATAATTAGTTCCAGAATTTAAA
AAGATTTACGGGATAATAATAGAAGCAGCGCTGCTGAATCCTTTCATTGG
TGGCTCTTGGGGAGCTGGGGAACCccgtggtgtggcgtcaaaacactgcggctccaggcaccag
gaactgggggaagggcaaaatttgcatctcgcaccaggcagtgctaggtggtttaggtggttttagccccttaaccaggcc
agggaggagagtttgaagcccagatggaaggtt

Figure 3.1 Mcr2 sequence. The mouse Mcr2 DNA sequence is shown in capitals (Total length 298 bp) in C57BL/6 strain flanked by contiguous sequence in non-capitals. The mouse Mcr2 (5'-3') sequence in capitals sequence and highlighted in red showing total length of 298 bases in C56/B6 strain flanked by contiguous fragments in non-capitals.

3.2 Results

3.2.1 The *Wt1* antisense locus

Upstream from the mouse *Wt1* promoter a number of spliced and unspliced (see Figure 3.2) antisense transcripts have been reported in testis, spleen and ovaries (See Appendix, Supplementary Table 1). From these only the unspliced AK172697 overlaps with *Wt1* promoter (by 15 nucleotides). AK165089 and also AK161318

appear to initiate immediately upstream of the *Wt1* promoter, being transcribed in the opposite direction to *Wt1* mRNA. These two transcripts are spliced to sequences very far upstream from *Wt1* (about 30 and 50 kb from *Wt1* promoter respectively) (Figure 3.2), so that none of these two reported RNAs include the Mcr2 sequence. In fact Mcr2 is not present in the Genbank database as an expressed sequence at all (Figure 3.2). In case of the human locus Mcr2 is present in transcripts, some of which overlap *Wt1* exon1, been originated in intron1 (Malik *et al*., 1995) (Figure 3.3).

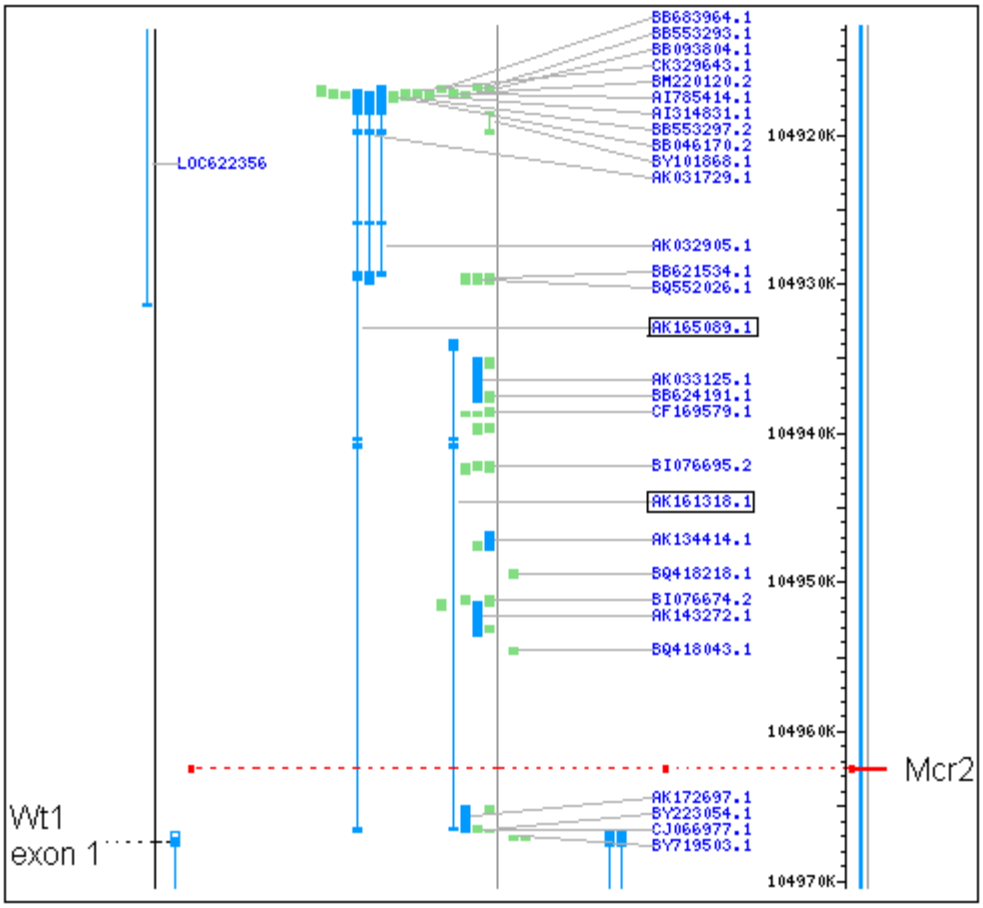

Figure 3.2 Transcripts reported within 55 kb of mouse *Wt1*. Mcr2 is marked in red, and is positioned 4.613 kb from *Wt1*. Far left, *Wt1* gene; middle, blue boxes: cDNA exons from specific tissue; green boxes: from mRNA without described source. For full description of source of all those cDNAs and mRNA see Appendix, Supplementary Table 1. Far right, chromosome 2 sale bar (kb). Highlighted transcripts splice out Mcr2. Figure adapted from NCB1 screen-dump.

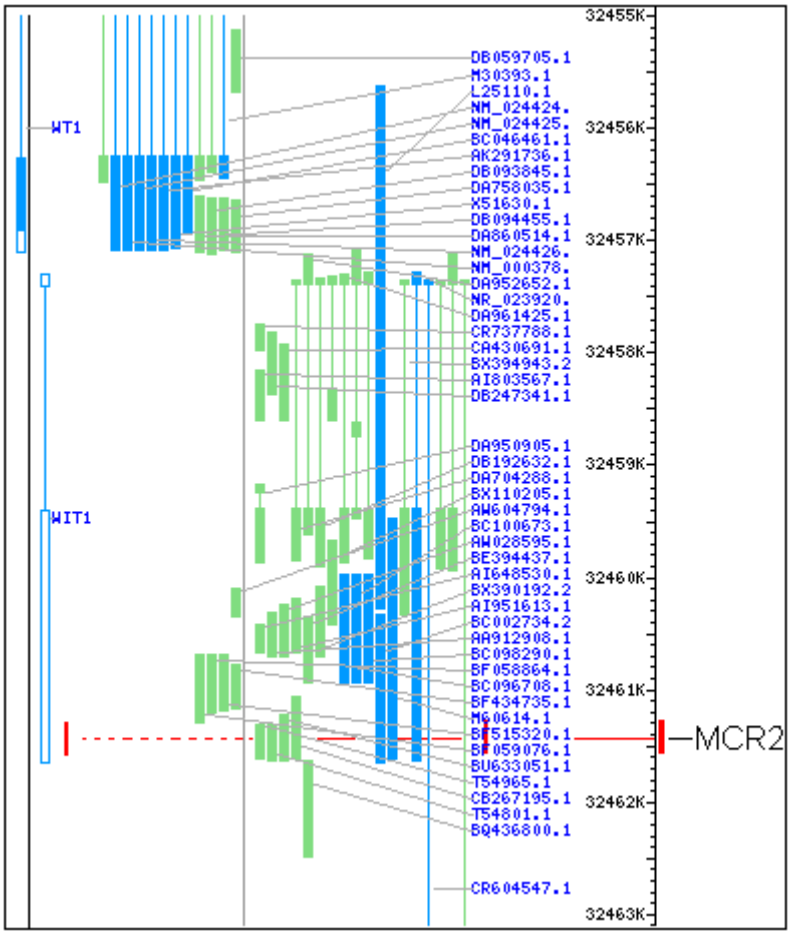

Figure 3.3 Transcripts reported within 8 kb upstream of human *WT1*. Scheme shows transcription reported within 8 kb of human *WT1*. MCR2 is marked in red. Far top left blue box is *WT1* (exon 1) followed down by *WIT1* (*WT1-AS*). Middle blue boxes: cDNA exons from specific tissue; green boxes: from mRNA without described source. For full description of source of all those cDNAs and mRNA see Appendix Supplementary, Table 2. Far right, chromosome 2 scale bar (kb). Figure adapted from NCB1 screen-dump.

3.2.2 Predictive analyses of functional properties of the Mcr2 sequence

3.2.2.1 Open reading frames at Mcr2

All six possible translational reading fames were interrogated in order to elucidate the protein coding capacity of Mcr2 (Figure 3.4). This was performed by using the public server provided by the Swiss Institute of Bioinformatics (http://www.isb-sib.ch/). The longest ORF was found on the sense 5'-3' translation frame 3, with a total of 65 amino acids including start and stop codons (4 kDa of predicted protein mass), 40 amino acids within Mcr2, then continuing towards *WT1*. Due to the minimal length of each

ORF it seems unlikely that Mcr2 is translated into a peptide. The lack of predicted translation of Mcr2 suggests that it may exist as a part of the ncRNA class.

5'-3' Frame 1
L S F L G **Stop** K H K N T N T L K E F S K V R R L K S L S **Stop** V L L L L L L L L F F F F F F F L F F
S P P P **PL F A K L N L G S G V L I V T S D W N S R W C A L D W K Q L S V H Q F H G L P Y L L**
W P R P G L H P H C G I N A E Q I E T Y P L Y N Stop F Q N L K R F T G Stop Stop Stop K Q R C
Stop I L S L V A L G E L G N P V V W R Q N T A A P G T R N W G K G K I C I S H Q A V L G G L G
G F S P L T R P G R R V **Stop** S P D G R
5'-3' Frame 2
Y H F **Stop** V K N I K T Q I L **Stop** K N F L R **Stop** E D **Stop** S L C H K F S S S S S S S S S S S F S S S
S F F F H R P H P **C L Q S Stop I W G Q E F Stop L Stop P Q T G I P D G A L W T G S N S Q F I N**
F Met G F H I C S G H G L V S I P T V A L Met Q N K L R H I L Y I I S S R I Stop K D L R D N N R S
S A A E S F H W W L L G S W G T P W C G V K T L R L Q A P G T G G R A K F A S R T R Q C **Stop**
V V **Stop** V V L A P **Stop** P G Q G G E F E A Q **Met** E G
5'-3' Frame 3
I I S R L K T **Stop** K H K Y F E R I F **Stop** G E K I K V S V I S S P P P P P P P L L L F L L L P F F F T
A P T L **V C K V E S G V R S S N C N L R L E F Q Met V R S G L E A T L S S S I S W A S I S A L A**
T A W S P S P L W H Stop C R T N Stop D I S S I Stop L V P E F K K I Y G I I I E A A L L N P F I G
G S W G A G E P R G V A S K H C G S R H Q E L G E G Q N L H L A P G S A R W F R W F **Stop** P L
N Q A R E E S L K P R W K V
3'-5' Frame 1
N L P S G L Q T L L P G L V K G L K P P K P P S T A W C E **Met** Q I L P F P Q F L V P G A A V F
Stop R H T T G **F P S S P R A T N E R I Q Q R C F Y Y Y P V N L F K F W N Stop L Y R G Y V S I C**
S A L Met P Q W G W R P G R G Q S R Y G S P Stop N Stop Stop T E S C F Q S R A H H L E F Q S
E V T I R T P D P R F N F A N K G G G G E K K R K K K K K K K R R R R R R R R T Y D R D F N L L
T L E N S F K V F V F L C F **Stop** P R N D
3'-5' Frame 2
T F H L G F K L S S L A W L R G **Stop** N H L N H L A L P G A R C K F C P S P S S W C L E P Q C F
D A T P R **G S P A P Q E P P Met K G F S S A A S I I I P Stop I F L N S G T N Y I E D Met S Q F V L**
H Stop C H S G D G D Q A V A R A D Met E A H E I D E L R V A S S P E R T I W N S S L R L Q L E
L L T P D S T L Q T R V G A V K K K G R R R K R R R G G G G G G G G E L **Met** T E T L I F S P **Stop**
K I L S K Y L C F Y V F N L E **Met** I
3'-5'Frame3
P S I W A S N S P P W P G **Stop** G A K T T **Stop** T T **Stop** H C L V R D A N F A L P P V P G A W S R
S V L T P H H G **V P Q L P K S H Q Stop K D S A A L L L L L S R K S F Stop I L E L I I Stop R I C L**
N L F C I N A T V G Met E T R P W P E Q I W K P Met K L Met N Stop E L L P V Q S A P S G I P V
Stop G Y N Stop N S Stop P Q I Q L C K Q G W G R **Stop** K K K E E E E E K E E E E E E E E E E E N L
Stop Q R L **Stop** S S H L R K F F Q S I C V F **Met** F L T **Stop** K **Stop Stop**

Figure 3.4 Mcr2 ORF prediction. Scheme showing predicted translation of the mouse Mcr2 region marked in grey and bold characters flanked by continuous neighbouring sequences. The largest possible translated region is given by the sense orientation 5'-3' on frame 3 shown underlined.

3.2.2.2 Secondary structure prediction

Because most of the ORFs were considered too short to encode proteins, the PSIPRED secondary structure prediction method (Bryson *et al*., 2005) was employed to elucidate if any discernable protein structural features were present on the longest ORF 5'-3' Frame 3. The PSIPRED Protein Structure Prediction Server aggregates into one location under several of the structure prediction methods. No metal response

elements were found or transcription factor motifs were found. However, its predicted amino acid sequence is expected to form a coil-helix-coil (Figure 3.5 B). Also a MAR motif was found by looking at possible matrix attachment region it also comprises amino acid 3 until 22 (Figure 3.5 A).

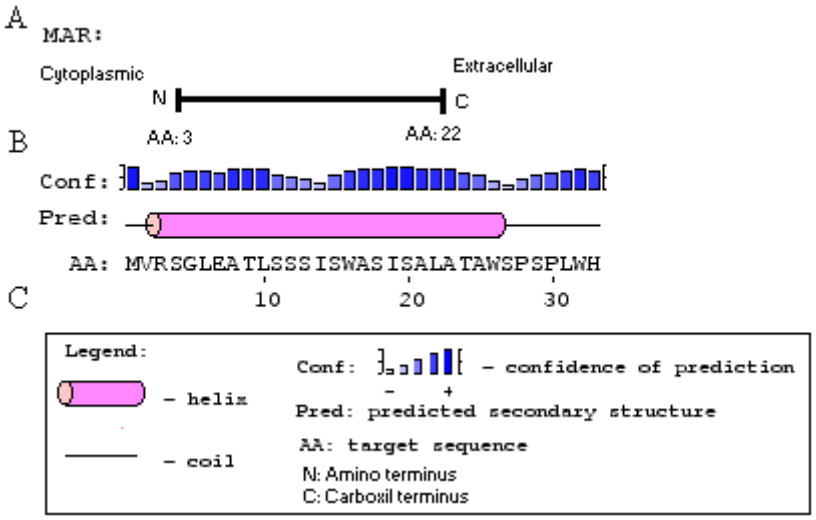

Figure 3.5 Schematic descriptions of secondary structures. (A) position of matrix attachment region; (B) position of helix domain; (C) legend related to B. Figure adapted from PSIPRED screen-dump.

3.2.2.3 CpG island prediction near Mcr2

Many developmental and in particular antisense ncRNAs genes have been found silenced due to hypermethylation. So that has been speculated that about half of mammalian genes, and, possibly every mammalian house-keeping gene have a CpG-rich region near by their 5' end (Bird, 1986). In *WT1* a CpG island cause hypermethylation associated with imprinting. In neoplasia occurs a different methylation pattern, aberrantly methylated region occurs in the first intron of the *WT1* gene in breast cancer (Laux *et al*., 1999) and ovarian cancer in *WT1-AS* (Kaenushi *et al*., 2004). To search for CpG islands software was used to define isochore plots GC content within 2 kb from Mcr2. After CpG analyses an island was found 481 bp from Mcr2 towards *WT1* direction (Figure 3.6).

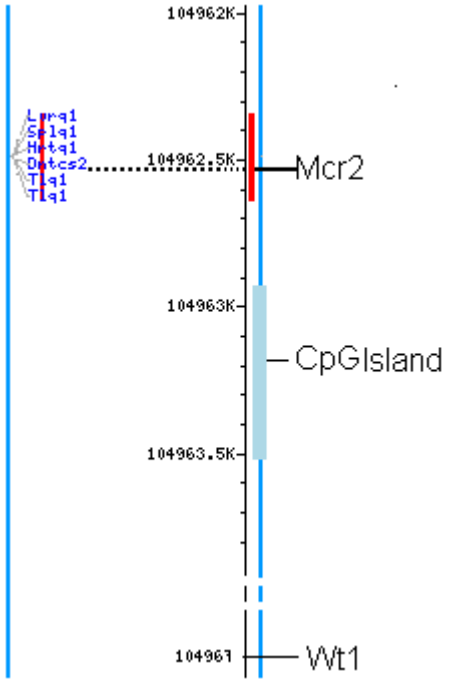

Figure 3.6 Map of Mcr2 including QTLs and CpG island spots. Scheme adapted from NCBI. Map viewer showing the positions of Mcr2 (red bar), contiguous CpG island (grey bar). Followed towards left by part of chromosome 2 from mouse strain C57BL/6. Far left, reported QLT (Lvrq1, Splq1, Hrtq1, Dntcs2, Tlq1, Tlq1 in blue) within Mcr2. Figure adapted from NCBI screen-dump.

3.2.2.4 Phenotype association for Mcr2 sequence.

Blast search of the mouse genome with Mcr2 identifies several QTLs annotated by Mouse Genome Informatics (MGI): Lvrq1, Splq1, Hrtq1, Dntcs2, Tlq1, Tlq1 (Figure 3.6). QTLs are large genomic sequences (several Mbp) linked to particular phenotypic traits in mice in this case. QTL markers called Hrtq1, Lvrq1 and Splq1 were discovered in heart, liver and spleen respectively by a linkage analysis performed on 552 10-week old male animals from a (M16i x L6) F2 intercross to identify QTLs associated with measurements of growth such as organ weight, growth rate, and adiposity. In heart, liver, and spleen weight differences were identified. L6-derived alleles conferred recessively inherited decrease in organ weight in the presence of these markers (Rocha *et al*., 2004).

More evidence was also found in studies of dental caries susceptibility using QTL analysis in mice. For this experiment genetic crosses of C3H/HeJ (caries-resistant)

and C57BL/6J (caries-susceptible) mice inoculated with Streptococcus mutants serotype C were performed. A region called Dntcs2 was identified as responsible for dental caries susceptibility (Nariyama *et al*., 2004). As suggested by the blast hit, variations in the Mcr2 sequence could be responsible for these traits. However the QTLs are very large and Mcr2 very small, so this is not very likely. In both cases organ weight difference (heart, liver, spleen) and susceptibility to dental caries have not been mapped to a gene so it remains plausible that these traits may map to Mcr2.

In a further QTL study to clarify the role of genomic elements associated with specific telomere length, two inter-fertile mice species were used, both harbouring dissimilar telomere length, *Mus musculus* (telomere length >25 kb) and *Mus spretus* (telomere length 5-15 kb). It was found that a QTL, Tlq1, for this trait which maps to chromosome 2 (Zhu *et al*., 1998). However subsequent work found that Tlq1 maps to a gene called *RTel* which is not very close to Mcr2 so in this case is confirmed to be a "miss mapping" (Ding *et al*., 2004).

3.2.3 Phylogenetic analysis of Mcr2

Conservation analysis of the *WT1* gene shows its presence throughout vertebrate genome evolution with some features specific to mammals as described earlier in Section 1.1.2.1. Other features such as the zinc fingers and the transregulatory domains are conserved between all gnathostome classes including the chick, alligator, X*enopus laevis* and zebrafish. However, the WT1+KTS isoform is found throughout the vertebrates whilst the 17 aa (+/-exon 5) deletion event is exclusive to mammals (Miles *et al*., 1998; Kent *et al*., 1995). Between mouse and human WT1 polypeptides an extremely high level of amino acid sequence conservation is observed (> 95%).

Functionally important elements are thought to be more likely to experience purifying selection pressure so that key regulatory domains involved in development are retained. Given that the genitourinary system has evolved considerably during vertebrate radiation, it has been speculated that the complexity of mammalian WT1 isoforms may be associated with changes to the genitourinary system. In contrast

alternative +/- KTS splicing might be linked to basic function conserved throughout vertebrate evolution.

The conservation of antisense RNAs at the WT1 locus has not been fully studied. As stated in section 1.2.2.1 antisense RNAs were first discovered in prokaryotes but are now recognised as being of great importance in the regulation of mammalian gene expression, in particular covering most of the transcription units of the mouse transcriptome, many of which appear to be lncRNAs, localized within the nucleus with or without polyadenylation (Lehner *et al*., 2002, Cheng *et al*., 2005). Many ncRNAs are of unclear significance and lack strong sequence conservation, prompting suggestions that they might be non-functional. Wang *et al*., (2004) stated that ncRNAs identified in a mouse cDNA library were poorly conserved, and therefore predicted to be non-functional. However, certain functional lncRNAs such as *Air* and *Xist* are also poorly conserved, which suggests that lack of conservation does not mean lack of function (reviewed in Pang *et al*., 2006). Nevertheless, miRNAs and snoRNAs are widely conserved among a diverse range of species (Huttenhofer, 2001; Lagos-Quintana, M. *et al.* 2001). Therefore, it might be that different types of ncRNAs can exhibit different patterns of sequence conservation, which can be expected as they are thought to play a variety of functions. Evolutionary conservation of sequences upstream of *WT1* could indicate novel functional regulatory domains. *WT1*-AS transcripts have been shown to be expressed in parallel to *WT1* in developing and paedriatic kidney *in vitro WT1-AS* levels affect *WT1* expression (Moorwood, *et al*., 1998).

In order to evaluate the conservation patterns of Mcr2 or other antisense elements upstream of *WT1,* alignments were performed using the genomes of 30 vertebrate species. The degree of sequence identity with the mouse genome was then calculated. Pair wise alignments with Mcr2 were generated using BLAT on DNA which is designed to find sequences of 95% and greater similarity (Kent, 2002) through the UCSC Genome Browser (http://genome.ucsc.edu, Rosenbloom, *et al*., 2010). Multiple alignments were generated using Multiz and other tools in the UCSC/Penn State Bioinformatics comparative genomics alignment pipeline. The conservation

measurements were created using the phastCons package from Adam Siepel at Cornell University. Details of the alignment parameters are noted in the genome wiki Mm9 multiple alignments. The evolutionary relationship used for conservation analysis is shown in Figure 3.7. Track displays of multiple alignments show three measures of evolutionary conservation across them all in one set. The vertebrate species tested were the placentals and euarchontoglires given below plus: Opossum, Platypus, Chicken, Lizard, Frog, Tetraodon, Fugu, Stickleback, Medaka, Zebrafish. Two more restricted groups were also tested to the euarchontoglires subset (10 species plus mouse): mouse, rat, Guinea Pig, Rabbit, Human, Chimp, Orangutan, Rhesus, Marmoset, Bush-baby, Tree Shrew. The euarchontoglires above plus: Shrew, Hedgehog, Dog, Cat, Horse, Cow, Armadillo, Elephant, Tenrec. The placental mammal conservation helps to identify sequences that are under different evolutionary pressures in mammals and non-mammal vertebrates. At the top of each alignment graphs resume mammal, euarchontoglires and vertebrates conservation. Gap annotation for all Figures shown (3.8-3.18) were used as follows: **Blank,** no bases in the aligned species. Possibly due to a lineage-specific insertion between the aligned blocks in the mouse genome or a lineage-specific deletion between the aligned blocks in the aligning species. **Double line:** aligning species has one or more unalignable bases in the gap region. Possibly due to excessive evolutionary distance between species or independent deleted regions between the aligned blocks in both species. **Pale yellow coloring:** aligning species has Ns in the gap region and reflects uncertainty in the relationship between the DNA of both species, due to lack of sequence in relevant portions of the aligning species. This description applies for all graphs.

Mcr1 was found to be mammalian specific (Figure 3.10) whereas Mcr2 was found to have partial conservation from medaka to rat (Figure 3.8). Mcr2 has a specific domain that is conserved from medaka to rat (except for the chicken) and another domain that is exclusive to non-fish vertebrates. In order to verify the limits of the conserved region up and downstream Mcr2, a wider sequence was analyzed. A preliminary PIPLOT (Figure 1.9) graph shows high conservation between human and mouse Mcr2 (98%), therefore it was expected that Mcr2 should appear as a plateau on

the alignment graph. Indeed this was confirmed to be the case. No further conservation was found outside the previously identified Mcr2 sequence (Figure 3.9). The genomic sequences of *Wt1* exon 1 and exon 1 A (codes for AWT1) were also analyzed (Figure 3.13 and 3.14). As expected *Wt1* exon1 shows a quite conserved pattern all across vertebrates. In contrast exon 1 A has a more conserved pattern within mammals plus the Lizard (Figure 3.14. Interestingly, exon 1 A shows more conserved region towards AWT1 code region, which is translated to protein. However exon 1 A did not show any conservation in Teleostei. In human it is known that *WT1-AS* and *AWT1* transcription originates in intron 1. Exon 1 A shows a poor conservation of its sequence outside of mammalian genomes. Indeed there is no conservation in aquatic vertebrates. This shows for the first time that *AWT1* is mammal+lizard-specific. In the case of euarchontoglires there is a more similar pattern of conservation of *AWT1* than the rest of mammals (Figure 3.14).

In Mcr2 two ultraconserved domains were identified, one of 112 bp and a second domain which of 111 bp (Figure 3.11 and 3.12). Phylogenic conservation of a transcript antisense to wt1, the cDNA isolated from 2 day mouse neonate ovary with an accession code AK165089 was also performed, and shown in figure 3.2 and 3.16. This transcript is spliced and includes exons up to 35 kb upstream of Wt1. Mcr2 itself is spliced out of AK165089. It contains significant ORFs with a maximum coding capacity of 86 amino acids. This element was found to share synteny with other murines but not with other vertebrates (Figure 3.16) Exons are more widely conserved than introns which suggest a function for the transcript. Traces of conservation appear to be from lower vertebrates becoming more extended in euarchontoglires. A more consistent pattern of conservation is observed in the unspliced antisense transcript that overlaps the *Wt1* promoter and was identified in spleen with accession number AK172697 (Figure 3.17). In this case it appears not well conserved in lower vertebrates, on the contrary is exhibit a more define pattern in euarchontoglires . This transcript also does not include Mcr2 sequence. Additionally conservation of two well known ncRNA transcripts conservation was analyzed. These were Wrap53 and H19. For the ncRNA H19, displays a wide conservation in mammals. In contrast Wrap53 has conserved domains at the

beginning and until the end of the transcript. Wrap53 has more synteny with the rat than all the rest of organisms (Figure 3.17 and Figure 3.18).

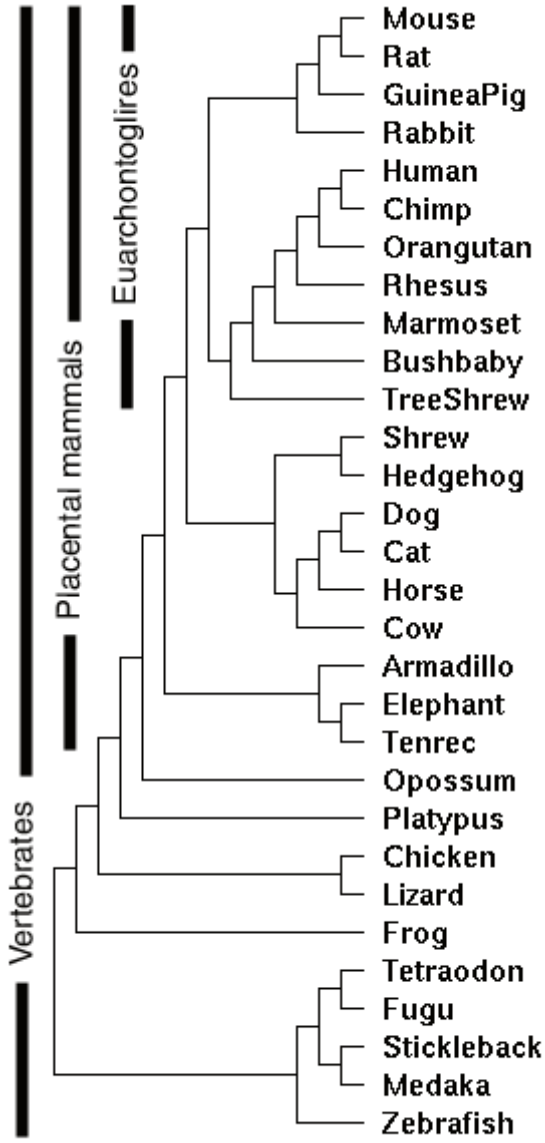

Figure 3.7 Phylogenetic distribution of vertebrate species used in the alignments.

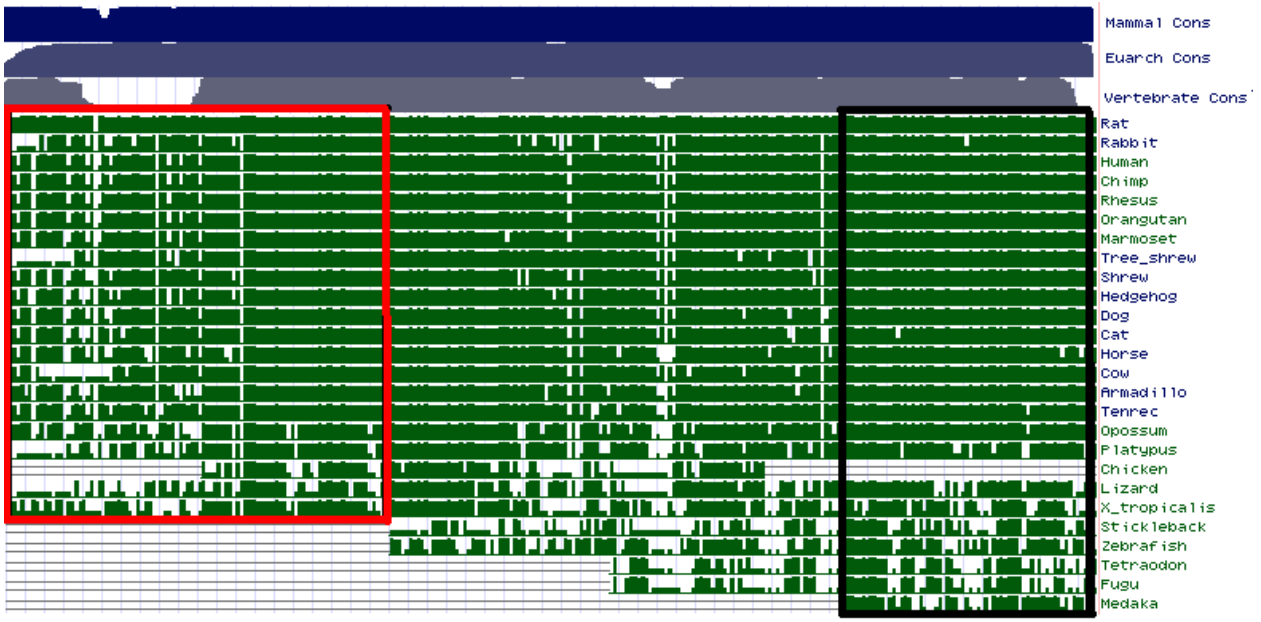

Figure 3.8 Alignments of vertebrate sequences with mouse Mcr2 (289 bp). Vertebrates conserved domain in which retinoic acid response element shown by the black square. Non-fish conserved domain vertebrates in red box.

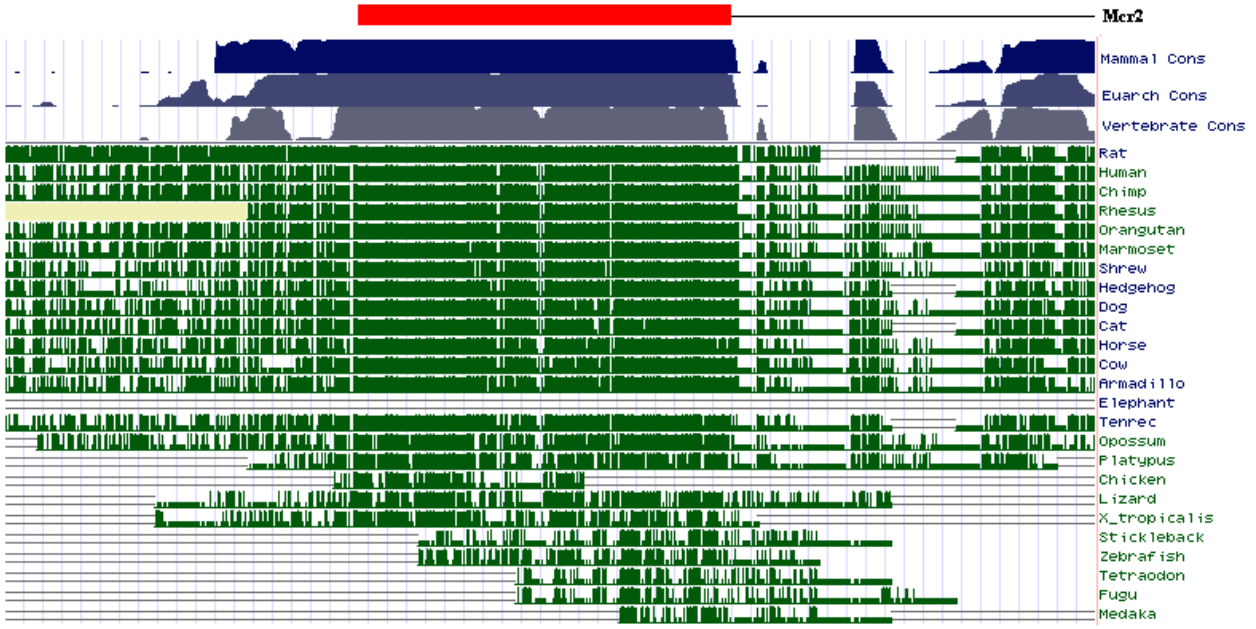

Figure 3.9 Mouse Mcr2 extended sequence alignment (599 bp). At the top Mcr2 position is referred in red bar.

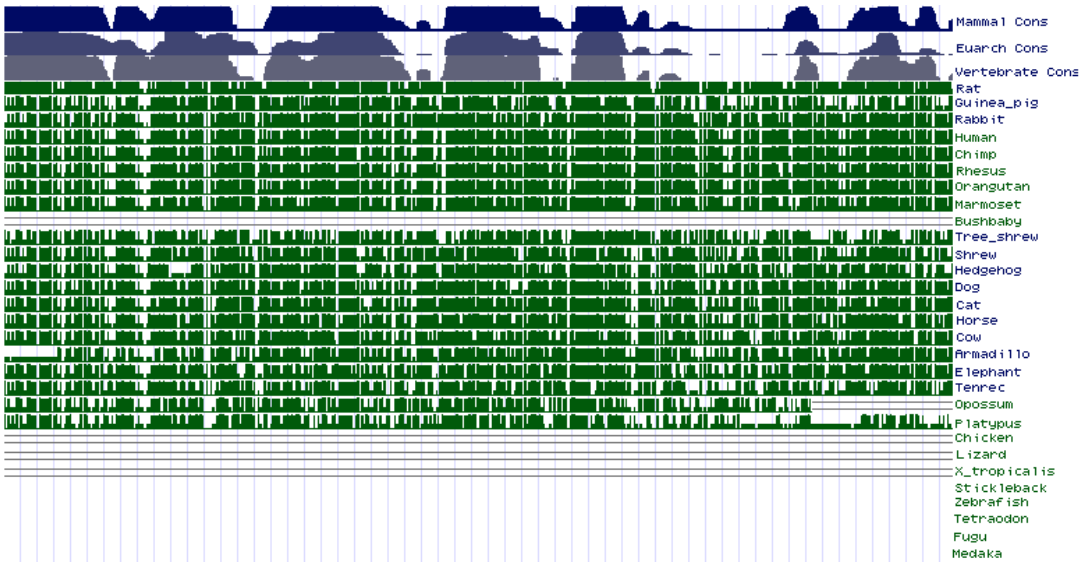

Figure 3.10 Mouse Mcr1 sequence alignment (495 pb).

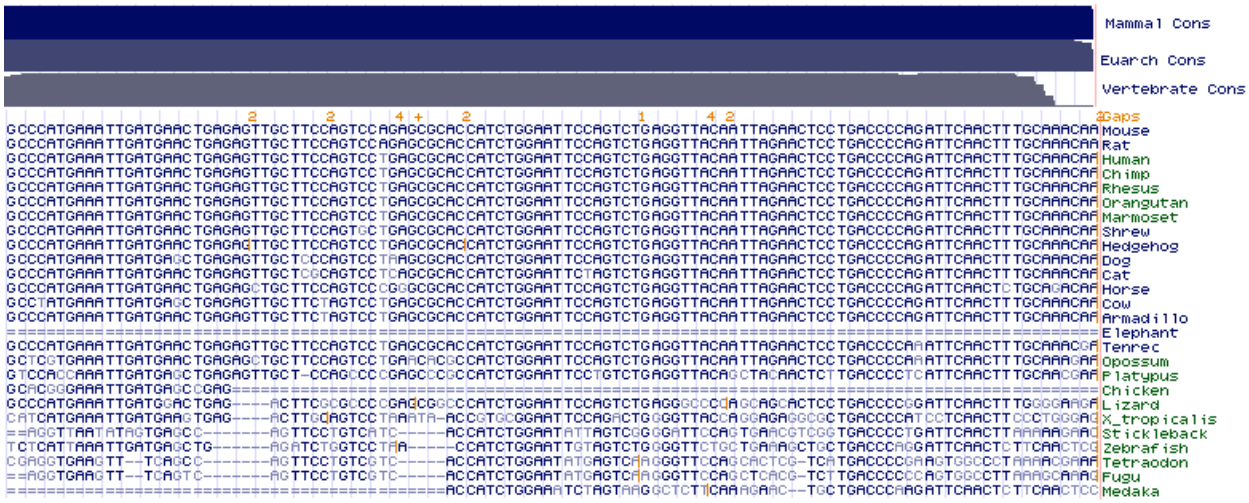

Figure 3.11 Conservation of the first Mcr2 alignment (112 bp).

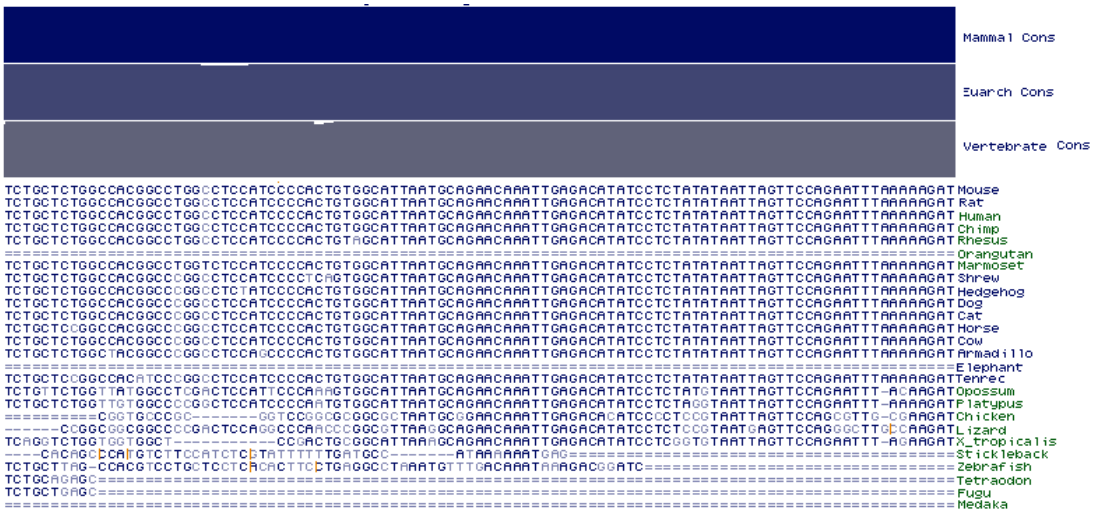

Figure 3.12 Conservation of the second ultraconserved domain (111 bp).

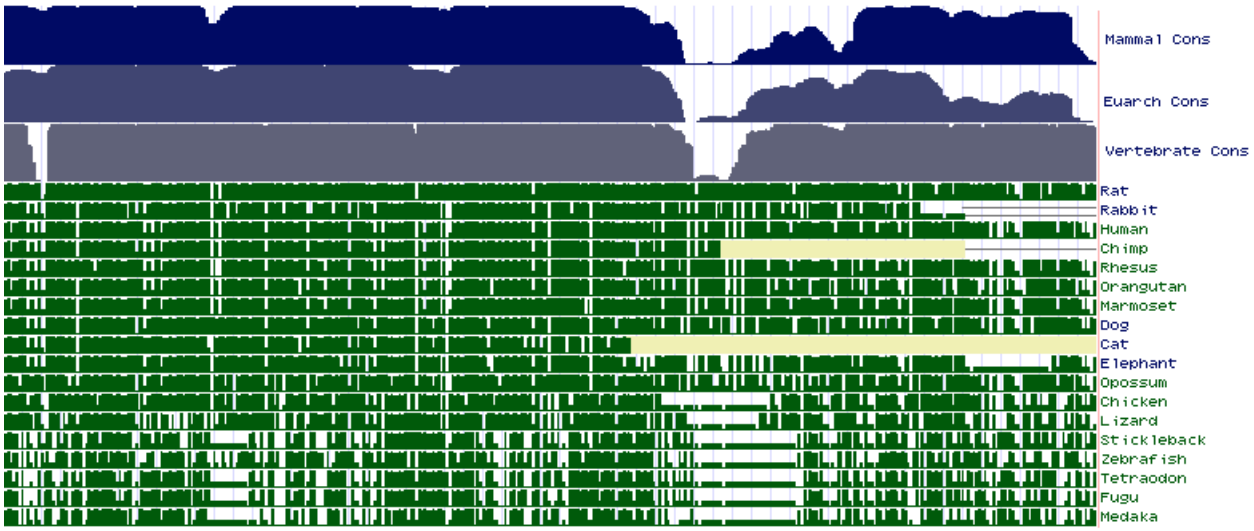

Figure 3.13 Alignments of vertebrate sequences with mouse Wt1 exon1 (399bp).

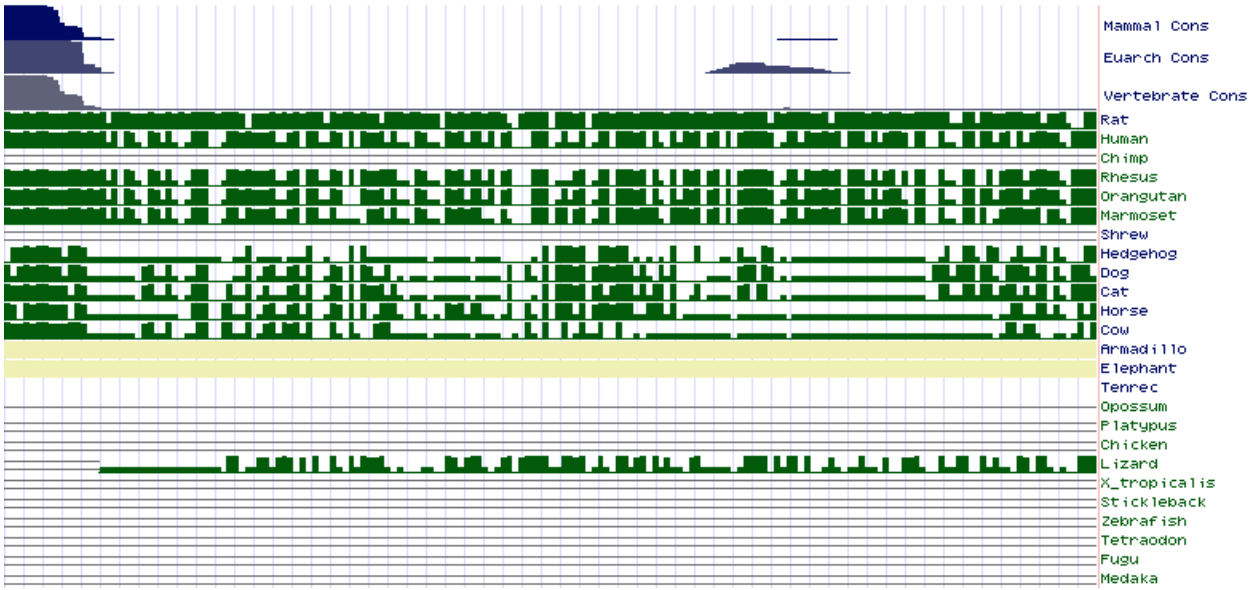

Figure 3.14 Alignments of vertebrate sequences with mouse exon1 A (181 bp).

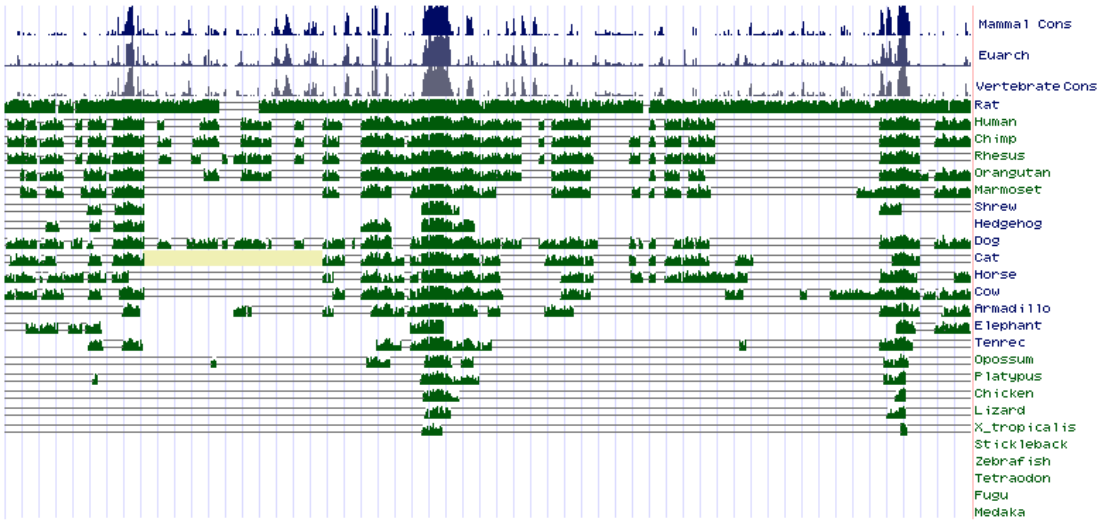

Figure 3.15 Alignments of vertebrate sequences with mouse AK165089 transcript (1,254 bp). At the bottom expressed exons are referred in red.

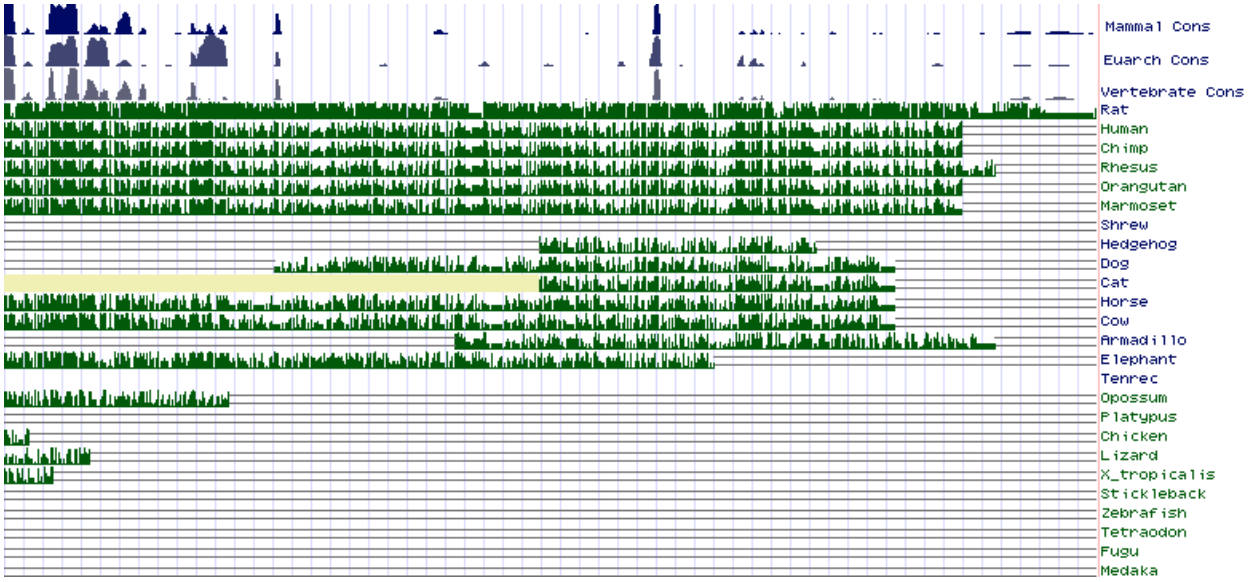

Figure 3.16 Alignments of vertebrate sequences with mouse AK172697 transcript (1677 bp).

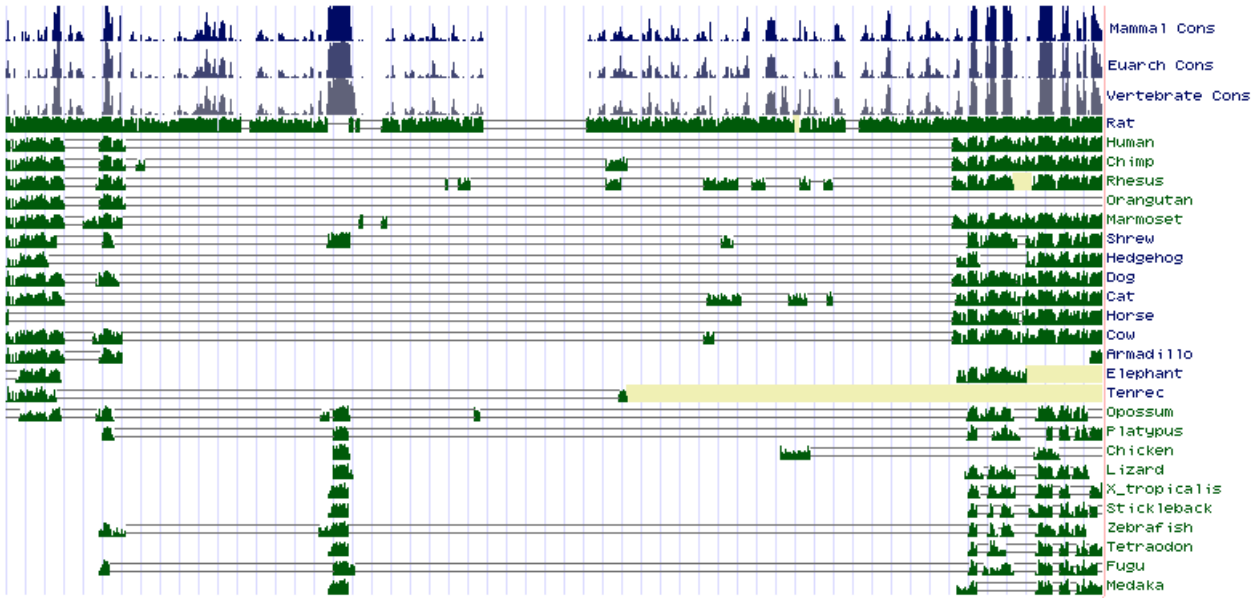

Figure 3.17 Alignments of vertebrate sequences with mouse *Wrap53* noncoding mRNA (1896 bp).

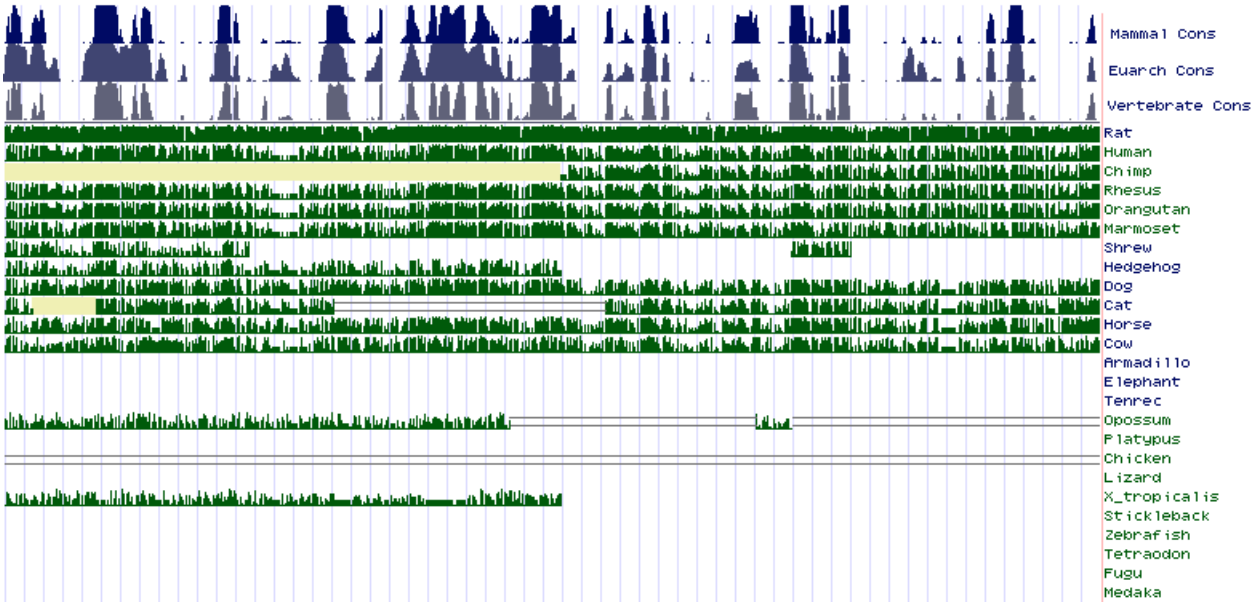

Figure 3.18 Alignments of vertebrate sequences with mouse *H19* (2615 bp).

3.5 Disscusion

Mcr2 has not favorable prediction of active translation to protein because of the many stop codons which would terminate its translation. The ORF present are unlikely to encode protein with functional structure. Finding between 3 to 7 stop codons for each frame analyzed in both sense and antisense orientation it would be unlikely to encode a Mcr2 protein. On the other hand some structural protein properties have been found in terms of secondary structure and MAR. No other structural properties or predicted DNA-Protein binding were found. It is more likely that Mcr2 exerts its active role as a RNA transcript. Also a putative CpG island was found through at 481 bp from Mcr2 towards *WT1* direction.

In terms of RNA expression GenBank displays diverse spliced and unspliced transcripts upstream the Wt1 gene in mouse and human. The vast majority of them are expressed in the antisense orientation. Most of them do not overlap with Wt1 except from the transcript AK172697 that overlaps the *Wt1* promoter by just 15 nucleotides. Mouse Mcr2 is not previously reported as an expressed transcript in

GenBank, or as part of one. In fact transcripts AK165089 and AK161318 splice out Mcr2 far upstream. In human, MCR2 forms part of the *WT1-AS-1* (accession code L25110.1) transcript which shows the same structure as the one reported by Huang *et al*., 1990. Also, in the human several transcripts overlap the *WT1* promoter except from the transcript reported by Eccles *et al*., (1994), which starts at intron 1 and spans exon 1 and continues upstream *WT1* now known as *WT1-AS.*

Mcr2 was recently reported to contain a retinoic acid response element (Bollig *et al*., 2009). An alignment of this was published showing conservation in 5 vertebrates showing homology between zebrafish and human. Differently to other vertebrates (Kent *et al*., 1995), fish possess two *wt1* genes *wt1*a and *wt1*b, which each show similar but non-identical spatial and temporal patterns of expression in nephrogenesis (Bollig *et al*., 2006). The retinoic acid response element was found to be involved in the regulation of development of intermediate mesoderm implying that the conserved element is an enhancer of wt1 a transcription. Although they found responsiveness to retinoic acid receptor in zebrafish, the percentage of identity between the whole 289 bp of Mcr2 in human and zebrafish is only 22%, whereas between mouse and human is 94%. Mcr2 contains different conservation domains, one that shares homology with most vertebrates, and another one that is exclusive of non-fish vertebrates. Thinking on a functional role for Mcr2, due to the fact that has two patterns of conservation within vertebrate domains, might be the case of having specific functions on aquatic or non-aquatic vertebrates. Interestingly another ncRNA, H19 was also only conserved in euarchontoglires. Also ultraconserved domains and MAR were found which suggests a possible transcriptional role. In the case of the ultraconserved domains might provide more evidence to support its role as transcriptional enhancer proposed by Bollig *et al*., (2009). Interestingly, other sequences were found to be widely conserved in mammalian organisms. This was the case for Mcr1 and exon 1 A. On the other hand, dissimilar pattern of conservation was found comparing AK17296 and AK165089.

APPENDIX

Supplementary Table 1 Full description transcripts annotated in Figure 3.2

Identification code	Description
BB683964.1	BB683964 RIKEN full-length enriched, 12 days embryo female mullerian duct Mus musculus cDNA clone 6820409P12 3-, mRNA sequence
BB553293.1	BB553293 RIKEN full-length enriched, 2 days pregnant adult female ovary Mus musculus cDNA clone E330005F08 3-, mRNA sequence
BB093804.1	BB093804 RIKEN full-length enriched, 12 days embryo, embryonic body between diaphragm region and neck Mus musculus cDNA clone 9430043P12 3-, mRNA sequence
CK329643.1	H8179B10-3 NIA Mouse Unique Gene Set Version 2 Mus musculus cDNA clone H8179B10 3-, mRNA sequence
BM220120.2	C0935D05-3 NIA Mouse 12.5-dpc Male Genital Ridge/Mesonephros cDNA Library (Long) Mus musculus cDNA clone NIA:C0935D05 IMAGE:30037960 3-, mRNA sequence
AI785414.1	uj41f10.x1 Sugano mouse kidney mkia Mus musculus cDNA clone IMAGE:1922539 3-, mRNA sequence
AI314831.1	uj31h06.x1 Sugano mouse kidney mkia Mus musculus cDNA clone IMAGE:1921595 3-, mRNA sequence
BB553297.2	BB553297 RIKEN full-length enriched, 2 days pregnant adult female ovary Mus musculus cDNA clone E330005F21 3-, mRNA sequence
BB046170.2	BB046170 RIKEN full-length enriched mouse cDNA library, C57BL/6J testis male 13 days embryo Mus musculus cDNA clone 6030498F17 3-, mRNA sequence
BY101868.1	BY101868 RIKEN full-length enriched, pooled tissues, adult spleen, etc. Mus musculus cDNA clone K630140O08 5-, mRNA sequence
AK031729.1	Mus musculus 13 days embryo male testis cDNA, RIKEN full-length enriched library, clone:6030498F17 product:unclassifiable, full insert sequence
AK032905.1	Mus musculus 12 days embryo male wolffian duct includes surrounding region cDNA, RIKEN full-length enriched library, clone:6720470H10 product:unclassifiable, full insert sequence
BB621534.1	BB621534 RIKEN full-length enriched mouse cDNA library, C57BL/6J

	testis male 13 days embryo Mus musculus cDNA clone 6030498F17 5-, mRNA sequence
BQ552026.1	H4013A02-5 NIA Mouse 7.4K cDNA Clone Set Mus musculus cDNA clone H4013A02 5-, mRNA sequence
AK165089.1	Mus musculus 2 days pregnant adult female ovary cDNA, RIKEN full-length enriched library, clone:E330005F21 product:hypothetical protein, full insert sequence
AK033125.1	Mus musculus 15 days embryo male testis cDNA, RIKEN full-length enriched library, clone:8030442G15 product:cytosolic 5' nucleotidase, type 1A, full insert sequence
BB624191.1	BB624191 RIKEN full-length enriched, 15 days embryo male testis Mus musculus cDNA clone 8030442G15 5-, mRNA sequence
CF169579.1	B0815E12-5 NIA Mouse Newborn Kidney cDNA Library (Long 1) Mus musculus cDNA clone NIA:B0815E12 IMAGE:30468923 5-, mRNA sequence
BI076695.2	L0209E12-3 NIA Mouse Newborn Ovary cDNA Library Mus musculus cDNA clone L0209E12 3-, mRNA sequence
AK161318.1	Mus musculus adult male testis cDNA, RIKEN full-length enriched library, clone:4930402L07 product:unclassifiable, full insert sequence
AK134414.1	Mus musculus 13 days embryo male testis cDNA, RIKEN full-length enriched library, clone:6030473K11 product:unclassifiable, full insert sequence
BQ418218.1	ik54e02.x3 Kaestner ngn3 wt Mus musculus cDNA 3-, mRNA sequence
BI076674.2	L0080C05-3 NIA Mouse E12.5 Female Mesonephros and Gonads cDNA Library Mus musculus cDNA clone L0080C05 3-, mRNA sequence
AK143272.1	Mus musculus 2 days pregnant adult female oviduct cDNA, RIKEN full-length enriched library, clone:E230026E04 product:unclassifiable, full insert sequence
BQ418043.1	ik54e02.y1 Kaestner ngn3 wt Mus musculus cDNA 5-, mRNA sequence
AK172697.1	Mus musculus activated spleen cDNA, RIKEN full-length enriched library, clone:F830301H19 product:unclassifiable, full insert sequence
BY223054.1	BY223054 RIKEN full-length enriched, activated spleen Mus musculus cDNA clone F830301H19 5-, mRNA sequence
CJ066977.1	CJ066977 RIKEN full-length enriched mouse cDNA library, C57BL/6J ovary female 2 days pregnant adult Mus musculus cDNA clone E330005F21 5-, mRNA

	sequence
BY719503.1	BY719503 RIKEN full-length enriched, 12 days embryo female mullerian duct Mus musculus cDNA clone 6820410K22 5-, mRNA sequence

Supplementary Table 2 Full description transcripts annotated in Figure 3.3

Accession code	Description
L25110.1	Human Wilms tumor 1 (WT1) mRNA, exon 1
DA952652.1	DA952652 SPLEN2 Homo sapiens cDNA clone SPLEN2030350 5-, mRNA sequence
NR_023920.1	Homo sapiens Wilms tumor upstream neighbor 1 (WIT1), non-coding RNA
DA961425.1	: DA961425 SPLEN2 Homo sapiens cDNA clone SPLEN2042186 5-, mRNA sequence
DA704288.1	DA704288 NT2RI2 Homo sapiens cDNA clone NT2RI2007592 5-, mRNA sequence
CR737788.1	Description: CR737788 Homo sapiens library (Ebert L) Homo sapiens cDNA clone IMAGp998B065082 ; IMAGE:2063141 5-, mRNA sequence
CA430691.1	UI-H-FL1-bgb-l-21-0-UI.s1 NCI_CGAP_FL1 Homo sapiens cDNA clone UI-H-FL1-bgb-l-21-0-UI 3-, mRNA sequence
BX394943.2	BX394943 Homo sapiens NEUROBLASTOMA COT 25-NORMALIZED Homo sapiens cDNA clone CS0DC026YK15 5-PRIME, mRNA sequence
AI803567.1	BX394943 Homo sapiens NEUROBLASTOMA COT 25-NORMALIZED Homo

	sapiens cDNA clone CS0DC026YK15 5-PRIME, mRNA sequence
DB247341.1	: DB247341 UTERU1 Homo sapiens cDNA clone UTERU1000235 5-, mRNA sequence
DA950905.1	DA950905 SPLEN2 Homo sapiens cDNA clone SPLEN2028049 5-, mRNA sequence
DB192632.1	DB192632 TOVAR2 Homo sapiens cDNA clone TOVAR2000753 5-, mRNA sequence
BX110205.1	: BX110205 Soares_NFL_T_GBC_S1 Homo sapiens cDNA clone IMAGp998O063860 ; IMAGE:1524701 5-, mRNA sequence
BC100673.1	Homo sapiens Wilms tumor upstream neighbor 1, mRNA (cDNA clone IMAGE:40023097)
AW604794.1	QV4-CT0363-010200-099-g09 CT0363 Homo sapiens cDNA, mRNA sequence
AW028595.1	wv33a08.x1 NCI_CGAP_Ov18 Homo sapiens cDNA clone IMAGE:2531318 3- similar to SW:WIT1_HUMAN Q06250 WILMS- TUMOR ASSOCIATED PROTEIN. ;, mRNA sequence
BE394437.1	601311703F1 NIH_MGC_44 Homo sapiens cDNA clone IMAGE:3633024 5-, mRNA sequence
AI648530.1	tz55a03.x1 NCI_CGAP_Ov35 Homo sapiens cDNA clone IMAGE:2292460 3- similar to SW:WIT1_HUMAN Q06250 WILMS- TUMOR ASSOCIATED PROTEIN. ;, mRNA sequence
BX390192.2	BX390192 Homo sapiens NEUROBLASTOMA

	COT 25-NORMALIZED Homo sapiens cDNA clone CS0DC026YK15 5-PRIME, mRNA sequence
AI951613.1	wv37d03.x1 NCI_CGAP_Ov18 Homo sapiens cDNA clone IMAGE:2531717 3- similar to SW:WIT1_HUMAN Q06250 WILMS- TUMOR ASSOCIATED PROTEIN. ;, mRNA sequence
AA912908.1	ol27f03.s1 Soares_NFL_T_GBC_S1 Homo sapiens cDNA clone IMAGE:1524701 3- similar to SW:WIT1_HUMAN Q06250 WILMS- TUMOR ASSOCIATED PROTEIN. ;, mRNA sequence
BC002734.2	Homo sapiens Wilms tumor upstream neighbor 1, mRNA (cDNA clone IMAGE:3633024)
BC098290.1	Homo sapiens Wilms tumor upstream neighbor 1, mRNA (cDNA clone IMAGE:40023096)
BF058864.1	: 7k35f06.x1 NCI_CGAP_Ov18 Homo sapiens cDNA clone IMAGE:3477634 3-, mRNA sequence
BC096708.1	Homo sapiens Wilms tumor upstream neighbor 1, mRNA (cDNA clone IMAGE:40023095)
BF434735.1	Description: 7p03g11.x1 NCI_CGAP_Ov18 Homo sapiens cDNA clone IMAGE:3644757 3-, mRNA sequence
M60614.1	Human Wilms' tumor (WIT-1) associated protein mRNA, complete cds
BF515320.1	UI-H-BW1-anl-g-07-0-UI.s1 NCI_CGAP_Sub7 Homo sapiens cDNA

	clone IMAGE:3082932 3-, mRNA sequence
BF059076.1	7k37e06.x1 NCI_CGAP_Ov18 Homo sapiens cDNA clone IMAGE:3477610 3-, mRNA sequence
BU633051.1	UI-H-FL1-bgt-g-19-0-UI.s1 NCI_CGAP_FL1 Homo sapiens cDNA clone UI-H-FL1-bgt-g-19-0-UI 3-, mRNA sequence
T54801.1	yb42d04.s1 Stratagene fetal spleen (#937205) Homo sapiens cDNA clone IMAGE:73831 3-, mRNA sequence
CB267195.1	1006101 Human Fat Cell 5--Stretch Plus cDNA Library Homo sapiens cDNA 5-, mRNA sequence
T54965.1	yb42d04.r1 Stratagene fetal spleen (#937205) Homo sapiens cDNA clone IMAGE:73831 5-, mRNA sequence
BQ436800.1	AGENCOURT_7769032 NIH_MGC_92 Homo sapiens cDNA clone IMAGE:6069449 5-, mRNA sequence
CR604547.1	full-length cDNA clone CS0DC024YP12 of Neuroblastoma Cot 25-normalized of Homo sapiens (human)

Chapter 4: Mcr2 expression in the *Davis* and *Trigger* transgenic models

4.1 Introduction

In order to elucidate a role *in vivo* for Mcr2 different transgenic mice strains were generated previously in our lab by Dr. K. Moorwood and Dr. J. Alsop. E14C4 ES cells were transfected with the Mcr2 targeting construct and targeted clone isolated. Targeted ES cells clones were selected and expanded. By blastocyst injection this ES cells clone was used to generate Mcr2 gene-targeted strains and then maintained on a C57xCBA genetic background. Two different strains were derived one with the Mcr2 sequence in the genome and another without this sequence. However, both strains have a transcriptional terminator sequence to abrogate through Mcr2 transcription so that even the strain with Mcr2 was designated to have truncated antisense expression. The strain with Mcr2 intact was named *Trigger* (for truncation only) and *Davis* (for deletion and truncation). *Trigger* and *Davis* were made in order to compare if Mcr2 could have a role at either at the DNA or RNA level or both. To characterize Mcr2 expression in the *Trigger* and *Davis* mouse models wild type (+/+) heterozygous (-/+) and homozygous (-/-) animals were compared. First, this Mcr2 expression was analyzed in wt kidney and *Trigger* $^{-/-}$ and *Davis* $^{-/-}$ strains were assessed to confirm whether correct truncation or deletion had occurred, respectively. Also to characterise if there were antisense, antisense expression or both (Mcr2) in *Trigger* and *Davis* models. For this, the expression in *Trigger* and *Davis* mouse models siblings was analyzed by RT-PCR using cDNA synthesized from a specific strand (sense or antisense). As discussed in Section 3.2.1, most of the transcription reported upstream *Wt1* occurs in the antisense orientation. Indeed the mouse kidney has several antisense transcripts which have been reported (Dalloso *et al*., 2007), however we did not know if that was the case for Mcr2. Also by RT-PCR has been performed to detect the common splicing contained by AK165089 and AK161318 in order to analyze its expression in our Mcr2 knockout model (*Davis* $^{-/-}$). For description of this splicing site see Figure 4.1. Particularly, this was tested to look if the expression of AK165089 and AK161318 might be disrupted. These predicted transcripts have been reported previously of mRNA, from ovary (AK165089) and testis (AK161318) (see Appendix, Table 1). The AK165089 transcript was shown to

be highly expressed in the developing kidney, suggesting that it might have an active role in development (Dallosso *et al*., 2007) (Figure 4.2). In a different aspect by looking at wild type mouse expression of Mcr2 it is of interest to see whether its allele-specific expression pattern parallels the pattern seen in the human. In human, WT1-AS is disrupted in WT and leukaemia had a potential oncogenic role due to loss of imprinting expression (Hancock *et al*., 2007). Although in the mouse there is no evidence of imprinting in some WT1-AS transcripts that have been analyzed, this epigenetic mechanism has not been analyzed at Mcr2.

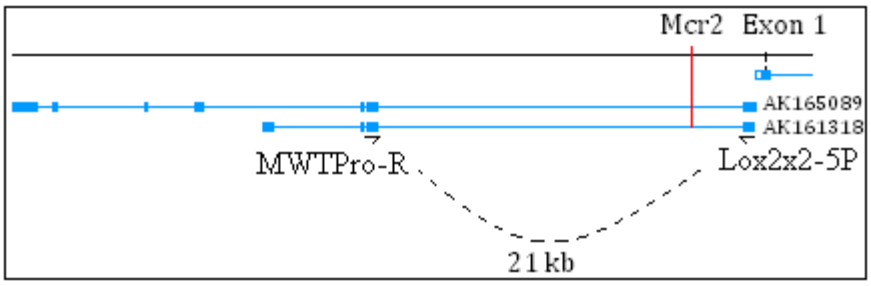

Figure 4.1 The mouse Wt1 locus in the region of Mcr2 showing spliced transcripts AK165089 and AK161318. Splicing of about 21 kb occurs around Mcr2 in transcripts AK165089 and AK161318. Both transcripts splice out Mcr2 (dotted line). The position of Mcr2 (vertical red line) is shown with respect to Wt1. Primers designed for amplifying the firs splicing are shown.

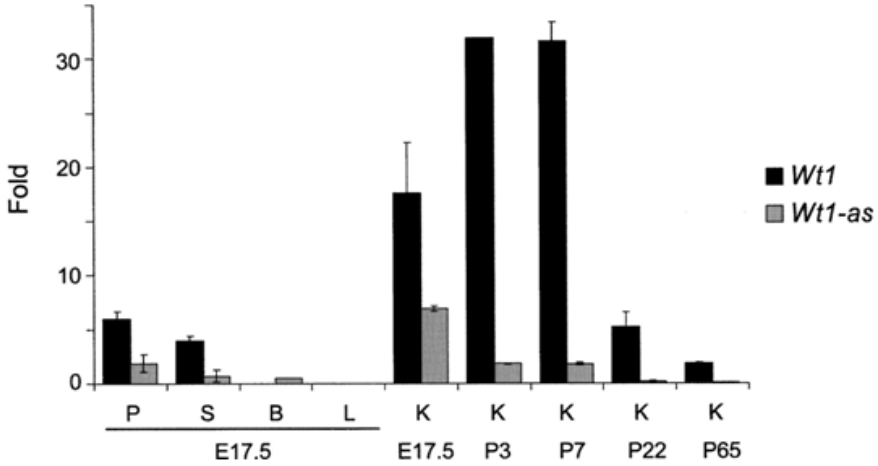

Figure 4.2 Graph showing q-PCR results displaying the expression of sense and antisense transcripts present in various tissues. P) placenta, S) spleen, B) brain, L) liver and K) kidney. Different stages were analyzed E17.5 and postnatal day (P) 3, 7, 22 and 65. This image was reproduced under the author permission (Dallosso *et al*., 2007).

4.2 Results

4.2.1 Detection of truncated and deleted alleles

4.2.1.1 Genotyping

To verify Mcr2 allele identity, specific primers were used to generate a product able to differentiate the truncated (*Trigger*) or deleted (*Davis*) allele from the wild type allele. PCR genotyping proved to be reproducible and consistent using ear biopsies as a DNA source and using TF/S primers (Figure 4.3). These primers amplified bands of 1.002 kb (wild type), 1.46 kb (*Davis* homozygous) and 1.9 kb (*Trigger* homozygous) that really distinguish the three possible alleles.

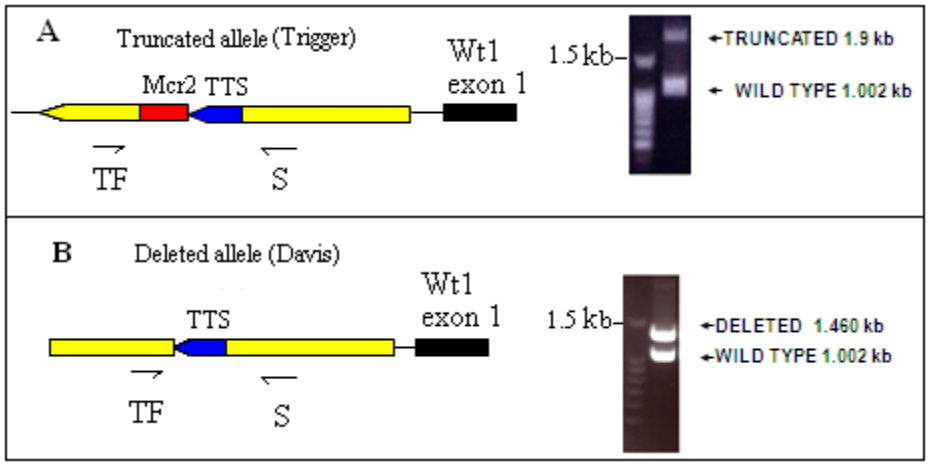

Figure 4.3 Illustration of TF/S primers used for genotyping. On left: structure of the *Trigger* (A) indicating Mcr2 in red and *Davis* (B) homozygous genomic structures indicating TF/S primer biding sites. On right: examples of typical PCR data (right panel) used to distinguish mutant and wild type alleles.

4.2.1.2 Mcr2 expression in the mouse kidney

In human, it has been documented that WT1-AS and WT1 might functionally interact because they have been found coordinately expressed, and in co-transfection assays WT1-AS can affect WT1 expression (Moorwood *et al.*, 1998). Interestingly, it was

found that Wt1-AS reaches its highest expression in the developing kidney, suggesting a functional role in development (Dalloso *et al*., 2007).

Although there is evidence of WT1-AS expression in human foetal kidney and also in mice it was of interest to detect Mcr2 expression in the mouse kidney. To do this, RT-PCR assays on kidney tissue were performed using CNL-B primers (Figure 4.5). RNA samples from *Davis* strain were used as negative controls. As expected agarose gels show a band of 243 bp in length, only when RT was present in wt sample. RNA from the *Davis* strain did not amplify a band using these primers (Figure 4.4)

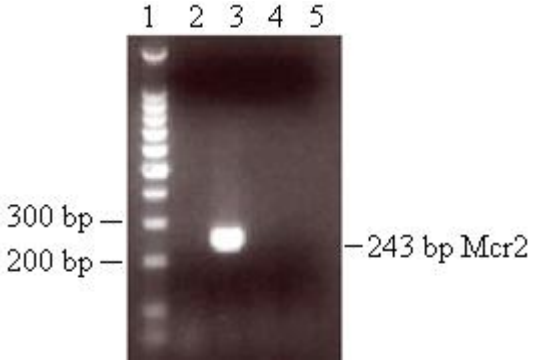

Figure 4.4 RT-PCR analysis of *Davis* wild type and homozygous mutant samples. Lane: 1) 100 bp ladder (Promega), 2) *Davis* $^{+/+}$ -RT, 3) *Davis* $^{+/+}$ +RT, 4) *Davis* $^{-/-}$–RT 5) *Davis* $^{-/-}$ +RT.

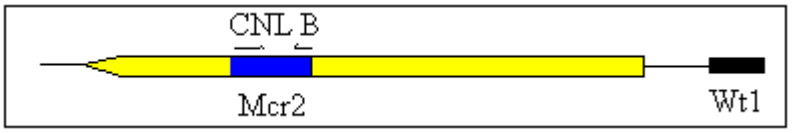

Figure 4.5 Illustration of CNL/B primers used for genotyping. Mcr2 is marked in blue and at the top CNL and B primers show their position. Far right is situated Wt1.

4.2.1.3 Analysis of Mcr2 expression from the truncated allele in *Trigger* mutant mice strain using random primers.

The knock-in mouse model *Trigger* contains a transcriptional terminator sequence which was designed for truncating antisense transcripts from Mcr2 sequence. To evaluate whether abrogation of Mcr2 occurs in this particular model, RT-PCR analysis from kidney (E17.5) RNA was perform under similar conditions to those

used to detect Mcr2 expression previously in the wild type samples (See previous section 4.2.1.2). Using CNlong/B primers evidence of Mcr2 transcription was found, suggesting that the transcriptional terminator sequence was not working properly and this strategy of knock down could not efficiently stop transcription though the Mcr2 sequence (Figure 4.6). However, since RT-PCR is not quantitative, additional experiments were performed to further evaluate Mcr2 expression in *Trigger* mutant mice.

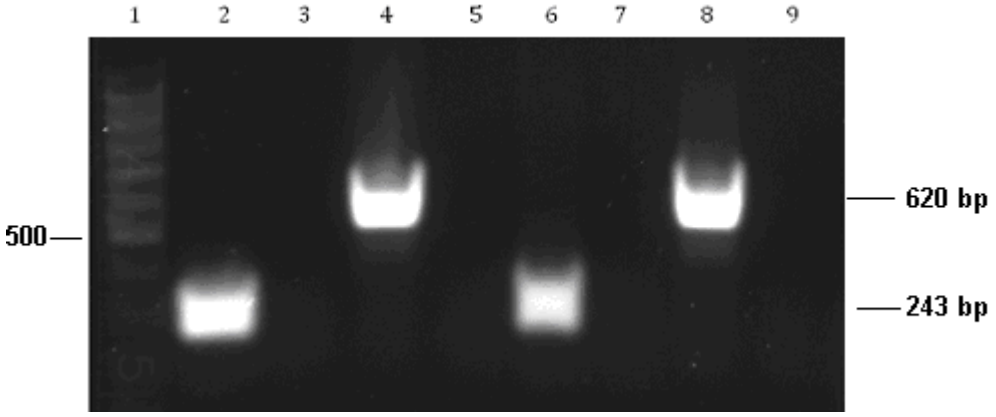

Figure 4.6 RT-PCR of Mcr2 expression in *Trigger* mutant mice. Lane: 1) 100 bp ladder (Promega), 2) +RT *Trigger*$^{+/+}$ Mcr2, 3) –RT *Trigger*$^{+/+}$ Mcr2, 4) Actin, +RT *Trigger*$^{+/+}$, 5) Actin, -RT *Trigger*$^{+/+}$, 6) +RT *Trigger*$^{-/-}$Mcr2, 7)-RT *Trigger*$^{-/-}$ Mcr2, 8)Actin +RT *Trigger*$^{-/-}$, 9) –RT *Trigger*$^{-/-}$ Actin.

4.2.1.4 Analysis of Mcr2 expression using strand specific cDNA

To address whether Mcr2 is transcribed in the antisense or the sense orientation, or both, single strand RT-PCR was performed. To do this, cDNA samples were first synthesized either sense or antisense (using A/B primers see Table 2.1 and Figure 4.7) and subsequently used as a template for amplification of the Mcr2 product region. RNA samples were kidney E17.5. Thus, specific primers were used, instead of random primers, to synthesize strand-specific cDNA. Primer A was used to copy sense RNA and primer B to copy the antisense RNA. When used in PCR, products derived from cDNA synthesis with primer A represent sense transcripts and products derived from cDNA synthesis with primer B- represent antisense transcript (Figure 4.8).

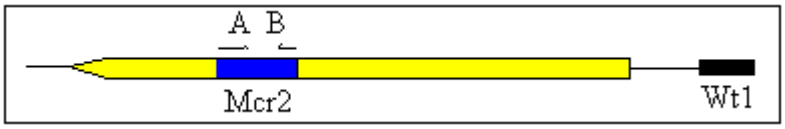

Figure 4.7 Illustration of A and B primers used for genotyping. Mcr2 is marked in blue and at the top A and B primers show their position. Far right is situated Wt1.

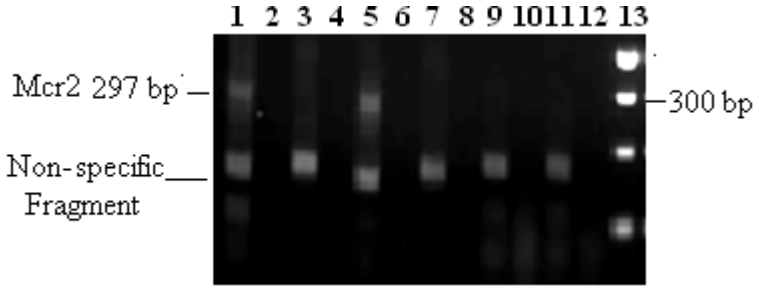

Figure 4.8 Strand-specific RT-PCR of Mcr2 expression in mouse kidney. Lane: 1) Antisense, *Trigger* $^{+/+}$ + RT; 2)Antisense, *Trigger* $^{+/+}$ –RT; 3)Sense, *Trigger* $^{+/+}$ +RT; 4)Sense, *Trigger* $^{+/+}$ –RT; 5)Antisense, *Trigger* $^{-/-}$ +RT; 6)Antisense, *Trigger* $^{-/-}$ –RT; 7)Sense, *Trigger*$^{-/-}$ +RT ; 8) Sense, *Trigger*$^{-/-}$ -RT; 9) Antisense, *Davis* $^{-/-}$ +RT; 10)Antisense, *Davis* $^{-/-}$ -RT; 11)Sense, *Davis* $^{-/-}$ +RT; 12) Sense, *Davis* $^{-/-}$ –RT; 13) 100 bp ladder (NEB).

A comparison was made between wild type (Mcr2 transcription is known to occur) and homozygous mutant kidneys from *Davis* and *Trigger* neonates. In wild type RNA amplification of Mcr2 was seen in the antisense orientation and not in the sense. Mcr2 was also expressed in *Trigger* $^{-/-}$ mutant mice but not in *Davis* $^{-/-}$ mice which were employed as a negative control (primer binding sequences are deleted in the *Davis* mutant allele). This confirms that the transcriptional terminator sequence is not working efficiently in *Trigger* in the *Trigger* mutant allele.

4.2.1.5 Measuring levels of transcription by qPCR in *Davis* and *Trigger* strain mice.

To estimate the levels of Mcr2 expression at E 17.5 from kidney total RNA, including in the *Trigger* strain quantitative PCR (qPCR) was performed by Dr. Hancock at Bristol University. The result of this experiment was comparable to those from the RT-PCR. In this assay two different homozygous mutant samples were employed for both *Davis* and *Trigger* and compared to wild type using A and B primers.

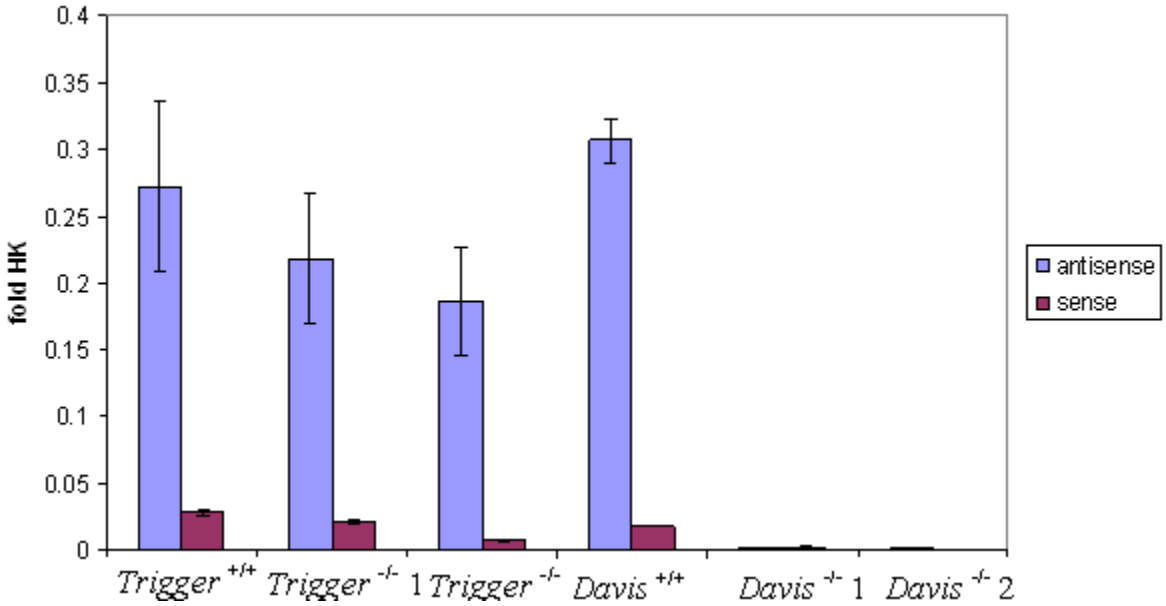

Figure 4.9 Quantitative PCR analysis of Mcr2 expression in *Trigger* and *Davis* mice. Graph displaying folds of PCR product. Blue bars indicate antisense transcription and red bars indicate sense transcription. This graph shows 1 wild type and 2 homozygous for each *Trigger* and *Davis* mutants. All samples were taken from kidney E17.5. Error bars show the range of triplicate measurements.

As expected, very little sense transcription at Mcr2 was detected in the analised kidneys. However abundant expression was seen in the wild type but also in *Trigger* $^{-/-}$ homozygous mutant sample. Levels of expression were measured and expressed as fold-changes. The Tbp housekeeping gene was used to normalize samples (Figure 4.8). A slight reduction in both *Trigger* homozygous with no expression was seen in the *Davis* samples.

4.2.1.6 Analysis of transcriptional terminator sequence function by testing the contiguous spliced WT1-AS transcript.

In the mouse kidney transcription at the WT1 locus has been shown in the antisense orientation for spliced transcripts containing two exons (accession code AK165089 and AK161318). These transcripts have been reported in ovary and testis respectively. In both cases signal was only seen using cDNA made from the antisense transcripts (Dalloso *et al*., 2007). Specific primers Lox2x2-5P/MWTPro-R were used to detect transcript expression of these transcripts (Table 2.1; Figure 4.1).

Following a hypothesis in which Mcr2 could act as an enhancer of other antisense transcripts in the developing kidney transcription of 17.5 Davis$^{+/+}$ and $^{-/-}$ kidneys were assessed from total RNA made from E17.5. In order to validate if the abrogation of the Mcr2 DNA sequence affects the expression of neighbouring transcripts AK165089/AK161318 expression was assessed at E17.5. After amplification PCR bands were amplified of the expected size but there was no change in expression of the spliced antisense transcript (Figure 4.10) although, perhaps a small decrease in antisense expression when the TTS is present.

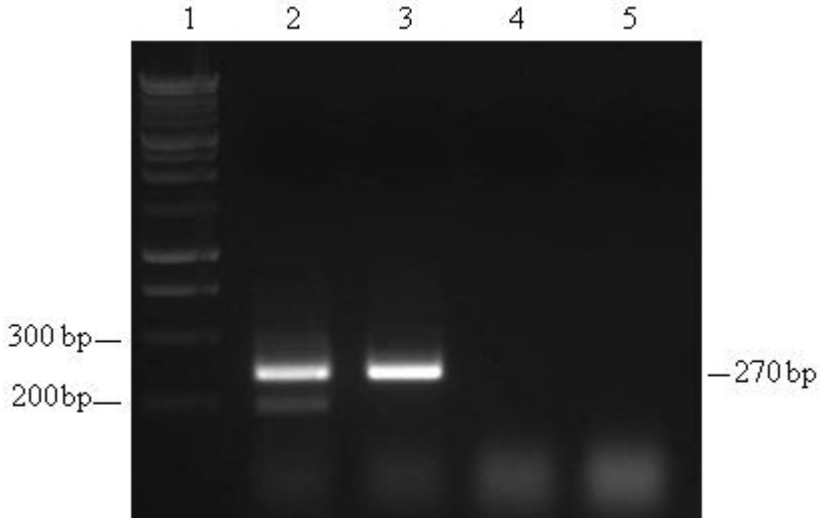

Figure 4.10 Expression of the spliced antisense transcripts. Detection of splicing present in AK165089/AK161318 transcripts. Expected fragment size: 270bp) Lane 1)1 kb ladder (NEB), 2) *Davis* $^{+/+}$ +RT, 3) *Davis* $^{-/-}$ +RT, 4) *Davis* $^{+/+}$ -RT, 5) *Davis* $^{-/-}$ -RT.

4.2.3 Imprinting study

4.2.3.1 Allele-specific expression of Mcr2.

As discussed earlier, (Section 1.2.2.5) in contrast to most of the transcriptome, a minority of genes are monoallelically transcribed in a parent-of-origin dependant manner. This is known as genomic imprinting and requires DNA elements to display allele-specific epigenetic modifications, such as differential DNA methylation. Intragenic CpG islands may serve as promoters of allele-specific antisense transcripts (Hutter *et al*., 2006) and as we have seen in Section 3.3.3 Mcr2 is located next to a CpG island.

To address the possibility that Mcr2 expression might be regulated by imprinting in Mcr2. Heterozygous mice (with deleted allele present in *Davis* $^{+/-}$) were generated and analyzed immediately after weaning at 22 days old. Two different groups of offspring one with Mcr2 deleted from the paternal allele (*Davis* $^{+/p}$) and the other one with Mcr2 deleted from the maternal allele (*Davis* $^{m/+}$) were generated by breeding homozygous male and female respectively with wild type mates (Figure 4.11).

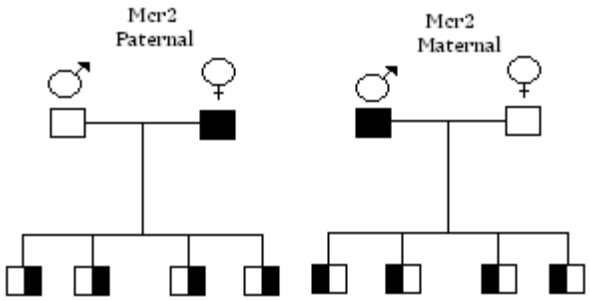

Figure 4.11 Crosses to obtain heterozygous mutant *Davis* mice with Mcr2 deleted from the paternal or maternal allele. Blank boxes are wild type strain (with Mcr2 intact) and filled boxes *Davis* homozygous mutants (with both Mcr2 alleles deleted). Half-filled boxes represent heterozygous offspring. Offspring with the half-filled box on the right represent *Davis* $^{p/-}$ and on the left *Davis* $^{-/m}$.

After RT-PCR amplification of RNA from kidney using CNL-B primers (used to detect the presence or absence of Mcr2; Figure 4.5) no evidence of parent-of-origin transcription (imprinting) was found. Amplification of Mcr2 sequences was seen in wild type and also both heterozygous (*Davis* $^{p/-}$ and *Davis* $^{-/m}$) mice.

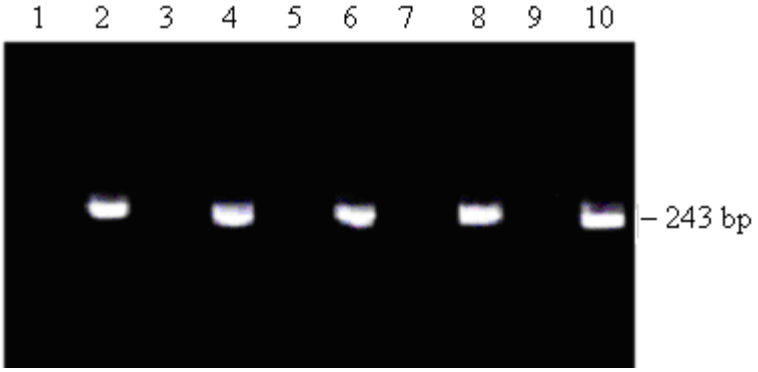

Figure 4.12 Analysis of Mcr2 allele-specific expression in (post-natal day 22) kidney samples. An RT-PCR product of 243 bp represents amplification of transcribed Mcr2 sequences were: Lane 1) *Davis* $^{p/m}$ -RT; 2) *Davis* $^{p/m}$ +RT; 3) *Davis* $^{p/-}$ -RT; 4) *Davis* $^{p/-}$ +RT; 5) *Davis* $^{p/-}$ -RT; 6) *Davis* $^{p/-}$ +RT; 7) *Davis* $^{-/m}$ -RT; 8) *Davis* $^{-/m}$ +RT; 9) *Davis* $^{-/m}$ -RT; 10) *Davis* $^{-/m}$ +RT.

As a result of this experiment heterozygous expression from Mcr2 Mats and Pats (Figure 4.12) was not conditional of the allele from were derived and all band signal had the same electrophoretic pattern as the Wt on lane 1 used as positive control. At least at this stage there is no evidence of imprinting in Mcr2.

4.2.3.2 Investigation of the allele specificity of expression in wild type mice using a naturally occurring sequence polymorphism.

Around 250 base pairs downstream from Mcr2 (between mcr2 and Wt1 exon 1) a polymorphism was found and sequenced by Dr. Kim Moorwood. This polymorphism gave a different length PCR- fragment in three different inbred mouse strains (CBA, C57 and 129) (Figure 4.13). Using a pair of primers designated SF-VR, products of 346 bp (C57) and 334 bp (CBA) were distinguishable on acrylamyde gel electrophoresis and consistent with sequence polymorphisms expected (Figure 4.14).

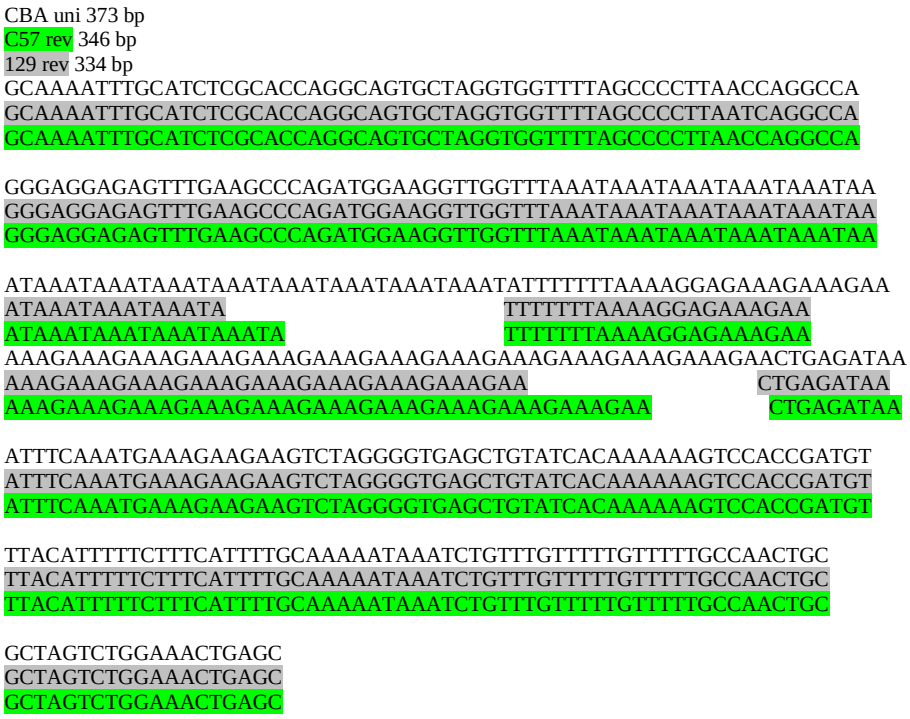

Figure 4.13 Alignment of sequences amplified by SF-VR primers. 129 is at the top followed by C57 (green) and CBL (grey).

4.2.3.3 SF-VR polymorphism imprinting analysis.

In order to look for evidence of imprinting in the region proximal to Mcr2 RT-PCR amplification was done using RNA from strains C57 and 129 (experiment performed by Dr. Kim Moorwood). Offspring were generated by crossing either C57 females or 129 females with C57 males or 129 males. Kidney RNA analysed at fetal stage (E17.5) and several post natal stages (P), however, no evidence of imprinted expression was found (Figure 4.14). Positions of the primers shown in Figure 4.15.

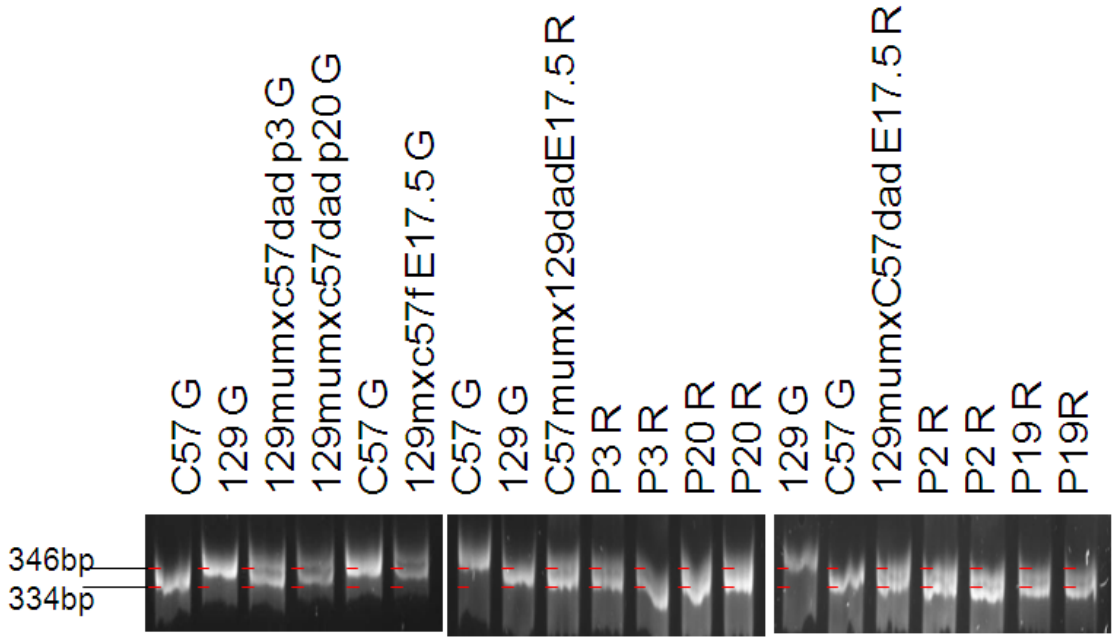

Figure 4.14 Allele specific expression by RT-PCR in an expressed polymorphism sequenced near to Mcr2 PCR products in polyacrylamide gels showing the polymorphism between C57 and 129. Genomic (G) DNA was used as a positive control for PCRs (left panel). RNA expression (R) was analysed by RT-PCR of kidney RNA containing either a C57 and 129 mother and C57 father (right panel). Ages of analyzed offspring are indicated (E=embryonic day and P=postnatal day).

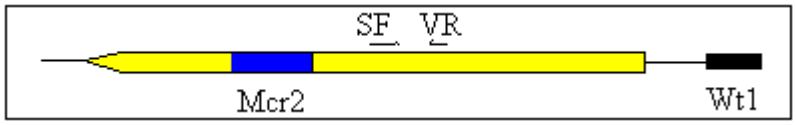

Figure 4.15 Illustration of SF/VR primers used for genotyping. Mcr2 is marked in blue and at the top SF and VR primers show their position. Far right is situated Wt1.

4.3 Discussion

By using a conventional PCR way it is possible to discriminate between wild type, heterozygous and homozygous mice in consistent, reduced time and expense compared with other methods. An alternative methodology to detect Wt1-as would have been strand-specific Northern blots. However, when strand-specific Northern hybridization was attempted in our laboratory was not possible to detect transcripts containing Mcr2 transcript because there was a strong signal from non-specific binding of the probe to 18S and 28S ribosomal RNAs that would have make it binding (Allsop, 2008). Perhaps because Wt1 antisense transcription level is relatively low, has not been successfully detected on Northern blot.

A genotyping method was established that allows positive identification of wild type, deletion (*Davis*) and truncation (*Trigger*) Mcr2 alleles, allowing discrimination. It was previously shown that Wt1-as transcripts are highly expressed in the developing kidney (Dallosso *et al*., 2007) RT-PCR amplification using primers specific for Mcr2 has shown that this conserved genomic region is expressed in the E17.5 mouse kidney. No expression was seen in *Davis* which carries only the Mcr2 deleted alleles. Therefore *Davis* $^{+/+}$ and *Davis* $^{-/-}$ mice could be used as a positive and negative controls, respectively, for comparison with transcription in the *Trigger* strain. Consistent results were obtained by conventional RT-PCR using both random priming and strand specific priming of cDNA synthesis, as well as in quantitative PCR reactions in each case, Mcr2 was detected in kidney samples from *Trigger* $^{-/-}$ mice, indicating that the transcriptional terminator sequences were not operating efficiently at all. By qPCR it was possible to see that Mcr2 expression in *Trigger* $^{-/-}$ mice perhaps was slightly diminished. Sequence analysis of the engineered mutation in both *Trigger* and *Davis* transgenic strains showed that the regions inserted by the gene targeting remained intact suggesting the transcriptional terminator sequences were not working as planned. In addition, looking at the expression of neighbouring transcripts there was no evidence they were disrupted when Mcr2 was deleted from the genome.

In contrast to what has been found in human (Hancock et al., 2008) Mcr2 transcripts in the mouse showed no evidence of imprinted expression. Imprinting of Mcr2 transcripts therefore, differ in human and mouse due to variability in the evolution of imprinting control elements, or could occur only at specific stages in the mouse. However, when looking at neighbouring elements (defined by the SF-VR primers) were not possible to find any evidence of imprinting at different stages in two different inbred strain backgrounds.

Chapter 5: Phenotypic screening of mice with genetic modification of Mcr2

5.1Introduction

Wt1 antisense transcription has been detected in several wt mouse tissues during both the embryonic stage (E17.5) and also postnatally (Figure 4.2) (Dallosso *et al*., 2007). In an effort to elucidate any relevant physiological role of Mcr2 in the biology of the mouse heterozygous and homozygous *Trigger* and *Davis* mice with genetically modified Mcr2 were monitored for any signs of morbidity or mortality in comparison to wt mice. Mortality was followed until adulthood but also this was evaluated by checking genotypes after birth and comparing allele frequency with Mendelian ratios to find if there was any lethality during gestation. Morbidity studies were carried out to observe any early sign of kidney disease by looking at the presence or absence of proteinurea which might indicate kidney malfunction (Menke *et al*., 2003; Lahiri *et al*., 2007). Analysis of the organs of these mutant mice was also carried out in adulthood to look for differences from wt siblings. A way to understand the physiological effect of a genetic modification is by comparing modified model organisms against the unmodified experimental controls quantitatively and qualitatively. Specifically weight, appearance and histological parameters were analyzed to define any potential phenotype.

Due to the polygenetic background of *Trigger* and *Davis* mice the most closely related animals as possible were used to maintain the most similar genetic background for the genetic model mice and the control wt mice. This was possible by inter-crossing heterozygous littermates to obtain wt, heterozygous and homozygous siblings. The cohort of animals studied was made up of individuals as closely related to each other as possible to enable any potential phenotype, especially a subtle one to be revealed. In the case of subtle effects or very variable wt phenotypes, successive cohorts were followed increasing the number of animals to enable reach statistical significance to be.

At 7 months old, various tissues were analyzed from adult mice to look at organ morphology through histological analysis. Contrary to what was expected the *Trigger* strain did not display correct truncation of Mcr2 antisense expression that would allow us to analyze the role of Mcr2 at the RNA level (see designed of *Trigger* genetic modification Figure 1.10). Therefore although the *Trigger* strain was used for preliminary analysis it was not studied as completely as the *Davis* strain. Therefore the *Davis* strain became the main focus of our experimental interest. As described in Chapter 4 much of our analysis has specifically focused on the kidney because of the involvement of Wt1 in kidney development and function. However in this Chapter the whole animal was studied in different way to enable discovery of the potential function of Mcr2 in other organ systems.

5.2 Results

5.2.1 Allelic inheritance study

Following previous reported transfection studies which show that WT1-AS transcription of *WT1-AS* can elevate Wt1 levels (Moorwood *et al*., 1998) we might have expected disruption of Mcr2 in the mouse we might have expected disruption of Mcr2 in the mouse to affect Wt1 protein levels. Since Wt1 has been shown essential for the organization of other organs from the kidney, we also expected that developmental defects might occur in for example heart and kidney as in the case of the *Wt1* null mouse model (Kreidberg *et al*., 1993). In contrast to these expectations only occasional, apparently random morbidity features were detected at post natal stage which may have contributed to occasional mortality of individuals in *Trigger*, *Davis* and wt mice (Table 5.4). *Trigger* and *Davis* strain line heterozygotes and homozygotes, both males and females were able to generate offspring and viable through adulthood.In order to test the possible influence of truncation or deletion of Mcr2 in *Davis* and *Trigger* heterozygotes and homozygotes, heterozygotes inter-crosses were counted and compared to expected Mendelian ratios. Genotyping was performed after weaning by PCR amplification from an ear clip biopsy as described on Figure 4.1. During inheritance, alleles at a single locus segregate according to the

second law of Mendel's inheritance (Mendel, 1866). Any variations from Mendel's ratio might be indicative of segregation dependant on a particular strain specific polymorphism or genomic imprinting or interestingly, if there is a decreasing number of homozygotes might be indicative of embryonic lethality. Genotype ratios were compared to the expected Mendelian ones using the Chi-squared test to determinate whether obtained values were significantly different from the expected ones. Whether or not the difference was classified as significant from one another relies upon the cutoff point called probability value (*P*). For the present study the cutoff point was $P<0.05$. The results for *Davis* mice genotypes were analyzed under the Chi-squared test with a total of 257 adult mice and shown in 5.1. With 2 degrees of freedom, $X^2=18.94$, indicated that two-tailed *P* value is less than 0.0001. By conventional criteria, this difference is considered to be extremely statistically significant indicating that the observe ratios are unlikely to occur by chance if Mendelian rules apply. In the *Davis* strain, wt offspring predominate, at the expense of both *Davis* heterozygotes and homozygotes (Table 5.1). According with the number of wt animals (94) versus the number of homozygotes born (52) nearly half of the *Davis* homozygous is reduced (41%). In the case of the *Trigger* strain (Table 5.2), there was no significant difference ($P>0.05$) between observe and expected ratios, the conclusion being that pups of all three genotypes were born. For *Trigger* $X^2= 5.34$ with 2 degrees of freedom, therefore the *P* value was 0.0693. By conventional criteria, since $0.0693 >0.05$ any differences between observed and expected values are not statistically significant.

Table 5.1 Frequency of genotypes obtained from *Davis* mice. A total of 257 *Davis* mice were obtained from heterozygous intercrosses. Table shows also expected number and percentage according to Mendelian inheritance. Wt= wild type, he= heterozygous, ho= homozygous.

Genotype	Animals born (Observed number)	Expected number	Expected %
wt	94	64.25	25%
he	111	128.5	50%
ho	52	64.25	25%
Total	257		

Table 5.2 Frequency of genotypes obtained from *Trigger* mice. A total of 100 mice born were obtained from *Trigger* heterozygous intercrosses. Table shows also expected number and percentage according to Mendelian inheritance. Wt= wild type, he= heterozygous, ho= homozygous

Genotype	Animals born (observed number)	Expected number	Expected %
wt	33	25	25%
he	39	50	50%
ho	28	25	25%
Total	100		

Due to these results is possible that (on the contrary of the normal values in the *Trigger* strain) *Davis* homozygous mice may experience lethality at gestational stage. However, this phenotype is incompletely penetrant, because, clearly, homozygous *Davis* mice are able to be born, viable and fertile, yet arise at a lower than expected frequency. This leads to the assumption that *Davis* homozygous intercrosses may give rise to smaller litters than wt intercross counterparts. To test this hypothesis further analysis was performed by looking at the number of offspring produced by intercrosses of each possible *Davis* genotype, wt, heterozygote or homozygote breeding pairs. If Mendelian laws apply, we might expect equal litter sizes for all genotypes as shown in Table 5.3 there is a reduction from an average litter size of 7.1 for the heterozygous intercrosses and 6.7 for homozygous intercrosses.These results suggest the possibility of embryonic lethality associated to some degree the *Davis* allele. Consistent causes of adult morbidity associated with the *Davis* allele (see Table 5.4) might have pointed to an incompletely penetrant embryonic lethality phenotype. However, no consistent features were found. Similarly some lethality if mice happened neonatally, before genotyping is possible and the dead pups are cannibalised. Thus, at this point the reason for the unexpectedly low number of *Davis* heterozygotes and homozygotes born to heterozygous intercrosses, and the smaller size of litters born to *Davis* homozygous intercrosses compared to wt intercrosses remains unknown.

Table 5.3 Average litter size produced by each intercross.

Intercross type	No. Litters counted	Total offspring	Average (No. Pups per litter)
wt	6	48	8
he	36	257	7.13
ho	14	94	6.7

Table 5.4 Compilation of observed morbid features in *Davis* mice.

Genotype	**Sex**	**Reason**	**Age at death**	**Clinical**
Ho	Female	FDC	Neonate	Unknown, coagulated blood in abdomen
Wt	Unknown	FDC	Neonate	Unknown, coagulated blood in abdomen
Wt	Unknown	FDC	Neonate	Unknown
He	Male	FDC	Neonate	Unknown
Wt	Female	FDC	Neonate	Unknown
Het	Female	FDC	3 months	Unknown
Ho	Female	Cull	3 months	Apparently intestines blocked
Wt	Male	Cull	3.5 months	Small and thin apparently ill
Ho	Male	FDC	4 months	Unknown
He	Female	Cull	4.5 months	Necrotic brain, sclerotic liver
Ho	Female	Cull	5 months	Prolapsed
Het	Male	Cull	5.5 months	Hyperactivity
Wt	Female	FDC	6 months	Unknown
Ho	Male	Cull	8 months	Enlarged stomach with an excess of liquid

5.2.2 Allometric scaling analysis

Allometric scaling is the term used to describe the mathematical relationship between similar organisms of different sizes. This principle can be used to predict differences in both metabolism and structural function between living organisms because size influences the rates of biological function from the level of the cell to population dynamics of plants and animals (West *et al*., 1997). Since the body function is related to size, there are many implications for the use of allometric scaling in medical research. Allometric principles have been applied to physiologic function such glomerular filtration rates (GFR) (Singer, 2001). In order to define any abnormality in organ growth the total size in terms of area, length and weight of each animal was measured as well as the weight of individual organs. For this a cohort each of Davis and *Trigger* of mice were sacrificed at 7 months of age and measured individually by sex and genotype. Organs where Wt1 is known to be expressed (at least during development) were dissected weighed and fixed in paraformaldehyde and embedded in wax blocks for subsequent analysis. These organs include Brain, Eye, Heart, Spleen, Kidneys, Testis Thymus, Liver and Abdominal and Renal fat pads. Because of intrinsic gender difference of weights were analyzed separately for males and females, this also would give us a confirmation in case if a difference appears, so that the observed dissimilarity might or not be able to be present in both genders. The values were analyzed using the statistical tool one-way analysis of variance (ANOVA) was performed to corroborate the values obtained and avoid redundancy with Tukey' Multiple Comparison (Tukey's test). Tukey's post hoc to see differences between three groups, this test can be used to compare all groups to each other to find where the differences lie. One way ANOVA looks for differences between three or more classes. This test is completed by Gaussian distribution by given P value that the groups are sampled within the same population. Whether differences between groups are valid or not is dependent upon the *P* value. The *P* values was defined as $P<0.05$. If $P<0.05$. Statistical test were performed using GraphPad Prism®.

5.2.2.1 *Trigger* weight analysis

From a cohort of 24 mice including equal numbers of male and female mice divided into same numbers of wt, heterozygotes and homozygotes. Organs were dissected and weighed. Graphs displaying average weights of whole carcasses and organs of male or female *Trigger* mice, comparing homozygotes, heterozygotes and wt's are shown in Figure 5.1 (i-xx). None of these weight measurements showed any statistical significant differences between the genotypes for each sex shown in Table 5.5 except only for sporadic cases as male eye and female left kidney. This could be explained by the finding that the terminator sequence, designated to truncate Wt1-AS RNA upstream of Mcr2 was not very effective, resulting in continued Mcr2 expression in tissues. Therefore any further analysis of this strain was abandoned.

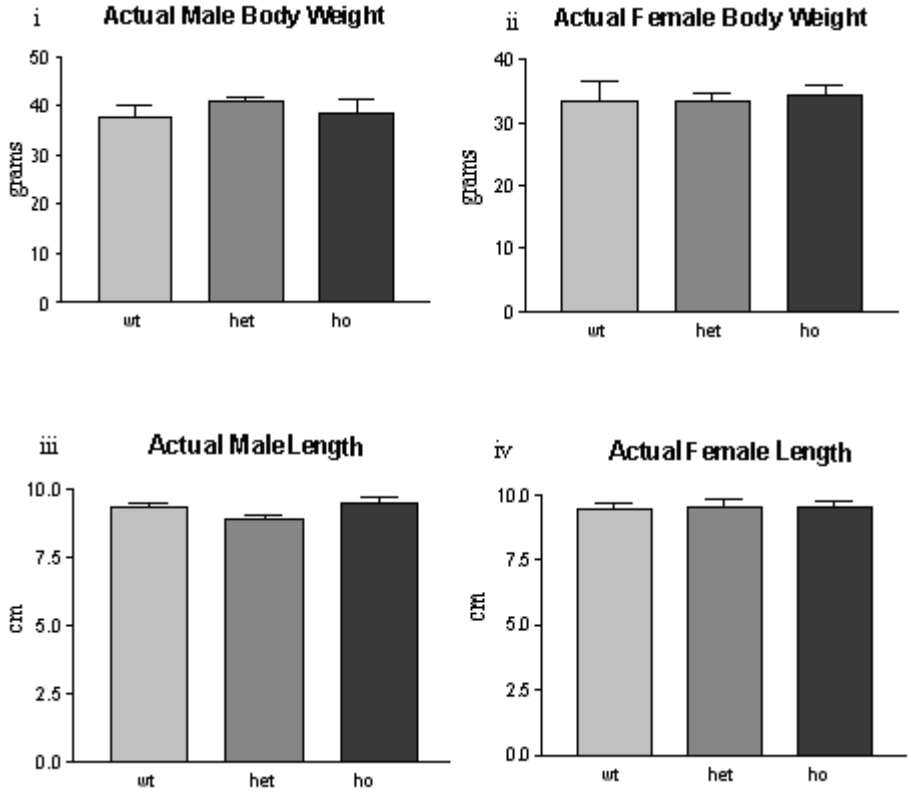

v Actual Male Brain Weight

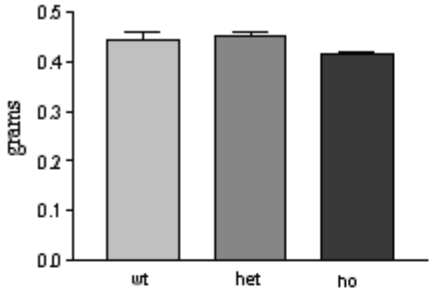

vi Actual Female Brain Weight

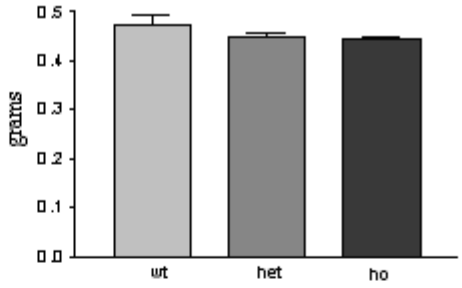

vii Actual Male Eye Weight

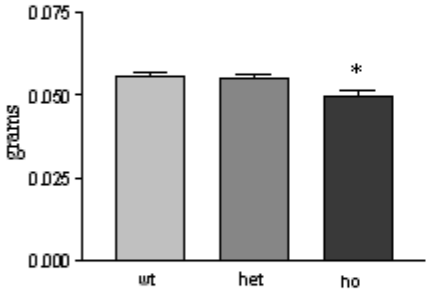

viii Actual Female Eye Weight

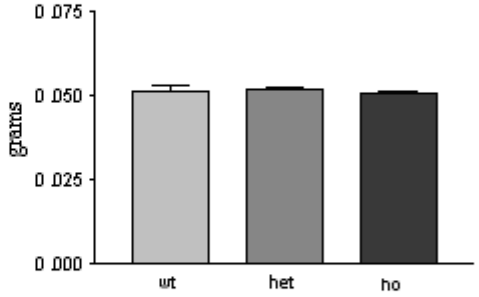

ix Actual Male Heart Weight

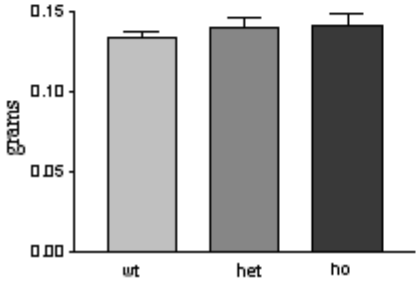

x Actual Female Heart Weight

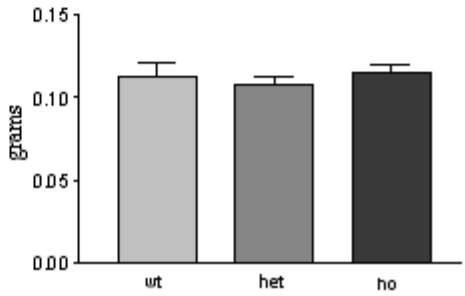

Actual Male Spleen Weight

xi

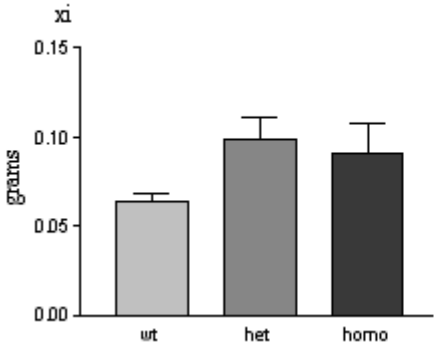

Actual Female Spleen Weight

xii

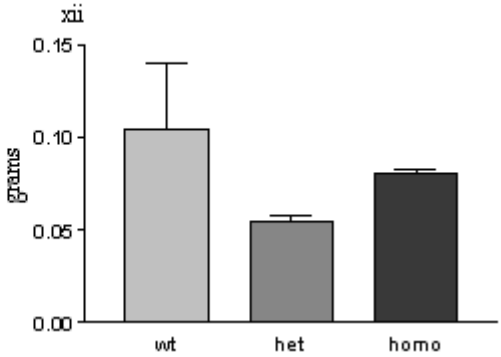

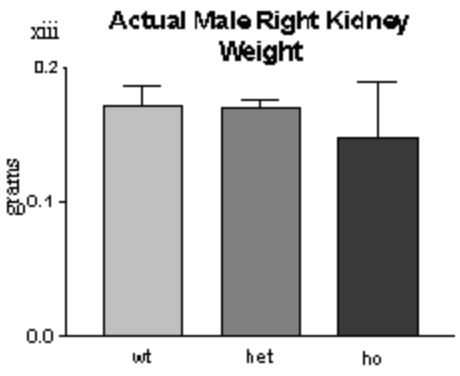
xiii
Actual Male Right Kidney Weight
grams
0.2
0.1
0.0
wt
het
ho

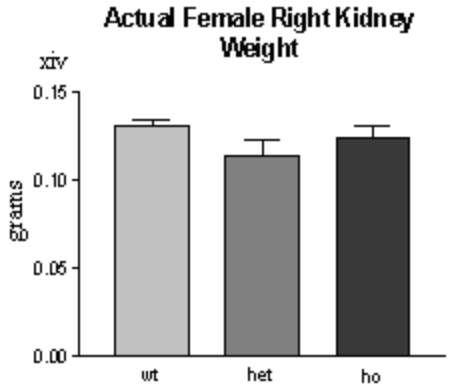
xiv
Actual Female Right Kidney Weight
grams
0.15
0.10
0.05
0.00
wt
het
ho

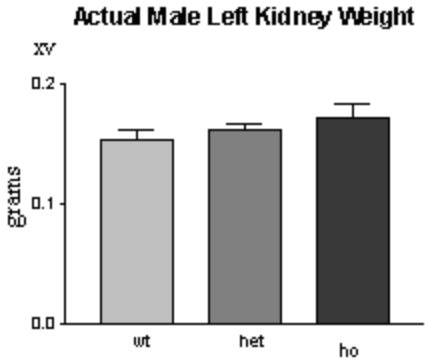
xv
Actual Male Left Kidney Weight
grams
0.2
0.1
0.0
wt
het
ho

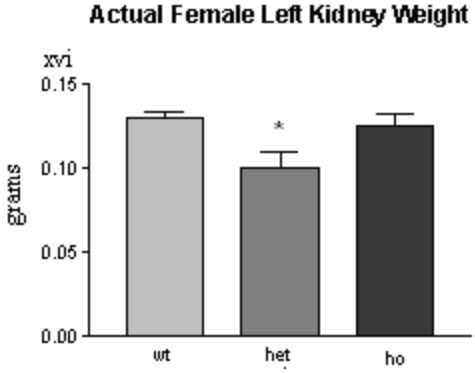
xvi
Actual Female Left Kidney Weight
grams
0.15
0.10
0.05
0.00
*
wt
het
ho

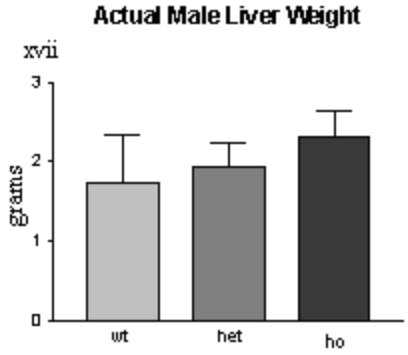
xvii
Actual Male Liver Weight
grams
3
2
1
0
wt
het
ho

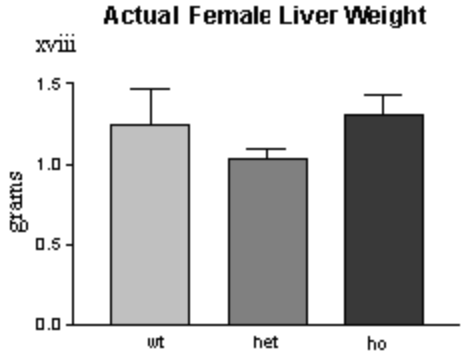
xviii
Actual Female Liver Weight
grams
1.5
1.0
0.5
0.0
wt
het
ho

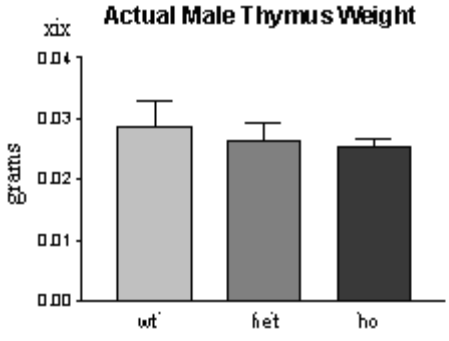
xix
Actual Male Thymus Weight
grams
0.04
0.03
0.02
0.01
0.00
wt
het
ho

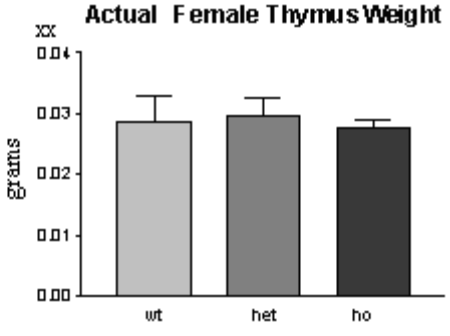
xx
Actual Female Thymus Weight
grams
0.04
0.03
0.02
0.01
0.00
wt
het
ho

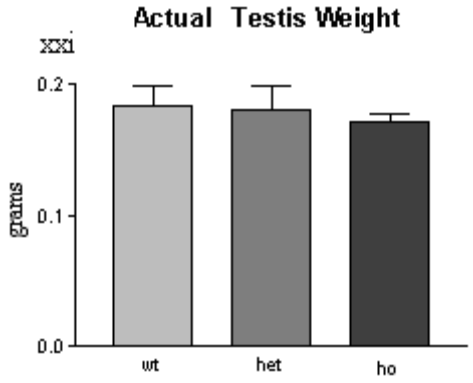

Figure 5.1 Graphs representing total body and individual organ weights in grams of 7-8 month old *Trigger* mice (i-xxi).

Table 5.5 Summary of the data presented in Figure 5.1 Data showing deviation from Wt controls. </> addressed the difference in size between groups, p values were categorized according to standard consensus **P*<0.05, ***P*<0.01, *** *P*<0.001, ns= non significant, wt= wild tpe, he= heterozygote, ho= homozygote.

7 Month Old Weight	*Trigger* Male	*Trigger* Female	Significant Difference	n
Total Body	*p*= 0.6009	*p*= 0.5271	ns	24
Brain	*p*= 0.0655	*p*= 0.3103	ns	24
Eye	*p*= 0.0384 * wt<he,ho	*p*= 0.8856	significant	24
Thymus	*p*= 0.7043	*p*= 0.7311	ns	24
Heart	*p*= 0.5334	*p*= 0.6900	ns	
Liver	*p*= 0.4572	*p*= 0.6414	ns	24
Right Kidney	*p*= 0.7713	*p*= 0.2773	ns	24
Left Kidney	*p*= 0.3696	*p*= 0.0362* he<wt, ho	significant	24
Spleen	*p*= 0.1559	*p*= 0.2806	ns	24
Testes (both)	*p*= 0.8326	---	ns	24

5.2.2.2 *Davis* weight analysis

The same analysis was made for the *Davis* strain with two consecutive cohorts with a pooled total sample number of 48. Graphs of the average weights are shown in Figure 5.2 (I-XXV). Cohorts of 4 animals for each sex, and genotype (n=24). Most of the measurements employed 2 cohorts (n=48). For a few of the measurements more or less animals were used. For the total weight analysis at 7 months (n=60), and a single cohort was used for recording total weight day 1, abdominal and renal fat paths only one cohort was raised (n=24). In the case of the total body weight a statistically significant difference was found with 17% difference between the wt and both heterozygotes and homozygotes, which were heavier (Figure 5.2 I and II). However this difference in weight is not reflected by body length (Figures 5.2 III and IV). To discover whether *Davis* homozygotes were already heavier than their wt and heterozygous littermate at birth, the total body weight of neonates was measured (Figure 5.2 V). No significant difference was observed at that stage suggesting that this phenotype develops with age.

By looking at the individual organs weights, a significant contribution to the increased total body weight of *Davis* homozygotes compared to wt's is not obvious for any particular organ. In some cases (e.g. male spleen, both genders left and right kidneys, male liver) there is a slight trend towards increased weight in *Davis* homozygotes compared with the wt counterparts. However, these differences are very slight and contradicted by opposite founded in trends towards some heavier organs in wt's compared to *Davis* homozygous (e.g. male and female heart, thymus, male testes, male abdominal fat and both genders of renal fat). In the case of the male brain weight this was difficult to reconcile, particularly as the apparent phenotype is not shown in females. This might have been an artifact due to the procedure of killing adult mice which has to be done by dislocation of the neck, sometimes damage the brain and is difficult to biopsy and weight integrally. The right and left kidneys were weighted separately due to the fact that in normal circumstances the right is bigger than the left.

However no differences between right and left kidney weight were found in this study. In summary no statistically significant increase in organ size in *Davis* homozygotes, compared to wt's was found. In fact the only case of statistical significance involves homozygotes showing decreased rather than increased weight. Therefore, the increased total body weight of *Davis* homozygotes is not due to increased organ weights.

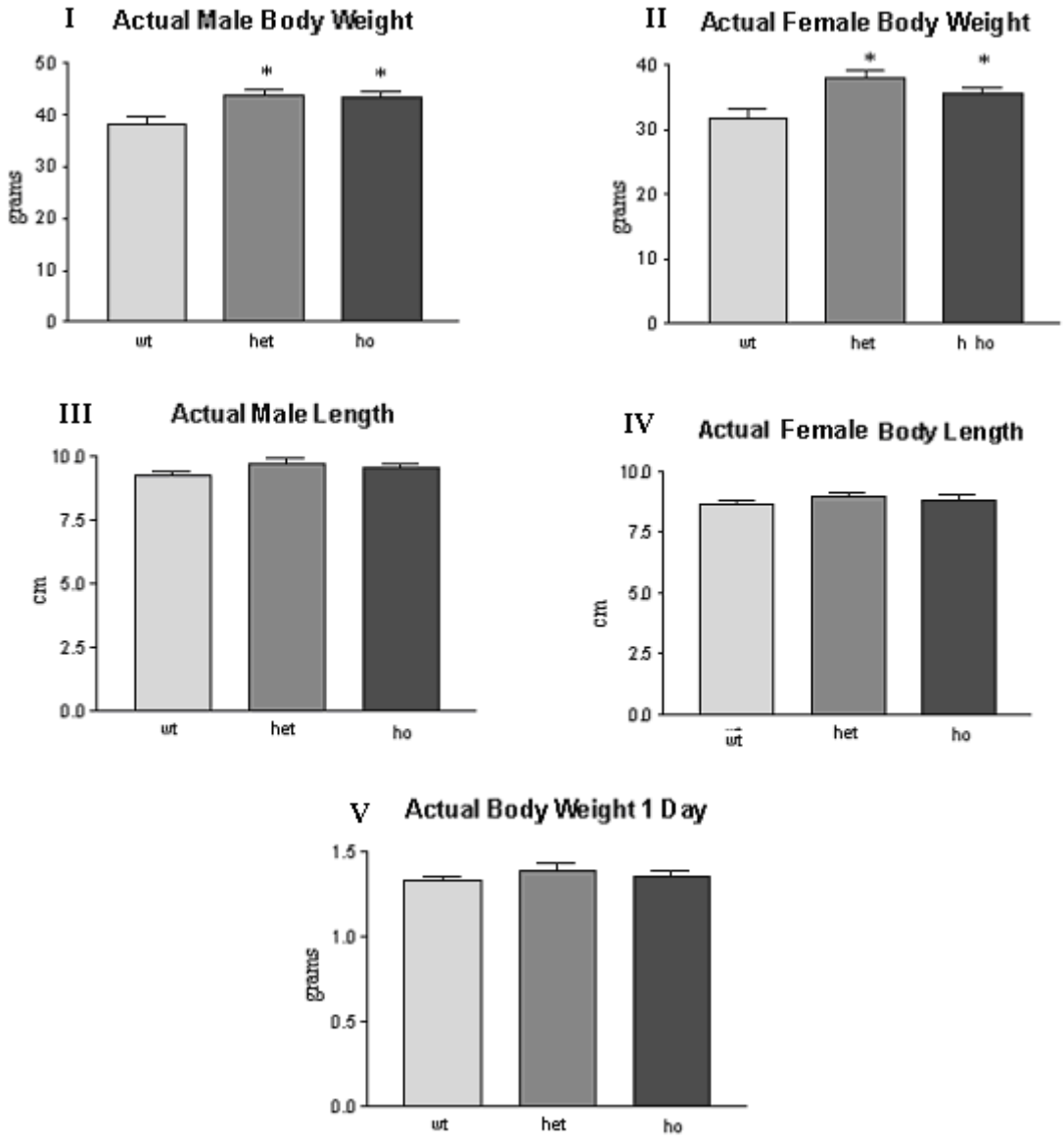

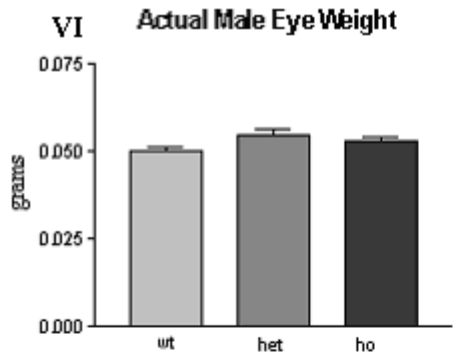
VI
Actual Male Eye Weight
grams
0.075
0.050
0.025
0.000
wt
het
ho

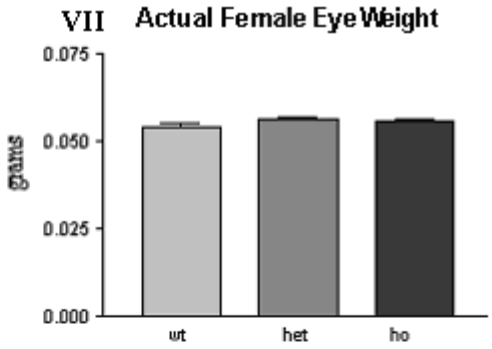
VII
Actual Female Eye Weight
grams
0.075
0.050
0.025
0.000
wt
het
ho

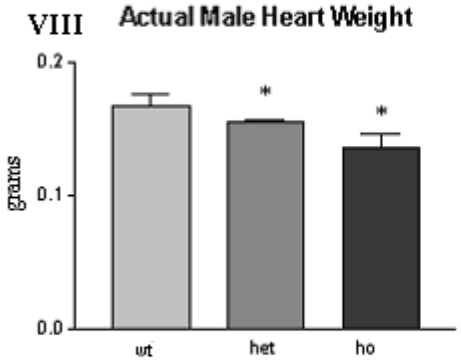
VIII
Actual Male Heart Weight
grams
0.2
0.1
0.0
*
*
wt
het
ho

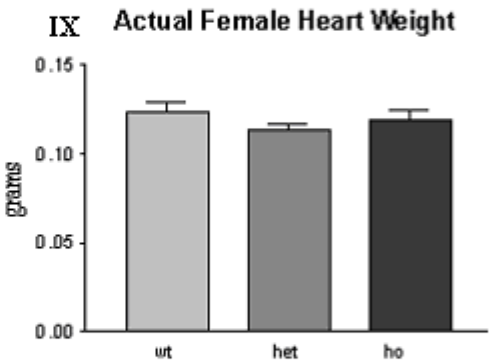
IX
Actual Female Heart Weight
grams
0.15
0.10
0.05
0.00
wt
het
ho

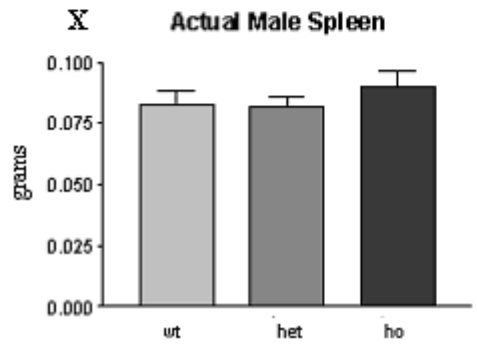
X
Actual Male Spleen
grams
0.100
0.075
0.050
0.025
0.000
wt
het
ho

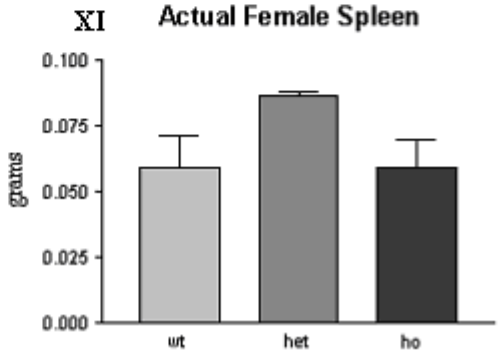
XI
Actual Female Spleen
grams
0.100
0.075
0.050
0.025
0.000
wt
het
ho

XII Actual Male Brain Weight

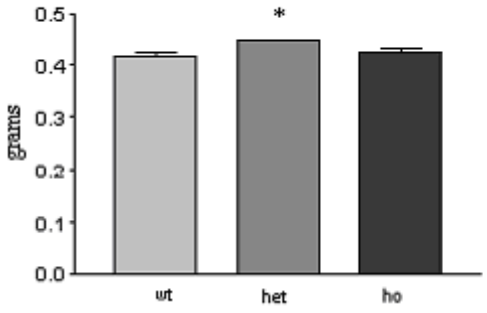

XIII Actual Female Brain Weight

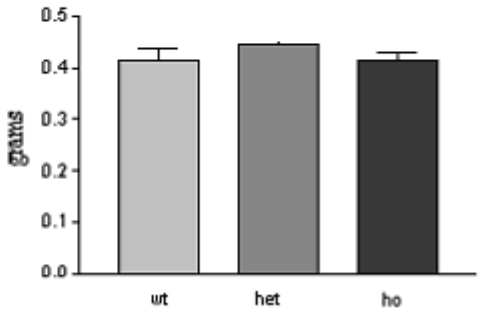

XIV Actual Male Right Kidney Weight

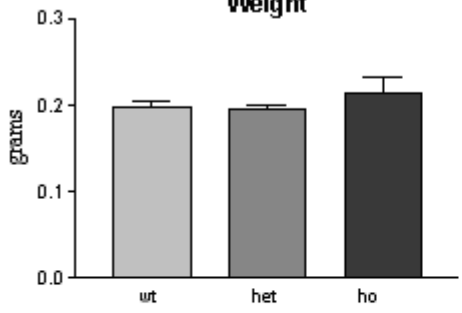

XV Actual Male Left Kidney Weight

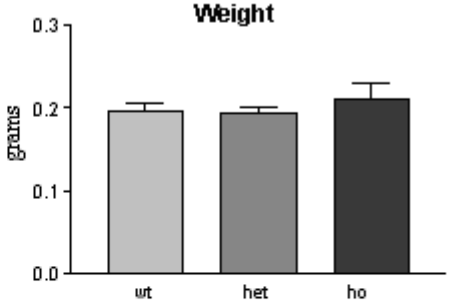

XVI Actual Female Right Kidney Weight

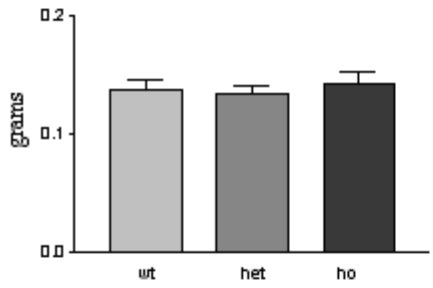

XVII Actual Female Left Kidney Weight

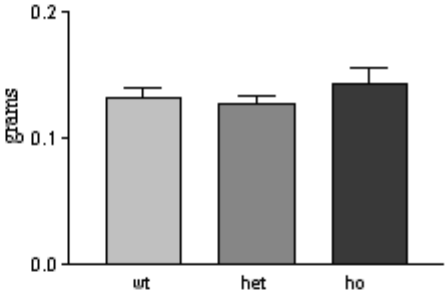

XVIII Actual Male Thymus Weight

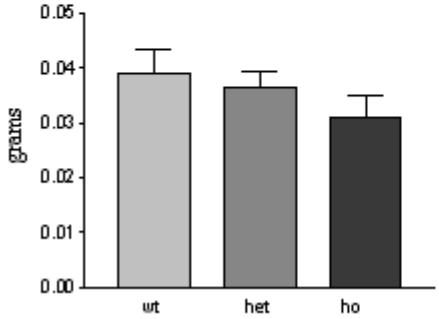

XIX Actual Female Thymus Weight

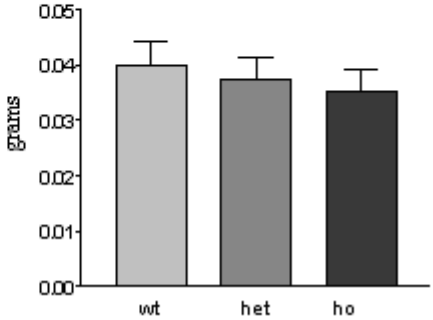

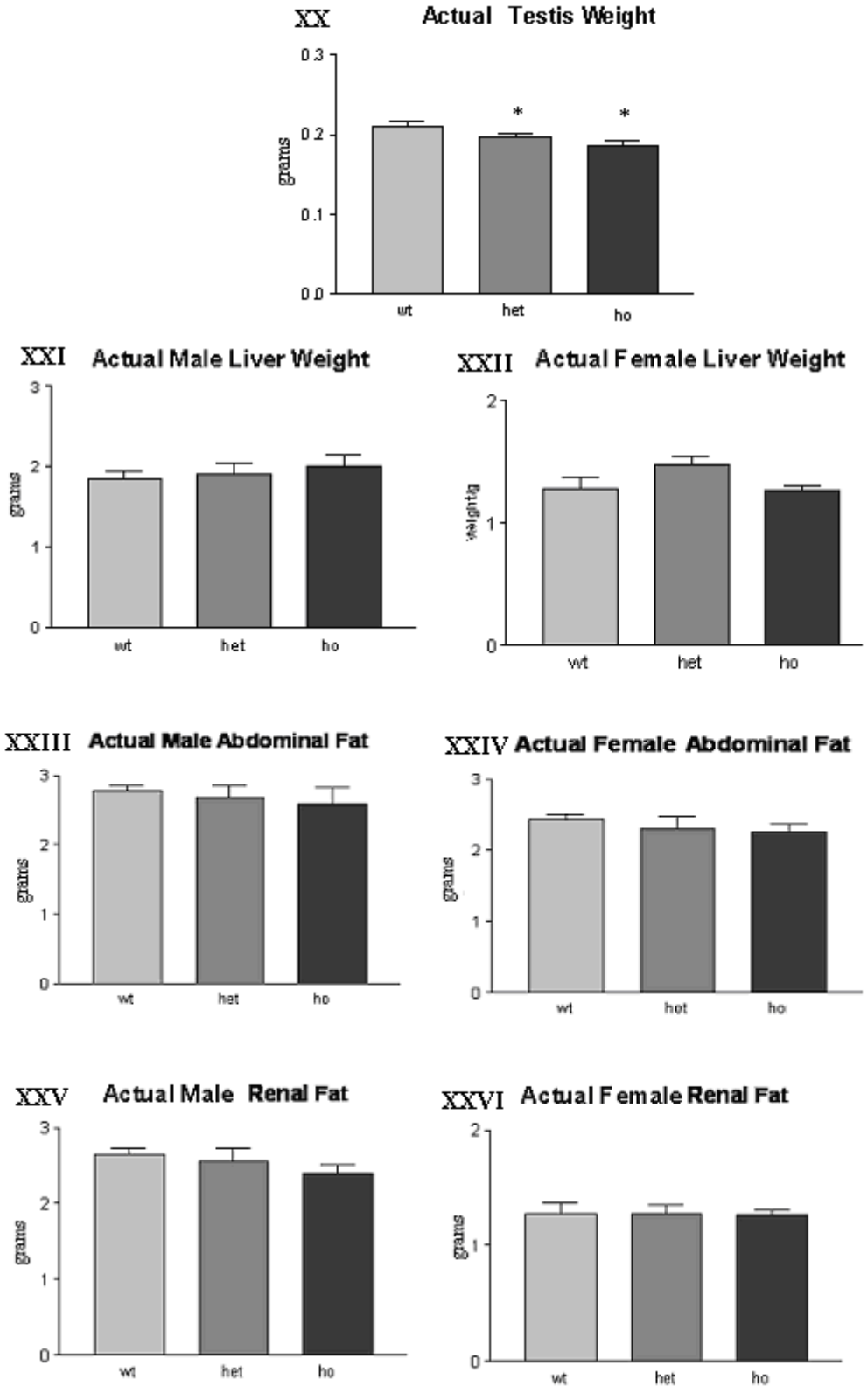

Figure 5.2 Graphics representing body and individual organ weights in grams of 7-8 month old *Davis* mice (I-XXVI).

Table 5.6 Summary of the data presented in Figures 5.2. Data showing deviation from Wt controls. </> addressed the difference in size between groups, *P* values were categorized according to standard consensus **P*<0.05, ***P*<0.01, *** *P*<0.001, ns= non significant.

7 Month Old *Davis* Mice Weight/Length	Male	Female	Significant difference	n
Total Body	P= 0.0092 ** wt< (ho/he)	P= 00085 ** wt< (ho/he)	Significant	60
Body length	P= 0.2466	P= 0.2185	ns	24
Brain	P= 0.0063 **(wt/ho)<he	P= 0.27	Significant	48
Eye	P= 0.06	P= 0.1154	ns	48
Thymus	P= 0.3847	P= 0.7165	ns	48
Heart	P=0.0337 * wt>he>ho	P= 0.2938	Significant	48
Liver	P=0.6284	P=0.1237	ns	48
Left Kidney	P= 0.450	P= 0.3040	ns	48
Right Kidney	P=0.5405	P=0.5365	ns	48
Spleen	P=0.4943	P=0.827	ns	48
Testis	P= 0.0387 * wt>he>ho	-----	Significant	48
Abdominal Fat	P=0.3922	P=0.483	ns	24
Renal Fat	P=0.3846	P=0.468	ns	24

5.2.3 Urine analysis of *Davis* and *Trigger*

Proteinurea is a frequent and early manifestation of glomerulonephritis mouse (Hoffstein *et al*., 1975). It can indicate functional disruption of the kidney. WT1 is essential for glomerular the maintenance of podocytes which perform glomerular filtration in the kidney (Guo *et al*., 2002; Menke *et al*., 2003). For this reason, we analyzed *Davis* and *Trigger* mouse urine for proteinurea. In fact proteinurea has been detected in transgenic mice expressing extra copies of a single isoform of Wt1 (-KTS) disrupting the Wt1 allele (Lahiri *et al*., 2007).

Urine samples were collected from cohorts of *Davis* and *Trigger* mice (n=24) at 6 months of age. Cohorts contained equal numbers of males and females of each genotype. 7 µl samples were analyzed by SDS-PAGE and protein visualized by staining with Coomassie Brilliant Blue staining. This method is sufficient to detect protein at >20 µg. As can be seen in Figure 5.3 no mice in the *Trigger* cohort had proteinurea, regardless of genotype. In the case of the *Davis* line, three mice displayed protein urea. (Lanes 9, 10, 11).

However, this phenotype did not correlate with genotype. The three positive samples were from females of the same single litter and were genotyped wt, wt and he respectively. Therefore proteinurea is not caused by the presence of the *Davis* allele in these particular mice. Kidneys from these two cohorts were not included in the weight study, but were studied hystologically.

Only 3 samples were detected with protein in the urine counting for 2 wt and one ho (Figure 5.3). This 3 individuals were littermates been born from the same parents. Kidney samples were not part of the class of weight however samples were hystomorphology analyzed.

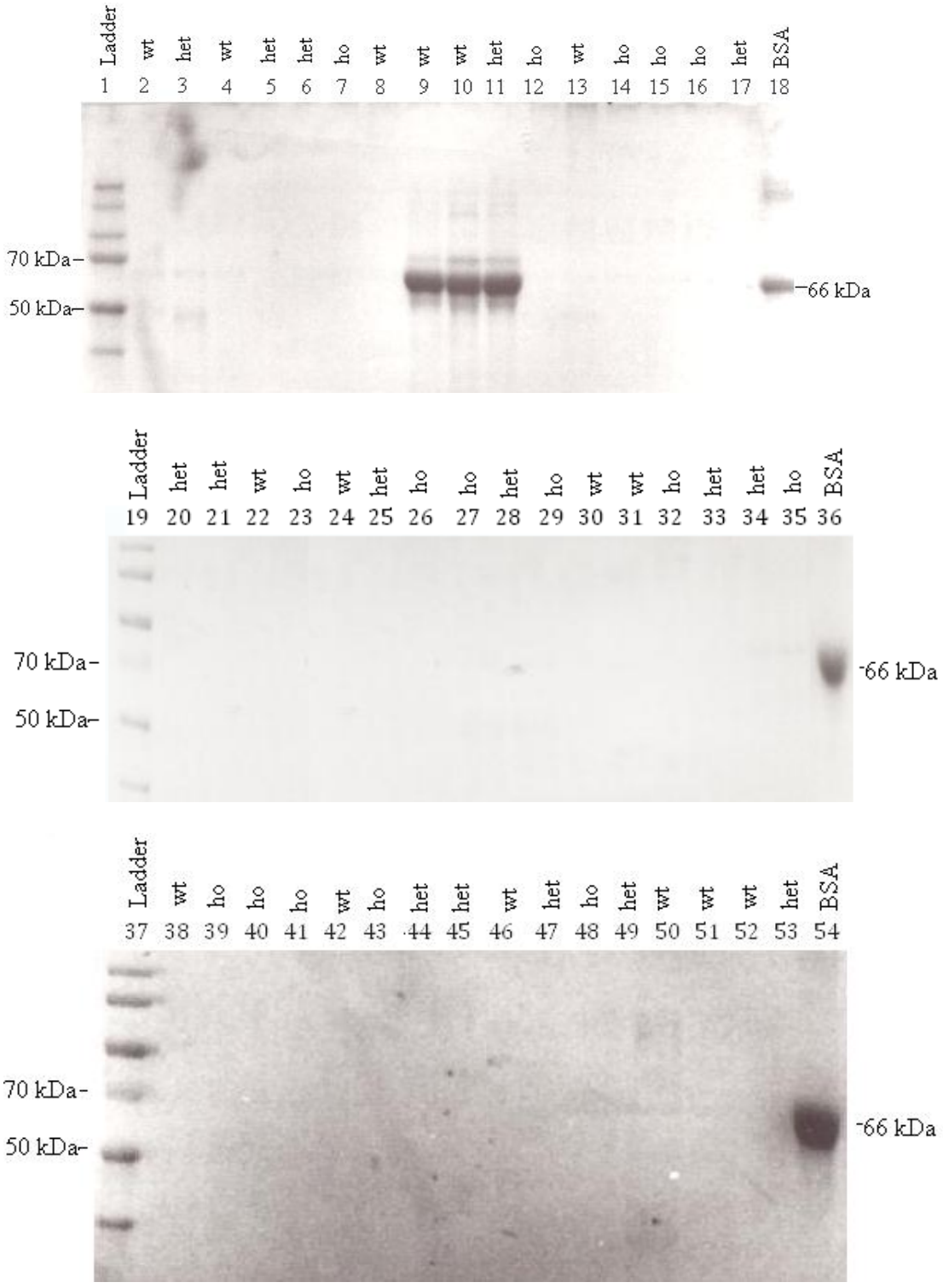

Figure 5.3 Urine analyses for early detection of proteinurea in *Davis* and *Trigger* mice. SDS-Polyacrylamide gel of *Davis* (1 to 27)and *Trigger* (28 to 54) urine samples. Lanes 1, 19 and 37: molecular weight ladders (Fermentas). Lanes 18, 36 and 54: bovine serum albumin as a positive control.

5.2.4 Segregation of polymorphic alleles in mice with abnormal kidneys.

As shown in section 4.2.3.2, by using SF-VR primers is possible to amplify strain-specific polymorphisms. During analysis of mouse wt1 antisense transcript expression by q-PCR in embryonic kidney, it was noticed that primers amplifying a sequence transcriptional upstream of the transcriptional terminator in *Trigger* homozygote mice gave rise to two different side peaks (personal communication). Subsequently by cloning and sequencing genomic PCR products, it was discovered that parental mouse strains combining to *Trigger* and *Davis*, namely C57BL/6, CBA and 129 had strain specific length polymorphism at the repetitive sequence between primers SF and VR. Due to proximity of the SF-VR sequence and Mcr2, if Mcr2 has any association with the formation of cystic kidneys of SF-VR might segregate with this pathological phenotype. A whole litter in which three females had kidney failure (Figure 5.3) was analysed including parents and grandparents. The SF-VR alleles are shown in Figure 5.10 including cystic individuals (2, 3 and 4), parents (5, 6) grandparents (7, 8), CBA and C57BL/6 genomic DNA as markers (10, 11) (Figure 5.4). Although no correlation between mice with abnormal kidneys was observed, mice inheriting the mother's C57BL/6 allele had cystic kidneys, whereas those that inherited the mother's CBA allele did not.

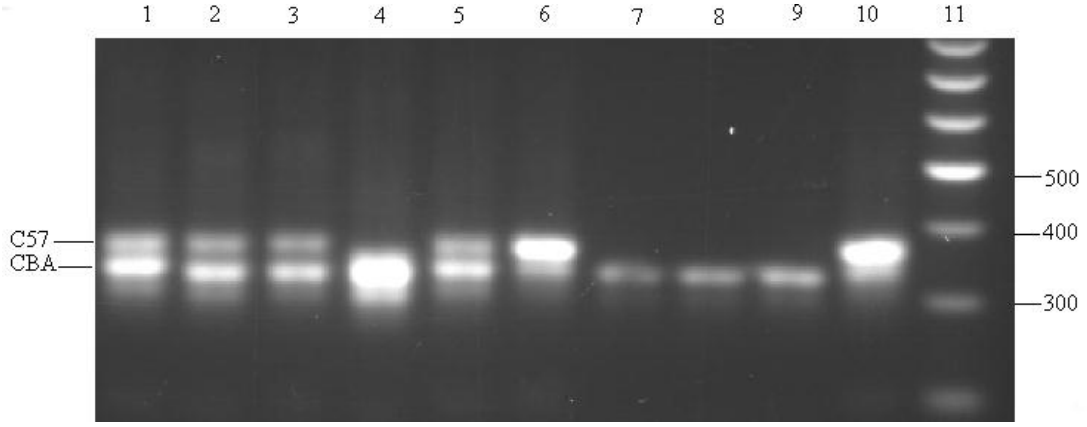

Figure 5.4 PCR showing distribution of SF-VR alleles in mice with abnormal kidneys. (1) He cystic littermate, (2) wt cystic littermate, (3) Ho cystic littermate, (4) heterozygote father, (5) heterozygote mother, (6) wt grandfather, (7) homozygote grandmother, (8) normal littermate, (9) normal littermate, (10) pure CBA, (11) pure C57, (12) 100 bp Ladder (Promega).

5.2.5 Histological analysis of *Davis* organs

To look for any abnormal organ morphology kidney, testis, liver, heart, spleen and thymus were dissected and histologically examined in a cohort of 24 (4 animals of same sex and genotype). The developmental expression of Wt1 in these tissues has been reported (Kreidberg *et al*., 1993), so an effect due to Mcr2 disruption was anticipated. A representative of each organ was sectioned from a wild-type, heterozygous and a *Davis* homozygous mouse. Organs were embedded in the same orientation and also stained in the same time in order to equalize conditions as much as possible. Most of the staining was done by haematoxylin and eosin (H&E) except in the kidney which was done by Periodic Acid Schiff (PAS) staining. All samples were males unless otherwise stated.

Kidney histology

Wt1 is expressed in the podocyte in the glomeruli of the adult kidney where it has a role in kidney function (Guo *et al*., 2002). For the case of the kidney PAS staining was used to visualise proximal and distal convoluted tubules were glycoproteins become visible with this staining. Proximal tubules show of pink staining within brush borders whereas distal tubules should not. A representative sample was analysed. Homozygote and wt kidneys were undistinguishable by histological analysis, showing that no obvious morphological kidney abnormality was associated with the *Davis* allele. All structures of the kidney were present in homozygous as well as in the wild-type kidney, displaying normal distribution. Within the kidney from the cortex (Co) to the capside (Ca) was possible to find glomeruli (G). They were present and appear normal, with a radial distribution surrounded by distal (D) and proximal (P) convoluted tubules (Figure 5.5). an example of a heterozygote kidney with no presence of peripheral tubules is shown in Figure 5.5 E. Protein in the urine was detected on this mouse (see Figure 5.3 lane 11).

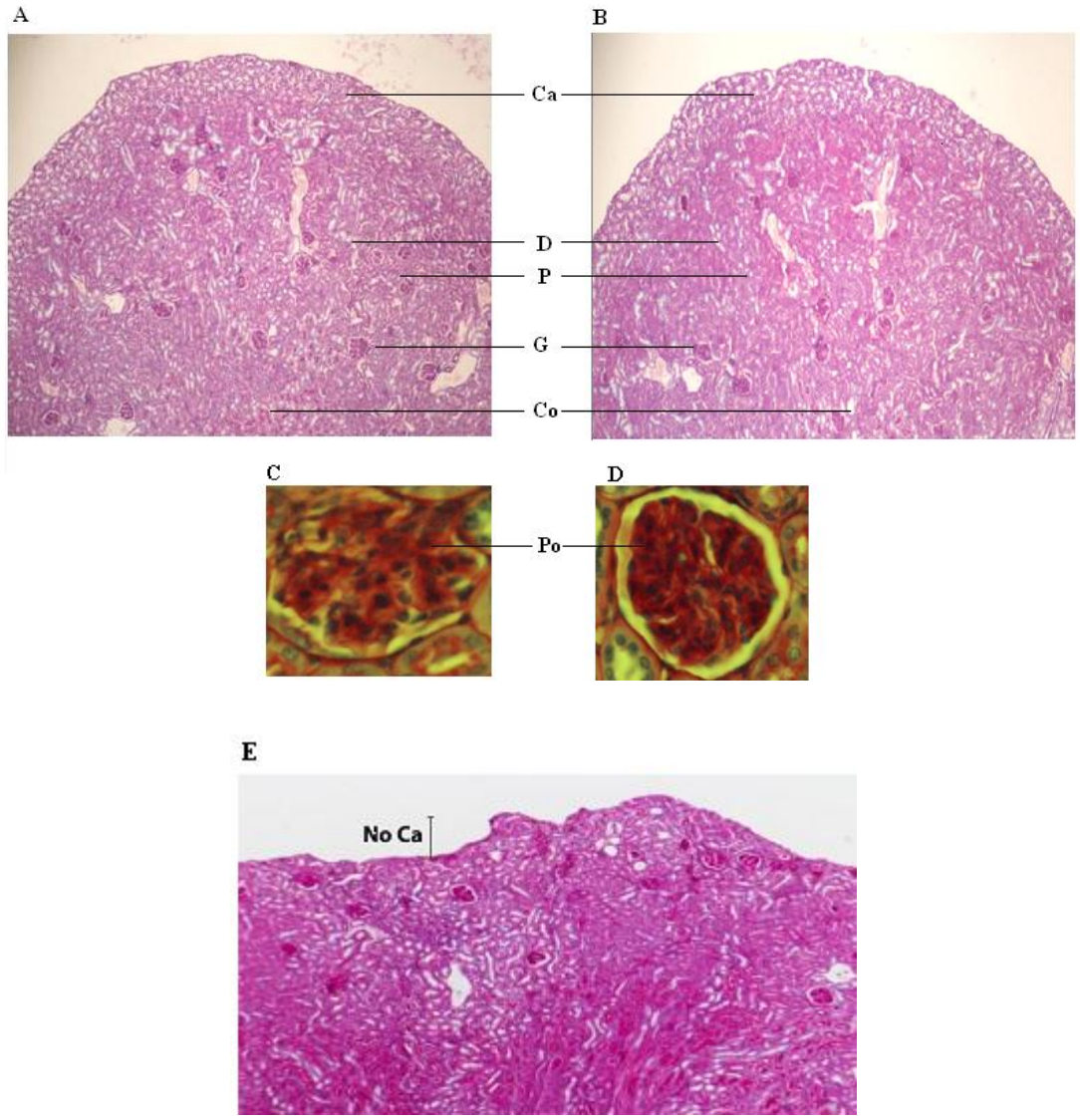

Figure 5.5 Histological analysis of *Davis* kidney. PAS stainining of sagittal sections in wt (A) and homozygous (B) kidney (20X) showing capsid (Ca), distal convoluted tubules (D); proximal convoluted tubules (P)and cortex(C). Below is shown the glomeruli (G) displaying the podocytes (Po) present wt (C) and homozygote (D) (40X). (E) Sagittal dissection of abnormal heterozygote kidney showing no presence of capsid (peripheral tubules) (20X).

Testis histology

As seen in the weight section (5.2.2.2), homozygous *Davis* testes were consistently found to be lighter than the testes of wt counterparts. H and E staining of a wt and homozygotes testes sections shown that although the size and number of the seminiferous tubules appeared to be the same, the distribution was not equal.

However, the number sertoli cells and mature sperm did not reveal any significant difference. On the histology analysis gaps were found between those tubules (Figure 5.6). No other parallel between testes pathology were discern. Although this genotypic dimorphism is consistent in the population, ho mice are able to generate offspring. So because of this mild feature we did not proceed to any further research about this particular subject. Sections of testes from 9-month-old mice were stained with Mayer's hematoxylin (Figure 5.6).

Seminiferous tubules were counted as well as the spermatozoa within those tubules. An arbitrary line in the middle of sagittal sections was draw in order to look at the number of tubules. The average of tubules in the testis for homozygous was 16.3 for the wt and 16.6 for the homozygote (P= 0.0869). The amount of mature sperm counted was also not significant between these two groups (P= 0.0611). No differences were noticed between wt and homozygous *Davis* mice which seemed to have the same amount of tubules and mature sperm.

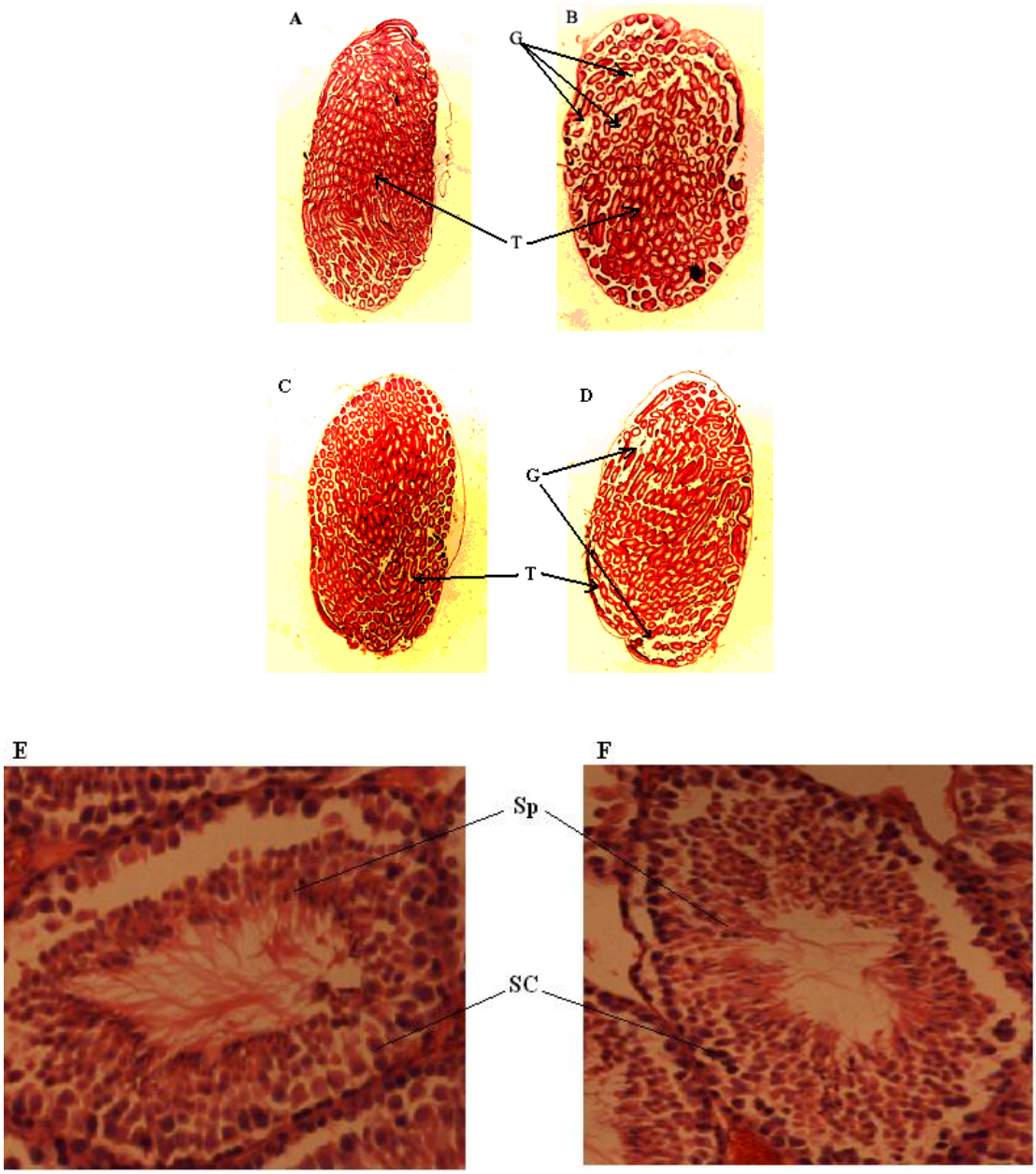

Figure 5.6 Histological analysis of *Davis* Testis. Sagittal dissection stained with H & E., comparing seminiferous tubules distribution in wt (A and C) and homozygous (B and D) (4X); below, wt (E) and homozygote (F) sections indicating Sertoli cells (SC) and mature sperm (SP) (40X).

Thymus histology

This organ did not statistically change in weight between genotypes. Consistent with this no difference in thymus morphology was found between *Davis* homozygotes and wt controls. Also no pathology was noted. Features of the thymus such as thymic corpuscles medulla and cortex were indistinguishable between wt and homozygotes as shown in Figure 5.7.

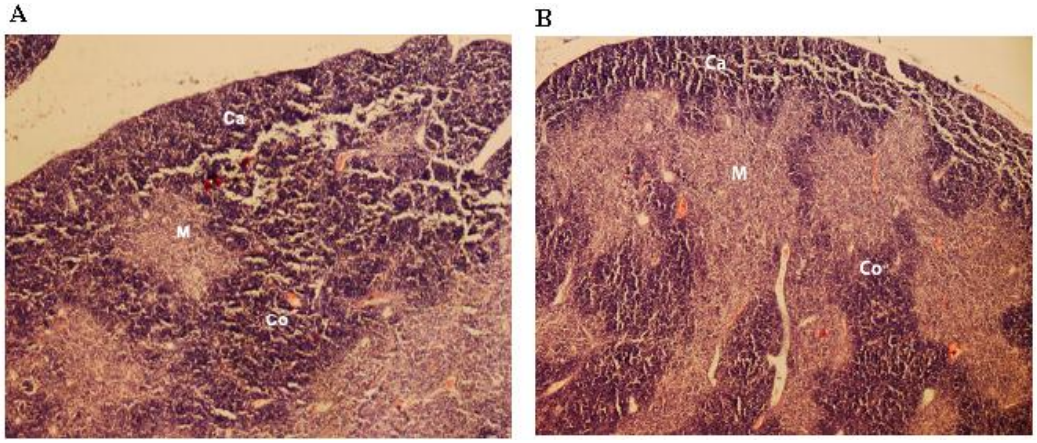

Figure 5.7 Histological analysis of *Davis* thymuses. (A) Sagittal sections of thymus from *Davis* wt and (B) homozygote stained with H & E (20X) showing capside (Ca), medulla (M) and cortex (C).

Liver and spleen histology

No observable differences were found by histological analyses of homozygous livers and their wt counterparts (Figure 5.8). Hepatocytes had an apparently similar distribution across wt and homozygous liver sections and no difference in number or shapes was obvious in the collected images. Heterozygous male mouse was found to have a sclerotic liver with apparently fat in the tissue (Figure 5.8 C). Abnormalities in livers were found in 3 males and 2 females (3 wt females; 1 male heterozygote and 1 female homozygote). The same mice with liver abnormalities also had spleen abnormalities. However, histological analysis of *Davis* homozygous and wt spleen did not reveal any feature exclusive to either genotype (Figure 5.8). Spleen cells did show common distribution between white and red pulp. Abnormal spleens displayed thickened and sometimes enlarged shapes with uneven epithelium surrounding the external area of the organ. However as was the case for livers, these abnormalities did not correlate with *Davis* genotype (Figure 5.8 F).

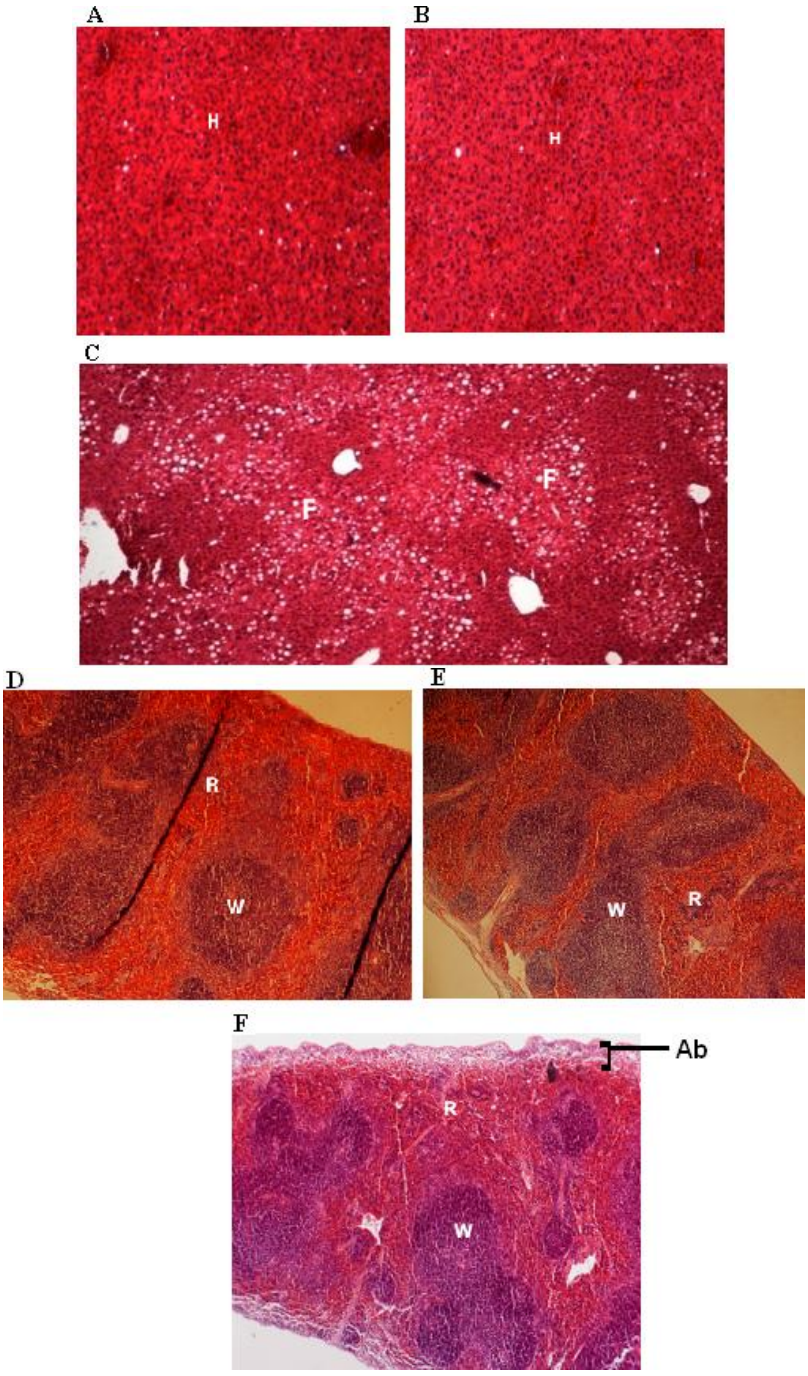

Figure 5.8 Histological analyses of *Davis* liver and spleen. Liver sections stained with H & E. (40X). Wt (A) and homozygote (B) liver sections show distribution of hepatocytes (H). (C) wt with apparently abnormal fat (F) content (20X). Longitudinal section of spleen organs stained by H & E. Wt (C), homozygote (D) and (F) displaying white (W) and red pulp (R) distribution and abnormal heterozygote with wrinkled surface (Ab) (20X).

Heart histology

Wt1 is needed for heart normal heart development. *Wt1* is expressed in the epicardium of the developing heart which is the external layer of tissue in the heart. In the homozygous *Wt1* knock-out mouse model (Kriedberg *et al*., 1993) the failure of the heart has been determined to be the cause of embryonic lethality at mid-gestation. In the weight study (see section 5.2.2.2) *Davis* homozygote male heart weight was significantly lower than wt; however this weight difference was not apparent in females. Sex-dependent differences were not expected for heart defect. *Davis* homozygote mouse heart has apparently undistinguishable from wt heart in terms of shape and distribution of cardiomyocites. No heart abnormality of pathology was found (Figure 5.9).

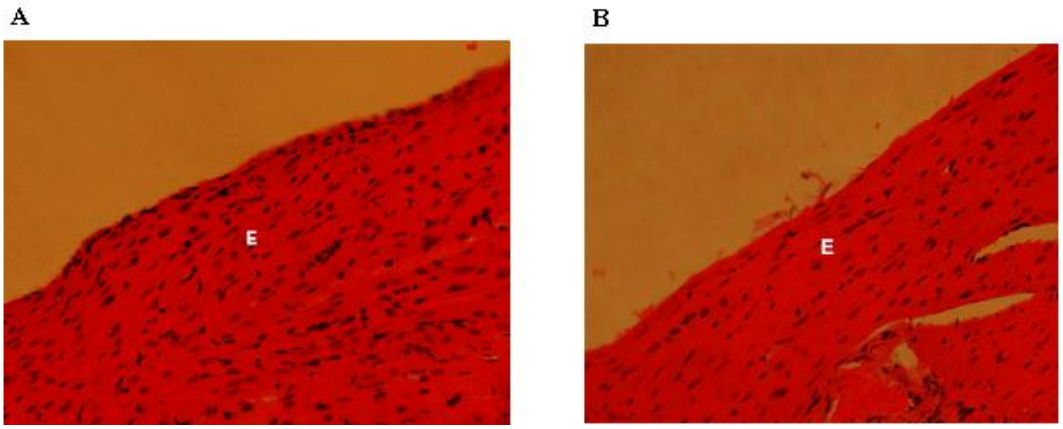

Figure 5.9 Histological analysis of *Davis* hearts. Stained sections with H & E show epicardum (E) tissue in wt (A) and homozygote (B) sections (40X).

5.2.6 Body composition of *Davis* mice.

The *Davis* weight study found that homozygotes had significantly higher weight than wt siblings (average of 17% higher, Section 5.2.2.2) even though, parallel increases in organ weight were not found. Indeed some organs of homozygous *Davis* mice were lighter were lighter than their wt siblings. Therefore, the analysis was extended to include a comparison of body size (area) and components such as bone, muscle and fat.

For this a new cohort of *Davis* mice 4 each per genotype including equal numbers of males and females (n=24) was analyzed at 7 months of age. Whole cadavers of *Davis*

mice were subjected to dual X-ray absorptiometry (DXA) which gives an estimate of fat mass, fat-free soft tissues mass and bone mass (Jabb *et al.*,1998; Zotti *et al.*, 2008). As shown in Table 5.7 no statistically significant differences between *Davis* wt, heterozygous, homozygous were found. Therefore the increased body weight of *Davis* homozygous mice is not account by these factors.

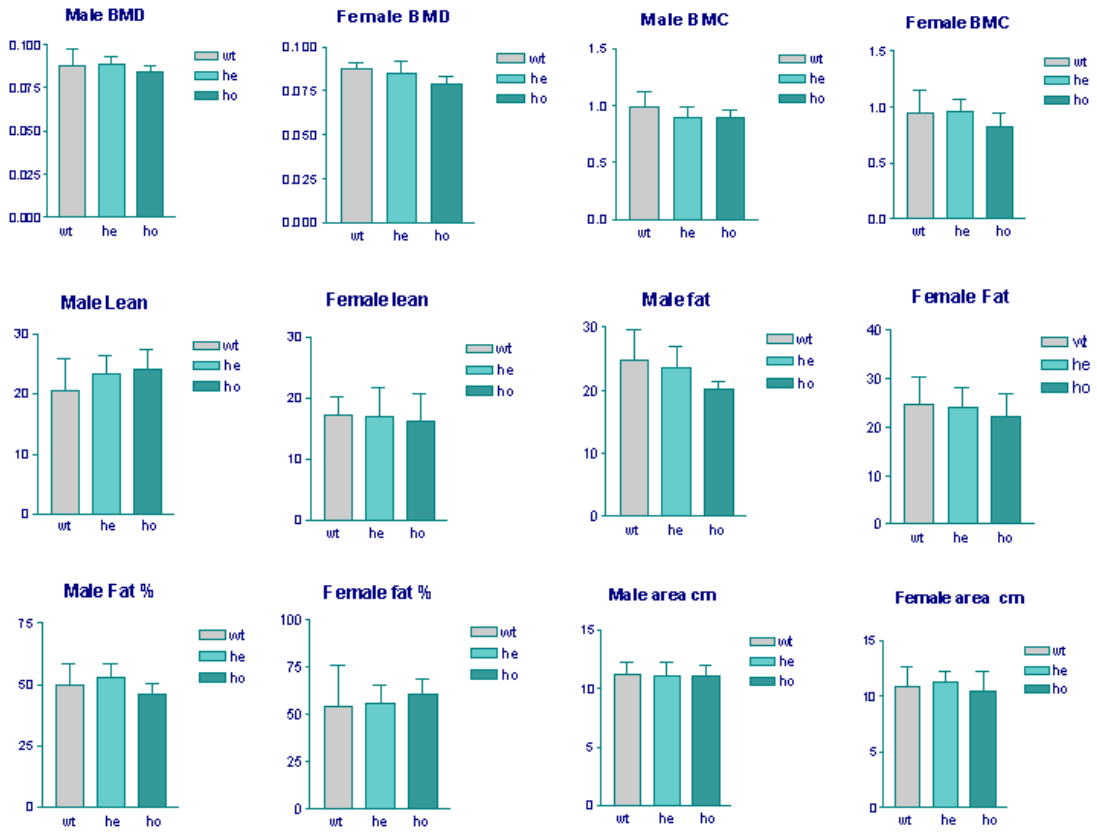

Figure 5.10 Average body composition of male and female *Davis* mice. Graphics show levels of lean, BMC, BMD, fat, fat% and areas values are expressed in g/cm^2. Wt=wild type, he=heterozygotes and ho= homozygote.

Table 5.7 Summary of P values obtained by using DXA measurements of body composition in *Davis* mice.

7 Month Old DXA	*Davis* Male	*Davis* Female
Bone Mineral density (BMD)	P=0.5661	P=0.0877
Lean content	P=0.4729	P=0.9422
Fat content	P=0.215	P=0.7695
Fat %	P=0.331	P=0.8072
Area cm^2	P=0.9542	P=0.7356

5.2.7 *Davis* dry weight study

After ruling out individual organs, bone, lean, fat as contributory factors to the increased total body weight of *Davis* homozygous to wt's, a remaining factor that could account for weight difference was water content which is controlled by the kidney. This was evaluated by comparing the weight of a mouse organ with the weight of the same organ after desiccation. 12 females (4 per genotype) at 7 months of age were used for this study. The liver was chosen for this analysis as a representative tissue because it is a suitable size to allow a difference in dry and wet weight to be measured using a fine balance.

After recording fresh (wet) weight, the livers were dried in an oven until no further decreasing in weight occurred indicating that a totally desiccated stage had been reached. Comparison of the average water content of organs from each genotype showed that liver water content was significantly higher (Figure 5.12) in heterozygous and homozygous *Davis* mice compared with wt counterparts. This was indicative of water retention in the tissue associated with the *Davis* allele. An average increment of 5.6 % in water content in ho and het vs. Wt *Davis* was observed.

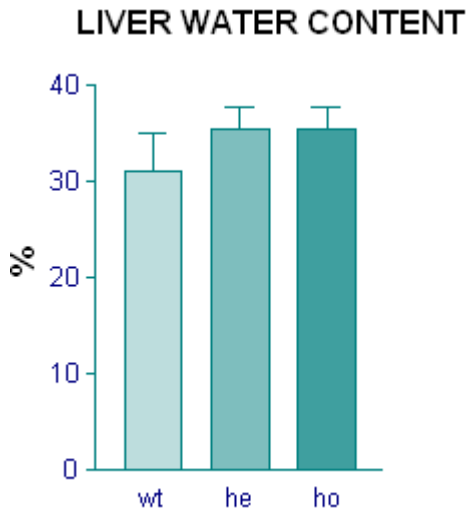

Figure 5.11 Average percentage of fresh organ weight lost from livers after desiccation. Graph shows the values obtained of water in the liver after desiccation expressed in percentage; wt= wild type, het= heterozygous and ho=homozygous.

5.2.8 *Davis* urine osmolarity

The body has a complex regulatory system which balances the water intake and losses to maintain the osmotic equilibrium. This system involves primarily hormones on the kidney. Thus normal renal function is crucial to maintenance of normal plasma concentration. An abnormal plasma concentration is likely to be reflected by excretion of urine with abnormal osmolarity level as well as causing abnormal fluid levels in the tissues of the body.

Given the significant difference in water content of *Davis* homozygous organs compared to wt, we sought further difference of altered excretory function in *Davis* homozygotes. To do this we examined urine osmolarity of 8 homozygous and wt female mice (n=16). Urine samples were collected and frozen after collection to avoid decomposition. In normal conditions urine osmolarity and concentration in the urine varies depending on the time lag between water and food consumption and sample collection. To reduce variability samples were taken on repeated occasions at the same time of the day having a collection of three samples per animal that were

pooled together. Osmolarity was measured twice per pooled sample and the average was recorded as the final value.

The values obtained from the wild type mice fitted within normal range reported previously (Ma *et al*, 1997). This result shows that *Davis* homozygotes had a significant increase in urine osmolarity compared with the wt control (*P*=0.0285) (Figure 5.13). This suggests that the abrogation of Mcr2 contributes to abnormal osmolarity in the urine. Thus, because the urine osmolarity is abnormally high the body increases due to the retention of water seen in *Davis* homozygous livers. Thus, urine osmolarity could indicate an excretory defect that could potentially explain the difference in total weight

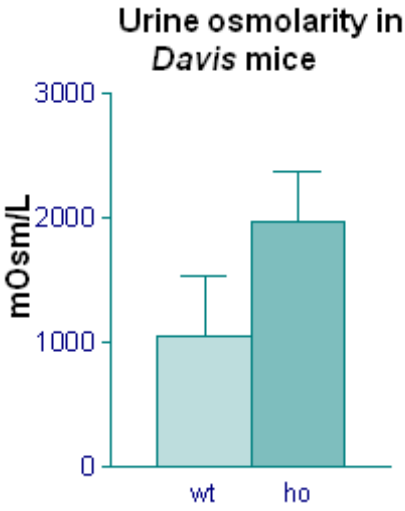

Figure 5.12 Graph showing urine osmolarity in *Davis* mice. Graph displays the result of urine osmolarity expressed in mOsm/L in Davis mutants and controls. Wt=wild type, ho= homozygous. A statistically significant difference was found between the two groups analyzed (*P*=0.0285).

5.2.9 *Davis* urine composition

Abnormal salt excretion has been associated with human disease (Gutkowska *et al*., 2009). For example, some types of nephrogenic diabetes insipidus are associated with significant natriuresis which is defined as the process of excretion of sodium in the urine via action of the kidneys. Previous studies have revealed an increased urinary sodium excretion on AQP3 protein null mice as well (Sasaki *et al*., 1998). The kidney

has a vital role in water excretion, transporting solute through the renal collecting duct system responsible for the final regulation of urinary sodium excretion (Kwon *et al*., 1999; 2000; Nielsen and Frokiaer, 2003).

The glomerular filtration rate (GFR) is the standard measure of renal function and considered the best index to measure renal disease. The clearance of creatinine is commonly used to estimate GFR, but this method has limitations. Mice have levels of noncreatinine chromogens, which make it hard to interpret. Instead in the mouse GFR is estimated by measuring electrolyte, creatinine and urea levels. In order to elucidate which factors might contribute to the increased osmolarity of homozygous mice, urine components were measured including Na^+, K^+, creatinine and urea.

The set of samples used in the osmolarity analysis served also to perform this analysis (see section 5.2.8). By comparing wt and homozygous levels trends in all of the readings indicate an increased concentration in homozygous compared to wt (Figure 5.13). However no significant differences between wt and homozygous were observed (Table 5.8).

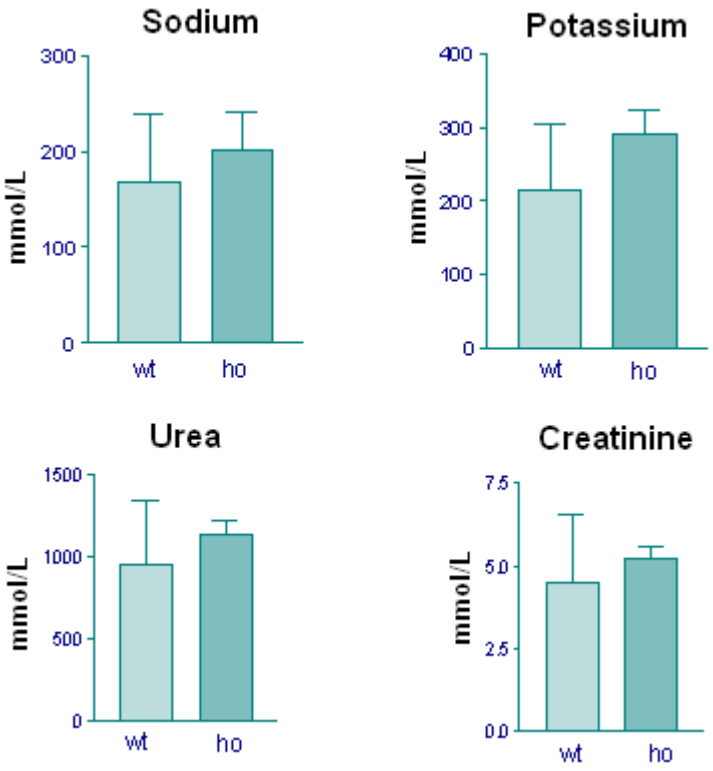

Figure 5.13 Graphics concentration of urine components in *Davis* mice. In analysis of urine components values expressed mmol/L indicate concentration levels in the urine. Wt=wild type, ho= homozygous.

Table 5.8 Summary of *P* values obtained measuring urine components in *Davis* mice.

	***P* values**
Na +	0.3618
K +	0.0823
Urea	0.3283
Creatinine	0.4602

5.2.10 Water ingestion by *Davis* mice

A study using 28 strains of mice concludes that size is not the main factor that affects water ingestion (Bachmanov *et al*., 2002). Water consumption can be affected by salinity, sugar concentration, food availability, temperature, humidity, and stress of the environment, however all those factors were fully controlled. To measure drinking habits of *Davis* homozygous and wt mice, 6 months old mice were housed in separate cages provided with measured quantity of water in their usual drinking bottles. The cages were left untouched for 15 days to minimize water leakage from the drinking bottles. At the end of the experiment the final volume of water remaining in the bottles was measured and the differences between start and final volumes taken as the volume drunk by each mouse. As a control, an empty cage was provided with water bottle in the same conditions. In this case if a considerable amount of liquid was lost, presumably through leakage. The value obtained from the negative control was subtracted from the drinking values. The results of this study indicate that there is a statistically significant difference (P=0.0195) between the water intake of *Davis* homozygotes and their wt littermates, with homozygotes drinking more (Figure 5.14). On average the values obtained of water intake during the experiment account for 82 ml in wt and 127 ml in homozygous. This is consistent with the finding of liquid retention in *Davis* homozygote organs. Further, given that this increased drinking is associated with more concentrated rather than more dilute, urine in *Davis* homozygous mice, compared with wt controls, suggests that an excretory abnormality is associated with deletion of Mcr2. In a single case it was found a *Davis* homozygote mouse with the stomach inflated and filled with water this might be a the case of an excretory defect (Figure 5.15).

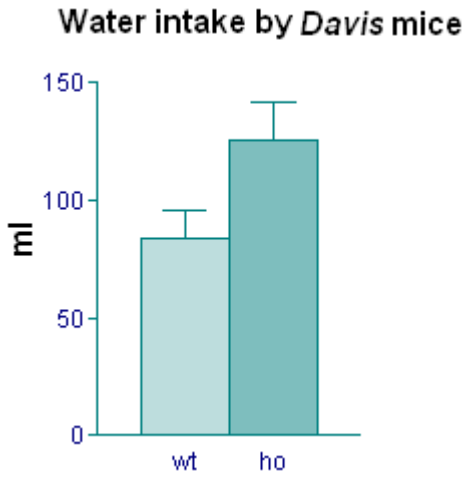

Figure 5.14 Measurement ingested water in *Davis* mice. Graphic shows the amount of ml of ingested water after 15 days. A statistically significant difference was found between the two groups analyzed (*P*=0.0295). Wt=wild type, Ho=homozygous.

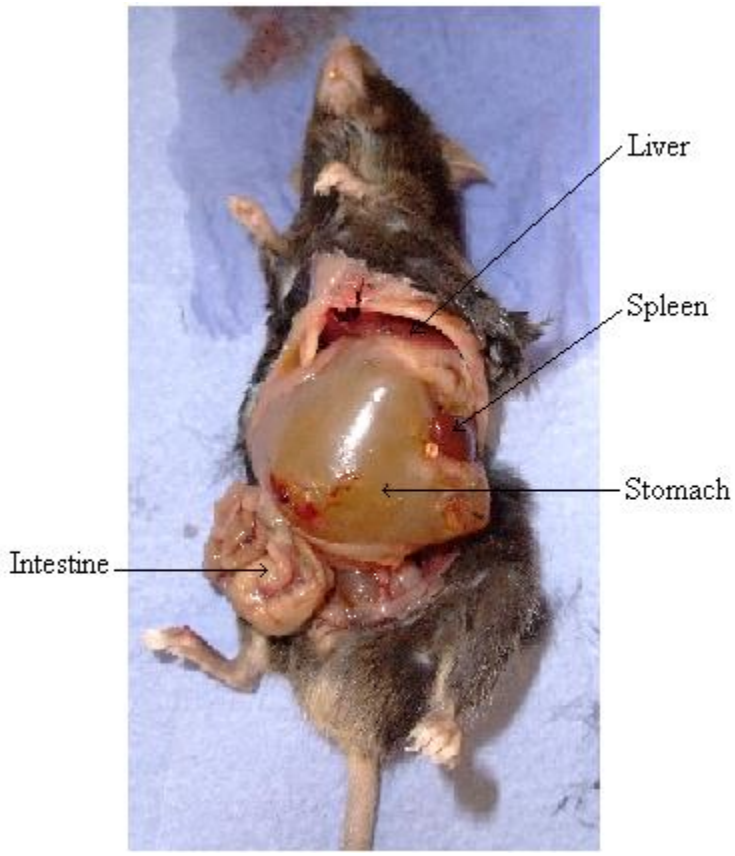

Figure 5.15 *Davis* male homozygote mouse with excessive liquid in the stomach. Arrows indicate organ distribution intestine, spleen, stomach and liver.

5.2.11 Effect of altered Mcr2 on *Wt1* gene

5.2.11.1 Levels *Wt1* and *AWt1* expression in *Davis* $^{-/-}$ and *Trigger* $^{-/-}$ at embryonic stage.

Wt1-AS is highly expressed at E 17.5 (see Section 4.1). At this embryonic stage we measured levels of expression of *Wt1* promoter and *Awt1*. The experiment was done in triplicates per sample were the media gave the error bar. Three samples from kidney littermates were assessed using two homozygous and one wt. Levels of expression were highly variable in *Trigger* $^{-/-}$ and *Davis* $^{-/-}$ compared to the wt controls (Figure 5.16). However the levels of *AWt1* expression were diminished in both *Trigger* and *Davis* homozygous (Figure 5.17). This qPCR experiments were performed by Dr. Anne Hancock.

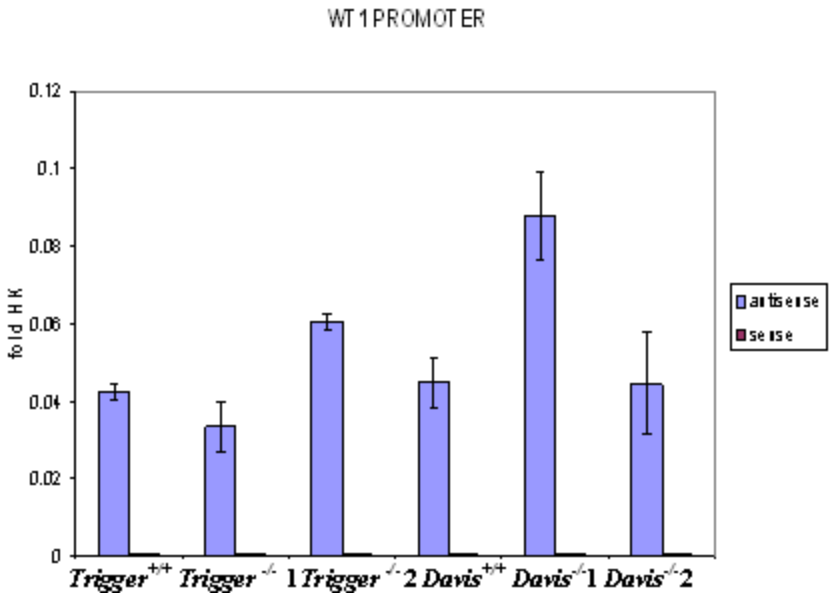

Figure 5.16 Quantitative PCR analysis of Wt1 expression in *Trigger* and *Davis* kidney. Graph displaying folds of PCR product of strand specific RT-PCR. Blue bars indicate antisense transcription and red bars indicate sense transcription. Error bars show the range of triplicate measurements. One wt was compared against two homozygous.

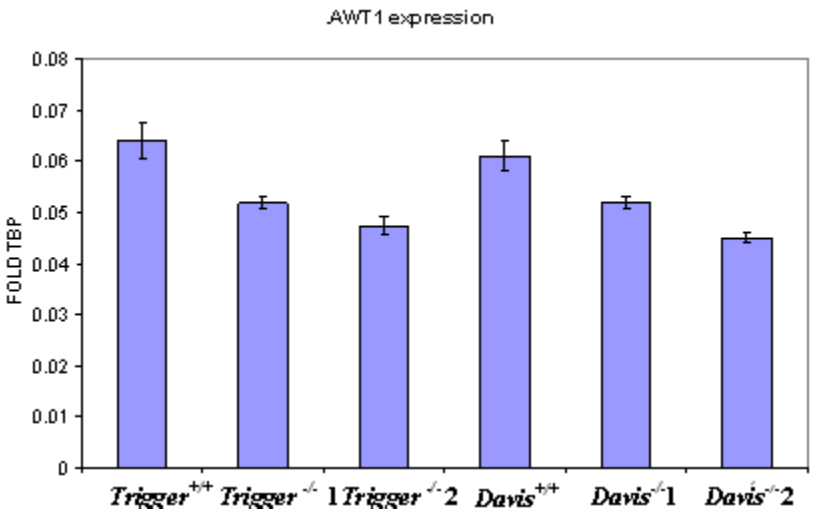

Figure 5.17 Quantitative PCR analysis of expression in *Trigger* and *Davis* kidney. Graph displaying folds of PCR product of strand specific RT-PCR. Blue bars levels of *Awt1* expression of *Trigger* and *Davis* mice. Error bars show the range of triplicate measurements. One wt was compared against two homozygous.

5.2.12 Effects of altered Mcr2 on WT1 protein

5.2.12.1 Western blot analyses from total kidney protein

Samples from *Davis* kidneys were analyzed at the day one of birth. Wt1 was detected using 6FH2 anybody against Wt1. Consistent with what we have found by looking at *Wt1* expression levels, no any changes of Wt1 protein were observed in *Davis* homozygous compared to the wt control. Cells expressing WT1 were used as a positive control (Figure 5.18).

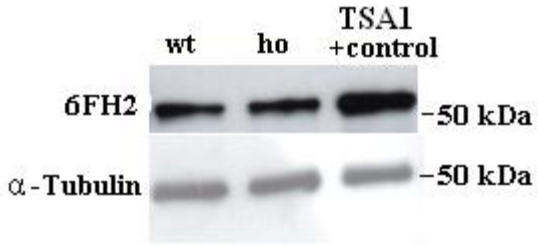

Figure 5.18 Western blot analysis of *Davis* kidney. Top panel shows detection of Wt1 using 6FH2 antibody. Panel below shows α-Tubulin that served as loading control. Wt= wild type, ho= homozygote, positive control TSA1.

5.2.12.2 C-19 immunohistochemistry in *Davis* kidney

As explained in section 1.3.2, parallel expression of *WT1* sense, antisense RNA, and also protein was observed in tissues from human foetal kidneys (Moorwood *et al*., 1998). Kidney sections form 7 months old homozygous and wt were analyzed in order to detect WT1 protein in the *Davis* glomeruli. This was performed by using C-19 antibody against Wt1. After performing this experiment not any discernable differences between *Davis* homozygous and wt were observed (Figure 5.19).

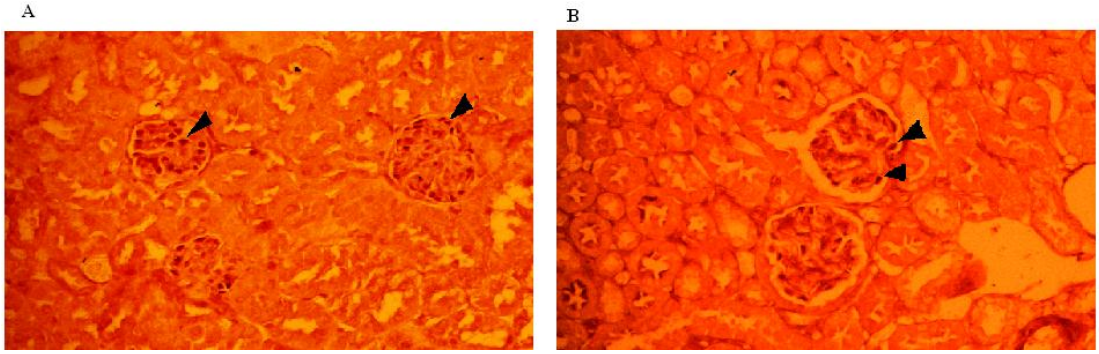

Figure 5.19 Detection of Wt1 by immnunohystochemistry in *Davis* kidney. Immunoperoxidase staining using C-19 antibody against Wt1 on kidney from wax section slides counterstained with methyl-green from 7 months kidney sections (40X). (A) Wt and (B) homozygote kidney display positive signal for Wt1 indicated by arrows.

5.3 Discussion

Consistent with RT-PCR data shown in Section 4.2.1.3 indicating that the transcriptional terminator sequence was inefficient on the *Trigger* strain, *Trigger* homozygote mice did not show any significant phenotype by analysis of body (organ weight, proteinurea), or effect upon Wt1 levels in the kidney (5.11). Therefore, we have not observed any phenotype resulting from loss of Mcr2 RNA. *Davis* mouse histology shows that Mcr2 is not necessary for completing the normal development of

the kidney as well as the other vital organs elsewhere than testis (Section 5.2.5). Probably due to defects in testis might be explained that heterozygous and homozygous intercrosses had a reduced number of pups born per litter (Table 5.3).

Also, nearly half of the expected numbers of *Davis* homozygous pups expected from a heterozygous intercross born which might indicate embryonic lethal. However after birth *Davis* mutants are viable and fertile.

During the time of study *Davis* and *Trigger* mice reached more than a year of age without presenting any health issues except from the case of the mouse with liquid in the stomach (Figure 5.15). The lack of obvious or dramatic phenotype made this study difficult since any differences between these genotypes were subtle. Pathologies found were independent of the genotype e.g. cystic kidneys, enlarged spleens and sclerotic livers, the latter two frequently in conjunction with each other. In the case of the case of cystic kidneys, we were able to detect proteinurea but again those cases did not correspond to a particular mutant genotype (Section 5.2.3). *Davis* brain and heart showed a significant difference in weight but only for males which proved not to be consistent as it would be expected to be found in both. For the case of the brain the deviation would be unlikely to be related with Mcr2 bias Wt1 given that the later is only expressed in a prominently small part of the brain called postrema within the fourth ventricle.

So any brain phenotype would be expected to be independent of Wt1. In the case of the testis, there was a clear difference in weight between all 3 genotypes (see section 5.2.2.2) may be explained by an aberrant distribution on the seminiferous tubules.
One of the most striking phenotypes found in this study was that both *Davis* heterozygous and homozygous were heavier of 17% on average, compared to wt controls (Section 5.2.2.2). These heavier animals were not longer and did not have increased area or increased individual organ weights (Section 5.2.6). However *Davis* homozygote mice had increased levels of water in the tissue (Section 5.2.7). DXA data, although not statistically significant shoes a tendency for fat to be more abundant in wt mice and for muscle to be more abundant in homozygote mice. Indeed water in the muscle is present in patients with edema (McMahon *et al*., 2010), which might indicate the bigger muscle volume in *Davis* homozygous. Urine osmolarity and concentration measurements (Section 5.2.8) did suggest excretory defect that indicate a functional abnormality in the kidney possibly linked to the abrogation of Mcr2. This

maybe a key piece of evidence to indicate a functional deficiency in the kidney despite the fact that proteinurea was not present in *Davis* homozygotes and kidney histology appear normal. Although electrolytes in the urine shown insignificant deviation from the controls however the tendency in all of them was to be more concentrated in homozygous mouse urine. Also the water intake results may indicate that *Davis* homozygous mice should not been dehydrated since they drink more that the wt mice. Nevertheless their urine is, surprisingly, not more dilute. This suggests an excretory defect.

Finally to elucidate if Mcr2 has any effect on Wt1 expression by immunohistochemistry and western blot indicates that there is no correlation between presence of Mcr2 and Wt1 protein. As reviewed in section 1.1.9.1.1 has been reported that changes in Wt1 levels are lethal due to incomplete development (Kreidberg *et al*., 1993), in contrast our *Davis* Mcr2 mutant display more subtle phenotypes which is consistent with the fact that no changes in levels of Wt1 protein were observed.

Chapter 6: Summary Discussion

Mcr2 did not have the role that we expected in the kidney in terms of affecting Wt1 levels. Because we found no changes in levels of Wt1 RNA or protein the role of Mcr2 as an enhancer of Wt1 could not be proved. However, we found other interesting features that suggest a role Mcr2 function in the mouse. In this Chapter an overview will be presented discussing what the results might suggest.

Initially, we considered intrinsic features of the Mcr2 sequence to help explain its potential functional roles. Due to shortness of its longest ORF was considered more likely to be a DNA regulatory element or as a part of a ncRNAs. This is not surprising taking in account that it has been estimated that most of the mammalian genome does not code for protein. Although the study of ncRNA is a rising field in the literature there are very few examples with ascribed roles and exact mechanisms of action in development or organ function remain speculative (Dennis, 2002; Brosius, 2005; Struhl, 2007; Pauler *et al*., 2007). Many expressed DNA sequences in the genome without protein coding capacity have an active function as RNA elements, with diverse biological roles (Table 1.4). New classes of ncRNA are still being described as in the case of RNA enhancers. This recently discovered group of ncRNAs can be defined as DNA sequences that bind the transcriptional co-activator p300/CBP, that bind histone H3 monomethylated at lysine 4, both located distally from transcriptional start sites (Heintzman *et al*., 2007, Visel *et al*., 2009). Interestingly as mentioned in Section 3.2.2.2 we have found a MAR that might involve attachment to histones. In a recent report Bollig *et al*., (2009) propose that at least part of the Mcr2 sequence acts as an eRNA which is responsive to retinoic acid in zebrafish. This retinoic acid responsive element controls *wt1a* expression in the zebrafish pronephros. As mentioned in Section 3.5 part of the sequence of Mcr2 has this retinoic acid element. Using PIPLOT (Figure 3.8) we found wide conservation of Mcr2 sequence in vertebrates which can be divided in two contiguous domains. One domain is present in most vertebrates (except from the chicken). Mouse Mcr2 conservation progressively extends its length of conservation from Medaka to *X*.

Tropicalis where remains well conserved in all non-fish vertebrates making a "bell curve" of conservation across non-fish species (Figure 3.9). Tacking in to account that Mcr2 is expressed in the kidney may lead to the following hypothesis: The fact that this novel region of conservation is present exclusively among the non-fish animals analyzed suggests that it may confer some kidney function which is distinct from that required in aquatic vertebrates which have a different excretory system. We also found a sequence exclusively conserved in mammals as in the case of Mcr1 suggesting that they may function in mammal-specific tissues.

By random priming we found Mcr2 expression in *Trigger* $^{-/-}$ neonate kidney cDNA despite the presence of a transcriptional terminator sequence inserted between Mcr2 and Wt1 exon1. This opened three possibilities: one that sense expression might account for transcription of Mcr2 given that the TTS is further downstream WT1 sense exons. The second scenario was having only antisense transcription but with liking of the construct designed to truncate Mcr2 transcription. The third option was to be bidirectionally expressed. To elucidate the direction of expression through Mcr2 cDNA was performed using strand-specific oligo primed RNA. In this case, expression was exclusively found in the antisense orientation, confirming the TTS sequence was not stopping Mcr2 expression in *Trigger* $^{-/-}$ neonate kidney cDNA. In a previous report by Dalloso and *et al*., (2007) the EST AK5089 was also found to be exclusively expressed in the antisense orientation by RPA. This evidence suggested that the orientation of transcription might be the same for Mcr2 due to the fact that they are both in the same locus relatively close to each other. Using a third approach, a qPCR reaction gave similar results, negligible sense expression. We can state that poor efficiency of premature transcriptional termination TTS was in the antisense orientation. Therefore we could conclude that the poor efficiency of TTS sequence function can account to detectable expression levels of Mcr2 in *Trigger* homozygote kidney.

Although the absence of Mcr2 in the knockout model could not correlate with up or down regulation of Wt1 sense, we were able to detect change in levels of *Awt1*. Davis

and surprisingly also *Trigger* homozygous mutant appear to have reduced Awt1 levels of expression (Section 5.2.11.1). As seen in Section 1.3.2 levels of Wt1-AS are able to modulate Wt1 sense. In the future it would be necessary to prove this experimentally by looking Awt1 protein levels.

Other examples have been described to display "concordant regulation". In some cases NATs augment the level of sense RNA or protein levels of other genes. Some examples as aHIFI (Faghihi, 2008), asEPO-R (Zahng, 2008) and Zeb-AS (Beltran, 2006). This could probably also be the case for Mcr2 and Awt1. Also if this result is confirmed might indicate that lower levels o Awt1 do not affect Wt1 expression. In addition to this in human we have spotted MCR2 to be part of WT1-AS (Figure 3.3). Also in human both AWT1 and WT1-AS have been proved to originate in intron 1 possibly its mechanism of transcription might be structurally linked due to the fact that abrogation of Mcr2 caused reduced levels of Awt1.

Loss of imprinting has been detected in WT1 antisense transcripts in WT (Malik, *et al*., 2000, Dalloso, *et al*., 2004) and ovarian carcinoma (Kaneushi, *et al*., 2005). Because WT1-AS is imprinted in the normal pediatric kidney, therefore we looked at the pediatric mouse kidney and other stages (Figure 4.13). However, imprinted expression was not seen in the mouse. In a separate approach strain specific genomic polymorphism was found expressed but also could not corroborate any evidence of imprinting. This was done by Dr. Km Moorwood using kidney RNA from embryos (E17.5), juvenile (P2, 3) and adults (P19, 20). Nevertheless evidence of Mcr2 imprinting might depend on examining different stages than the ones analyzed.

Davis and *Trigger* mutant mice were examined for phenotypic changes that could indicate a function for Mcr2. At the histological level aberrant organization of seminiferous tubules was observed in *Davis* homozygous testes, however no differences in amount of the seminiferous tubules and number of mature sperm was found. Infertility has been reported in number mouse knockout models, as in the case of mice lacking the *Cstf2t* gene, a paralog of the 64,000 *M*r subunit of the cleavage stimulation factor (CstF-64). In this model male infertility was observed, however,

this did not relate to changes in weight that were found between mutants and wt mice (Das *et al*., 2001). In a conditional Wt1 knockout mouse Gao *et al*., (2006), reported disruption of seminiferous tubules. However, this was not the same defect seen in *Davis* homozygous mutant mice.

Statistical analyses of 257 *Davis* mutant mice a deviation was seen in the expected number of homozygous mutants. This was the most significant phenotype observed in the present study, indicating lethality in *Davis* genetically modified mice. Viability was lost in a significant proportion of homozygous and heterozygous embryos in relation to wild type littermates. This might also be linked with abnormal liquid homeostasis which may have perturbed viability of the mutant embryos. In a similar analysis of genotype number for the Trigger strain no significant result was observed, implying that the effect seen in the *Davis* line has been something directly associated with mcr2 DNA function. However it was not possible to uncover the cause of loss viability associated with Trigger mutant genotypes.

Because of the normal variability in weight between individual mice a study of the association of body weight with genotype required a large cohort of mice. Analyzing total body weight in 7 month old mice gave the first clue of body proportion abnormality in the *Davis* strain. The *Davis* homozygotes or heterozygotes were 17% heavier compared to wild type litter mates. None of the organs where Wt1 is shown to be expressed were found to be increased in weight and in fact, some of the, some were decreased, as in testes and heart. The next step was to define if this was due to animal size. After measuring body length and bone mineral content, density (BMC, BMD) it was clear that these variables were not altered between *Davis* homozygote mutant and wild type animals. Also, no difference was detected by in fat pad weight and actual fat content measured by DXA, perhaps due to a small number of animals analyzed. We only analyzed 4 males and females per each genotype (n=24). The weight component remaining after considering these analyses was the amount of water in the tissue. Liquid retention was commonly has an effect on body weight in cases of edema (Manley *et al*., 2000). A crude diagnostic test for edema simply

involves pressing the abdomen, and observing whether if recovers its normal shape. Using this test edema was not evident.

It was possible to find a difference when measuring the water content of the liver representative organ from mutant and wild type *Davis* animal, comparing liver weights pre- and post- desiccation. After measuring dried livers the *Davis* homozygote liver was found to retain on average 5.6% more water than their wt counterparts. If the deregulation of liquid homeostasis was the reason for this phenotype we might expect to obtain significantly different values for urine osmolarity between *Davis* homozygotes mutants and wild-type siblings. Measurements of liquid retention in the liver, urine osmolarity and total body weight in small cohorts of mice suggested that indeed this was the case.

This suggested that urine in the *Davis* homozygous mutants was more concentrated than in wt possibly because of kidney dysfunction. However no differences in morphology were seen upon histological staining of kidney tissue sections with PAS. Also, although proteinurea was not observable on polyacrylamide gels the presumptive kidney defect might have been too subtle to be resolved by these methods. The most common method for measuring functional kidney efficiency is by linking metabolite concentration with creatinine levels, a compound that generally has a relatively constant clearance rate. However, some studies have shown variability even no related with of water intake and diet (Chilcott *et al.*, 1985). However we could not detect evidence of kidney malfunction by measuring levels of GFR. This may be because there are other chromogens that might mask the actual creatinine in the urine making measurement redundant. Possibly a better way to measure this might be supplying intravenous doses of creatinine and subsequently measuring levels after metabolic response. On the other hand, after measuring other urine components (Na^+, K^+ and urea) readings showed that the urine concentration tended to be higher in *Davis* homozygous than in wt siblings. Although this might change if the sample size were increased (for example in the case of Na^+), it can be taken as evidence that the main factor involved in this abnormality is water content.

However it is worthwhile to taking into account that the observed differences are very mild and did not provoke a significant level of mortality in *Davis* homozygous mutants to expect worse effects at older ages. In just a single case a *Davis* $^{-/-}$ mouse was found with water retained in an enlarged stomach in an 8 month old mouse (Figure 5.15). Possibly more cases would have appeared if had been possible to study an older *Davis*. *Davis* $^{-/-}$ not only had higher urine osmolarity but also appeared to drink more water than controls, therefore, behaving as if they were dehydrated.

Due to abnormal concentration of the urine, liquid retention within tissues and heavier weight in total body it appears that Davis homozygous mutant mice could have excretory defects. These mice drink more water but could possibly control high osmolarity in tissues through hormonal regulation (Figure 6.1). Liquid retention might have been by measuring the total amount of urine produced, however this is difficult to measure accurately due to small sample volumes.

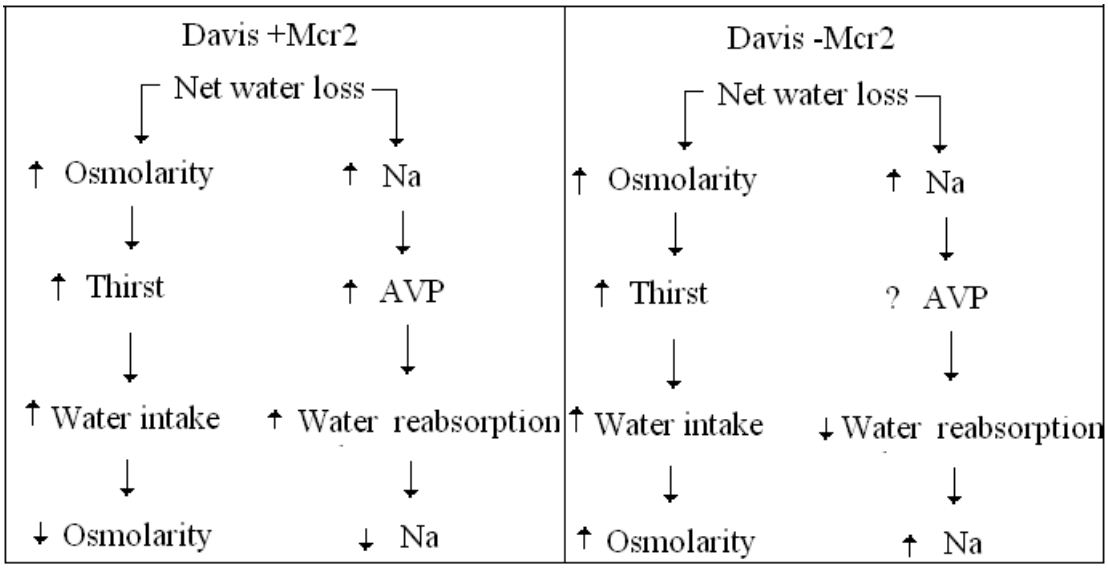

Figure 6.1 Hypothetical model of mechanisms in water homeostasis in Davis + and – Mcr2. Left panel indicates how water loss is compensate by thirst and hormonal and salt components (Arginine vasopressin and Na). On the Right panel exemplifies how loss of Mcr2 produces less water reabsorption and possible augment in Na and Osmolarity.

Also if would have been of interest to measure the urine concentration with 24 hours of water depravation to see the effect on ADH levels in wt control and also homozygous counterparts Also other peptides that are expressed in the membrane should be looked at as for example aquaporins which are involved in liquid homeostasis in the kidney (Nielsen *et al*., 2002). However, mice deficient with in aquaporins exhibited proteinurea and other abnormal phenotypes from those seen in *Davis* mutant mice (reviewed by Verkman and Yang, 2002).

Furthermore lethality due to edema has been detected in mice at E14.5 following disruption of the gene encoding Peptidylglycine alpha-amidating monooxigenase (PAM) which catalyzes the COOH-terminal amidation of peptide hormones (Czysyk *et al*., 2006). Homozygous mutants die in utero between E14.5 and E15.5 with severe edema. In a different mouse model Yang, *et al*., (2005) found embryonic lethality of homozygous knockout Dicer$^{ex1/2}$ mice occurred at E14.5. As described in Section 1.2.1.2 dicer is protein that produces short interfering RNAs (siRNAs) out of long double-stranded RNAs during RNA interference. Yang *et al*., (2005) postulate that Dicer might exerts its function on mouse embryonic angiogenesis possibly by processing of microRNAs. Interestingly, this embryonic stage is similar to the one that Czyzyk *et al*., (2006) detected. This might suggest E11.5 to look at edema in Davis transgenic mice due to the fact that potential lethality due to reduced levels heterozygous and homozygous animals were obtained. Although some homozygous and heterozygous were born, lethality might be explained as a matter of incomplete penetrance by this means that in some individuals the phenotype possibly as aberrant water homeostasis occurs.

The ability to detect a relevant function for Mcr2 was not a straight forward process. It would be that a Mcr2 ncRNA causes a subtle phenotype that would be missed in further superficial genetic screens, but might still be strongly disadvantageous in the wild. Similarly, modifications in ultraconserved enhancers produced no discernable abnormality (Poulin *et al*., 2005). In this case, Poulin *et al* (2005) made knock-out mice with a deletion of an ultraconserved enhancer element named Dc2. This did not show any phenotypic observable differences. Authors previously have stipulated that

ncRNAs may give a milder phenotypic effect and more on the side of regulatory defects not been primarily source of protein “building” cell components (Mattick and Makuning, 2006). We do not know if the lack of more obvious phenotype was due to the fact the *Davis* mutation was studied in a mixed genetic background. For this reason at the moment *Davis* mouse model is being backcrossed to a different strain background. Initial screening performed by Dr. Kim Moorwood and Dr. Joanne Stewart-Cox has confirmed the difference in weight observed in *Davis* mutant mice described in the present study.

Initially we thought that with such high degree of sequence conservation, suggesting severe evolutionary constraint, would predict a lack of tolerance to mutation on Mcr2 function. Although still far from elucidating the exact mechanism, this work indicates a novel role for Mcr2 in regulating liquid homeostasis in the mouse body

References

(2004). "Finishing the euchromatic sequence of the human genome." Nature **431**(7011): 931-945.

Acs, G., T. Pasha, et al. (2004). "WT1 is differentially expressed in serous, endometrioid, clear cell, and mucinous carcinomas of the peritoneum, fallopian tube, ovary, and endometrium." Int J Gynecol Pathol **23**(2): 110-118.

Alberta, J. A., G. M. Springett, et al. (2003). "Role of the WT1 tumor suppressor in murine hematopoiesis." Blood **101**(7): 2570-2574.

Alenina, N., T. Baranova, et al. (2002). "Cell type-specific expression of the Mas proto-oncogene in testis." J Histochem Cytochem **50**(5): 691-696.

Alff-Steinberger, C. (1984). "Evidence for a coding pattern on the non-coding strand of the E. coli genome." Nucleic Acids Res **12**(5): 2235-2241.

Alff-Steinberger, C. (1987). "Codon usage in Homo sapiens: evidence for a coding pattern on the non-coding strand and evolutionary implications of dinucleotide discrimination." J Theor Biol **124**(1): 89-95.

Algar, E. M., T. Khromykh, et al. (1996). "A WT1 antisense oligonucleotide inhibits proliferation and induces apoptosis in myeloid leukaemia cell lines." Oncogene **12**(5): 1005-1014.

Andersen, B. B. and B. Pakkenberg (2003). "Stereological quantitation in cerebella from people with schizophrenia." Br J Psychiatry **182**: 354-361.

Arima, T., T. Matsuda, et al. (1997). "Association of IGF2 and H19 imprinting with choriocarcinoma development." Cancer Genet Cytogenet **93**(1): 39-47.

Avner, P. and E. Heard (2001). "X-chromosome inactivation: counting, choice and initiation." Nat Rev Genet **2**(1): 59-67.

Baccarini, P., M. Fiorentino, et al. (1993). "Detection of anti-sense transcripts of the insulin-like growth factor-2 gene in Wilms' tumor." Am J Pathol **143**(6): 1535-1542.

Bachmanov, A. A., D. R. Reed, et al. (2002). "Food intake, water intake, and drinking spout side preference of 28 mouse strains." Behav Genet **32**(6)23-45

Baird, P. N., N. Groves, et al. (1992). "Identification of mutations in the WT1 gene in tumours from patients with the WAGR syndrome." Oncogene **7**(11): 2141-2149.

Ballermann, B. J. (2005). "Glomerular endothelial cell differentiation." Kidney Int **67**(5): 1668-1671.

Barbaux, S., P. Niaudet, et al. (1997). "Donor splice-site mutations in WT1 are responsible for Frasier syndrome." Nat Genet **17**(4): 467-470.

Bartel, D. P. (2004). "MicroRNAs: genomics, biogenesis, mechanism, and function." Cell **116**(2): 281-297.

Baudry, D., M. Faussillon, et al. (2002). "Changes in WT1 splicing are associated with a specific gene expression profile in Wilms' tumour." Oncogene **21**(36): 5566-5573.

Beckwith, J. B. (1983). "Wilms' tumor and other renal tumors of childhood: a selective review from the National Wilms' Tumor Study Pathology Center." Hum Pathol **14**(6): 481-492.

Beckwith, J. B., N. B. Kiviat, et al. (1990). "Nephrogenic rests, nephroblastomatosis, and the pathogenesis of Wilms' tumor." Pediatr Pathol **10**(1-2): 1-36.

Bejerano, G., M. Pheasant, et al. (2004). "Ultraconserved Elements in the Human Genome." Science **304**(5675): 1321-1325.

Beltran, M., I. Puig, et al. (2008). "A natural antisense transcript regulates Zeb2/Sip1 gene expression during Snail1-induced epithelial-mesenchymal transition." Genes Dev **22**(6): 756-769.

Benzow, K. A. and M. D. Koob (2002). "The KLHL1-antisense transcript (KLHL1AS) is evolutionarily conserved." Mamm Genome **13**(3): 134-141.

Bernstein, E. and C. D. Allis (2005). "RNA meets chromatin." Genes Dev **19**(14): 1635-1655.

Bird, A. P. (1986). "CpG-rich islands and the function of DNA methylation." Nature **321**(6067): 209-213.

Birney, E., J. A. Stamatoyannopoulos, et al. (2007). "Identification and analysis of functional elements in 1% of the human genome by the ENCODE pilot project." Nature **447**(7146): 799-816.

Blalock, J. E. (1990). "Complementarity of peptides specified by 'sense' and 'antisense' strands of DNA." Trends Biotechnol **8**(6): 140-144.

Blalock, J. E. and K. L. Bost (1986). "Binding of peptides that are specified by complementary RNAs." Biochem J **234**(3): 679-683.

Boehm, M. and F. Slack (2005). "A developmental timing microRNA and its target regulate life span in C. elegans." Science **310**(5756): 1954-1957.

Bolland, D. J., A. L. Wood, et al. (2007). "Antisense intergenic transcription precedes Igh D-to-J recombination and is controlled by the intronic enhancer Emu." Mol Cell Biol **27**(15): 5523-5533.

Bolland, D. J., A. L. Wood, et al. (2004). "Antisense intergenic transcription in V(D)J recombination." Nat Immunol **5**(6): 630-637.

Bollig, F., B. Perner, et al. (2009). "A highly conserved retinoic acid responsive element controls wt1a expression in the zebrafish pronephros." Development **136**(17): 2883-2892.

Bonetta, L., S. E. Kuehn, et al. (1990). "Wilms tumor locus on 11p13 defined by multiple CpG island-associated transcripts." Science **250**(4983): 994-997.

Borel, F., K. C. Barilla, et al. (1996). "Effects of Denys-Drash syndrome point mutations on the DNA binding activity of the Wilms' tumor suppressor protein WT1." Biochemistry **35**(37): 12070-12076.

Boumil, R. M. and J. T. Lee (2001). "Forty years of decoding the silence in X-chromosome inactivation." Hum Mol Genet **10**(20): 2225-2232.

Braidotti, G., T. Baubec, et al. (2004). "The Air noncoding RNA: an imprinted cis-silencing transcript." Cold Spring Harb Symp Quant Biol **69**: 55-66.

Brannan, C. I., E. C. Dees, et al. (1990). "The product of the H19 gene may function as an RNA." Mol Cell Biol **10**(1): 28-36.

Brantl, S. (2002). "Antisense RNAs in plasmids: control of replication and maintenance." Plasmid **48**(3): 165-173.

Brantl, S. and E. G. Wagner (2002). "An antisense RNA-mediated transcriptional attenuation mechanism functions in Escherichia coli." J Bacteriol **184**(10): 2740-2747.

Brosius, J. (2005). "Waste not, want not--transcript excess in multicellular eukaryotes." Trends Genet **21**(5): 287-288.

Bruening, W., N. Bardeesy, et al. (1992). "Germline intronic and exonic mutations in the Wilms' tumour gene (WT1) affecting urogenital development." Nat Genet **1**(2): 144-148.

Bruening, W., P. Moffett, et al. (1996). "Identification of nuclear localization signals within the zinc fingers of the WT1 tumor suppressor gene product." FEBS Lett **393**(1): 41-47.

Bruening, W. and J. Pelletier (1996). "A non-AUG translational initiation event generates novel WT1 isoforms." J Biol Chem **271**(15): 8646-8654.

Bryson, K., L. J. McGuffin, et al. (2005). "Protein structure prediction servers at University College London." Nucleic Acids Res **33**(Web Server issue): W36-38.

Buckler, A. J., J. Pelletier, et al. (1991). "Isolation, characterization, and expression of the murine Wilms' tumor gene (WT1) during kidney development." Mol Cell Biol **11**(3): 1707-1712.

Burd, C. G. and G. Dreyfuss (1994). "Conserved structures and diversity of functions of RNA-binding proteins." Science **265**(5172): 615-621.

Calin, G. A., A. Cimmino, et al. (2008). "MiR-15a and miR-16-1 cluster functions in human leukemia." Proc Natl Acad Sci U S A **105**(13): 5166-5171.

Calin, G. A., C. D. Dumitru, et al. (2002). "Frequent deletions and down-regulation of micro- RNA genes miR15 and miR16 at 13q14 in chronic lymphocytic leukemia." Proc Natl Acad Sci U S A **99**(24): 15524-15529.

Calin, G. A., C. G. Liu, et al. (2004). "MicroRNA profiling reveals distinct signatures in B cell chronic lymphocytic leukemias." Proc Natl Acad Sci U S A **101**(32): 11755-11760.

Calin, G. A., C. Sevignani, et al. (2004). "Human microRNA genes are frequently located at fragile sites and genomic regions involved in cancers." Proc Natl Acad Sci U S A **101**(9): 2999-3004.

Call, K. M., T. Glaser, et al. (1990). "Isolation and characterization of a zinc finger polypeptide gene at the human chromosome 11 Wilms' tumor locus." Cell **60**(3): 509-520.

Campbell, C. E., A. Huang, et al. (1994). "Antisense transcripts and protein binding motifs within the Wilms tumour (WT1) locus." Oncogene **9**(2): 583-595.

Caricasole, A., A. Duarte, et al. (1996). "RNA binding by the Wilms tumor suppressor zinc finger proteins." Proc Natl Acad Sci U S A **93**(15): 7562-7566.

Carleton, M., M. A. Cleary, et al. (2007). "MicroRNAs and cell cycle regulation." Cell Cycle **6**(17): 2127-2132.

Carninci, P., T. Kasukawa, et al. (2005). "The transcriptional landscape of the mammalian genome." Science **309**(5740): 1559-1563.

Carpenter, B., K. J. Hill, et al. (2004). "BASP1 is a transcriptional cosuppressor for the Wilms' tumor suppressor protein WT1." Mol Cell Biol **24**(2): 537-549.

Cathro, H. P. and M. H. Stoler (2005). "The utility of calretinin, inhibin, and WT1 immunohistochemical staining in the differential diagnosis of ovarian tumors." Hum Pathol **36**(2): 195-201.

Chamberlain, S. J. and C. I. Brannan (2001). "The Prader-Willi syndrome imprinting center activates the paternally expressed murine Ube3a antisense transcript but represses paternal Ube3a." Genomics **73**(3): 316-322.

Chao, W., K. D. Huynh, et al. (2002). "CTCF, a candidate trans-acting factor for X-inactivation choice." Science **295**(5553): 345-347.

Charles, A. K., K. W. Brown, et al. (1998). "Microdissecting the genetic events in nephrogenic rests and Wilms' tumor development." Am J Pathol **153**(3): 991-1000.

Chen, F. and Y.-P. P. Chen (2010). "Exploring the ncRNA-ncRNA patterns based on bridging rules." J. of Biomedical Informatics **43**(4): 569-577.

Chen, J. L., M. A. Blasco, et al. (2000). "Secondary structure of vertebrate telomerase RNA." Cell **100**(5): 503-514.

Cheng, J., P. Kapranov, et al. (2005). "Transcriptional maps of 10 human chromosomes at 5-nucleotide resolution." Science **308**(5725): 1149-1154.

Clarke, B. L. and J. E. Blalock (1990). "Steroidogenic activity of a peptide specified by the reversed sequence of corticotropin mRNA." Proc Natl Acad Sci U S A **87**(24): 9708-9711.

Clemson, C. M., J. C. Chow, et al. (1998). "Stabilization and localization of Xist RNA are controlled by separate mechanisms and are not sufficient for X inactivation." J Cell Biol **142**(1): 13-23.

Coker, R. K., G. J. Laurent, et al. (1998). "A novel transforming growth factor beta2 antisense transcript in mammalian lung." Biochem J **332 (Pt 2)**: 297-301.

Coppes, M. J., G. J. Liefers, et al. (1993). "Homozygous somatic Wt1 point mutations in sporadic unilateral Wilms tumor." Proc Natl Acad Sci U S A **90**(4): 1416-1419.

Core, L. J., J. J. Waterfall, et al. (2008). "Nascent RNA sequencing reveals widespread pausing and divergent initiation at human promoters." Science **322**(5909): 1845-1848.

Costa, F. F. (2005). "Non-coding RNAs: new players in eukaryotic biology." Gene **357**(2): 83-94.

Costa, F. F. (2007). "Non-coding RNAs: lost in translation?" Gene **386**(1-2): 1-10.

Crampton, N., W. A. Bonass, et al. (2006). "Collision events between RNA polymerases in convergent transcription studied by atomic force microscopy." Nucleic Acids Res **34**(19): 5416-5425.

Czyzyk, T. A., Y. Ning, et al. (2005). "Deletion of peptide amidation enzymatic activity leads to edema and embryonic lethality in the mouse." Dev Biol **287**(2): 301-313.

Dass, B., E. N. Attaya, et al. (2001). "Overexpression of the CstF-64 and CPSF-160 polyadenylation protein messenger RNAs in mouse male germ cells." Biol Reprod **64**(6): 1722-1729.

Dallosso, A. R., A. L. Hancock, et al. (2004). "Genomic imprinting at the WT1 gene involves a novel coding transcript (AWT1) that shows deregulation in Wilms' tumours." Hum Mol Genet **13**(4): 405-415.

Dallosso, A. R., A. L. Hancock, et al. (2007). "Alternately spliced WT1 antisense transcripts interact with WT1 sense RNA and show epigenetic and splicing defects in cancer." RNA **13**(12): 2287-2299.

Dame, C., K. M. Kirschner, et al. (2006). "Wilms tumor suppressor, Wt1, is a transcriptional activator of the erythropoietin gene." Blood **107**(11): 4282-4290.

Davies, R. C., C. Calvio, et al. (1998). "WT1 interacts with the splicing factor U2AF65 in an isoform-dependent manner and can be incorporated into spliceosomes." Genes Dev **12**(20): 3217-3225.

Dennis, C. (2002). "Small RNAs: the genome's guiding hand?" Nature **420**(6917): 732.

Denys, P., P. Malvaux, et al. (1967). "[Association of an anatomo-pathological syndrome of male pseudohermaphroditism, Wilms' tumor, parenchymatous nephropathy and XX/XY mosaicism]." Arch Fr Pediatr **24**(7): 729-739.

Dey, B. R., V. P. Sukhatme, et al. (1994). "Repression of the transforming growth factor-beta 1 gene by the Wilms' tumor suppressor WT1 gene product." Mol Endocrinol **8**(5): 595-602.

Ding, H., M. Schertzer, et al. (2004). "Regulation of murine telomere length by Rtel: an essential gene encoding a helicase-like protein." Cell **117**(7): 873-886.

Discenza, M. T., S. He, et al. (2003). "WT1 is a modifier of the Pax2 mutant phenotype: cooperation and interaction between WT1 and Pax2." Oncogene **22**(50): 8145-8155.

Discenza, M. T. and J. Pelletier (2004). "Insights into the physiological role of WT1 from studies of genetically modified mice." Physiol Genomics **16**(3): 287-300.

Dressler, G. R. and E. C. Douglass (1992). "Pax-2 is a DNA-binding protein expressed in embryonic kidney and Wilms tumor." Proc Natl Acad Sci U S A **89**(4): 1179-1183.

Du, X., P. Hublitz, et al. (2002). "The LIM-only coactivator FHL2 modulates WT1 transcriptional activity during gonadal differentiation." Biochim Biophys Acta **1577**(1): 93-101.

Eccles, M. R., G. Grubb, et al. (1994). "Cloning of novel Wilms tumor gene (WT1) cDNAs; evidence for antisense transcription of WT1." Oncogene **9**(7): 2059-2063.

Ellisen, L. W., N. Carlesso, et al. (2001). "The Wilms tumor suppressor WT1 directs stage-specific quiescence and differentiation of human hematopoietic progenitor cells." EMBO J **20**(8): 1897-1909.

Englert, C., X. Hou, et al. (1995a). "WT1 suppresses synthesis of the epidermal growth factor receptor and induces apoptosis." EMBO J **14**(19): 4662-4675.

Englert, C., S. Maheswaran, et al. (1997b). "Induction of p21 by the Wilms' tumor suppressor gene WT1." Cancer Res **57**(8): 1429-1434.

Englert, C., M. Vidal, et al. (1995). "Truncated WT1 mutants alter the subnuclear localization of the wild-type protein." Proc Natl Acad Sci U S A **92**(26): 11960-11964.

Faghihi, M. A., F. Modarresi, et al. (2008). "Expression of a noncoding RNA is elevated in Alzheimer's disease and drives rapid feed-forward regulation of beta-secretase." Nat Med **14**(7): 723-730.

Faghihi, M. A. and C. Wahlestedt (2009). "Regulatory roles of natural antisense transcripts." Nat Rev Mol Cell Biol **10**(9): 637-643.

Faghihi, M. A., M. Zhang, et al. (2010). "Evidence for natural antisense transcript-mediated inhibition of microRNA function." Genome Biol **11**(5): R56.

Favor, J., R. Sandulache, et al. (1996). "The mouse Pax2(1Neu) mutation is identical to a human PAX2 mutation in a family with renal-coloboma syndrome and results in developmental defects of the brain, ear, eye, and kidney." Proc Natl Acad Sci U S A **93**(24): 13870-13875.

Fournier, C., Y. Goto, et al. (2002). "Allele-specific histone lysine methylation marks regulatory regions at imprinted mouse genes." EMBO J **21**(23): 6560-6570.

Fraizer, G. C., P. Patmasiriwat, et al. (1995). "Expression of the tumor suppressor gene WT1 in both human and mouse bone marrow." Blood **86**(12): 4704-4706.

Francke, U., L. B. Holmes, et al. (1979). "Aniridia-Wilms' tumor association: evidence for specific deletion of 11p13." Cytogenet Cell Genet **24**(3): 185-192.

Frasier, S. D., R. A. Bashore, et al. (1964). "Gonadoblastoma Associated with Pure Gonadal Dysgenesis in Monozygous Twins." J Pediatr **64**: 740-745.

Gao, F., S. Maiti, et al. (2006). "The Wilms tumor gene, Wt1, is required for Sox9 expression and maintenance of tubular architecture in the developing testis." Proc Natl Acad Sci U S A **103**(32): 11987-11992.

Garzon, R., G. A. Calin, et al. (2009). "MicroRNAs in Cancer." Annu Rev Med **60**: 167-179.

Ge, X., W. S. Rubinstein, et al. (2008). "Genome-wide analysis of antisense transcription with Affymetrix exon array." BMC Genomics **9**: 27.

Ge, X. and S. M. Wang (2008). "Identifying nonspecific SAGE tags by context of gene expression." Methods Mol Biol **387**: 199-204.

Gessler, M. and G. A. Bruns (1993). "Sequence of the WT1 upstream region including the Wit-1 gene." Genomics **17**(2): 499-501.

Gessler, M., A. Konig, et al. (1992). "The genomic organization and expression of the WT1 gene." Genomics **12**(4): 807-813.

Gessler, M., A. Poustka, et al. (1990). "Homozygous deletion in Wilms tumours of a zinc-finger gene identified by chromosome jumping." Nature **343**(6260): 774-778.

Ghanem, M. A., T. H. Van der Kwast, et al. (2000). "Expression and prognostic value of Wilms' tumor 1 and early growth response 1 proteins in nephroblastoma." Clin Cancer Res **6**(11): 4265-4271.

Ginger, M. R., A. N. Shore, et al. (2006). "A noncoding RNA is a potential marker of cell fate during mammary gland development." Proc Natl Acad Sci U S A **103**(15): 5781-5786.

Glaser, T., J. Lane, et al. (1990). "A mouse model of the aniridia-Wilms tumor deletion syndrome." Science **250**(4982): 823-827.

Goodstadt, L. and C. P. Ponting (2006). "Phylogenetic reconstruction of orthology, paralogy, and conserved synteny for dog and human." PLoS Comput Biol **2**(9): e133.

Green, L. M., K. J. Wagner, et al. (2009). "Dynamic interaction between WT1 and BASP1 in transcriptional regulation during differentiation." Nucleic Acids Res **37**(2): 431-440.

Grubb, G. R., K. Yun, et al. (1994). "Expression of WT1 protein in fetal kidneys and Wilms tumors." Lab Invest **71**(4): 472-479.

Grundy, P., A. Koufos, et al. (1988). "Familial predisposition to Wilms' tumour does not map to the short arm of chromosome 11." Nature **336**(6197): 374-376.

Gu, W., S. Hu, et al. (2010). "High expression of WT1 gene in acute myeloid leukemias with more predominant WT1+17AA isoforms at relapse." Leuk Res **34**(1): 46-49.

Guo, J. K., A. L. Menke, et al. (2002). "WT1 is a key regulator of podocyte function: reduced expression levels cause crescentic glomerulonephritis and mesangial sclerosis." Hum Mol Genet **11**(6): 651-659.

Gupta, S., K. Joshi, et al. (2009). "High frequency of loss of allelic integrity at Wilms' tumor suppressor gene-1 locus in advanced breast tumors associated with aggressiveness of the tumor." Indian J Cancer **46**(4): 303-310.

Gutkowska, J., T. L. Broderick, et al. (2009). "Downregulation of oxytocin and natriuretic peptides in diabetes: possible implications in cardiomyopathy." J Physiol **587**(Pt 19): 4725-4736.

Gutkowska, J., M. Jankowski, et al. (2000). "Corticotropin-releasing hormone causes antidiuresis and antinatriuresis by stimulating vasopressin and inhibiting atrial natriuretic peptide release in male rats." Proc Natl Acad Sci U S A **97**(1): 483-488.

Haber, D. A., A. J. Buckler, et al. (1990). "An internal deletion within an 11p13 zinc finger gene contributes to the development of Wilms' tumor." Cell **61**(7): 1257-1269.

Haber, D. A., R. L. Sohn, et al. (1991). "Alternative splicing and genomic structure of the Wilms tumor gene WT1." Proc Natl Acad Sci U S A **88**(21): 9618-9622.

Hamilton, T. B., K. C. Barilla, et al. (1995). "High affinity binding sites for the Wilms' tumour suppressor protein WT1." Nucleic Acids Res **23**(2): 277-284.

Hammes, A., J. K. Guo, et al. (2001). "Two splice variants of the Wilms' tumor 1 gene have distinct functions during sex determination and nephron formation." Cell **106**(3): 319-329.

Han, Y., S. San-Marina, et al. (2004). "Transcriptional activation of c-myc proto-oncogene by WT1 protein." Oncogene **23**(41): 6933-6941.

Hancock, A. L., K. W. Brown, et al. (2007). "A CTCF-binding silencer regulates the imprinted genes AWT1 and WT1-AS and exhibits sequential epigenetic defects during Wilms' tumourigenesis." Hum Mol Genet **16**(3): 343-354.

Hao, Y., T. Crenshaw, et al. (1993). "Tumour-suppressor activity of H19 RNA." Nature **365**(6448): 764-767.

Harrington, M. A., B. Konicek, et al. (1993). "Inhibition of colony-stimulating factor-1 promoter activity by the product of the Wilms' tumor locus." J Biol Chem **268**(28): 21271-21275.

Hartwig, S., J. Ho, et al. (2010). "Genomic characterization of Wilms' tumor suppressor 1 targets in nephron progenitor cells during kidney development." Development **137**(7): 1189-1203.

Haselbacher, G. K., J. C. Irminger, et al. (1987). "Insulin-like growth factor II in human adrenal pheochromocytomas and Wilms tumors: expression at the mRNA and protein level." Proc Natl Acad Sci U S A **84**(4): 1104-1106.

Hastie, N. D. (1994). "The genetics of Wilms' tumor--a case of disrupted development." Annu Rev Genet **28**: 523-558.

He, L., J. M. Thomson, et al. (2005). "A microRNA polycistron as a potential human oncogene." Nature **435**(7043): 828-833.

He, Y., B. Vogelstein, et al. (2008). "The antisense transcriptomes of human cells." Science **322**(5909): 1855-1857.

Heintzman, N. D., R. K. Stuart, et al. (2007). "Distinct and predictive chromatin signatures of transcriptional promoters and enhancers in the human genome." Nat Genet **39**(3): 311-318.

Herzer, U., A. Crocoll, et al. (1999). "The Wilms tumor suppressor gene wt1 is required for development of the spleen." Curr Biol **9**(15): 837-840.

Hoffsten, P. E., C. L. Hill, et al. (1975). "Studies of abluminuria and proteinuria in normal mice and mice with immune complex glomerulonephritis." J Lab Clin Med **86**(6): 920-930.

Hofmann, W., H. D. Royer, et al. (1993). "Characterization of the transcriptional regulatory region of the human WT1 gene." Oncogene **8**(11): 3123-3132.

Holmes, G., S. Boterashvili, et al. (1997). "Two N-terminal self-association domains are required for the dominant negative transcriptional activity of WT1 Denys-Drash mutant proteins." Biochem Biophys Res Commun **233**(3): 723-728.

Hossain, A. and G. F. Saunders (2001). "The human sex-determining gene SRY is a direct target of WT1." J Biol Chem **276**(20): 16817-16823.

Hsu, S. Y., M. Kubo, et al. (1995). "Wilms' tumor protein WT1 as an ovarian transcription factor: decreases in expression during follicle development and repression of inhibin-alpha gene promoter." Mol Endocrinol **9**(10): 1356-1366.

Hu, Z., J. Chen, et al. (2008). "Genetic variants of miRNA sequences and non-small cell lung cancer survival." J Clin Invest **118**(7): 2600-2608.

Hutter, B., V. Helms, et al. (2006). "Tandem repeats in the CpG islands of imprinted genes." Genomics **88**(3): 323-332.

Huang, A., C. E. Campbell, et al. (1990). "Tissue, developmental, and tumor-specific expression of divergent transcripts in Wilms tumor." Science **250**(4983): 991-994.

Huang, T. H., D. E. Laux, et al. (1997). "Identification of DNA methylation markers for human breast carcinomas using the methylation-sensitive restriction fingerprinting technique." Cancer Res **57**(6): 1030-1034.

Huff, V., D. A. Compton, et al. (1988). "Lack of linkage of familial Wilms' tumour to chromosomal band 11p13." Nature **336**(6197): 377-378.

Huttenhofer, A., P. Schattner, et al. (2005). "Non-coding RNAs: hope or hype?" Trends Genet **21**(5): 289-297.

Huttenhofer, A., M. Kiefmann, et al. (2001). "RNomics: an experimental approach that identifies 201 candidates for novel, small, non-messenger RNAs in mouse." EMBO J **20**(11): 2943-2953.

Iben, S. and B. Royer-Pokora (1999). "Analysis of native WT1 protein from frozen human kidney and Wilms' tumors." Oncogene **18**(15): 2533-2536.

Ito, K., Y. Oji, et al. (2006). "Antiapoptotic function of 17AA(+)WT1 (Wilms' tumor gene) isoforms on the intrinsic apoptosis pathway." Oncogene **25**(30): 4217-4229.

Jin, P., D. C. Zarnescu, et al. (2004). "Biochemical and genetic interaction between the fragile X mental retardation protein and the microRNA pathway." Nat Neurosci **7**(2): 113-117.

Johnstone, R. W., R. H. See, et al. (1996). "A novel repressor, par-4, modulates transcription and growth suppression functions of the Wilms' tumor suppressor WT1." Mol Cell Biol **16**(12): 6945-6956.

Juan, V., C. Crain, et al. (2000). "Evidence for evolutionarily conserved secondary structure in the H19 tumor suppressor RNA." Nucleic Acids Res **28**(5): 1221-1227.

Junqueira, L. C. (1999). Hitologia Basica. Rio de Janeiro.

Kanduri, C. (2008). "Functional insights into long antisense noncoding RNA Kcnq1ot1 mediated bidirectional silencing." RNA Biol **5**(4): 208-211.

Kaneuchi, M., M. Sasaki, et al. (2005). "WT1 and WT1-AS genes are inactivated by promoter methylation in ovarian clear cell adenocarcinoma." Cancer **104**(9): 1924-1930.

Kapranov, P., J. Cheng, et al. (2007a). "RNA maps reveal new RNA classes and a possible function for pervasive transcription." Science **316**(5830): 1484-1488.

Kapranov, P., A. T. Willingham, et al. (2007b). "Genome-wide transcription and the implications for genomic organization." Nat Rev Genet **8**(6): 413-423.

Katayama, S., Y. Tomaru, et al. (2005). "Antisense transcription in the mammalian transcriptome." Science **309**(5740): 1564-1566.

Kawasaki, H. and K. Taira (2004). "Induction of DNA methylation and gene silencing by short interfering RNAs in human cells." Nature **431**(7005): 211-217.

Kennedy, D., T. Ramsdale, et al. (1996). "An RNA recognition motif in Wilms' tumour protein (WT1) revealed by structural modelling." Nat Genet **12**(3): 329-331.

Kent, J., A. M. Coriat, et al. (1995). "The evolution of WT1 sequence and expression pattern in the vertebrates." Oncogene **11**(9): 1781-1792.

Kent, W. J., C. W. Sugnet, et al. (2002). "The human genome browser at UCSC." Genome Res **12**(6): 996-1006

Kim, V. N. (2005). "Small RNAs: classification, biogenesis, and function." Mol Cells **19**(1): 1-15.

Kirschner, K. M., N. Wagner, et al. (2006). "The Wilms tumor suppressor Wt1 promotes cell adhesion through transcriptional activation of the alpha4integrin gene." J Biol Chem **281**(42): 31930-31939.

Kittler, R. and F. Buchholz (2003). "RNA interference: gene silencing in the fast lane." Semin Cancer Biol **13**(4): 259-265.

Kiyosawa, H. (2007). "[Mouse natural antisense RNA]." Tanpakushitsu Kakusan Koso **52**(5): 441-448.

Kiyosawa, H., I. Yamanaka, et al. (2003). "Antisense transcripts with FANTOM2 clone set and their implications for gene regulation." Genome Res **13**(6B): 1324-1334.

Klamt, B., A. Koziell, et al. (1998). "Frasier syndrome is caused by defective alternative splicing of WT1 leading to an altered ratio of WT1 +/-KTS splice isoforms." Hum Mol Genet **7**(4): 709-714.

Kleymenova, E. V., X. Yuan, et al. (1998). "Identification of a tumor-specific methylation site in the Wilms tumor suppressor gene." Oncogene **16**(6): 713-720.

Knudson, A. G., Jr. (1971). "Mutation and cancer: statistical study of retinoblastoma." Proc Natl Acad Sci U S A **68**(4): 820-823.

Konecny, J., M. Eckert, et al. (1993). "Neutral adaptation of the genetic code to double-strand coding." J Mol Evol **36**(5): 407-416.

Koufos, A., M. F. Hansen, et al. (1984). "Loss of alleles at loci on human chromosome 11 during genesis of Wilms' tumour." Nature **309**(5964): 170-172.

Kreidberg, J. A., H. Sariola, et al. (1993). "WT-1 is required for early kidney development." Cell **74**(4): 679-691.

Krystal, G. W., B. C. Armstrong, et al. (1990). "N-myc mRNA forms an RNA-RNA duplex with endogenous antisense transcripts." Mol Cell Biol **10**(8): 4180-4191.

Kubota, S., T. Hattori, et al. (1999). "Involvement of cis-acting repressive element(s) in the 3'-untranslated region of human connective tissue growth factor gene." FEBS Lett **450**(1-2): 84-88.

Kwon, T. H., J. Frokiaer, et al. (1999). "Reduced abundance of aquaporins in rats with bilateral ischemia-induced acute renal failure: prevention by alpha-MSH." Am J Physiol **277**(3 Pt 2): F413-427.

Ladomery, M. R., J. Slight, et al. (1999). "Presence of WT1, the Wilm's tumor suppressor gene product, in nuclear poly(A)(+) ribonucleoprotein." J Biol Chem **274**(51): 36520-36526.

Lagos-Quintana, M., R. Rauhut, et al. (2001). "Identification of novel genes coding for small expressed RNAs." Science **294**(5543): 853-858

Lahiri, D., J. R. Dutton, et al. (2007). "Nephropathy and defective spermatogenesis in mice transgenic for a single isoform of the Wilms' tumour suppressor protein, WT1-KTS, together with one disrupted Wt1 allele." Mol Reprod Dev **74**(3): 300-311.

Lai, E. C. (2002). "Micro RNAs are complementary to 3' UTR sequence motifs that mediate negative post-transcriptional regulation." Nat Genet **30**(4): 363-364.

Laity, J. H., J. Chung, et al. (2000). "Alternative splicing of Wilms' tumor suppressor protein modulates DNA binding activity through isoform-specific DNA-induced conformational changes." Biochemistry **39**(18): 5341-5348.

Larsson, S. H., J. P. Charlieu, et al. (1995). "Subnuclear localization of WT1 in splicing or transcription factor domains is regulated by alternative splicing." Cell **81**(3): 391-401.

Latham, K. E. (2005). "X chromosome imprinting and inactivation in preimplantation mammalian embryos." Trends in Genetics **21**(2): 120-127.

Laux, D. E., E. M. Curran, et al. (1999). "Hypermethylation of the Wilms' tumor suppressor gene CpG island in human breast carcinomas." Breast Cancer Res Treat **56**(1): 35-43.

Lavorgna, G., D. Dahary, et al. (2004). "In search of antisense." Trends Biochem Sci **29**(2): 88-94.

Lee, J. T., L. S. Davidow, et al. (1999). "Tsix, a gene antisense to Xist at the X-inactivation centre." Nat Genet **21**(4): 400-404.

Lee, S. B. and D. A. Haber (2001). "Wilms tumor and the WT1 gene." Exp Cell Res **264**(1): 74-99.

Lee, S. B., K. Huang, et al. (1999). "The Wilms tumor suppressor WT1 encodes a transcriptional activator of amphiregulin." Cell **98**(5): 663-673.

Lehner, B., G. Williams, et al. (2002). "Antisense transcripts in the human genome." Trends Genet **18**(2): 63-65.

Leighton, P. A., J. R. Saam, et al. (1995). "An enhancer deletion affects both H19 and Igf2 expression." Genes Dev **9**(17): 2079-2089.

Lewis, A. and L. Redrup (2005). "Genetic imprinting: conflict at the Callipyge locus." Curr Biol **15**(8): R291-294.

Lewis, W. H., H. Yeger, et al. (1988). "Homozygous deletion of a DNA marker from chromosome 11p13 in sporadic Wilms tumor." Genomics **3**(1): 25-31.

Li, A. W., G. Seyoum, et al. (1996). "Expression of the rat BFGF antisense RNA transcript is tissue-specific and developmentally regulated." Mol Cell Endocrinol **118**(1-2): 113-123.

Li, M., M. Yu, et al. (1996). "[Inhibitory effects of malignant phenotype of human bladder cancer cell line by c-Ha-ras, c-myc antisense oligodeoxynucleotide]." Zhonghua Wai Ke Za Zhi **34**(1): 7-9.

Lin, S. L., D. Chang, et al. (2003). "A novel RNA splicing-mediated gene silencing mechanism potential for genome evolution." Biochem Biophys Res Commun **310**(3): 754-760.

Little, M., G. Holmes, et al. (1999). "WT1: what has the last decade told us?" Bioessays **21**(3): 191-202.

Little, M. and C. Wells (1997). "A clinical overview of WT1 gene mutations." Hum Mutat **9**(3): 209-225.

Little, M. H., K. A. Williamson, et al. (1993). "Evidence that WT1 mutations in Denys-Drash syndrome patients may act in a dominant-negative fashion." Hum Mol Genet **2**(3): 259-264.

Loeb, D. M., E. Evron, et al. (2001). "Wilms' tumor suppressor gene (WT1) is expressed in primary breast tumors despite tumor-specific promoter methylation." Cancer Res **61**(3): 921-925.

Loeb, D. M., D. Korz, et al. (2002). "Cyclin E is a target of WT1 transcriptional repression." J Biol Chem **277**(22): 19627-19632.

Lu, C., S. S. Tej, et al. (2005). "Elucidation of the small RNA component of the transcriptome." Science **309**(5740): 1567-1569.

Lu, J., G. Getz, et al. (2005). "MicroRNA expression profiles classify human cancers." Nature **435**(7043): 834-838.

Luo, G., C. Hofmann, et al. (1995). "BMP-7 is an inducer of nephrogenesis, and is also required for eye development and skeletal patterning." Genes Dev **9**(22): 2808-2820.

Lyle, R., D. Watanabe, et al. (2000). "The imprinted antisense RNA at the Igf2r locus overlaps but does not imprint Mas1." Nat Genet **25**(1): 19-21.

Ma, T., B. Yang, et al. (1998). "Severely impaired urinary concentrating ability in transgenic mice lacking aquaporin-1 water channels." J Biol Chem **273**(8): 4296-4299.

Madden, S. L., D. M. Cook, et al. (1991). "Transcriptional repression mediated by the WT1 Wilms tumor gene product." Science **253**(5027): 1550-1553.

Madden, S. L., D. M. Cook, et al. (1993a). "A structure-function analysis of transcriptional repression mediated by the WT1, Wilms' tumor suppressor protein." Oncogene **8**(7): 1713-1720.

Madden, S. L. and F. J. Rauscher, 3rd (1993b). "Positive and negative regulation of transcription and cell growth mediated by the EGR family of zinc-finger gene products." Ann N Y Acad Sci **684**: 75-84.

Maheswaran, S., C. Englert, et al. (1995). "The WT1 gene product stabilizes p53 and inhibits p53-mediated apoptosis." Genes Dev **9**(17): 2143-2156.

Maheswaran, S., C. Englert, et al. (1998). "E1B 55K sequesters WT1 along with p53 within a cytoplasmic body in adenovirus-transformed kidney cells." Oncogene **16**(16): 2041-2050.

Maheswaran, S., S. Park, et al. (1993). "Physical and functional interaction between WT1 and p53 proteins." Proc Natl Acad Sci U S A **90**(11): 5100-5104.

Malik, K. T., J. I. Wallace, et al. (1995). "Identification of an antisense WT1 promoter in intron 1: implications for WT1 gene regulation." Oncogene **11**(8): 1589-1595.

Mallory, A. C. and H. Vaucheret (2006). "Functions of microRNAs and related small RNAs in plants." Nat Genet **38 Suppl**: S31-36.

Mancini-Dinardo, D., S. J. Steele, et al. (2006). "Elongation of the Kcnq1ot1 transcript is required for genomic imprinting of neighboring genes." Genes Dev **20**(10): 1268-1282.

Manley, G. T., M. Fujimura, et al. (2000). "Aquaporin-4 deletion in mice reduces brain edema after acute water intoxication and ischemic stroke." Nat Med **6**(2): 159-163.

Martinez-Estrada, O. M., L. A. Lettice, et al. (2010). "Wt1 is required for cardiovascular progenitor cell formation through transcriptional control of Snail and E-cadherin." Nat Genet **42**(1): 89-93.

Matsunaga, E. (1981). "Genetics of Wilms' tumor." Hum Genet **57**(3): 231-246.

Mattick, J. S. (2005). "The functional genomics of noncoding RNA." Science **309**(5740): 1527-1528.

Mattick, J. S. (2007). "A new paradigm for developmental biology." J Exp Biol **210**(Pt 9): 1526-1547.

Matzke, M. A. and J. A. Birchler (2005). "RNAi-mediated pathways in the nucleus." Nat Rev Genet **6**(1): 24-35.

Mayo, M. W., C. Y. Wang, et al. (1999). "WT1 modulates apoptosis by transcriptionally upregulating the bcl-2 proto-oncogene." EMBO J **18**(14): 3990-4003.

McCann, A. H., N. Miller, et al. (1996). "Biallelic expression of the IGF2 gene in human breast disease." Hum Mol Genet **5**(8): 1123-1127.

McCann, S., J. Sullivan, et al. (1995). "Repression of the c-myb gene by WT1 protein in T and B cell lines." J Biol Chem **270**(40): 23785-23789.

McMahon, C. J., J. S. Wu, et al. (2010). "Muscle edema." AJR Am J Roentgenol **194**(4): W284-292.

McManus, M. T. (2003). "MicroRNAs and cancer." Semin Cancer Biol **13**(4): 253-258.

Meister, G. and T. Tuschl (2004). "Mechanisms of gene silencing by double-stranded RNA." Nature **431**(7006): 343-349.

Menke, A., L. McInnes, et al. (1998). "The Wilms' tumor suppressor WT1: approaches to gene function." Kidney Int **53**(6): 1512-1518.

Menke, A. L., A. R. Clarke, et al. (2002). "Genetic interactions between the Wilms' tumor 1 gene and the p53 gene." Cancer Res **62**(22): 6615-6620.

Menke, A. L. and A. Schedl (2003). "WT1 and glomerular function." Semin Cell Dev Biol **14**(4): 233-240.

Menke, A. L., A. Shvarts, et al. (1997). "Wilms' tumor 1-KTS isoforms induce p53-independent apoptosis that can be partially rescued by expression of the epidermal growth factor receptor or the insulin receptor." Cancer Res **57**(7): 1353-1363.

Menke, A. L., A. J. van der Eb, et al. (1998). "The Wilms' tumor 1 gene: oncogene or tumor suppressor gene?" Int Rev Cytol **181**: 151-212.

Merino, E., P. Balbas, et al. (1994). "Antisense overlapping open reading frames in genes from bacteria to humans." Nucleic Acids Res **22**(10): 1903-1908.

Miles, C., G. Elgar, et al. (1998). "Complete sequencing of the Fugu WAGR region from WT1 to PAX6: dramatic compaction and conservation of synteny with human chromosome 11p13." Proc Natl Acad Sci U S A **95**(22): 13068-13072.

Miles, C. G., J. Slight, et al. (2003). "Mice lacking the 68-amino-acid, mammal-specific N-terminal extension of WT1 develop normally and are fertile." Mol Cell Biol **23**(7): 2608-2613.

Moore, A. W., L. McInnes, et al. (1999). "YAC complementation shows a requirement for Wt1 in the development of epicardium, adrenal gland and throughout nephrogenesis." Development **126**(9): 1845-1857.

Moorwood, K., A. K. Charles, et al. (1998). "Antisense WT1 transcription parallels sense mRNA and protein expression in fetal kidney and can elevate protein levels in vitro." J Pathol **185**(4): 352-359.

Moorwood, K., A. Salpekar, et al. (1999). "Transactivation of the WT1 antisense promoter is unique to the WT1[+/-] isoform." FEBS Lett **456**(1): 131-136.

Morey, C. and P. Avner (2004). "Employment opportunities for non-coding RNAs." FEBS Lett **567**(1): 27-34.

Morrison, D. J., M. A. English, et al. (2005). "WT1 induces apoptosis through transcriptional regulation of the proapoptotic Bcl-2 family member Bak." Cancer Res **65**(18): 8174-8182.

Mueller, R. F. (1994). "The Denys-Drash syndrome." J Med Genet **31**(6): 471-477.

Murphy, P. R. and R. S. Knee (1994). "Identification and characterization of an antisense RNA transcript (gfg) from the human basic fibroblast growth factor gene." Mol Endocrinol **8**(7): 852-859.

Nakagama, H., G. Heinrich, et al. (1995). "Sequence and structural requirements for high-affinity DNA binding by the WT1 gene product." Mol Cell Biol **15**(3): 1489-1498.

Nariyama, M., K. Shimizu, et al. (2004). "Identification of chromosomes associated with dental caries susceptibility using quantitative trait locus analysis in mice." Caries Res **38**(2): 79-84

Natoli, T. A., J. Liu, et al. (2002). "A mutant form of the Wilms' tumor suppressor gene WT1 observed in Denys-Drash syndrome interferes with glomerular capillary development." J Am Soc Nephrol **13**(8): 2058-2067.

Natoli, T. A., A. McDonald, et al. (2002). "A mammal-specific exon of WT1 is not required for development or fertility." Mol Cell Biol **22**(12): 4433-4438.

Nei, M., P. Xu, et al. (2001). "Estimation of divergence times from multiprotein sequences for a few mammalian species and several distantly related organisms." Proc Natl Acad Sci U S A **98**(5): 2497-2502.

Nielsen, S. and J. Frokiaer (2003). "[The 2003 Nobel Prize in chemistry to Peter Agre for the discovery of aquaporin channels]." Ugeskr Laeger **165**(50): 4863-4865.

Nishinakamura, R., Y. Matsumoto, et al. (2001). "Murine homolog of SALL1 is essential for ureteric bud invasion in kidney development." Development **128**(16): 3105-3115.

Norden, J., T. Grieskamp, et al. (2010). "Wt1 and retinoic acid signaling in the subcoelomic mesenchyme control the development of the pleuropericardial membranes and the sinus horns." Circ Res **106**(7): 1212-1220.

O'Donnell, K. A., E. A. Wentzel, et al. (2005). "c-Myc-regulated microRNAs modulate E2F1 expression." Nature **435**(7043): 839-843.

O'Neill, M. J. (2005). "The influence of non-coding RNAs on allele-specific gene expression in mammals." Hum Mol Genet **14 Spec No 1**: R113-120.

Ogawa, O., M. R. Eccles, et al. (1993). "Relaxation of insulin-like growth factor II gene imprinting implicated in Wilms' tumour." Nature **362**(6422): 749-751.

Oji, Y., S. Miyoshi, et al. (2002). "Overexpression of the Wilms' tumor gene WT1 in de novo lung cancers." Int J Cancer **100**(3): 297-303.

Okada, Y., C. Tashiro, et al. (2008). "Comparative expression analysis uncovers novel features of endogenous antisense transcription." Hum Mol Genet **17**(11): 1631-1640.

Orkin, S. H., D. S. Goldman, et al. (1984). "Development of homozygosity for chromosome 11p markers in Wilms' tumour." Nature **309**(5964): 172-174.

Palmer, R. E., A. Kotsianti, et al. (2001). "WT1 regulates the expression of the major glomerular podocyte membrane protein Podocalyxin." Curr Biol **11**(22): 1805-1809.

Pang, K. C., M. C. Frith, et al. (2006). "Rapid evolution of noncoding RNAs: lack of conservation does not mean lack of function." Trends Genet **22**(1): 1-5.

Park, S., A. Bernard, et al. (1993). "Inactivation of WT1 in nephrogenic rests, genetic precursors to Wilms' tumour." Nat Genet **5**(4): 363-367.

Patek, C. E., D. G. Brownstein, et al. (2008). "Effects on kidney disease, fertility and development in mice inheriting a protein-truncating Denys-Drash syndrome allele (Wt1tmT396)." Transgenic Res **17**(3): 459-475.

Patek, C. E., M. H. Little, et al. (1999). "A zinc finger truncation of murine WT1 results in the characteristic urogenital abnormalities of Denys-Drash syndrome." Proc Natl Acad Sci U S A **96**(6): 2931-2936.

Pauler, F. M., M. V. Koerner, et al. (2007). "Silencing by imprinted noncoding RNAs: is transcription the answer?" Trends Genet **23**(6): 284-292.

Pavletich, N. P. and C. O. Pabo (1993). "Crystal structure of a five-finger GLI-DNA complex: new perspectives on zinc fingers." Science **261**(5129): 1701-1707.

Pelletier, J., W. Bruening, et al. (1991a). "Germline mutations in the Wilms' tumor suppressor gene are associated with abnormal urogenital development in Denys-Drash syndrome." Cell **67**(2): 437-447.

Pelletier, J., M. Schalling, et al. (1991b). "Expression of the Wilms' tumor gene WT1 in the murine urogenital system." Genes Dev **5**(8): 1345-1356.

Pennacchio, L. A., N. Ahituv, et al. (2006). "In vivo enhancer analysis of human conserved non-coding sequences." Nature **444**(7118): 499-502.

Perlot, T. and F. W. Alt (2008). "Cis-regulatory elements and epigenetic changes control genomic rearrangements of the IgH locus." Adv Immunol **99**: 1-32.

Peterson, J. A. and A. M. Myers (1993). "Functional analysis of mRNA 3' end formation signals in the convergent and overlapping transcription units of the S. cerevisiae genes RHO1 and MRP2." Nucleic Acids Res **21**(23): 5500-5508.

Phelan, S. A., C. Lindberg, et al. (1994). "Wilms' tumor gene, WT1, mRNA is down-regulated during induction of erythroid and megakaryocytic differentiation of K562 cells." Cell Growth Differ **5**(6): 677-686.

Plass, C., F. Yu, et al. (1999). "Restriction landmark genome scanning for aberrant methylation in primary refractory and relapsed acute myeloid leukemia; involvement of the WIT-1 gene." Oncogene **18**(20): 3159-3165.

Potter, S. S. and W. W. Branford (1998). "Evolutionary conservation and tissue-specific processing of Hoxa 11 antisense transcripts." Mamm Genome **9**(10): 799-806.

Poulin, F., M. A. Nobrega, et al. (2005). "In vivo characterization of a vertebrate ultraconserved enhancer." Genomics **85**(6): 774-781.

Poy, M. N., L. Eliasson, et al. (2004). "A pancreatic islet-specific microRNA regulates insulin secretion." Nature **432**(7014): 226-230.

Prasanth, K. V., S. G. Prasanth, et al. (2005). "Regulating gene expression through RNA nuclear retention." Cell **123**(2): 249-263.

Prasanth, K. V. and D. L. Spector (2007). "Eukaryotic regulatory RNAs: an answer to the 'genome complexity' conundrum." Genes Dev **21**(1): 11-42.

Prescott, E. M. and N. J. Proudfoot (2002). "Transcriptional collision between convergent genes in budding yeast." Proc Natl Acad Sci U S A **99**(13): 8796-8801.

Pritchard-Jones, K., S. Fleming, et al. (1990). "The candidate Wilms' tumour gene is involved in genitourinary development." Nature **346**(6280): 194-197.

Puig, O., A. Gottschalk, et al. (1999). "Interaction of the U1 snRNP with nonconserved intronic sequences affects 5' splice site selection." Genes Dev **13**(5): 569-580.

Rainier, S., L. A. Johnson, et al. (1993). "Relaxation of imprinted genes in human cancer." Nature **362**(6422): 747-749.

Rao, M. K., J. Pham, et al. (2006). "Tissue-specific RNAi reveals that WT1 expression in nurse cells controls germ cell survival and spermatogenesis." Genes Dev **20**(2): 147-152.

Ratelade, J., C. Arrondel, et al. (2010). "A murine model of Denys-Drash syndrome reveals novel transcriptional targets of WT1 in podocytes." Hum Mol Genet **19**(1): 1-15.

Rauscher, F. J., 3rd (1993). "Tumor suppressor genes which encode transcriptional repressors: studies on the EGR and Wilms' tumor (WT1) gene products." Adv Exp Med Biol **348**: 23-29.

Rauscher, F. J., 3rd, J. F. Morris, et al. (1990). "Binding of the Wilms' tumor locus zinc finger protein to the EGR-1 consensus sequence." Science **250**(4985): 1259-1262.

Ravasi, T., H. Suzuki, et al. (2006). "Experimental validation of the regulated expression of large numbers of non-coding RNAs from the mouse genome." Genome Res **16**(1): 11-19.

Reddy, J. C., S. Hosono, et al. (1995a). "The transcriptional effect of WT1 is modulated by choice of expression vector." J Biol Chem **270**(50): 29976-29982.

Reddy, J. C., J. C. Morris, et al. (1995b). "WT1-mediated transcriptional activation is inhibited by dominant negative mutant proteins." J Biol Chem **270**(18): 10878-10884.

Reeve, A. E., P. J. Housiaux, et al. (1984). "Loss of a Harvey ras allele in sporadic Wilms' tumour." Nature **309**(5964): 174-176.

Reik, W., M. Constancia, et al. (2003). "Regulation of supply and demand for maternal nutrients in mammals by imprinted genes." J Physiol **547**(Pt 1): 35-44.

Reik, W. and W. Dean (2001). "DNA methylation and mammalian epigenetics." Electrophoresis **22**(14): 2838-2843.

Reik, W. and A. Lewis (2005). "Co-evolution of X-chromosome inactivation and imprinting in mammals." Nat Rev Genet **6**(5): 403-410.

Reik, W. and J. Walter (2001). "Evolution of imprinting mechanisms: the battle of the sexes begins in the zygote." Nat Genet **27**(3): 255-256.

Renshaw, J., R. M. Orr, et al. (2004). "Disruption of WT1 gene expression and exon 5 splicing following cytotoxic drug treatment: antisense down-regulation of exon 5 alters target gene expression and inhibits cell survival." Mol Cancer Ther **3**(11): 1467-1484.

Riccardi, V. M. (1980). "Chromosomes, embryonal tumors, and birth defects." Am J Ophthalmol **89**(5): 749-751.

Riccio, A., A. Sparago, et al. (2009). "Inherited and Sporadic Epimutations at the IGF2-H19 locus in Beckwith-Wiedemann syndrome and Wilms' tumor." Endocr Dev **14**: 1-9.

Rivera, M. N. and D. A. Haber (2005). "Wilms' tumour: connecting tumorigenesis and organ development in the kidney." Nat Rev Cancer **5**(9): 699-712.

Roberts, S. G. (2005). "Transcriptional regulation by WT1 in development." Curr Opin Genet Dev **15**(5): 542-547.

Rocha, J. L., E. J. Eisen, et al. (2004). "A large-sample QTL study in mice: I. Growth." Mamm Genome **15**(2): 83-99

Ronai, D., M. D. Iglesias-Ussel, et al. (2007). "Detection of chromatin-associated single-stranded DNA in regions targeted for somatic hypermutation." J Exp Med **204**(1): 181-190.

Rose, E. A., T. Glaser, et al. (1990). "Complete physical map of the WAGR region of 11p13 localizes a candidate Wilms' tumor gene." Cell **60**(3): 495-508.

Rosenbloom, K. R., T. R. Dreszer, et al. (2010). "ENCODE whole-genome data in the UCSC Genome Browser." Nucleic Acids Res **38**(Database issue): D620-625.

Rosok, O. and M. Sioud (2004). "Systematic identification of sense-antisense transcripts in mammalian cells." Nat Biotechnol **22**(1): 104-108.

Rougeulle, C. and E. Heard (2002). "Antisense RNA in imprinting: spreading silence through Air." Trends Genet **18**(9): 434-437.

Ryan, G., V. Steele-Perkins, et al. (1995). "Repression of Pax-2 by WT1 during normal kidney development." Development **121**(3): 867-875.

Sado, T., Z. Wang, et al. (2001). "Regulation of imprinted X-chromosome inactivation in mice by Tsix." Development **128**(8): 1275-1286.

Sakamoto, Y., Y. Mariya, et al. (2009). "WT1 mRNA level in peripheral blood is a sensitive biomarker for monitoring minimal residual disease in acute myeloid leukemia." Tohoku J Exp Med **219**(2): 169-176.

Sarfstein, R. and H. Werner (2006). "The WT1 Wilms' tumor suppressor gene is a downstream target for insulin-like growth factor-I (IGF-I) action in PC12 cells." J Neurochem **99**(3): 818-826.

Sasaki, S., K. Ishibashi, et al. (1998). "Aquaporin-2 and -3: representatives of two subgroups of the aquaporin family colocalized in the kidney collecting duct." Annu Rev Physiol **60**: 199-220.

Sastry, S. S. and P. L. Hoffman (1995). "The influence of RNA and DNA template structures during transcript elongation by RNA polymerases." Biochem Biophys Res Commun **211**(1): 106-114.

Saxen, L. and H. Sariola (1987). "Early organogenesis of the kidney." Pediatr Nephrol **1**(3): 385-392.

Scharnhorst, V., A. J. van der Eb, et al. (2001). "WT1 proteins: functions in growth and differentiation." Gene **273**(2): 141-161.

Schmidt, J. V., J. M. Levorse, et al. (1999). "Enhancer competition between H19 and Igf2 does not mediate their imprinting." Proc Natl Acad Sci U S A **96**(17): 9733-9738.

Scholz, H. and K. M. Kirschner (2005). "A role for the Wilms' tumor protein WT1 in organ development." Physiology (Bethesda) **20**: 54-59.

Schroeder, W. T., L. Y. Chao, et al. (1987). "Nonrandom loss of maternal chromosome 11 alleles in Wilms tumors." Am J Hum Genet **40**(5): 413-420.

Seidl, C. I., S. H. Stricker, et al. (2006). "The imprinted Air ncRNA is an atypical RNAPII transcript that evades splicing and escapes nuclear export." EMBO J **25**(15): 3565-3575.

Semba, K., R. Saito-Ueno, et al. (1996). "cDNA cloning and its pronephros-specific expression of the Wilms' tumor suppressor gene, WT1, from Xenopus laevis." Gene **175**(1-2): 167-172.

Shannon, R. S., J. R. Mann, et al. (1982). "Wilms's tumour and aniridia: clinical and cytogenetic features." Arch Dis Child **57**(9): 685-690.

Sharma, P. M., M. Bowman, et al. (1994). "RNA editing in the Wilms' tumor susceptibility gene, WT1." Genes Dev **8**(6): 720-731.

Shen, H., W. Xu, et al. (2007). "Down-regulation of WT1/+17AA gene expression using RNAi and modulating leukemia cell chemotherapy resistance." Haematologica **92**(9): 1270-1272.

Shen, J., C. B. Ambrosone, et al. (2009). "Novel genetic variants in microRNA genes and familial breast cancer." Int J Cancer **124**(5): 1178-1182.

Shimizu, M., T. Toki, et al. (2000). "Immunohistochemical detection of the Wilms' tumor gene (WT1) in epithelial ovarian tumors." Int J Gynecol Pathol **19**(2): 158-163.

Siehl, J. M., M. Reinwald, et al. (2004). "Expression of Wilms' tumor gene 1 at different stages of acute myeloid leukemia and analysis of its major splice variants." Ann Hematol **83**(12): 745-750.

Singer, M. A. (2001). "Of mice and men and elephants: metabolic rate sets glomerular filtration rate." Am J Kidney Dis **37**(1): 164-178.

Simpson, L. A., E. A. Burwell, et al. (2006). "The antiapoptotic gene A1/BFL1 is a WT1 target gene that mediates granulocytic differentiation and resistance to chemotherapy." Blood **107**(12): 4695-4702.

Sleutels, F. and D. P. Barlow (2002). "The origins of genomic imprinting in mammals." Adv Genet **46**: 119-163.

Sleutels, F., G. Tjon, et al. (2003). "Imprinted silencing of Slc22a2 and Slc22a3 does not need transcriptional overlap between Igf2r and Air." EMBO J **22**(14): 3696-3704.

Sleutels, F., R. Zwart, et al. (2002). "The non-coding Air RNA is required for silencing autosomal imprinted genes." Nature **415**(6873): 810-813.

Srichai, M. B., M. Konieczkowski, et al. (2004). "A WT1 co-regulator controls podocyte phenotype by shuttling between adhesion structures and nucleus." J Biol Chem **279**(14): 14398-14408.

Stein, L. D., Z. Bao, et al. (2003). "The genome sequence of Caenorhabditis briggsae: a platform for comparative genomics." PLoS Biol **1**(2): E45.

Storz, G. (2002). "An expanding universe of noncoding RNAs." Science **296**(5571): 1260-1263.

Stougaard, P., S. Molin, et al. (1981). "RNAs involved in copy-number control and incompatibility of plasmid R1." Proc Natl Acad Sci U S A **78**(10): 6008-6012.

Struhl, K. (2007). "Transcriptional noise and the fidelity of initiation by RNA polymerase II." Nat Struct Mol Biol **14**(2): 103-105.

Taft, R. J., M. Pheasant, et al. (2007). "The relationship between non-protein-coding DNA and eukaryotic complexity." Bioessays **29**(3): 288-299.

Tasheva, E. S. and D. J. Roufa (1995). "A densely methylated DNA island is associated with a chromosomal replication origin in the human RPS14 locus." Somat Cell Mol Genet **21**(6): 369-383.

Tomari, Y. and P. D. Zamore (2005). "MicroRNA biogenesis: drosha can't cut it without a partner." Curr Biol **15**(2): R61-64.

Tomizawa, J., T. Itoh, et al. (1981). "Inhibition of ColE1 RNA primer formation by a plasmid-specified small RNA." Proc Natl Acad Sci U S A **78**(3): 1421-1425.

Tufarelli, C., J. A. Stanley, et al. (2003). "Transcription of antisense RNA leading to gene silencing and methylation as a novel cause of human genetic disease." Nat Genet **34**(2): 157-165.

Udtha, M., S. J. Lee, et al. (2003). "Upregulation of c-MYC in WT1-mutant tumors: assessment of WT1 putative transcriptional targets using cDNA microarray expression profiling of genetically defined Wilms' tumors." Oncogene **22**(24): 3821-3826.

Varanasi, R., N. Bardeesy, et al. (1994). "Fine structure analysis of the WT1 gene in sporadic Wilms tumors." Proc Natl Acad Sci U S A **91**(9): 3554-3558.

Venter, J. C., M. D. Adams, et al. (2001). "The sequence of the human genome." Science **291**(5507): 1304-1351.

Verkman, A. S. and B. Yang (2002). "Aquaporin gene delivery to kidney." Kidney Int **61**(1 Suppl): S120-124.

Visel, A., M. J. Blow, et al. (2009). "ChIP-seq accurately predicts tissue-specific activity of enhancers." Nature **457**(7231): 854-858.

Voinnet, O. (2009). "Origin, biogenesis, and activity of plant microRNAs." Cell **136**(4): 669-687.

Volinia, S., G. A. Calin, et al. (2006). "A microRNA expression signature of human solid tumors defines cancer gene targets." Proc Natl Acad Sci U S A **103**(7): 2257-2261.

Vu, T. H., N. V. Chuyen, et al. (2003). "Loss of imprinting of IGF2 sense and antisense transcripts in Wilms' tumor." Cancer Res **63**(8): 1900-1905.

Wagner, K. D., N. Wagner, et al. (2003). "The complex life of WT1." J Cell Sci **116**(Pt 9): 1653-1658.

Wagner, K. D., N. Wagner, et al. (2002). "The Wilms' tumor gene Wt1 is required for normal development of the retina." EMBO J **21**(6): 1398-1405.

Wagner, N., K. D. Wagner, et al. (2005). "A splice variant of the Wilms' tumour suppressor Wt1 is required for normal development of the olfactory system." Development **132**(6): 1327-1336.

Wagner, N., K. D. Wagner, et al. (2004). "The major podocyte protein nephrin is transcriptionally activated by the Wilms' tumor suppressor WT1." J Am Soc Nephrol **15**(12): 3044-3051.

Wahlestedt, C. (2006). "Natural antisense and noncoding RNA transcripts as potential drug targets." Drug Discov Today **11**(11-12): 503-508.

Waldstrom, M. and A. Grove (2005). "Immunohistochemical expression of wilms tumor gene protein in different histologic subtypes of ovarian carcinomas." Arch Pathol Lab Med **129**(1): 85-88.

Wang, J. Y. and K. Drlica (2004). "Computational identification of antisense oligonucleotides that rapidly hybridize to RNA." Oligonucleotides **14**(3): 167-175.

Wang, W., S. B. Lee, et al. (2001). "A functional interaction with CBP contributes to transcriptional activation by the Wilms tumor suppressor WT1." J Biol Chem **276**(20): 16810-16816.

Wang, Z. Y., Q. Q. Qiu, et al. (1993). "The Wilms' tumor gene product WT1 activates or suppresses transcription through separate functional domains." J Biol Chem **268**(13): 9172-9175.

Wang, Z. Y., Q. Q. Qiu, et al. (1995a). "WT1, the Wilms' tumor suppressor gene product, represses transcription through an interactive nuclear protein." Oncogene **10**(6): 1243-1247.

Wang, Z. Y., Q. Q. Qiu, et al. (1995b). "Products of alternatively spliced transcripts of the Wilms' tumor suppressor gene, wt1, have altered DNA binding specificity and regulate transcription in different ways." Oncogene **10**(3): 415-422.

Ward, A. (1997). "Beck-Wiedemann syndrome and Wilms' tumour." Mol Hum Reprod **3**(2): 157-168.

Ward, A., J. A. Pooler, et al. (1995). "Repression of promoters for the mouse insulin-like growth factor II-encoding gene (Igf-2) by products of the Wilms' tumour suppressor gene wt1." Gene **167**(1-2): 239-243.

Waterston, R. H., K. Lindblad-Toh, et al. (2002). "Initial sequencing and comparative analysis of the mouse genome." Nature **420**(6915): 520-562.

Werner, H., F. J. Rauscher, 3rd, et al. (1994). "Transcriptional repression of the insulin-like growth factor I receptor (IGF-I-R) gene by the tumor suppressor WT1 involves binding to sequences both upstream and downstream of the IGF-I-R gene transcription start site." J Biol Chem **269**(17): 12577-12582.

West, G. B., J. H. Brown, et al. (1997). "A general model for the origin of allometric scaling laws in biology." Science **276**(5309): 122-126.

Wilhelm, D. and C. Englert (2002). "The Wilms tumor suppressor WT1 regulates early gonad development by activation of Sf1." Genes Dev **16**(14): 1839-1851.

Wilimas, J. A., E. C. Douglass, et al. (1988). "Reduced therapy for Wilms' tumor: analysis of treatment results from a single institution." J Clin Oncol **6**(10): 1630-1635.

Wilkins, J. F. and D. Haig (2003). "Inbreeding, maternal care and genomic imprinting." J Theor Biol **221**(4): 559-564.

Will, C. L., C. Schneider, et al. (2001). "A novel U2 and U11/U12 snRNP protein that associates with the pre-mRNA branch site." EMBO J **20**(16): 4536-4546.

Williams, J. C., K. W. Brown, et al. (1989). "Maternal allele loss in Wilms' tumour." Lancet **1**(8632): 283-284.

Williamson, C. M., M. D. Turner, et al. (2006). "Identification of an imprinting control region affecting the expression of all transcripts in the Gnas cluster." Nat Genet **38**(3): 350-355.

Willingham, A. T., A. P. Orth, et al. (2005). "A strategy for probing the function of noncoding RNAs finds a repressor of NFAT." Science **309**(5740): 1570-1573.

Wutz, A., O. W. Smrzka, et al. (1997). "Imprinted expression of the Igf2r gene depends on an intronic CpG island." Nature **389**(6652): 745-749.

Yamasaki, Y., T. Kayashima, et al. (2005). "Neuron-specific relaxation of Igf2r imprinting is associated with neuron-specific histone modifications and lack of its antisense transcript Air." Hum Mol Genet **14**(17): 2511-2520.

Yang, W. J., D. D. Yang, et al. (2005). "Dicer is required for embryonic angiogenesis during mouse development." J Biol Chem **280**(10): 9330-9335.

Yeger, H., C. Cullinane, et al. (1992). "Coordinate expression of Wilms' tumor genes correlates with Wilms' tumor phenotypes." Cell Growth Differ **3**(12): 855-864.

Yelin, R., D. Dahary, et al. (2003). "Widespread occurrence of antisense transcription in the human genome." Nat Biotechnol **21**(4): 379-386.

Yomo, T. and S. Ohno (1989). "Concordant evolution of coding and noncoding regions of DNA made possible by the universal rule of TA/CG deficiency-TG/CT excess." Proc Natl Acad Sci U S A **86**(21): 8452-8456.

Yomo, T. and I. Urabe (1994). "A frame-specific symmetry of complementary strands of DNA suggests the existence of genes on the antisense strand." J Mol Evol **38**(2): 113-120.

Yomo, T., I. Urabe, et al. (1992). "No stop codons in the antisense strands of the genes for nylon oligomer degradation." Proc Natl Acad Sci U S A **89**(9): 3780-3784.

Yu, Q., H. C. Chang, et al. (2008). "Transcription factor-dependent chromatin remodeling of Il18r1 during Th1 and Th2 differentiation." J Immunol **181**(5): 3346-3352.

Zenker, M., T. Aigner, et al. (2004). "Human laminin beta2 deficiency causes congenital nephrosis with mesangial sclerosis and distinct eye abnormalities." Hum Mol Genet **13**(21): 2625-2632.

Zhang, Q., J. Zhang, et al. (2008). "Synergistic upregulation of erythropoietin receptor (EPO-R) expression by sense and antisense EPO-R transcripts in the canine lung." Proc Natl Acad Sci U S A **105**(21): 7612-7617.

Zhang, Y., J. Li, et al. (2007). "NATsDB: Natural Antisense Transcripts DataBase." Nucleic Acids Res **35**(Database issue): D156-161.

Zull, J. E. and S. K. Smith (1990). "Is genetic code redundancy related to retention of structural information in both DNA strands?" Trends Biochem Sci **15**(7): 257-261.

Zwart, R., F. Sleutels, et al. (2001). "Bidirectional action of the Igf2r imprint control element on upstream and downstream imprinted genes." Genes Dev **15**(18): 2361-2366.

Zotti, A., R. Poggi, et al. (2009). "Exceptional bone density DXA values of the rostrum of a deep-diving marine mammal: a new technical insight in the adaptation of bone to aquatic life." Skeletal Radiology **38**(12): 1123-1125.